RELATIVE HEPATOTOXOCITY, CARCINOGENICITY, AND TOXICOGENOMICS OF SELECT DEHYDROPYRROLIZIDINE ALKALOIDS IN MICE

by

Michael J. Clayton

A dissertation submitted in partial fulfillment
of the requirements for the degree of:

DOCTOR OF PHILOSOPHY
In
Animal Health and Disease

Approved:

Arnaud Van Wettere, DVM, Ph.D. Major Professor	Bryan L Stegelmeier, DVM, Ph.D. Co-Major Professor
Jeffery O. Hall, DVM, Ph.D. Committee Member	Aaron Thomas, Ph.D. Committee Member
Korry Hintze, Ph.D. Committee Member	D. Richard Cutler, Ph.D. Vice Provost of Graduate Studies

UTAH STATE UNIVERSITY
Logan, Utah
2023

ABSTRACT

Relative Hepatotoxicity, Carcinogenicity, and Toxicogenomics of Select

Dehydropyrrolizidine Alkaloids in Mice.

by

Michael J. Clayton, Doctor of Philosophy

Utah State University, 2023

Major Professor: Arnaud J. Van Wettere, DVM, PhD, Diplomate ACVP
Department: Animal, Dairy and Veterinary Sciences

Dehydropyrrolizidine alkaloids are arguably the most important group of plant derived toxins in terms of impact on human and animal health. Dehydropyrrolizidine alkaloids are a large group of chemically related compounds, found in 3% of flowering plants worldwide. These toxins contaminate herbal products, grain, and hay, resulting in human and animal exposure. There are at least 350 identified toxic PAs, isolated from more than 6,000 plants. Dehydropyrrolizidine alkaloids are primarily hepatotoxic but have also been proven genotoxic and carcinogenic in certain circumstances. Riddelliine is the only member of this group of toxins to be classified as reasonably expected to be a human carcinogen by the National Toxicology Program. In the following three experiments, select purified dehydropyrrolizidine alkaloids were compared by their relative hepatotoxic, carcinogenic, and toxicogenomic effects in mice. In the first experiment, seven compounds were administered to C57BL6/j mice by oral gavage for ten days at

varying doses (1,2,4,8,15,30,45,90,180,360 mg/kg/day). Microscopic lesions, serum biochemical assays, and hepatic concentrations of pyrroles were compared. Distribution and severity of hepatic necrosis differed between compounds. Serum biochemical assays indicative of hepatic injury correlated with hepatic necrosis. Riddelliine caused the greatest concentration of pyrroles in the liver. In a second experiment, heterozygous p53 knockout mice were exposed to five dehydropyrrolizidine alkaloids to compare carcinogenic potential. There was no statistically significant difference for any of the five compounds in the frequency of neoplasia when compared to the control mice. This indicates that short duration exposure to hepatotoxic doses may be less likely to cause cancer compared to long-term low-dose exposure. In a third experiment, three dehydropyrrolizidine alkaloids, riddelliine, senecionine and heliotrine were administered to C57BL6/j mice at a common dose for 8 days. Whole genome RNA expression was compared for each compound at two time-points, 1-day and 28-days after exposure. Riddelliine and senecionine were hepatotoxic and caused similar changes in gene expression related to cancer development and metabolism; suggesting senecionine is probably carcinogenic. Heliotrine was not hepatotoxic and caused minimal changes in gene expression. Dysregulated genes tended to return to normal expression after 28 days, indicating recovery following short-duration hepatotoxic doses of the toxins.

(404 pages)

PUBLIC ABSTRACT

Relative Hepatotoxicity, Carcinogenicity, and Toxicogenomics of Select Dehydropyrrolizidine Alkaloids in Mice.

Michael J. Clayton

Dehydropyrrolizidine alkaloids are arguably the most important plant derived toxins in terms of impact on human and animal health. Dehydropyrrolizidine alkaloids are a large group of chemically related compounds found in 3% of flowering plants worldwide. Human exposure occurs from ingestion of herbal products including teas supplements or contaminated grain. Animals are exposed through contaminated feed or grazing. There are at least 350 identified toxic PAs, from more than 6,000 plants. The toxins primarily cause liver damage, but some are proven to cause cancer. Individual dehydropyrrolizidine alkaloids vary in their toxic effects. Riddelliine is the only dehydropyrrolizidine alkaloid with extensive evidence of its cancer-causing effects. The purpose of the research presented herein is to characterize and compare the relative toxic and cancer-causing effects of select dehydropyrrolizidine alkaloids. In the first experiment, seven compounds are administered to C57BL6/j mice by oral gavage for ten days at varying doses. Microscopic liver damage, liver enzymes, and liver concentrations of the toxic metabolite were compared. There was variation in the characteristics and severity of liver damage between compounds. Liver enzymes indicative of liver damage were observed. Riddelliine caused the greatest concentration of the toxic metabolite in the liver. In the second experiment, five dehydropyrrolizidine alkaloids were administered to genetically modified mice for ten days at the same dose. These mice are designed to develop cancer

more readily. There was no statistically significant difference in the development of cancer between the mice exposed to any of the five compounds compared to the control group, in. This indicates that short-duration exposure to dehydropyrrolizidine alkaloids at high doses may be less likely to cause cancer than long term low-dose exposure. In the third experiment, three dehydropyrrolizidine alkaloids were administered to mice at a common dose for 8 days. Whole genome RNA expression was compared for each compound at two time-points. Two of the compounds, riddelliine and senecionine, caused liver damage and similar gene expression changes. The dysregulated genes were related to cancer development and metabolism, indicating that senecionine may also cause cancer. Dysregulated genes tended to return to normal expression levels after 28 days, indicating recovery.

ACKNOWLEDGMENTS

There are many people to whom I owe my gratitude for their assistance in helping me complete this doctoral dissertation, and become board certified by the American College of Veterinary Pathologists. First, I must thank my committee members, Dr.'s Arnaud Van Wettere, Bryan Stegelmeier, Jeff Hall, Aaron Thomas, and Korey Hintze. Each of these brilliant individuals provided critical feedback and mentorship which enabled me to create quality experimental designs and to carry out the research with few unexpected complications. This doctoral program was part of a combined program also including a residency in veterinary pathology. The pathologists at the Utah Veterinary Diagnostic Laboratory and the USDA Poisonous Plant Research Laboratory have been generous and selfless with their time and always willing to impart their wisdom and knowledge for my benefit. Dr.'s Tom Baldwin, Bryan Stegelmeier, Arnaud Van Wettere, Gordon Hullinger, Jackie Kurz, and Carmen Lau have been instrumental in helping me learn the skills required of a veterinary pathologist. These people have gone above and beyond what is required and expected of them in looking out for me professionally and personally over the last six years. It is thanks to all of you that I was able to pass the ACVP phase I and II board examinations on my first attempt. Each of these individuals have also shown me what it means to be a good colleague and supervisor. Dr. Baldwin and Dr. Stegelmeier have treated me like family, while also insisting on the kind of work that I can be proud of at the end of this program. I find it difficult to find words sufficient to express my gratitude to these giants in their respective fields but thank you both so very much. Dr. Van Wettere also deserves specific mention for being the singular individual to consistently be in my corner. Dr. Van Wettere was critical in helping me stay on task

from start to finish. He is truly a remarkable mentor and I feel lucky to call him my friend after this long program.

The research that is presented in this dissertation was funded by the United States Department of Agriculture, Division of Animal Research Sciences, Poisonous Plant Research Laboratory. I would like to thank Dr. Daniel Cook, research leader for the Poisonous Plant Research Laboratory, for providing facilities, staff, and funding support that made this dissertation possible. Ed Knoppel and Joseph Jacobsen deserve huge thanks for doing the actual work that made the research possible, and teaching and helping me learn skills related to animal research which I lacked upon arrival. Lee Balls, Darrin Thornley and other animal care staff performed essential mouse work to help me complete my experiments as well. Dr. Dale Gardner also performed a great deal of work which was essential for the completion of my research projects. Dr. Gardner was always willing to take the time to share the wealth of knowledge he has, and to perform necessary testing for my projects. The entire staff of the Poisonous Plant Research Laboratory helped me by sharing their knowledge, teaching me new processes, and allowing me to occasionally assist them in some of the high-level research that the PPRL is known for. Thank you very much Dr.'s Kevin Welch, Zane Davis, Ben Green, Anita McCollum, Steve Lee, and Clint Stonecipher.

Finally, I must thank my family. My Wife Kate has supported me through veterinary school, clinical practice, then a combined PhD and residency in veterinary pathology. She always embraces these changes and supports me in pursuit of my dreams. My kids, Max and Emma June, who help keep me grounded and remind me of where my priorities belong. My mother and father-in-law, Dr. Jill Muir and Scott Muir, who have

been unwavering in their support, and always happy to proofread a document on short notice. My mom and Dad, Blaine and Jan Clayton, for making me into the person I am today. I love you both. Thank you all.

Michael J. Clayton

CONTENTS

Page

LIST OF TABLES

Page

LIST OF FIGURES

Page

CHAPTER I INTRODUCTION AND BACKGROUND INFORMATION

Introduction:

Dehydropyrrolizidine alkaloids (also known as pyrrolizidine alkaloids; abbreviated as PAs) are a large group of chemically related, plant-derived toxins. PAs are estimated to be present in approximately 3% of the worlds flowering plants, and are one of the most important groups of plant derived toxins in terms of impact on human and animal health.[1] This group of toxins includes more than 600 individual compounds from at least 6,000 different plant species.[1,2] PA containing plants belong to the *Senecio*, *Heliotropium, Symphytum, Crotalaria, Cynoglossum,* and *Trichodesma* genera.[3] PAs commonly poison both humans and animals. Animal exposure occurs from ingestion of contaminated hay, grain, silage, or commercial feed products, or from grazing.[4,5] Human exposure can occur from ingestion of contaminated foods, herbal teas, or other herbal products.[6–10] Contamination of food sources occurs either when PA-containing plants are inadvertently co-harvested with crops, mainly grain. If seeds from PA containing plants are co-harvested with grains and then processed into flour, the bread and other products made from that flour will contain toxic PAs. This type of crop contamination has led to large outbreaks of poisoning, sometimes affecting thousands of people.[8,11,12] Contamination of animal products can occur when agricultural animals are fed or otherwise exposed to PA containing plants. It has been proven that PAs can be carried over into milk, eggs, honey, and possibly meat.[6,13,14] Exposure from herbal teas, supplements, or homeopathic treatments is a common scenario. This may be the result of inadvertent consumption because the PA plant was mistakenly identified, or even purposeful ingestion of

homeopathic treatments such as comfrey which are known to contain toxic PAs, but have a historic or cultural place as a home remedy.[9,14] The chemical structure of PAs consists of a common base structure referred to as a necine base, composed of two five membered ring structures with a single nitrogen atom in the center. There are one or two side chains that extend from carbons 7 and 9, referred to as necic acids which provide the immense variation within this chemical class. PAs can be considered protoxins as they require metabolic activation in order to exert their toxic effects.[1,3] After ingestion, metabolic activation occurs via the cytochrome p450 (CYP450) enzymes mainly in the liver. Because the liver contains the greatest concentration of CYP450 enzymes, PAs are mainly hepatotoxic, but they can also cause pneumotoxicity.[15–17] PAs are also genotoxic, cytotoxic, mutagenic some have been proven carcinogenic under some conditions.[3,18,19] Detoxification occurs mainly by glutathione conjugation, with glucuronidation playing a smaller role.[1,20] There has been a great deal of research into the toxic mechanisms, histopathological and biochemical effects of PAs. Experiments in which different PAs are directly compared to one another have shown that PAs can vary dramatically in their toxic potential.[21–24] As there are hundreds of documented toxic PAs there is much to be investigated regarding these chemicals and their relative toxic and carcinogenic effects. Next generation sequencing tools, sometimes referred to as toxicogenomics, are quickly becoming a mainstay in toxicology research. [25,26] These tools include transcriptomic, proteomic and metabolomic methods, which have recently been applied to the field of PA toxicity research and will be discussed at length later in this chapter and in chapter 4.

This dissertation will consist of five chapters. Chapter one includes an introduction and a literature review to provide the necessary background information which is pertinent to

the subsequent chapters. The following three chapters describe three individual research experiments on the comparative toxicity of select PAs in mice. Chapter 2 includes the first experiment, which was a comparative study on the immediate effects of five PAs and two PA N-oxides: riddelliine, senecionine, seneciphylline, heliotrine, lasiocarpine, riddelliine N-oxide, and senecionine N-oxide. Mice were exposed to various doses of these toxins by oral gavage for ten days, and then necropsied one day after dosing (day 11). Notable findings from this experiment include a ranking of these selected PAs by severity of hepatotoxicity, characterization of the liver lesions, comparing concentrations of hepatic PA metabolite or pyrrole concentrations, and correlation of certain serum biochemical assays with PA hepatotoxicosis. Senecionine, seneciphylline, and senecionine N-oxide were the most toxic; riddelliine and riddelliine N-oxide were intermediate; and lasiocarpine and heliotrine were the least toxic. All PAs except heliotrine caused some degree of hepatocellular degeneration and necrosis, but the distribution of the lesion within the hepatic lobule differed. Only riddelliine and its N-oxide had a centrilobular distribution, as is typically described in the literature for PA hepatotoxicosis. Riddelliine induced greater concentrations of hepatic pyrroles than all other compounds at comparable doses. Serum biochemical concentrations of alanine aminotransferase (ALT) and alkaline phosphatase (ALP) had strong positive correlations with hepatic necrosis scores. The second experiment, discussed in chapter 3 is a comparison of the carcinogenic potential of five PAs (riddelliine, senecionine, seneciphylline, lasiocarpine and heliotrine) in a heterozygous p53 knockout mouse model (B6.129S2-Trp53tm1Tyj/J). This animal model was determined suitable for experimental comparisons of PA-induced neoplasia in a previous experiment performed by Brown et

al. (2015). [27] Mice were exposed to these PAs at a common molar dose (0.129 mmol/kg/day) for ten days, by oral gavage. The selected dose was based on information obtained from the first experiment. Ultimately no statistical difference was detected between any of the PA groups and the control group by Dunnett's test with a poly-k correction for mortality. The poly-k correction is necessary in long-term carcinogenicity studies in which there is a difference in mortality between groups. The poly-k correction is intended to prevent underestimation of carcinogenicity in groups that did not live as long.[28] Riddelliine-exposed mice had the greatest number of liver hemangiosarcomas, though not statistically significant. Riddelliine was used as a positive control for carcinogenicity as it is the single PA with the strongest proof of carcinogenicity in rodents. These results suggest that short duration exposure to hepatotoxic doses of PAs may be less likely to induce carcinogenesis compared to long-term, low-dose exposure. However, there was a relatively high proportion of control mice with background neoplasia and the lack of statistical significance may be related to the animal model or experimental model used. Additionally, differences in mortality between groups occurred which likely contributed to the incidence of neoplasia in the control group. Although not statistically significant, differences in the number of neoplasms between groups suggested that the PAs used are not equally carcinogenic. The third experiment described in chapter 4 is a comparison of the toxicogenomic effects of three PAs on whole genome RNA expression. Riddelliine, senecionine and heliotrine were administered by oral gavage to mice for 8 days. The original plan was to treat mice for ten days, as in the other two experiments, but severe weight loss in the senecionine-exposed group necessitated early discontinuation of dosing. Mice were exposed to a common molar dose (0.129

mmol/kg/day) of each PA. Groups of five mice from each PA group were necropsied the day after dosing, and ten remaining mice were necropsied four weeks later. Whole genome RNA expression was performed on five mice from each PA group at both time points. Heliotrine exposure had no significant effects on biological pathways indicative of PA exposure and had the smallest number of differentially expressed genes (DEGs). Senecionine and riddelliine exposed mice had DEGs involved in biologic pathways related to cancer development, metabolism, and the cell cycle. Senecionine exposure caused the greatest number of dysregulated genes at both time points. Comparison of gene expression between the two time points showed that mice generally recovered following PA exposure. Upregulated and downregulated DEGs generally returned to normal or trended towards normal following the 28-day period of recovery. At the later time point, senecionine-exposed mice had more DEGs, but a greater proportion of the DEGs in the riddelliine-exposed mice belonged to cancer related biologic pathways. Additional endpoints compared included histopathology of the liver, serum biochemistry concentrations and hepatic pyrrole concentrations. Heliotrine had no significant effect on any of these endpoints, suggesting that heliotrine is not toxic to mice at the dose used in this experiment. Senecionine caused the most severe hepatic necrosis, which was characterized by multifocal groups of necrotic hepatocytes. Riddelliine caused mainly individual cell necrosis. Senecionine and riddelliine exposed mice had increased concentrations of serum biochemical assays indicative of hepatocellular injury, which had positive correlations with hepatic necrosis scores. Senecionine-exposure also resulted in the greatest concentration of hepatic pyrroles. This hepatic pyrrole concentration result

contrasts with the results of the initial experiment, in which riddelliine induced the greatest hepatic pyrrole concentrations.

This review will discuss the chemistry, toxicology, metabolism, and toxicogenomics of PAs. The information presented is intended to provide the reader with background information necessary to understand the experiments described in the following chapters. It is by no means a completely comprehensive review of PAs, as this would include enough information to fill a large textbook.

Sources of Dehydropyrrolizidine Alkaloid Exposure

The majority of known PAs come from plants in the Compositae, Leguminosae, and Boraginaceae families and the *Senecio, Crotalaria, Cynoglossum, Amsinckia, Heliotropium, Symphytum* and *Echium* genera. These plants are found throughout the world. With few exceptions, most of these plants do not contain a single compound but rather they contain mixtures of various PAs. Concentrations of PAs within the plants show considerable variation. The majority of PA containing plants contain the toxin in the above ground portion of the plant, but some plants have PAs in the root and seeds as well.[1,21]

Natural exposure to PAs occurs through ingestion. Pyrrolizidine alkaloid exposure in animals can occur through grazing poisonous plants, or from contamination of hay or grain. Nonnative PA containing plants often act as invasive weeds that contaminate crops. Alternatively, native PA containing plants can grow as monocultures in places where the land is disturbed. Most PA containing plants are thought to be nonpalatable for

animals, but as with other plant toxins if hungry grazing animals are placed on land where PAs are present without good forage available, those grazing animals are likely to eat the forage that is present. If these plants contaminate crops that are dried into hay, animals will typically readily eat the contaminated plants regardless of palatability.[29] This contamination can be present in commercially produced animal feed products as well. A recent study tested 48 samples of commercial feed for horses and found that 43% of the samples had concentrations that were greater than the recommended 90 ug/kg limit.[5] Another study in Belgium found PA contamination in feed samples meant for horses, rabbits and birds.[30] The process of ensiling partially, but not completely, degrades pyrrolizidine alkaloids when present, resulting in a 25% to 90% reduction of pyrrolizidine alkaloid content.[31] The risk from silage depends on the PAs and the contamination content before ensiling and the amount of reduction that occurs. Though ensiling is a possible mechanism that might allow use of contaminated feedstuffs, it would be prudent to test the ensiled feed prior to use.

People are exposed to pyrrolizidine alkaloids by either purposeful or accidental ingestion. Accidental ingestion occurs as the result of contamination of plant products such as herbal teas or supplements or animal products including milk, honey, eggs, grain, or pollen.[10,32,33] Mulder et al. (2018) recently measured PA concentrations in a variety of plant and animal food products and found a significant number of plant products are contaminated, with teas being the worst offenders. By contrast, relatively few of the animal products are contaminated, and only eggs and milk, no meat, had detectable concentrations of PAs.[34] Honey may can also be considered as an animal product. The study by Mulder et al. (2018) did not test honey samples, but other reports have

determined that PA contamination of honey occurs frequently. Dubecke et al. (2011) analyzed 3,917 honey samples and 119 samples of bee pollen using LC-MS/MS. They detected PA concentrations in 66% of the raw honey, 94% of retail honey, and 60% of bee pollen samples. Raw honey is meant to specify bulk honey that is not yet packaged for sale, while retail honey was obtained in packaged containers sold at supermarkets. The reason for the larger percentage in the retail honeys is thought to be the fact that retail honey is usually a blend of multiple honeys which often originate from different areas and a variety of plants. PA concentrations in the honey samples ranged from 1-225 µg /kg while bee pollen concentrations ranged from 11 to 37,855 µg /kg. Honey samples from South America and Central America tended to have greater PA concentrations than those from Europe. [35] Purposeful ingestion occurs due to the use of herbal preparations of known PA containing plants which are used as homeopathic treatments in the form of tinctures, teas and other supplements.[10] The most common source of exposure in people currently is thought to be through the ingestion of herbal teas.[36] Bodi et al. (2014) tested hundreds of samples of various commercially sold herbal teas, and found that more than 50% had detectable concentrations of PAs, with mean concentrations ranging from 51.7 to 1,856.4 mcg/kg. They also found that senecionine was the most commonly detected PA.[14] This is noteworthy, as multiple experiments comparing toxic potential of Pas have determined that senecionine is among the most toxic of Pas.[21,23,37–39] Huybrechts et al. (2015) found that in the Belgian food market, tea and honey were the most important sources of PA exposure, while milk samples were also found to contain PAs.[30] Kaltner et al. (2020) examined culinary herbs and spices from different geographic regions and determined that many (58% of samples analyzed) contained concentrations of PAs, of

particular concern was oregano and cumin imported from Turkey.[40] Candrian et al. (1984) demonstrated PA carryover into milk by feeding drosophila the milk of rats treated with seneciphylline and senkirkine. The same mutagenic effects were induced by feeding the milk as were observed by administering pure alkaloids to drosophila.[41] Hoogenboom et al. (2011) determined that there is a dose dependent carryover of PAs to milk in dairy cows by feeding dairy cows increasing amounts of dry ragwort. The overall carryover in milk was low, ranging from 0.1-4% of the total PAs, but depending on the dose the cows receive, this could be of concern to those consuming dairy products.[13] The PA constituents in milk did not necessarily match those in the plant and there were no N-oxides in milk. Mulder et al. (2020) similarly analyzed carryover to milk in dairy cows fed 200 g/day of various PA containing plants and found a carryover percentage ranging from 0.05-1.4%, resulting in concentrations of total PAs in milk of 12.1 +/- 0.5. In this study, they also detected PA N-oxides in milk.[42] Milk processing and its effects on PA content have also been studied. It was determined that pasteurization and sterilization procedures did not affect the PA content, but that microbial fermentation as is used in the making of cheese and yogurt did reduce PA concentrations.[43] Eggs can also be contaminated with PAs if hens are inadvertently fed PA containing plants.[6] Mulder et al. (2016) investigated carryover rates in eggs and poultry meat. They determined that carryover ranged from 0.02-0.23% in eggs and found that the concentration of PAs in meat were slightly lower than those in the eggs. This is one of few publications that detected PA concentrations in meat, and the author mentioned that these concentrations were found in birds that were dosed just prior to euthanasia.[44] Although meat is often mentioned as a potential source of PAs, careful review of the literature finds few

examples of meat containing PAs, and tracing some citations to their source finds a paucity of evidence to support this claim.

Despite an abundance of peer reviewed scientific literature detailing the risks associated with ingestion of dehydropyrrolizidine alkaloid containing plants, purposeful ingestion of PA containing plants for purported medicinal and health benefits still occurs.[45–47] Comfrey (*Symphytum officianale*) has been used frequently in herbal preparations, teas and even eaten in salads. This plant has numerous purported beneficial effects though evidence for these benefits is lacking. Comfrey is known to contain toxic pyrrolizidine alkaloids, has been linked to multiple cases of hepatic venoocclusive disease in people, and has been experimentally proven to be hepatotoxic, genotoxic and carcinogenic.[22,46,48,49] Mei et al. (2005) compared the mutagenicity of Comfrey and riddelliine in rats. Comfrey was proven more mutagenic than riddelliine.[50] Riddelliine is the single PA with the strongest proof of carcinogenicity, so it is noteworthy that a purported homeopathic cure-all like Comfrey induced more mutation. Despite the large body of scientific evidence to the contrary, there are those who persist in claiming Comfreys safety and efficacy, including multiple journal articles published in the fields of homeopathy and ethnopharmaceuticals.[47,51,52] Some of these reports discuss only topical use, which is unlikely to cause hepatotoxicity given the need for metabolic activation of PAs. Avila et al. (2020) recently attempted to dismantle the credibility of case reports of comfrey toxicity, while disregarding experimental data regarding toxic potential and proven toxicosis.[53] This highlights the disconnect between alternative and complimentary medicine and the scientific and medical communities. Comfrey was

banned for commercial sale by the United States Food and Drug Administration (FDA) in 2001.[54]

Crotalaria juncea, which is known to contain PAs, has been purposefully ingested as a remedy for hemoptysis, impetigo, or to treat common colds in various parts of the world.[55,56] A recent review of plants of the *Gynura* genus, which is a member of the Compositae family, cited multiple studies claiming medicinal properties which can treat a range of ailments ranging from diabetes to cancer. These plants are known to contain multiple pyrrolizidine alkaloids including seneciphylline and senecionine, which are among the most toxic PAs.[45] A similar review by Sarkar et al. (2021) cited numerous scientific studies which claimed that *Heliotropium indicum* has "antioxidant, analgesic, antimicrobial, anticancer, antituberculosis, antiplasmodial, anticataract, antifertility, wound healing, antiinflammatory, antinociceptive, antihyperglycemic, anthelmintic, diuretic, antitussive, antiglaucoma, antiallergic, and larvicidal activity's".[57] Claims of such diverse therapeutic benefits for any substance warrant skepticism. An additional study from Letsyo et al. (2017) found that many herbal medicines used in Ghana commonly contain potentially toxic concentrations of PAs.[7] Despite published claims of therapeutic benefits from PA containing plants, ingestion of these plants should be avoided. Methods of detection in foodstuffs and other consumed products is an ongoing area of research. Most of the detection methods employed use mass spectrometry or dual mass spectrometry technology, usually following high performance liquid chromatography separation.[58] Other groups have proposed that quantitative nuclear magnetic resonance may improve sensitivity in detection methods.[59] A recent approach using electrochemical methods for detection of pyrrolizidine alkaloids also shows

promise.[60] These methods enable the continual discovery of previously unknown pyrrolizidine alkaloid compounds.[58]

Examples of Dehydropyrrolizidine Alkaloid Poisoning in Humans and Animals

Dehydropyrrolizidine Alkaloid Poisoning in Humans

Poisoning by ingestion of PAs in humans occurs sporadically and is often difficult to directly attribute to PA exposure. Large scale exposures affecting multiple people is most likely to be the result of inadvertent contamination of crops by PA containing plants. Such occurrences may involve mixing of seeds from PA containing plants with cereal grains during harvest. These events are uncommon, and most frequently occur in developing countries during times of drought or famine.[61] It is thought that the most common cause of human exposure to PAs currently is ingestion of herbal teas, though honey and milk may also contain PAs.[14] Acute toxicosis in people is clinically characterized by severe abdominal pain, emesis, and diarrhea. Gross lesions in acute poisoning include hepatomegaly and ascites. Microscopic lesions during acute PA intoxication include hepatocellular necrosis with congestion.[55,62–64] Subacute poisoning also leads to hepatomegaly and ascites, additionally there is endothelial hyperplasia in sinusoids and medial arterial hypertrophy. These changes may occlude blood vessels and result in hepatic sinusoidal obstruction syndrome (HSOS) which is characteristic in people poisoned with PAs.[62] Chronic toxicosis is characterized by hepatomegaly, splenomegaly, ascites, hepatic veno-occlusion, fibrosis, cirrhosis, portal hypertension, lymphadenopathy, anemia, hemosiderosis, widespread hemorrhage, nephritis, and thymic cortical necrosis.[55] Exposure to small amounts of pyrrolizidine alkaloids may lead to lung

lesions without liver lesions.[55] "Bread poisoning" was first documented in the 1920 in Africa, and was caused by grain contamination with *Senecio ilicifolius* or *S. burchellii*, which was processed into flour and made into bread.[65] In the 1950's it was established in the USSR that *Heliotropium lasiocarpium* contamination of grain was the cause of several endemic liver diseases.[66] Another outbreak of PA poisoning occurred in 1975 in India, due to contamination of grain with *Crotalaria nana* seeds. This outbreak affected at least 67 people and killed 28 of them.[67] From 1974 to 1976 in Afghanistan numerous people developed severe ascites and emaciation following a period of severe drought conditions. These individuals were diagnosed with hepatic veno-occlusive disease, and it was determined that the cause was grain contamination with *Heliotropium spp*. This particular outbreak affected at least 7,800 people, with approximately 1,600 deaths. When the contaminating plants were examined and tested, it was determined that heliotrine was the main PA, with several others in smaller concentrations.[11,12] Smaller such outbreaks attributed to ingestion of PA contaminated flour occurred in Afghanistan in 1999 and 2008.[11] Between 1931 and 1945 approximately 1,500 cases of hepatic veno-occlusive disease were reported in Uzbekistan and attributed to *Heliotropium spp*. poisoning.[11] In 1992, a blockade led to a two month delay in harvesting a wheat crop in Tadjikistan, allowing *Heliotropium lasiocarpium* to grow among the wheat. The blockade also resulted in a food -shortage, so the grain was needed. The contaminated wheat was distributed to the population and made into bread. By March of 1993, 3,906 cases were reported with a fatality rate of 1.3%.[8,68] *Heliotropium* sp. poisoning is endemic in central Asia due to contamination of the wheat crop. These large-scale outbreaks of poisoning occur infrequently, and typically result in an investigation and ultimately a diagnosis. It is

currently understood that herbal teas are the most common source of PA ingestion in people. This type of exposure which affects individuals sporadically is less likely to spark an investigation and diagnosis, and even less likely to be reported in the literature. Epidemiologic data regarding regional prevalence of PA exposure is not available, but studies in which food sources are analyzed indicate that human exposure occurs frequently. In 1985, a thirteen-year-old boy who regularly drank comfrey tea was admitted to a hospital with hepatomegaly and ascites. The boy had been previously diagnosed with Crohn's disease three years earlier, for which physicians had prescribed corticosteroids and sulphasalazine. Despite an improvement on these medications, the boy's parents promptly discontinued these medications and visited a naturopath who then prescribed comfrey tea. Eventually the boy was diagnosed with hepatic veno-occlusive disease (VOD).[69] An 18-month-old boy who had been given an herbal tea which supposedly contained peppermint and colsfoot starting at 3-months of age was diagnosed with hepatic VOD. The tea was analyzed and contained seneciphylline. It was estimated that the boy was exposed to 60 mcg/day. In this case, the VOD was reversible and the boy recovered after the tea was discontinued.[70] In the southwestern United States Gordolobo yerba is a popular herbal tea made from *Gnaphalium macounii* which can be mistaken for the PA containing plant *Senecio longilobus*. Such cases of mistaken identification have resulted in fatal exposure in an infant and cirrhosis in a six-month old child who were fed this tea.[55,71] In another case, a pregnant woman drank comfrey tea daily throughout her pregnancy. The estimated PA exposure was 7 mcg/day. The woman had no signs of PA toxicosis, but her fetus was born with hepatic VOD and died at two-days of age.[72] A nearly identical case was reported in the 1980s, in which the pregnant

woman reported regular consumption of Coltsfoot tea as a cough remedy, The tea was found to be contaminated by *Tussilago farfara* and *Petasites officinalis*, which contain the PAs senecionine and senkirkine. In this case, the woman's infant died of hepatic VOD 38 days after birth.[55,73] These cases highlight two important concepts regarding PA toxicosis, first that PAs can cross the placenta and intoxicate a fetus, and second that young people and fetuses are more susceptible to PA toxicosis than adults. A 47-year-old woman was instructed by a homeopathic doctor to use comfrey tea as a remedy for complaints of fatigue, abdominal pain and allergies. She reported drinking up to ten cups of comfrey tea per day and taking comfrey tablets "by the handful". Four years later she presented with severe ascites and was eventually diagnosed with hepatic VOD.[9] As recently as 2013 multiple infant mortalities due to hepatic sinusoidal obstruction were reported when a *Senecio* sp. was mistaken for a medicinal plant that is administered as an enema to infants.[74] Human exposure to PAs continues to be a significant problem, and diagnosis of the cause is a challenge without the benefit of volunteered history of exposure. Ma et al. (2021) recently demonstrated that detection of pyrrole-hemoglobin adducts in blood may be a suitable biomarker to detect pyrrolizidine alkaloid exposure in people, presenting a potential solution to a challenge in diagnosing PA induced liver damage.[75]

Dehydropyrrolizidine Alkaloid Poisoning in Animals

PA exposure in animals is considered a common occurrence both for agricultural animals and wildlife. PA toxicosis is a particular concern in livestock that produce food for human consumption. It has been proven that PAs can contaminate milk if fed to dairy animals. Eggs similarly can be contaminated with PAs if the laying hens are fed PA-

containing plants.[6,44] Honey can also be contaminated with PAs if bees are placed in areas where PA containing plants are present.[66] Pyrrolizidine alkaloid poisoning was first recognized in grazing animals. As early as 1787, *Senecio jacobea* was identified as the cause of poisoning in grazing animals. In 1884 during the westward expansion of the United States, "Missouri river bottom disease" was recognized as being caused by ingestion of prairie ragwort (*Senecio plattensis*) or arrowhead rattlebox (*Crotalaria sagittalis*). This disease has been estimated to have killed nearly 1,800 horses in Western Iowa and eastern Nebraska in 1892.[61] Additional diseases in animals attribute to PA exposure include "Pictou disease" of cattle in Canada, "Winton disease" of cattle and horses in New Zealand, "Schweinsberger disease" of horses in Germany, Molteno cattle sickness in South Africa, and various hepatic diseases with cirrhosis in range animals worldwide. Clinical signs in animals include neurologic signs, diarrhea, ascites and hematologic effects.[4,55]

Recently *Senecio madagascarensis*, otherwise known as fireweed, began causing serious problems as an invasive species on the Hawaiian Islands. It is thought that this plant was introduced to Hawaii via Australia in the 1980's. Fireweed had been found to contain a variety of PAs including senecivernine, senecionine, integerrimine, senkirkine, mucronatinine, retrorsine, usaramine, otosenine, acetylsenkirkine, desacetyldoronine, florosenine and doronine.[61,76,77] Because PAs are found nearly ubiquitously in the environment, wildlife exposure can be assumed as a somewhat frequent occurrence, however little if any epidemiologic data to support this claim is available. Recently in a yet to be published experiment which is a collaboration between the United States Department of Agriculture, Poisonous Plant Research Laboratory (Logan, Utah) and

researchers from the Colorado State University (Fort Collins, Colorado) a variety of hunter collected gamebirds in Hawaii were submitted and tested for the presence of hepatic pyrrole concentrations by HPLC MS/MS. Hepatic pyrrole concentrations were detected in 8 of 22 wild turkeys, 41 of 51 California quail, 4 of 4 black francolins, 47 of 78 Erckel's francolins, 16 of 50 red-necked phalaropes, and one chukar. This means that among the birds submitted, 56.8% had proven exposure to PA containing plants. Gross observations detected the presence of plant material suspected to be fireweed in the ventriculus of some of the birds. Histopathologic evaluation of the livers detected the presence of bile duct hyperplasia in some of the birds with pyrrole concentrations; however, the lesion was present in some birds that had no detectable pyrrole concentrations. Other birds with significant hepatic pyrrole concentrations did not appear to have hepatic disease as their livers were microscopically normal. In wild quail, hepatic necrosis was infrequent and did not clearly correlate with hepatic pyrrole concentrations. Some birds had bile duct hyperplasia which is often considered compatible with PA exposure, but this lesion similarly did no correlated with hepatic pyrrole concentrations. It is possible that the bile duct hyperplasia in these birds was not due to PA exposure, or that the hepatic pyrroles had been metabolized and excreted until concentrations were below detection. Though chicks are very sensitive to PA poisoning, older birds or other species may have different susceptibilities.[62,78] These results suggest that these birds can tolerate these PA exposures with little or no detrimental effects. Regardless of the direct effects on the gamebirds, as PAs were identified in avian muscle, secondary poisoning is a concern. Though meat is typically considered a low-risk product for PA exposure, any exposure to genotoxic carcinogens is troubling. Some health agencies have established

acceptable exposure limits for PA exposures. Recent identification of PA adducts in humans suggests that even minute doses may be detrimental [44,79] Egg contamination is also troubling. Mulder et al. (2016) clearly demonstrated that PAs are consistently transferred to eggs when PA containing plants are fed to laying hens. They also reported relatively small PA concentrations in skeletal muscle.[44]

PA poisoning has been reported in many domestic and wildlife species including cattle, sheep, goats, horses, pigs, a gazelle, deer, chickens, turkeys, and more.[80–86] Sheep grazed on pastures with *Heliotropium europaeum* developed megalocytosis and hepatocellular loss and fibrosis.[87] Calves dosed with *Cynoglossum officinale* at doses of 60 mg/kg of total alkaloid mixture developed massive hepatic necrosis. At the lower dose of 15 mg/kg chronic lesions including megalocytosis with karyomegaly, periportal fibrosis and bile duct proliferation were observed.[88] Natural exposure to *Cynoglossum officinale* contaminated hey caused similar microscopic lesions.[89] Chronic low-dose exposure to *Senecio erraticus* in calves resulted in the same lesions.[90] *Senecio grisebachii* containing 0.29% PAs on a dry weight basis orally dosed to calves resulted in elevations of gamma glutamyltransferase (GGT), aspartate aminotransferase (AST) and alkaline phosphatase (ALP). These calves which all weighed between 85-89 kg., were dosed at 15, 24 and 45 g of dried plant. The PA in this plant was a mixture of seneciphylline, senecionine and retrorsine. Microscopic lesions included hepatocellular necrosis, hepatocyte loss and fibrosis and bile duct proliferation.[91] *Senecio riddellii* was fed to calves for 20 days resulting in weight loss, depression, reduced feed intake, hind limb ataxia, ascites, edema and eventually death. Microscopic findings in this study included hepatocellular necrosis and collapse of lobules, fibrosis, portal edema, hepatocyte

anisokaryosis and cytomegaly, and bile duct proliferation.[1] Experimental chronic poisoning with *Senecio jacobea* in pigs resulted in karyomegaly and megalocytosis in hepatocytes and renal tubular epithelial cells.[92]

Differences In Susceptibility:

Factors that influence susceptibility to the toxic effects of PAs include species, strain (e.g. mouse models), sex, nutritional status, and age.[55] There is considerable variation in susceptibility to PA poisoning between species. The most sensitive agricultural species include pigs and poultry, followed by horses and cattle, with sheep and goats being resistant to poisoning.[93] When comparing the regularly used laboratory rodents, rats are more sensitive than mice. Sheep, guinea pigs, gerbils, rabbits, hamsters and Japanese quail are said to be resistant to PA poisoning, while rats, cattle, horses and chickens are susceptible.[94,95]

Differences in susceptibility between sexes have also been described. Males are generally considered more sensitive to PA poisoning than females. On the other hand, Luo et al. (2019) exposed pregnant rats to monocrotaline and demonstrated that female fetuses were more susceptible to hepatotoxicity and developmental toxicity. They also determined that the difference between males and females was due to greater CYP450 metabolism in the females, as females had greater expression levels of CYP3A than males.[96] It has also been shown that there are sex differences in glutathione conjugation. Liang et al. (2011) demonstrated that male mice had lower concentrations of glutamate-cysteine ligase and glutathione peroxidase, which are involved in glutathione conjugation in males when compared to females. They subsequently correlated this difference with

enhanced hepatic injury from single dose exposure to the PA isoline.[97] These examples demonstrate that resistance and susceptibility depend on multiple factors, mostly relating to phase I or II metabolism.

Nutritional status also affects susceptibility to PA toxicosis. PA exposure can result in copper poisoning in areas where the forage contains normal copper concentrations.[98] Dosing of retrorsine to nursing Wistar rats resulted in increased hepatic copper accumulation in suckling pups, demonstrating that PAs accumulate in milk, and that they affect hepatic copper storage.[99] Zinc supplementation has been proven to have a protective effect against PA intoxication. PA consumption has also been shown to affect hepatic iron concentrations.[98] In rats dosed with *Senecio jacobea* and *Senecio vulgaris* a protective effect was observed when dietary cysteine was added to the ration. The addition of dietary methionine had no effect.[100] In rats, copper and iron concentrations in the liver were increased following exposure to *Senecio* spp.[101] Lower concentrations of dietary protein have been shown to increase severity of PA toxicosis. PA exposure also results in a reduction of plasma and liver concentrations of vitamins A and E.[98]

Dehydropyrrolizidine Alkaloid Chemistry:

The chemical structure of PAs consists of a necine base, common to all PAs, and one or two side chains attached at the carbon 7 and/or 9 positions (See figure 1.1). The necine base of PAs are classified into one of four categories, retronecine, heliotridine, otonecine, or platynecine, depending on saturation and steric conformation. PAs are typically referred to by their common or trivial names, as their proper chemical names are cumbersome. These common names are typically derived from the species or genus

names of the plant source of the PA. For example, the chemical 15-ethylidine-12β-hydroxy-12α,13β-dimethylsenec-1-enine is commonly referred to as senecionine, named after the *Senecio* species in which it was discovered. [102] Toxic PAs have a double bond between carbons 1 and 2 and fall into either the retronecine or heliotridine categories (see figure 1.2). Depending on the side chains attached to the carbons 7 and 9 of the ring structure, PAs can be classified as monoesters, diesters, or macrocyclic diesters.[15] Monoester PAs have a single monocarboxylic acids side chain (e.g. heliotrine, figure 1.3), while diesters have dicarboxylic acids attached at carbon 1 and 7 (e.g. lasiocarpine, figure 3) and macrocyclic diesters have an additional ring structure formed by two ester bonds and extending from the carbon 1 and 7 positions (e.g. senecionine, figure 1.3).[1,15,55,102] While in the plant, PAs exist mainly as N-oxides.[82] PA N-oxides have an oxygen atom bound to the nitrogen, see figure 1 (b). PA N-oxides are typically considered less toxic than the parent PA, and N-oxidation is considered a detoxification reaction in PA metabolism. PA N-oxides are more water soluble and are thought to be more easily excreted than the parent PA which is more lipid soluble.[61] In terms of toxic potential, all PAs are not equal. Multiple studies have demonstrated that differences in toxicity between PAs with different chemical structures. In addition to chemical characteristics of the necine base such as the critical double bond between carbons 1 and 2, there are marked differences in the toxic potential between PAs of the same base structure but varying necic acid side chains.[21,23,24,103]

(a) dehydropyrrolizidine alkaloid

(b) dehydropyrrolizidine alkaloid N-oxide

Figure 1.1: General chemical structure of a toxic PA and PA N-oxide. The necine base is composed of two five membered rings with a nitrogen at the center, and variable carboxylic acid side chains (R1 and R2). Variation in both the base and the necic acids provide the diversity within this group of toxins. Though many pyrrolizidine alkaloids are not toxic, those that have a double bond between carbons 1 and 2 as shown in this image (dehydropyrrolizidine alkaloids) are toxic and have been associated with poisoning.

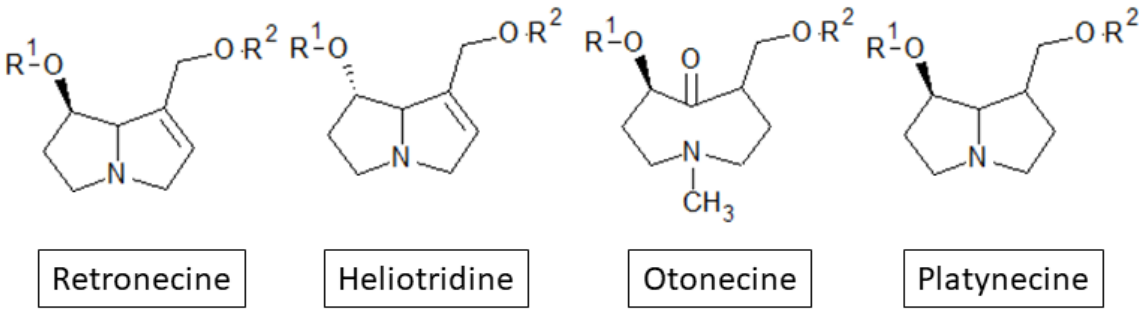

Figure 1.2: Chemical structures of necine bases of PAs. PAs with documented toxicity belong to the retronecine and heliotridine groups, which are stereoisomers. Platynecine PAs are non-toxic, likely due to the saturated ring structure. R1 and R2 represent the variable carboxylic acid side chains attached to carbons 7 and 9, which provide the immense variation found in this class of chemical compounds.

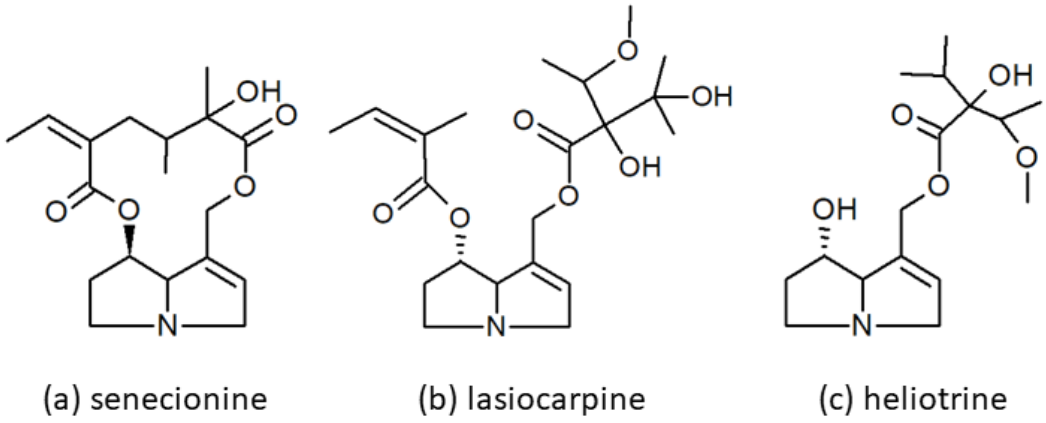

Figure 1.3: Examples of PA chemical structures. Image a, senecionine, is a macrocyclic diester retronecine-type PA, in which two ester bonds are attached to carbons 7 and 9 forming an additional ring structure. Macrocyclic diester PAs are the most toxic for some species. Image b, lasiocarpine, is a diester heliotridine-type PA with two separate side chains. Image c, heliotrine, is a monoester heliotridine type-PA.

Dehydropyrrolizidine Alkaloid Toxicity:

PAs are hepatotoxic, pneumotoxic, genotoxic and under some conditions they are carcinogenic. [1,19,104] A great deal of research has been performed to characterize the mechanism of toxicity and the metabolic fate of PAs.

Absorption:

Natural PA exposure occurs via ingestion. Once in the gastrointestinal tract, PAs are mainly absorbed by simple diffusion.[105] There may also be active transport, as evidenced by a recent study which found that monocrotaline was determined to be a substrate for

organic cation transporter 1.[106] Approximately 80% of ingested PAs are rapidly excreted unchanged in urine and feces, with urinary excretion being the main route. Pulmonary excretion occurs as a minor route. Most of the PAs are present in the liver and kidneys, with small amounts in the lungs and spleen.[55] There are alkaloid dependent (most likely structurally differences) between individual PAs in absorption.[105] Toxicokinetic characterization has been described for a small number of PAs including riddelliine, senecionine, adonifoline, monocrotaline, and few others. PAs are potent antimitotic compounds. This has been demonstrated both in vitro and in vivo.[107–109] Because of these antimitotic effects, some PAs have been investigated as antitumor agents including indicine N-oxide. These investigations included evaluation of pharmacokinetics of these agents. The distribution half-life, elimination half-life, and plasma clearance of indicine N-oxide were 8 min, 84 min and 62 ml/min/m^2, respectively. One patient with renal disease had a prolonged elimination half-life.[110] Indicine N-oxide had a biphasic elimination curve indicating a two-compartment model. Toxic effects of indicine N-oxide in these human cancer patients included leukopenia, thrombocytopenia, myelosuppression, nausea and vomiting. No therapeutic benefit was observed.[111] An additional study compared the pharmacology of senecionine and adonifoline and their metabolites. In this study there were differences in the pharmacokinetics following IV administration compared to oral dosing. The elimination half-lives of senecionine and adonifoline were 306.3 minutes and 237.6 minutes respectively.[112] Because there is a paucity of evidence for therapeutic benefits from PA exposure, pharmacokinetic data has limited utility, hence the scarcity of such data. Riddelliine is another of the few PAs for which toxicokinetic studies have been completed. Toxicokinetics were performed using a

dose of 10 mg/kg in rats and 25 mg/kg in mice and compared riddelliine to riddelliine N-oxide and retronecine. This study found that riddelliine N-oxide had a longer elimination half-life in serum than riddelliine did in both male and female rats and mice.[113] These studies found differences in the absorption and excretion characteristics of individual PAs.[110–113] Given these differences, it is not advisable to extrapolate toxicokinetic information from one PA to another. Toxicokinetic properties should be considered structurally specific for each individual PA. PAs have been proven to generally be genotoxic carcinogens, and as such there is no safe amount of exposure that should be considered acceptable. PAs, like all genotoxic carcinogens should be avoided whenever possible. Tu et al. (2014) showed that retrorsine is a high affinity substrate the organic cation transported molecule, which is evidence of a potential receptor mediated mode of cell entry for PAs.[114] However, PAs vary in their solubility and passive diffusion is still considered the main method of absorption.

Metabolism:

PAs require metabolic activation to exert their toxic effects.[1,15,115] PAs are metabolized by common pathways to form pyrrolic derivatives. Formation of pyrrolic esters is the primary mechanism by which the cytotoxic, genotoxic, and carcinogenic effects occur.[115] There are four metabolic pathways by which PAs are metabolized after absorption. These include hydrolysis of ester bonds, N-oxidation of the necine base, N-glucuronidation, and two-step oxidation of the necine base at C3 or C8, followed by spontaneous dehydration to a dehydropyrrolizidine.[62,115,116] The pyrrolic ester metabolites are reactive and can readily interact with endogenous components including water and glutathione to form detoxified products.[115] Hydrolysis, glucuronidation and N-oxidation are considered

detoxification mechanisms whereas dehydrogenation results in the toxic effects. Hydrolysis results in the breakdown of the PA into its necine base, a mono- or dicarboxylic acid and the specific necic acid. The necine base can then be further oxidized to an N-oxide or dehydrogenated to a reactive pyrrole.[55] The phase 1 metabolism reaction that produces the toxic pyrrole is mediated by the CYP450 enzymes. The greatest concentrations of CYP450 enzymes are found in the liver, hence liver is the major target organ. CYP450 enzymes are responsible for C oxidation and N oxidation of the necine base to form pyrrolic esters and PA N oxides. In people, it is mainly the CYP3A and CYP2B isoforms that are responsible for bioactivation of PAs.[62,116] In vitro work has found that a greater number of CYP450 enzymes were capable of bioactivating the retronecine type PAs, when compared to the otonecine type. They incubated human liver microsomes with a variety of CYP450 enzymes and found the seven retronecine PAs tested were bioactivated by CYP3A4, CYP3A5, CYP2A6, CYP1A1, CYP1A2, CYP2B6, CYP2C9, CYP2C19, CYP2D6, and CYP2E1, while the two otonecine type PAs were only bioactivated by CYP3A4, CYP3A5.[117] Phenobarbital induces both CYP2B and CYP3A enzymes, and administration of phenobarbital to rats prior to dosing resulted in enhanced metabolism and toxicity of riddelliine. The main metabolites of riddelliine by liver microsomes in F344 female rats were riddelliine N-oxide and dehydroretronecine. Phenobarbital-treated rats produced 3.5 times more metabolites compared to untreated rats, because phenobarbital induces CYP2A1, CYP2A2, CYP2B, and CYP3A.[118] Administration of phenobarbital prior to dosing with monocrotaline similarly resulted in enhanced toxic effects including poor weight gain and more severe lung lesions.[119] Didehydroretronecine was identified as the toxic metabolite that results

from metabolism of monocrotaline as with other PAs having a retronecine base structure.[120] It has similarly been proven that treatment with inhibitors of CYP3A enzymes resulted in reduced metabolism of riddelliine, clivorine and lasiocarpine in rats.[115] Species differences in PA metabolism are significant, Huan et al. (1998) provided an illustrative example by demonstrating that CYP3A converted senecionine to senecionine N-oxide in sheep while converting senecionine to its pyrrolic toxic metabolite in guinea pigs.[121] Flavin-containing monooxygenases also participate in N-oxidation reactions of PAs. Conversion of senecionine to its N-oxide is mainly catalyzed by flavin containing monooxygenases in pig liver, lung and kidney.[81,122] PA N-oxides are more water soluble than their parent compounds and are purportedly less toxic, however they can be reduced back to their parent compounds by bacterial floral enzymes.[55] Hydrolysis can occur as a result of catalysis from microsomal and cytosolic carboxylesterases.[115] Microsomal mixed function oxidases can also mediate hydrolysis, as well as reduction reactions. Hydrolysis may be a detoxifying reaction, as the products of this reaction are more water soluble and can be more easily excreted.[66] Phase II metabolism is mainly achieved by glutathione conjugation, which is the predominant detoxification reaction after the PA is bioactivated into a electrophilic pyrrole. Glutathione conjugation results in binding with one or two glutathione molecules forming wither 7-glutathionyl-6,7-dihydro-1-hydroxymethyl-5H-pyrrolizine (7-GSH-DHP) or 7,9-diglutathionyl-6,7-dihydro-1-hydroxymethyl-5H-pyrrolizine (7, 9-diGSH-DHP). Cytosolic and microsomal glutathione S-transferases enzymatically catalyze glutathione conjugation[115]. Glutathione s-transferases are dimeric enzymes that catalyze conjugation of glutathione to a variety of electrophiles, including PAs.[123] It has recently been

discovered that glucuronidation also participates in phase II metabolism of PAs.[20,116] In this work, they demonstrated that rabbits, cattle, sheep, pigs and humans had greater glucuronidation of PAs than mice, rats, dogs and guinea pigs. Differences in metabolism is considered one of the main reasons that species differ in susceptibility to the toxic effects of these compounds. Metabolism is a critical aspect of PA toxicity, as PAs are protoxins and essentially non-toxic until they are bioactivated. The main purpose of the research described herein is to characterize differences in toxic potential between individual PAs. These differences are also likely due to differences in metabolism. One of the potential theories to explain differences in toxic potential is the production of unique toxic metabolites following bioactivation. As an example, senecionine bioactivation results in the formation of a compound called trans-4-hydroxy-2-hexenal. This additional metabolite has also been shown to induce hepatic necrosis. Trans-4-hydroxy-2-hexenal is also capable of forming DNA adducts by binding to deoxyguanosine.[24,37,124] Bioactivated pyrroles are reactive electrophiles, and can bind to cellular proteins or nucleic acids, resulting in cellular injury and DNA damage. Figure 4 below is a flow-chart showing the various pathways by which PAs are metabolized following absorption.

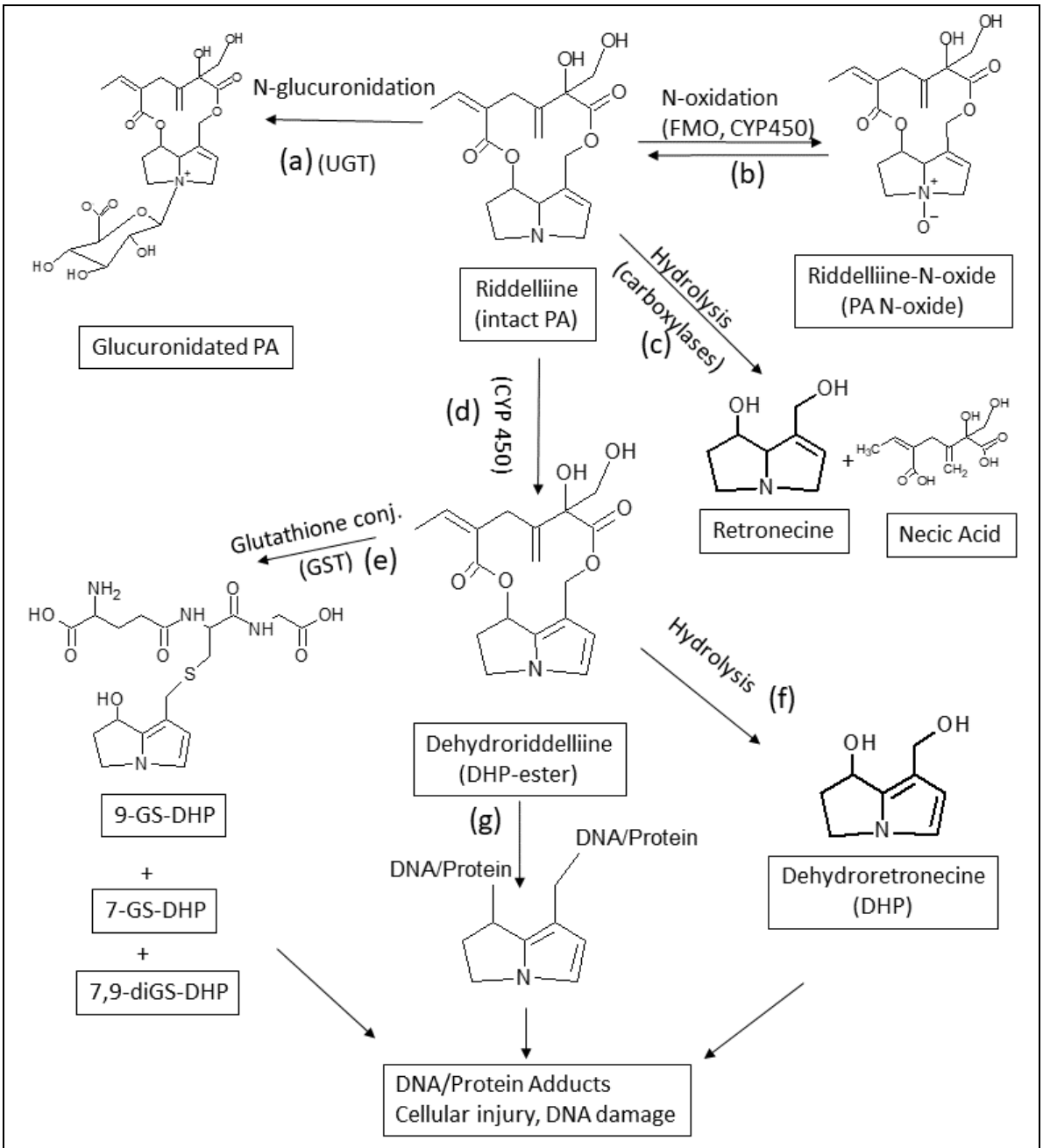

Figure 1.4: PA metabolism flow chart. The intact PA can follow 4 metabolic routes; (a) glucuronidation, catalyzed by UDP glucuronosyltransferase (UGT); (b) N-oxidation, catalyzed either by cytochrome p450 (CYP450) or flavin-containing monooxygenases (FMO) resulting in production of PA N-oxide, (c) Hydrolysis, may be catalyzed by carboxylesterases, into the necine base and necic acid(s), or (d) Bioactivation (phase I metabolism) by members of the CYP450 family of enzymes, resulting in production of a reactive pyrrolic ester (DHP-ester). The reactive pyrrole can then follow three different

metabolic pathways; (e) glutathione conjugation, mediated by glutathione s-transferase, (f) hydrolysis, separating, or (g) binding with cellular macromolecules resulting in cellular injury and production of DNA and protein adducts. Glutathione bound pyrroles and hydrolyzed pyrroles may also result in DNA/protein adducts and cellular injury or DNA damage.

Mechanism of Toxicity:

Bioactivation, or phase I metabolism of PAs is the first step in the toxic mechanism as described above in the section on metabolism and illustrated in figure 4. The general mechanism of toxicity is the formation of pyrrole adducts with nucleic acids and cellular proteins.[125] PAs are ingested and absorbed by simple diffusion in the gastrointestinal tract. Following absorption, PAs are metabolized by cytochrome P450 enzymes in an oxidation reaction to didehydropyrrolizidine alkaloids, also called "pyrroles". Pyrroles are electrophilic and can form covalent bonds with proteins and nucleic acids. The product of these covalent bonds are pyrrole-DNA adducts or pyrrole-protein adducts.[62,104,125] PAs interact with these cellular components via two electrophilic positions at carbons C7 and C9. Metabolic activation of PAs reduces glutathione (GSH) concentrations in some cells, diminishing the cells' ability to respond to oxidative injury and contributing to cellular injury. Pretreatment with GSH or GSH stimulators such as N-acetylcysteine have been shown to reduce the toxic effects of PAs.[125] Little information is known regarding specific protein targets PA toxic metabolites bind to or interact with following bioactivation.[125] Toxic PA metabolites are thought to bind to cellular macromolecules mainly at the site of bioactivation, hence the metabolites are thought to be volatile binding to structures nearby.[15] Studies of monocrotaline have shown that

pyrroles form adducts with galectin-1, protein-disulfide isomerase, probable protein-disulfide isomerase (ER60), b- or g-cytoplasmic actin, and cytoskeletal tropomyosin in pulmonary endothelial cells.[126] It is not known whether these same proteins are affected by other PAs or in other cell lines. Monocrotaline seems to be somewhat unique in its ability to cause pulmonary injury, therefore studies of other specific PAs are needed to determine whether specific proteins are targeted.[17] Another study demonstrated that monocrotaline could interact with F-actin resulting in increased matrix metalloproteinase activity in hepatic sinusoidal endothelial cells. They first determined that F-actin depolymerization leads to increased MMP activity, and then that inhibition of matrix metalloproteinases prevented the development of sinusoidal obstruction syndrome in rats following monocrotaline exposure.[127] The formation of pyrrole-protein adducts may cause direct cytotoxicity.[128] In addition to the formation of DNA and protein adducts, glutathione adducts form after binding to pyrrolic esters. Glutathione is a detoxifying reaction in PA metabolism, but there is also evidence that these glutathione bound pyrroles may also result in cellular injury and DNA damage.[129] It is also theorized that recycling of reactive pyrroles can result in additional damage, when bound pyrroles are hydrolyzed or otherwise freed from their substrate, and then again bind to additional cellular macromolecules.[4] Other pyrrole conjugates which form after bioactivation can be reactive and cause DNA damage and cellular injury. He et al. (2016) found that riddelliine and monocrotaline metabolism produces 7-*N*-acetylcysteine-pyrrole conjugate, which is a potent reactive metabolite and can bind to DNA and other cellular macromolecules.[130] It is possible that other retronecine PAs also produce this metabolite,

and that other PAs produce additional undiscovered or uncharacterized metabolites that result in differences in their toxic potential.

Hepatotoxicity:

PAs are biologically inactive prior to bioactivation by CYP450 enzymes. The CYP450 enzymes are mainly expressed in the liver although other organs, including the lung and kidney express smaller concentrations.[131] The toxic metabolites produced following bioactivation of PAs mainly cause damage at the site of bioactivation as a result of DNA or protein adduct formation. In other words, the toxic pyrrole does not travel far after it is produced. This bioactivation relationship explains why the liver is the main target organ of PA toxicosis. Pulmonary disease is also reported, but the majority of experimentally produced pulmonary lesions are caused by exposure to monocrotaline, and monocrotaline may be unique in this ability.[17,119,126] Monocrotaline has been used to develop an experimental animal model of pulmonary hypertension in rats, which has also been applied to non-human primates.[16,119] For most PAs, greater doses are required to induce pulmonary lesions when compared to the hepatotoxic doses.[103] Monocrotaline administration in rats seems to be the exception to this, where lower doses can cause pulmonary lesions, and greater doses of monocrotaline are needed to induce hepatotoxicity.[16,17] The bioactivation reaction that results in cellular injury takes place mainly in hepatocytes and endothelial cells.[22] The result of acute PA toxicosis is hepatocyte swelling, hypertrophy and degeneration, followed by hepatocellular necrosis depending on dose. Affected hepatocytes are enlarged with hypereosinophilic cytoplasm, or groups of contiguous hepatocytes are replaced by cellular debris (necrosis), depending on dose. The lesion typically affects a specific area of the hepatic lobule, either the

centrilobular or periportal areas.[22,29] The reported distribution of this lesion varies depending on the source. Some sources report the lesion as affecting mainly centrilobular areas, while others describe degeneration and necrosis affecting mainly periportal areas. High doses can result in massive necrosis.[84,92,132–134] It is thought that the site of cellular injury corresponds with the site of bioactivation; therefore, the lesion distribution should correspond to the distribution of the CYP450 enzymes responsible for bioactivation. The concentration of CYP450 enzymes are said to be greatest in the centrilobular regions, up to 1.3 times the concentrations found in the midzonal and periportal areas.[135,136] It is worth noting that these reports are based on specific compounds i.e. acetaminophen and phenobarbital, and may vary between CYPs and species. When considering the large number of CYP450 enzymes and the fact that CYP450 enzyme specificity for PAs differs between species, these generalizations may be oversimplified. PA research highlighting differences between individual PA regarding toxic potential in the same species or the same cell line indicates that PA specificity for CYP450 enzymes should be characterized for individual PAs, and individual species. Chronic PA exposure leads to the development of a variety of lesions which are not observed in acute exposure. Among the more characteristic lesions associated with PA exposure is hepatomegalocytosis (also referred to as megalocytosis). Megalocytosis is characterized by marked enlargement of hepatocytes are their nuclei, 2.5 times larger than normal hepatocytes. [137,138] The ultrastructural characteristics of megalocytic hepatocytes include both nuclear and cytoplasmic abnormalities. Megalohepatocytes were round, oval or polygonal. Megalohepatocytes often have polyploid nuclei.[139] Microvilli were often dilated, and a microvillous border was not visible around the space of Disse. The space of Disse was

inapparent adjacent to the megalohepatocyte. Nuclear characteristics include enlarged, misshapen nuclei with numerous cytoplasmic-nuclear invaginations which were sometimes large and contained cytoplasm and numerous organelles. Rarely, cytoplasmic invaginations were separated and formed intranuclear inclusions composed of membrane-bound organelles. Nucleoli contained irregular fibrillary components which were separated into small packets. Cytoplasmic abnormalities include increased numbers of organelles, modifications to and reduction in the rough endoplasmic reticulum, reduced numbers of ribosomes, increased amounts of smooth endoplasmic reticulum and enlarged Golgi apparatuses. Most mitochondria were small and irregular with electron dense granules within the matrices. Rough endoplasmic reticulum consisted of short strands in close proximity with adjacent mitochondria. Smooth and rough endoplasmic reticulum were continuous with smooth laminated membranous bodies. Multiple Golgi apparatuses were present.[137,138] Megalocytosis is often accompanied by additional chronic lesions such as bile duct proliferation and periportal fibrosis. Megalocytosis should not be mistaken for fused cells (syncytia) which can be seen in acute toxicosis.[1,2] Veno-occlusive disease is also reported as a chronic lesion attributed to PA exposure in certain species, including dogs, rats, and humans.[115,127,127] Veno-occlusive disease is sometimes used interchangeably with the term hepatic sinusoidal obstructive syndrome (HSOS). HSOS is characterized by congestion and necrosis affecting centrilobular areas. This lesion is said to progress to fibrosis and cirrhosis with chronic exposure.[127,134] The research described in this dissertation will use only short-term, high-dose exposure in mice. This exposure is like natural exposures when livestock are exposed to contaminated feed. Livestock are unlikely to experience chronic low dose PA exposures as feeds are

rarely uniformly contaminated or they are most often intermittently available. Alternatively, animals exposed in pastures and ranges are usually seasonally used and exposures are short or intermittent. Similarly, epidemic human exposures occur as the result of contaminated grain, flour and food. However, deliberate exposures such as occur when PA containing plants are used are medicinal or herbals are likely to have extended exposures.

Genotoxicity:

Genotoxicity is defined as the capability of an agent to cause chromosomal or DNA damage. Damage to DNA has the potential to result in mutation; therefore, all genotoxins are potentially mutagenic. Genotoxins can induce a variety of mutations, including point mutations, deletions, insertions, gene amplifications, and chromosomal aberrations.[140] Similar to the hepatotoxic effects of PAs, the genotoxic mechanism by which PAs induce DNA damage is mediated by metabolic activation as a first step.[62] Pyrrolizidine alkaloids have been shown to induce a variety of genotoxic injuries such as DNA adduct formation, DNA-binding, DNA cross linking, DNA strand breakage, unscheduled DNA synthesis, DNA-protein cross linking, sister chromatid exchange, and chromosomal damage.[104,115] The mechanism by which PAs are thought to cause DNA adducts is metabolism of the parent PA to a dehydro-PA or dehydroretronecine such as dehydroretronecine, the dehydro-PA and/or dehydroretronecine can then bind to DNA forming specific DNA adducts.[141] A variety of methods have been used to characterize the genotoxic potential of PAs. The 32P-postlabeling assay is a sensitive test for the detection and quantitation of DNA adducts.[142] Yang et al. (2001) developed a 32P-post-labeling assay specifically for PA induced DNA damage.[143] This assay had the added

benefit of characterizing the specific types of DNA adducts that form following PA induced cytotoxicity and DNA damage. They used ^{32}P-postlabeling with high performance liquid chromatography to determine that riddelliine induces formation of eight PA derived DNA adducts. Two of the adducts were epimers of DHP-2'-deoxyguanosine 3'-monophosphate and the other six could only be classified as DHP-modified-dinucleotides.[143,144] This same assay has been used since its development to identify DHP-DNA adducts both in vivo and in vitro since its development.[144–147] Hadi et al. (2021) demonstrated that europine, lycopsamine, retrorsine, riddelliine, seneciphylline, echimidine, and lasiocarpine exhibit genotoxicity in the HepG2 cell line using the micronucleus induction test.[148] Heliotrine has been shown to induce chromosomal damage and sex-linked recessive mutations in Drosophila.[149] Integerrimine, obtained from the plant *Senecio brasiliensis*, when fed to *Drosophila melanogaster* resulted in the induction of mitotic recombination events.[150] Seneciphylline and senkirkine similarly induced sex-linked recessive lethal mutations when administered as pure alkaloids and after ingestion of milk from rats treated with these alkaloids.[41] Mutations in salmonella, sister chromatid exchanges, S-phase and unscheduled DNA synthesis have also been documented. In vitro exposure to heliotrine, monocrotaline, seneciphylline and senkirkine induced the formation of sister chromatid exchanges (SCEs) in V79 Chinese hamster cells. In this study, coculture with chicken hepatocytes resulted in greater SCE induction when compared with addition of rat liver homogenate, likely due a greater amount of enzymatic activation.[151] Additional methods have been used in multiple studies using both in vitro and in vivo experiments to verify the genotoxicity of various pyrrolizidine alkaloids.[104,109,152–154] Individual PAs vary in their

genotoxic potential. Macrocyclic diester PAs exhibit the greatest genotoxicity and hepatotoxicity, specifically those with either a retronecine for heliotridine base.[115] Rutz et al. (2020) tested several PAs by multiple genotoxicity and cytotoxicity assays and developed a model to rank the PAs according to genotoxic potential. They found that lasiocarpine was the most genotoxic, followed closely by retrorsine, riddelliine, senecionine, and seneciphylline. Heliotrine and echimidine were the next most genotoxic, and the least were indicine, lycopsamine and monocrotaline. Monocrotaline is notably the only macrocyclic diester PA in this study that was not among the most genotoxic, and lasiocarpine was the only open diester which showed substantial genotoxic potential. The PAs with the lowest genotoxic potential were all open diester or monoester PAs.[155] A similar study by Louisse et al. (2019) compared genotoxic potential of several PAs using the γH2AX assay and found that the group with the greatest genotoxic potential included 17 PAs, including 12 retronecine macrocyclic diesters, two heliotridine open diesters, and three retronecine open diesters. The group with middle-ranking genotoxicty included two otonecine macrocyclic diesters and three retronecine macrocyclic diesters. The PAs with the lowest genotoxicty by this assay included two heliotridine monoesters, one retronecine monoester and monocrotaline (a retronecine macrocyclic monoester). This study had a fourth group that demonstrated even lower genotoxic potential and included several necine bases and PA-N oxides.[156] These studies consistently find that macrocyclic diesters have the greatest genotoxic potential.

Carcinogenicity:

Chemical carcinogens cause neoplasia through a variety of different mechanisms, including direct DNA damage through the formation of DNA adducts, or by secondary

mechanisms including oxidative damage, altered DNA methylation, lipid peroxidation, or dysregulation of endocrine signaling pathways. Chemical carcinogens can be classified as genotoxic or non-genotoxic. Genotoxic carcinogens cause genetic damage, resulting in mutations which can then result in neoplasia. Non-genotoxic carcinogens induce neoplasia without direct genetic damage, with effects such as DNA methylation, hormonal effects, induction of cell proliferation and others.[157,158] As discussed in the previous section, PAs are genotoxic. PAs have been shown to be carcinogenic in mice and rats and can therefore be classified as genotoxic carcinogens. PAs induce neoplasia by induction of DNA adducts, DNA cross-linking, DNA-protein cross linking, DNA strand breakage, and unscheduled DNA synthesis.[104,159] Lipid peroxidation has been observed in vitro following exposure to the PA senecionine.[160] Other secondary, non-genotoxic affects have not been observed in PA induced carcinogenicity.[145] After bioactivation, PA toxic metabolites referred to as pyrroles, DHP, or dehydroPAs, are able to bind to DNA via two functional groups at carbons number 7 and 9. These groups can bind with DNA and/or protein, resulting in DNA crosslinking and /or DNA-protein crosslinking.[145] Both in vitro and in vivo studies have proven that PAs induce the formation of DNA and protein adducts. Candrian et al. (1985) treated rats with labeled senecionine and seneciphylline and demonstrated via HPLC and radioactivity analysis that alkaloids were covalently bound to DNA. In this study, alkaloids were present in lungs and kidneys, and livers of female rats.[152] Kim et al. (1995) demonstrated that the amount of DNA crosslinking had a direct correlation with the severity of toxicity, therefore the mechanism that results in hepatotoxicity is the same mechanism that leads to tumor formation.[161] The ^{32}P-postlabeling assay described in the genotoxicity section

was used to identify DNA adducts following exposure to riddelliine, and these adducts were quantified. They determined that the same eight adducts were present in the livers of mice after treatment with riddelliine for 3 and 6 months. Statistical analysis found that there was not a correlation between the concentrations of the DNA adducts and the prevalence of liver hemangiosarcomas or hepatocellular neoplasms. This suggests that additional mechanisms such as DNA repair are also involved in the development of these tumors.[162] In vitro, dehydroriddelliine (DHR) was capable of binding to DNA, 3N-dGMP, 5N-dGMP, and 3N-dAMP.[19,162] Dehydroretronecine-modified 7-deoxyguanosin-N2-yl epimers (DHR-3′-dGMP) have also been identified in rats following riddelliine exposure (Yang et al., 2001).[143] These studies have been performed using a variety of different PAs. Macrocyclic diester PAs seem to exhibit the greatest genotoxicity and tumorigenicity, in addition to hepatotoxicity.[115]

Carcinogenicity Studies in Rodents:

The vast majority of experimental studies in which neoplasia was induced by PA exposure have been performed in mice and rats. PA carcinogenicity has been demonstrated by feeding mice and rats whole plant, mixtures or isolated PAs. Hepatic hemangiosarcoma, hepatocellular carcinoma and hepatocellular adenoma have been reported in mice and rats following PA exposure.[21,55] There are many reasons that mice and rats are the preferred laboratory animal species, including size, care requirements, and the breadth of genetic knowledge available for transcriptomic studies. Regarding PA research, one of the main reasons these animals are preferred is their small size and relative short lifespan. The current state of PA research is such that researchers are mainly interested in the effects of individual PAs. Most PA containing plants contain

mixtures of PAs, and the process of isolating and purifying individual PAs is costly and time consuming. *Senecio riddellii* (Riddells ragwort) is a unique plant in that it typically contains primarily riddelliine, simplifying isolation of nearly pure (>93%) N-oxide and free base riddelliine. Additionally some collections have extremely high PA concentrations ranging from 10% to nearly 18% over 5 years.[163] As the other PA containing plants have much lower PA concentration and they contain mixtures of alkaloids, Extreme effort and large volumes of plant material are needed to produce small quantities of purified PAs. This process is time consuming and costly. A variety of neoplasms have been experimentally induced in rats. Hemangioendothelial sarcomas and hepatic adenomas have been experimentally in rats following exposure to clivorine, senkirkine, petasitenine, and seneciphylline.[164–168] Central nervous system tumors were detected after exposure to hydroxysenkirkine and retronecine.[169] Hepatic adenomas, carcinomas or other liver tumors have been observed following exposure to heliotrine, jacobine, monocrotaline, retrorsine, symphytine, senecionine, and isatadine. [164,168,170–177] Intraperitoneal injection of dehydro-heliotrine was reported to induce tumors in the liver, lungs, intestines and other organs. [170] Pancreatic islet cell tumors were observed following exposure to heliotrine and lycopasamine.[177,178] Subcutaneous injection of dehydroretronecine or retronecine resulted in development of rhabdomyosarcomas in 51.6% and 3.3% of rats in one study, and 10% of the monocrotaline treated rats developed other tumors.[179] Campbell et al. administered seneciphylline to birds both by injection and in feed and observed the development of primary liver tumors in the treated birds. To the authors knowledge, this is the only report of experimental PA-induced neoplasia in non-rodent species.[180] A variety of other tumors such as bladder tumors,

lung adenocarcinomas, adrenal adenomas, and skin tumors have been detected in rats following exposure to heliotrine, lasiocarpine, intermedine, monocrotaline and dehydromonocrotaline, to name a few.[115] Some of these studies used injection rather than oral exposure, and some used plant material rather than purified individual PAs. Brown et al. (2015) exposed groups of heterozygous p53 knockout male by oral gavage to riddelliine doses ranging from 5-45 mg/kg/day for ten days. A separate group was exposed to 1 mg/kg/day for 12 months via riddelliine infused pelleted feed. Liver hemangiosarcomas were the most frequent neoplasm observed in this study, however a variety of tumors were present. In addition to hemangiosarcomas, mice developed mammary carcinomas, lymphomas, leukemias, malignant ependymoma, bronchioloalveolar tumors, osteosarcomas, and several other singular neoplasms. They found a statistically significant trend in the development of neoplasia related to dose in the groups gavaged for ten days. The group that was exposed for the full 12-months also had a statistically significant increase in neoplasia compared to the control group.[27]

The strongest evidence of PA induced carcinogenicity comes from a large study performed by the National Toxicology Program (NTP) using riddelliine. The NTP is a division of the United States Department of Health and Human Services responsible for investigating the effects of various substances for a variety of toxicologic effects, including carcinogenicity. The NTP publishes periodic reports on carcinogens, evaluating existing evidence for carcinogenicity and performs research experiments on select candidate toxins and/or carcinogens. The NTP standards for carcinogenicity studies require that a strict set of standards are followed. The International Agency for Research on Cancer (IARC), a division of the World Health Organization (WHO) has a similar

mission. The IARC tends to be more cautious in terms of the evidence required for classification as a possible, or probable carcinogen when compared to the NTP. Both the NTP and the IARC have classified multiple PAs as potential carcinogens. NTP carcinogenicity studies require groups of 50 male and 50 female mice or rats are treated with various doses for two years duration. The NTP performed a large study on the carcinogenicity of riddelliine in rats and mice. These experiments resulted in the strongest evidence of carcinogenicity for PAs to date.[162]

National Toxicology Program Studies on Riddelliine:

Riddelliine is a noteworthy compound, as a great deal of the PA research has been conducted using this specific alkaloid. Riddelliine is a macrocyclic diester of composed of a retronecine base, bound to riddellic acid found mainly from plants in the *Senecio* genus.[55] Figure 4 shows the chemical structure and metabolic pathways of riddelliine. *Senecio riddellii*, also called Riddell's ragwort is also somewhat unique when compared to other PA containing plants. As indicated previously, it typically contains mostly riddelliine and riddelliine N-oxide*S. riddellii* often has 5 to 10 greater PA concentrations when compared to other PA containing plants.[61,163] These characteristics make riddelliine a convenient choice for research purposes when considering the difficulty of extracting, purifying and preparing appropriate solutions for dosing. Riddelliine was nominated by the FDA for in depth study by the NTP because of evidence of carcinogenicity, potential for human exposure, and its impact on livestock.[162] In 1993, the NTP study published a study on the toxicology of riddelliine in mice and rats. F344/N rats and B6C3F mice were treated by oral gavage with doses ranging from 0.33 to 25 mg/kg body weight five times per week, for two weeks, and in for thirteen weeks in an additional experiment. In the

two-week study, most male rats in the highest dosing group died or were euthanized before the endo of the study. Male rats developed dose dependent hemorrhagic centrilobular hepatocellular necrosis, hepatocyte karyomegaly and cytologic changes, pulmonary hemorrhage, and other lesions. Female rats had fewer and less severe lesions comparatively. In B6C3F mice dosed similarly, the only findings were a dose responsive increase in liver weight, likely indicating cell swelling, and hepatocytomegaly.[55] This study shows that male rats are more sensitive than females, and that rats are more sensitive than mice. In the thirteen-week study, 19 of 20 male rats in the 25 mg/kg (high dose) group died during the treatment period and five of 20 female rats died in the fourteen-week recovery period. Treated rats developed hepatocytomegaly and karyomegaly (megalocytosis), cytoplasmic vacuoles, centrilobular necrosis with mixed infiltrating inflammatory cells, and bile duct hyperplasia. There were also vascular lesions in the kidneys and lungs. After the fourteen-week period, the cytologic changes in the hepatocytes persisted and bile duct hyperplasia became more severe. Three of the female rats (2 of 10 in the 10 mg/kg group at 13 weeks, and 1 of 5 of the 10 mg/kg group after the fourteen-week recovery period) developed hepatic adenomas. In mice, no deaths occurred during the treatment recovery periods. Weight gain was reduced in the two highest dose groups. Centrilobular hepatocyte enlargement was observed in the highest dosing group. Bile duct hyperplasia was observed in high dose females. The 1993 NTP report also evaluated mutagenicity in Salmonella typhimurium, and determined that with S9 activation, riddelliine was mutagenic. These short-term studies were designed to evaluate the toxic effects of riddelliine, but also determined that long-term carcinogenicity studies were warranted. Subsequently, the NTP designed a large study on

the carcinogenicity of riddelliine in mice and rats. In 2003 the NTP published the results of these carcinogenicity studies.[162] In this study groups of 50 male and 50 female rats and mice were exposed by oral gavage to incrementally increasing doses of riddelliine. Groups of 50 male and 50 female rats were exposed to 1 mg/kg riddelliine per day, and additional groups of 50 females received doses ranging from 0.01 to 0.33 mg/kg/day. In the 1 mg/kg dose group, 86% of male and 76% of females developed hemangiosarcomas. Other neoplasms in rats observed with statistical significance included hepatic adenomas and leukemia. They analyzed the livers of these rats and detected the same eight DNA adducts characterized by Yang et al. (2001) via ^{32}P-post-labeling, clearly demonstrating a link between riddelliine exposure, DNA adduct formation, and the development of hemangiosarcomas and other tumors.[143,162] The same study exposed groups of 50 male and 50 female mice to doses of 3 mg/kg/day by oral gavage, and additional groups of 50 male mice were exposed to doses of 0.1, 0.3, or 1 mg/kg/day for two years. Liver hemangiosarcomas were observed in 62% of the male mice give 3 mg/kg. Females in the 3 mg/kg group had in increased number of lung tumors. They also repeated the mutagenicity studies in Salmonella, showing that S9 activation is needed to induce mutations. Lastly, they performed in vitro studies using Chinese hamster ovary cells, and showed that sister chromatid exchange was induced by riddelliine exposure. This study concluded that riddelliine had “clear evidence of carcinogenic activity” in rats and mice. Clear evidence requires the highest standard of proof in NTP studies. Furthermore, they determined that riddelliine is “reasonably anticipated to cause cancer in humans”.[181] An older (1978) NTP two-year carcinogenicity study on lasiocarpine determined that it was carcinogenic in rats.[182] The experimental protocols used in NTP long-term

carcinogenicity studies remain as the gold standard for identifying carcinogens. The time and resources these studies require must be justified by the need for this knowledge. Comparative studies have clearly proven that all PAs are not created equal; however, it may not be feasible to perform studies using NTP standards on each individual PA to determine which are carcinogenic and which are not, or to compare which PAs are more carcinogenic than others. Rather, we may now use riddelliine as a positive control in carcinogenicity studies comparing multiple PAs both in vitro and in vivo. If a PA causes similar changes as riddelliine, it is reasonable to assume that it is a carcinogen. In the experiments described in this dissertation, comparisons will be made between individual PAs, and riddelliine will be used as a positive control in terms of carcinogenicity.

Evidence of Carcinogenicity in Humans:

Direct evidence of chemically induced carcinogenesis in humans is difficult to obtain. The cause-and-effect relationship from carcinogen to tumor is rarely obtained. Rather, epidemiologic data and circumstantial evidence are often used to make assumptions regarding the cause of cancer. PA induced carcinogenesis has not been clearly proven in humans, and experimental evidence in animals is used to determine risks. It was noted as early as 1956 that some South African tribes who regularly consume herbal teas containing *Senecio* spp. had a high incidence of cirrhosis and primary liver cancer.[180] Whole genome sequencing has provided numerous tools in cancer research, one of which is referred to as mutational signature analysis. A mutational signature is produced by transcriptomic software based on whole genome sequencing from numerous neoplasms. Mutational signature analysis uses patterns of mutations which have been characterized in many neoplasms to characterize patterns within various tumors. This technology has

many potential uses including cancer pathogenesis, but as it is new technology, there is disagreement regarding its use and interpretation.[183] Currently, mutational signatures are mainly used to identify driver mutations within neoplasms.[184] Mutational signature analysis has been applied to other suspected carcinogens including tobacco smoking and aflatoxins with promising results.[185,186] He et al. (2021) used mutational signature analysis to determine whether human liver tumors were attributable to PA exposure. After validating a specific mutational signature from PAs using laboratory animals, the authors applied this tool to hepatic carcinomas from a variety of geographic locations. They surprisingly detected pyrrole-protein adducts in 11 out of 34 hepatic carcinomas. They also detected the pyrrolizidine alkaloid specific mutational signature in samples from 193 out of 398 hepatic carcinoma samples from mainland China, 34 of 78 samples from Hong Kong, 62 of 282 samples from Japan, 13 of 218 samples from South Korea, 7 of 28 samples from Southeast Asia, 8 of 290 samples from North America, and 11 of 219 samples from Europe. This study confirms the potential a link between PA exposure and human hepatocellular carcinoma, and also denoted differences in PA exposure risk based on geographic location.[185] Further validation of the specificity of the mutational signature is needed to confirm these findings.

Toxicogenomics of Pyrrolizidine Alkaloids:

Toxicogenomics is a rapidly growing component of toxicology studies. This discipline involves the use of genomic, proteomic, and metabonomic tools in toxicology research.[26] These tools have potential to provide a great deal of information regarding mechanisms and response to candidate toxins. Gene expression profiling has become a mainstay in toxicogenomic studies as the ability to sequence the entire genome and characterize RNA

expression has become easier and less costly. Proteomics is the next level of endpoints and is necessary to further characterize which proteins actually participate in the response to toxicant-induced injury. Metabolomics represents an additional tool that can be applied to investigate the metabolic consequences of toxicant induced injury.[26] A growing number of studies on pyrrolizidine alkaloid toxicity have incorporated these toxicogenomics tools. These studies involve the use of both in vitro and in vivo methods, each of which has its own advantages.[187] In vivo studies have the benefit of correlating genetic changes with critical endpoints like histopathology, serum biochemistry, and clinical signs, which strengthens the conclusion that the genetic changes are toxicant induced. In vitro studies can be performed faster and with less cost and reduce genetic variation caused by the presence of multiple cell types, which can make interpretation of in vivo genomic data difficult. Ebmeyer et al. (2020) exposed male Fischer rats to doses ranging from 0.1 to 3.3 mg/kg/day of heliotrine, echimidine, lasiocarpine, senecionine, senkirkine, and platyphylline by oral gavage for 28 days, then performed whole genome microarray analysis on liver tissue. They found that all PAs of the retronecine and heliotridine types (unsaturated PAs) affected genes involved in cell cycle regulation and DNA damage. Notably, they did not observe histopathologic lesions of PA-induced hepatotoxicosis, which indicates that the DNA damage PAs cause occurs independently from and at lower doses than hepatocellular necrosis. In that study, senecionine caused the greatest number of differentially expressed genes (DEGs), followed in descending order by senkirkine, heliotrine, echimidine, lasiocarpine, and last was platyphylline. Functional analysis determined that the PAs in this study affected pathways involved in DNA repair, cell cycle, xenobiotic metabolism, transcriptional activity, and apoptosis.[188]

Buchmueller et al. (2021) exposed rats to 3.3 mg/kg/day of echimidine, heliotrine, lasiocarpine, senecionine, senkirkine, and platyphylline by oral gavage for 28 days. Following treatment, they performed whole genome microarray analysis on lung tissue to characterize gene expression changes following PA exposure. They found that heliotrine exposure caused the greatest number of DEGs, followed in descending order by echimidine, senkirkine, senecionine, platyphylline and last was lasiocarpine. The lasiocarpine exposed mice only had one DEG. In this study they also performed gene expression on the kidneys of all exposed rats and found no significant differences compared to the control group.[189] Single dose senecionine exposure in mice was shown to cause dysregulation of the hepatocytes transporter genes of the solute carrier (SLC) and ATP-binding cassette (ABC) family's concurrently with liver sinusoidal endothelial cell necrosis. Genes involved in transcriptional regulation and the Wnt signaling pathway were also affected.[39] The Wnt signaling pathway is involved in the development of a variety of neoplasms.[190] Huang et al. (2017) exposed mice to hepatotoxic doses of monocrotaline and measured both microRNA and mRNA expression in liver. They showed a dose related increase in the number of dysregulated mRNAs. They also showed that eleven microRNAs were altered by monocrotaline exposure. They then integrated the altered microRNA and mRNA data to determine that eight genes were significantly upregulated. Kyoto encyclopedia of genes and genome (KEGG) pathway enrichment analysis on these eight genes affected the KEGG pathway "Phagosome".[191] Chen et al. (2012) also evaluated microRNA expression in rats exposed to riddelliine. They found dysregulation of 47 microRNAs, involved in biologic pathways related to hepatotoxicity and hepatic neoplasia, such as "liver proliferation", "liver necrosis/cell death",

"hepatocellular carcinoma", "liver hepatomegaly", "liver inflammation" and "liver fibrosis".[192] Two studies were conducted by the same group to investigate the effects of riddelliine and comfrey on gene expression profiles in the liver of rats. In the initial study (Mei et al. 2007), they exposed rats to 1 mg/kg/day riddelliine, 5 days per week, for 12 weeks, then performed whole genome microarray on liver tissue. There was a total of 919 DEGs, (490 downregulated and 429 upregulated). They used Ingenuity Pathway Analysis to perform pathway enrichment analysis, and pathways related to cancer, cell death, tissue development, cell morphology, cell-to-cell signaling, and cellular development were significantly affected. They also found dysregulation in genes involved in phase I and phase II metabolism of PAs. The CYP 450 genes Cyp2c12, Cyp2e1, Cyp3a9, and Cyp26CYP3a9 were upregulated, and CYP3a9 had the greatest increased fold-change. Phase II metabolism genes Gsta3 was upregulated and Gstm1 and Gstm2 were downregulated. Four ABC genes were dysregulated as well. They also found 17 DEGs that associated with endothelial cells.[193] The same group (Mei et al. 2006) had previously investigated the gene expression effects from feeding comfrey root to Big Blue transgenic rats. It was mentioned earlier that comfrey is a plant with a long history of use as a homeopathic treatment, and as a tea, but its oral use was banned for sale in the U.S. in 2001. In Mei's study rats were fed a diet containing 8% comfrey root for the same 12-week period. They performed whole genome microarray and found that 2,726 genes were differentially expressed. Many genes associated with metabolism were dysregulated, including CYP450 genes, glutathione s-transferases, and ABC transporters. Genes associated with endothelial cell injury and liver injury were also found to be dysregulated. Pathway enrichment analysis found that pathways involved in liver cancer.

A subsequent study (Guo et al. 2007) directly compared the gene expression under the same conditions as the two previously mentioned experiments, namely riddelliine (1 mg/kg/day, 5-days/wk, for 12 weeks) to comfrey (8% comfrey root in diet for 12 weeks). They found that comfrey and riddelliine induced similar changes in gene expression, in fact comfrey exposure resulted in a greater number of DEGs than riddelliine exposure (1,841 DEGs to 639 DEGs respectively). Again they found that pathways relating to cancer and metabolism were affected.[194] This comparison is noteworthy because based on the effects on gene expression alone, comfrey appears to be more genotoxic, and possibly more carcinogenic than riddelliine. Given that riddelliine is the single PA with the strongest evidence of carcinogenicity, people should probably avoid comfrey at all costs. Comfrey can still be found as an herbal supplement or tea. Proteomics have been applied to PA research as well. Wang et al. (2022) performed proteomics on mouse liver after single dose exposure to senecionine and performed the same proteomic assay in vitro using senecionine-exposed human hepatic sinusoidal endothelial cells. Gene ontology (GO) enrichment analysis found that the treated mice had protein alterations related to the following GO terms, “cellular process”, “metabolic process”, “biological regulation”, “response to stimulus”, and “localization”. A total of 231 proteins were dysregulated in the exposed mice. In the in vitro study they found that 50 proteins were dysregulated, and that thrombospondin-1 (TSP1) was overexpressed and had a strong positive correlation with several other overexpressed proteins such as matrix metalloproteinase-9, and a few others. They concluded that TSP1 is a major contributor to the development of PA induced hepatic sinusoidal obstruction syndrome.[195]

In Vitro Toxicogenomic Studies:

Luckert et al. (2015) exposed human hepatocytes to echimidine, senecionine, heliotrine and senkirkine, and performed whole genome microarray. Each of these PAs caused numerous DEGs. The number of DEGs was greatest for senecionine (8,623 DEGs) followed by echimidine (4,556 DEGs), senkirkine (3,406 DEGs), and heliotrine (1,806 DEGs). They found that all four PAs dysregulated multiple CYP450 genes. CYP3A4 was upregulated by all PAs except heliotrine, and many other CYP450 genes were dysregulated by one or more. They also found dysregulation with genes encoding for glucuronosyltransferases, glutathione s-transferases, sulfotransferases, ATP-binding cassettes, and soluble carriers. Functional analysis detected effects on the Ingenuity Pathway Analysis pathways "cholangiocellular carcinoma", "bile duct formation", "hepatocellular carcinoma", "proliferation of liver cancer cells", "biliary tract cancer" and "growth of liver tumor".[38] These pathways clearly highlight the link between PAs and liver cancer, and the fact that they occurred in human hepatocytes is significant in correlating the proof of carcinogenesis in rodents with human liver cancer risks. Abdelfatah et al. (2022) used HepG2 clone 9 cells, designed to overexpress CYP3A4 to measure transcriptomic changes caused by exposure to lasiocarpine, riddelliine, lycopsamine, echimidine, and monocrotaline. They found that lasiocarpine, riddelliine, monocrotaline, and echimidine, but not lycopsamine, affected canonical pathways involved in DNA damage repair and the cell cycle. The effects on gene expression occurred in a concentration dependent manner. Other affected pathways included DNA methylation and transcriptional repression.[196] CYP3A4 is reportedly the main enzyme responsible for PA bioactivation in people. Toxicogenomic research on PA toxicosis and

carcinogenesis is early in its development but has already added a great deal of knowledge regarding the mechanism of toxicity, metabolism, and carcinogenic potential of PAs.

Despite the vast amount of research performed on the risks associated with PA exposure, these compounds continue to pose a significant risk factor for human and animal health. The research described in this dissertation will contribute to this body of knowledge and characterize relative similarities and differences between individual PAs.

References:

1. Stegelmeier, B. L. *et al.* Pyrrolizidine alkaloid plants, metabolism and toxicity. *J Nat Toxins* **8**, 95–116 (1999).
2. Haschek, W. M., Rousseaux, C. G. & Wallig, M. A. Toxicologic Pathology: An Introduction. in *Haschek and Rousseaux's Handbook of Toxicologic Pathology* 1–9 (Elsevier, 2013). doi:10.1016/B978-0-12-415759-0.00094-7.
3. Stegelmeier, B. L., Colegate, S. M. & Brown, A. W. Dehydropyrrolizidine Alkaloid Toxicity, Cytotoxicity, and Carcinogenicity. *Toxins (Basel)* **8**, 356 (2016).
4. Stegelmeier, B. L. Pyrrolizidine Alkaloid–Containing Toxic Plants (Senecio, Crotalaria, Cynoglossum, Amsinckia, Heliotropium, and Echium spp.). *Veterinary Clinics: Food Animal Practice* **27**, 419–428 (2011).
5. Rückert, C., Emmerich, I., Hertzsch, R. & Vervuert, I. Pyrrolizidine alkaloids in commercial feedstuffs for horses. *Equine Vet J* **51**, 495–499 (2019).

6. Edgar, J. A. & Smith, L. W. Transfer of pyrrolizidine alkaloids into eggs: food safety implications. (1998).

7. Letsyo, E., Jerz, G., Winterhalter, P. & Beuerle, T. Toxic pyrrolizidine alkaloids in herbal medicines commonly used in Ghana. *J Ethnopharmacol* **202**, 154–161 (2017).

8. Chauvin, P., Dillon, J. C. & Moren, A. [An outbreak of Heliotrope food poisoning, Tadjikistan, November 1992-March 1993]. *Sante* **4**, 263–268 (1994).

9. Bach, N., Thung, S. N. & Schaffner, F. Comfrey herb tea-induced hepatic veno-occlusive disease. *Am J Med* **87**, 97–99 (1989).

10. Steinhoff, B. Pyrrolizidine alkaloid contamination in herbal medicinal products: Limits and occurrence. *Food Chem Toxicol* **130**, 262–266 (2019).

11. Kakar, F. *et al.* An Outbreak of Hepatic Veno-Occlusive Disease in Western Afghanistan Associated with Exposure to Wheat Flour Contaminated with Pyrrolizidine Alkaloids. *J Toxicol* **2010**, 313280 (2010).

12. Mohabbat, O. *et al.* AN OUTBREAK OF HEPATIC VENO-OCCLUSIVE DISEASE IN NORTH-WESTERN AFGHANISTAN. *The Lancet* **308**, 269–271 (1976).

13. Hoogenboom, L. a. P. *et al.* Carry-over of pyrrolizidine alkaloids from feed to milk in dairy cows. *Food Addit Contam Part A Chem Anal Control Expo Risk Assess* **28**, 359–372 (2011).

14. Bodi, D. *et al.* Determination of pyrrolizidine alkaloids in tea, herbal drugs and honey. *Food Addit Contam Part A Chem Anal Control Expo Risk Assess* **31**, 1886–1895 (2014).

15. Moreira, R., Pereira, D. M., Valentão, P. & Andrade, P. B. Pyrrolizidine Alkaloids: Chemistry, Pharmacology, Toxicology and Food Safety. *Int J Mol Sci* **19**, 1668 (2018).

16. Bueno-Beti, C., Sassi, Y., Hajjar, R. J. & Hadri, L. Pulmonary Artery Hypertension Model in Rats by Monocrotaline Administration. *Methods Mol Biol* **1816**, 233–241 (2018).

17. Gomez-Arroyo, J. G. *et al.* The monocrotaline model of pulmonary hypertension in perspective. *American Journal of Physiology-Lung Cellular and Molecular Physiology* **302**, L363–L369 (2012).

18. Mei, N., Heflich, R. H., Chou, M. W. & Chen, T. Mutations Induced by the Carcinogenic Pyrrolizidine Alkaloid Riddelliine in the Liver cII Gene of Transgenic Big Blue Rats. *Chem. Res. Toxicol.* **17**, 814–818 (2004).

19. Chan, P. C., Haseman, J. K., Prejean, J. D. & Nyska, A. Toxicity and carcinogenicity of riddelliine in rats and mice. *Toxicology Letters* **144**, 295–311 (2003).

20. He, Y.-Q. *et al.* Glucuronidation, a new metabolic pathway for pyrrolizidine alkaloids. *Chem Res Toxicol* **23**, 591–599 (2010).

21. Brown, A. Relative Toxicity of Select Dehydropyrrolizidine Alkaloids and Evaluation of a Heterozygous P53 Knockout Mouse Model for Dehydropyrrolizidine Alkaloid Induced Carcinogenesis. *All Graduate Theses and Dissertations* (2015) doi:https://doi.org/10.26076/7997-d859.

22. Brown, A. W. *et al.* The comparative toxicity of a reduced, crude comfrey (Symphytum officinale) alkaloid extract and the pure, comfrey-derived pyrrolizidine

alkaloids, lycopsamine and intermedine in chicks (Gallus gallus domesticus). *J Appl Toxicol* **36**, 716–725 (2016).

23. Field, R. A., Stegelmeier, B. L., Colegate, S. M., Brown, A. W. & Green, B. T. An in vitro comparison of the cytotoxic potential of selected dehydropyrrolizidine alkaloids and some N-oxides. *Toxicon* **97**, 36–45 (2015).
24. Griffin, D. S. & Segall, H. J. Genotoxicity and cytotoxicity of selected pyrrolizidine alkaloids, a possible alkenal metabolite of the alkaloids, and related alkenals. *Toxicol Appl Pharmacol* **86**, 227–234 (1986).
25. Ellinger-Ziegelbauer, H., Aubrecht, J., Kleinjans, J. C. & Ahr, H.-J. Application of toxicogenomics to study mechanisms of genotoxicity and carcinogenicity. *Toxicol Lett* **186**, 36–44 (2009).
26. Hamadeh, H. K., Amin, R. P., Paules, R. S. & Afshari, C. A. An Overview of Toxicogenomics. *Current Issues in Molecular Biology* **4**, 45–56 (2002).
27. Heterozygous p53 knockout mouse model for dehydropyrrolizidine alkaloid-induced carcinogenesis. *J Appl Toxicol* **35**, 1557–1563 (2015).
28. Schaarschmidt, F., Sill, M. & Hothorn, L. A. Poly-k-trend tests for survival adjusted analysis of tumor rates formulated as approximate multiple contrast test. *J Biopharm Stat* **18**, 934–948 (2008).
29. Stegelmeier, B. L., Davis, T. Z., Clayton, M. J. & Gardner, D. R. Identifying Plant Poisoning in Livestock in North America. *Vet Clin North Am Food Anim Pract* **36**, 661–671 (2020).

30. Huybrechts, B. & Callebaut, A. Pyrrolizidine alkaloids in food and feed on the Belgian market. *Food Addit Contam Part A Chem Anal Control Expo Risk Assess* **32**, 1939–1951 (2015).

31. Driehuis, F., Wilkinson, J. M., Jiang, Y., Ogunade, I. & Adesogan, A. T. Silage review: Animal and human health risks from silage. *J Dairy Sci* **101**, 4093–4110 (2018).

32. Schrenk, D. *et al.* Pyrrolizidine alkaloids in food and phytomedicine: Occurrence, exposure, toxicity, mechanisms, and risk assessment - A review. *Food Chem Toxicol* **136**, 111107 (2020).

33. Brugnerotto, P. *et al.* Pyrrolizidine alkaloids and beehive products: A review. *Food Chem* **342**, 128384 (2021).

34. Mulder, P. P. J. *et al.* Occurrence of pyrrolizidine alkaloids in animal- and plant-derived food: results of a survey across Europe. *Food Addit Contam Part A Chem Anal Control Expo Risk Assess* **35**, 118–133 (2018).

35. Dübecke, A., Beckh, G. & Lüllmann, C. Pyrrolizidine alkaloids in honey and bee pollen. *Food Additives & Contaminants: Part A* **28**, 348–358 (2011).

36. Dusemund, B. *et al.* Risk assessment of pyrrolizidine alkaloids in food of plant and animal origin. *Food Chem Toxicol* **115**, 63–72 (2018).

37. Segall, H. J., Wilson, D. W., Dallas, J. L. & Haddon, W. F. Trans-4-Hydroxy-2-Hexenal: a Reactive Metabolite from the Macrocyclic Pyrrolizidine Alkaloid Senecionine. *Science* **229**, 472–475 (1985).

38. Luckert, C., Hessel, S., Lenze, D. & Lampen, A. Disturbance of gene expression in primary human hepatocytes by hepatotoxic pyrrolizidine alkaloids: A whole genome transcriptome analysis. *Toxicology in Vitro* **29**, 1669–1682 (2015).

39. Hessel-Pras, S. *et al.* The pyrrolizidine alkaloid senecionine induces CYP-dependent destruction of sinusoidal endothelial cells and cholestasis in mice. *Arch Toxicol* **94**, 219–229 (2020).

40. Kaltner, F., Rychlik, M., Gareis, M. & Gottschalk, C. Occurrence and Risk Assessment of Pyrrolizidine Alkaloids in Spices and Culinary Herbs from Various Geographical Origins. *Toxins (Basel)* **12**, 155 (2020).

41. Candrian, U., Lüthy, J., Graf, U. & Schlatter, C. Mutagenic activity of the pyrrolizidine alkaloids seneciphylline and senkirkine in Drosophila and their transfer into rat milk. *Food Chem Toxicol* **22**, 223–225 (1984).

42. Mulder, P. P. J. *et al.* Transfer of pyrrolizidine alkaloids from ragwort, common groundsel and viper's bugloss to milk from dairy cows. *Food Addit Contam Part A Chem Anal Control Expo Risk Assess* **37**, 1906–1921 (2020).

43. de Nijs, M., Mulder, P. P. J., Klijnstra, M. D., Driehuis, F. & Hoogenboom, R. L. A. P. Fate of pyrrolizidine alkaloids during processing of milk of cows treated with ragwort. *Food Addit Contam Part A Chem Anal Control Expo Risk Assess* **34**, 2212–2219 (2017).

44. Mulder, P. P. J. *et al.* Transfer of pyrrolizidine alkaloids from various herbs to eggs and meat in laying hens. *Food Addit Contam Part A Chem Anal Control Expo Risk Assess* **33**, 1826–1839 (2016).

45. Bari, M. S. *et al.* Ethnomedicinal uses, phytochemistry, and biological activities of plants of the genus Gynura. *J Ethnopharmacol* **271**, 113834 (2021).

46. F, S. & Hk, S. The efficacy and safety of comfrey. *Public health nutrition* **3**, (2000).

47. Frost, R., MacPherson, H. & O'Meara, S. A critical scoping review of external uses of comfrey (Symphytum spp.). *Complement Ther Med* **21**, 724–745 (2013).

48. Mattocks, A. R. Toxic pyrrolizidine alkaloids in comfrey. *Lancet* **2**, 1136–1137 (1980).

49. Mei, N. *et al.* METABOLISM, GENOTOXICITY, AND CARCINOGENICITY OF COMFREY. *J Toxicol Environ Health B Crit Rev* **13**, 509–526 (2010).

50. Mei, N., Guo, L., Fu, P. P., Heflich, R. H. & Chen, T. Mutagenicity of comfrey (Symphytum Officinale) in rat liver. *Br J Cancer* **92**, 873–875 (2005).

51. Staiger, C. Comfrey: a clinical overview. *Phytother Res* **26**, 1441–1448 (2012).

52. Staiger, C. Comfrey root: from tradition to modern clinical trials. *Wien Med Wochenschr* **163**, 58–64 (2013).

53. Avila, C., Breakspear, I., Hawrelak, J., Salmond, S. & Evans, S. A systematic review and quality assessment of case reports of adverse events for borage (Borago officinalis), coltsfoot (Tussilago farfara) and comfrey (Symphytum officinale). *Fitoterapia* **142**, 104519 (2020).

54. Nutrition, C. for F. S. and A. Safety Alerts & Advisories - FDA Advises Dietary Supplement Manufacturers to Remove Comfrey Products From the Market. http://wayback.archive-it.org/7993/20161022045127/http://www.fda.gov/Food/RecallsOutbreaksEmergencies/SafetyAlertsAdvisories/ucm111219.htm.

55. Chan, P. NTP technical report on the toxicity studies of Riddelliine (CAS No. 23246-96-0) Administered by Gavage to F344 Rats and B6C3F1 Mice. *Toxic Rep Ser* **27**, 1-D9 (1993).

56. Roeder, E. & Wiedenfeld, H. Pyrrolizidine alkaloids in medicinal plants of Mongolia, Nepal and Tibet. *Die Pharmazie - An International Journal of Pharmaceutical Sciences* **64**, 699–716 (2009).

57. Sarkar, C. *et al.* Heliotropium indicum L.: From Farm to a Source of Bioactive Compounds with Therapeutic Activity. *Evid Based Complement Alternat Med* **2021**, 9965481 (2021).

58. Robertson, J. & Stevens, K. Pyrrolizidine alkaloids: occurrence, biology, and chemical synthesis. *Nat Prod Rep* **34**, 62–89 (2017).

59. Cairns, E. *et al.* Structure of Echivulgarine, a Pyrrolizidine Alkaloid Isolated from the Pollen of Echium vulgare. *J. Agric. Food Chem.* **63**, 7421–7427 (2015).

60. Senturk, H., Eksin, E., Zeybek, U. & Erdem, A. Detection of Senecionine in Dietary Sources by Single-Use Electrochemical Sensor. *Micromachines (Basel)* **12**, 1585 (2021).

61. Molyneux, R. J., Gardner, D. L., Colegate, S. M. & Edgar, J. A. Pyrrolizidine alkaloid toxicity in livestock: a paradigm for human poisoning? *Food Addit Contam Part A Chem Anal Control Expo Risk Assess* **28**, 293–307 (2011).

62. He, Y., Zhu, L., Ma, J. & Lin, G. Metabolism-mediated cytotoxicity and genotoxicity of pyrrolizidine alkaloids. *Arch Toxicol* **95**, 1917–1942 (2021).

63. Peterson, J. E. & C. C. J. Culvenor. Hepatotoxic Pyrrolizidine Alkaloids. in *Handbook of Natural Toxins Volume 1. Plant and Fungal Toxins* vol. 1 637–671 (Marcel Dekker Inc., 1983).

64. Edgar, J. A., Colegate, S. M., Boppré, M. & Molyneux, R. J. Pyrrolizidine alkaloids in food: a spectrum of potential health consequences. *Food Addit Contam Part A Chem Anal Control Expo Risk Assess* **28**, 308–324 (2011).

65. Willmot, F. & Robertson, G. SENECIO DISEASE, OR CIRRHOSIS OF THE LIVER DUE TO SENECIO POISONING. *The Lancet* **196**, 848–849 (1920).

66. Wiedenfeld, H. & Edgar, J. Toxicity of pyrrolizidine alkaloids to humans and ruminants. *Phytochem Rev* **10**, 137–151 (2011).

67. Tandon, B. N., Tandon, H. D., Tandon, R. K., Narndranathan, M. & Joshi, Y. K. An epidemic of veno-occlusive disease of liver in central India. *Lancet* **2**, 271–272 (1976).

68. Mayer, F. & Lüthy, J. Heliotrope poisoning in Tadjikistan. *Lancet* **342**, 246–247 (1993).

69. Weston, C. F., Cooper, B. T., Davies, J. D. & Levine, D. F. Veno-occlusive disease of the liver secondary to ingestion of comfrey. *Br Med J (Clin Res Ed)* **295**, 183 (1987).

70. Sperl, W. *et al.* Reversible hepatic veno-occlusive disease in an infant after consumption of pyrrolizidine-containing herbal tea. *Eur J Pediatr* **154**, 112–116 (1995).

71. Huxtable, R. J. New aspects of the toxicology and pharmacology of pyrrolizidine alkaloids. *Gen Pharmacol* **10**, 159–167 (1979).

72. Rasenack, R., Müller, C., Kleinschmidt, M., Rasenack, J. & Wiedenfeld, H. Veno-occlusive disease in a fetus caused by pyrrolizidine alkaloids of food origin. *Fetal Diagn Ther* **18**, 223–225 (2003).

73. Roulet, M., Laurini, R., Rivier, L. & Calame, A. Hepatic veno-occlusive disease in newborn infant of a woman drinking herbal tea. *The Journal of Pediatrics* **112**, 433–436 (1988).

74. Van Schalkwyk, F. J., Stander, M. A., Nsizwane, M., Mathee, A. & Van Wyk, B.-E. Fatal pyrrolizidine alkaloid poisoning of infants caused by adulterated Senecio coronatus. *Forensic Sci Int* **320**, 110680 (2021).

75. Ma, J. *et al.* Clinical application of pyrrole-hemoglobin adducts as a biomarker of pyrrolizidine alkaloid exposure in humans. *Arch Toxicol* **95**, 759–765 (2021).

76. Gardner, D. R., Thorne, M. S., Molyneux, R. J., Pfister, J. A. & Seawright, A. A. Pyrrolizidine alkaloids in Senecio madagascariensis from Australia and Hawaii and assessment of possible livestock poisoning. *Biochemical Systematics and Ecology* **34**, 736–744 (2006).

77. Le Roux, J., Wieczorek, A., Oshiro, C. & Vorsino, A. Disentangling the dynamics of invasive fireweed (Senecio madagascariensis Poir Species Complex) in the Hawaiian Islands. *Biological Invasions* **12**, 2251–2264 (2010).

78. Schoental, R. Toxicology and Carcinogenic Action of Pyrrolizidine Alkaloids. *Cancer Research* **28**, 2237–2246 (1968).

79. Mulder, P. P. J., Sánchez, P. L., These, A., Preiss-Weigert, A. & Castellari, M. Occurrence of Pyrrolizidine Alkaloids in food. *EFSA Supporting Publications* **12**, 859E (2015).

80. Cheeke, P. R. & Pierson-Goeger, M. L. Toxicity of Senecio jacobaea and pyrrolizidine alkaloids in various laboratory animals and avian species. *Toxicology Letters* **18**, 343–349 (1983).

81. Miranda, C. L. *et al.* Flavin-containing monooxygenase: a major detoxifying enzyme for the pyrrolizidine alkaloid senecionine in guinea pig tissues. *Biochem Biophys Res Commun* **178**, 546–552 (1991).

82. Molyneux, R. J., Johnson, A. E., Olsen, J. D. & Baker, D. C. Toxicity of pyrrolizidine alkaloids from Riddell groundsel (Senecio riddellii) to cattle. *Am J Vet Res* **52**, 146–151 (1991).

83. Abu Damir, H., Adam, S. E. & Tartour, G. The effects of Heliotropium ovalifolium on goats and sheep. *Br Vet J* **138**, 463–472 (1982).

84. Stegelmeier, B. L., Gardner, D. R., James, L. F. & Molyneux, R. J. Pyrrole detection and the pathologic progression of Cynoglossum officinale (houndstongue) poisoning in horses. *J Vet Diagn Invest* **8**, 81–90 (1996).

85. Creeper, J. H., Mitchell, A. A., Jubb, T. F. & Colegate, S. M. Pyrrolizidine alkaloid poisoning of horses grazing a native heliotrope (Heliotropium ovalifolium). *Aust Vet J* **77**, 401–402 (1999).

86. Mendel, V. E. *et al.* Pyrrolizidine alkaloid-induced liver disease in horses: an early diagnosis. *Am J Vet Res* **49**, 572–578 (1988).

87. Bull, L. B., Dick, A. T., Keast, J. C. & Edgar, G. An experimental investigation of the hepatotoxic and other effects on sheep of consumption of Heliotropium europaeum L. : Heliotrope poisoning of sheep. *Aust. J. Agric. Res.* **7**, 281–332 (1956).

88. Baker, D. C., Pfister, J. A., Molyneux, R. J. & Kechele, P. Cynoglossum officinale toxicity in calves. *J Comp Pathol* **104**, 403–410 (1991).

89. Baker, D. C., Smart, R. A., Ralphs, M. & Molyneux, R. J. Hound's-tongue (Cynoglossum officinale) poisoning in a calf. *J Am Vet Med Assoc* **194**, 929–930 (1989).

90. Araya, O. & Fuentealba, I. C. Chronic hepato-toxicity of Senecio erraticus in calves from two 50-day feeding periods in consecutive years. *Vet Hum Toxicol* **32**, 555–557 (1990).

91. Preliasco, M. *et al.* Senecio grisebachii Baker: Pyrrolizidine alkaloids and experimental poisoning in calves. *Toxicon* **133**, 68–73 (2017).

92. Harding, J. D. J., Lewis, G., Done, J. T. & Allcroft, R. Experimental Poisoning by Senecio jacobaea in Pigs. *Pathologia veterinaria* **1**, 204–220 (1964).

93. Prakash, A. S., Pereira, T. N., Reilly, P. E. B. & Seawright, A. A. Pyrrolizidine alkaloids in human diet. *Mutation Research/Genetic Toxicology and Environmental Mutagenesis* **443**, 53–67 (1999).

94. Huan, J.-Y., Miranda, C. L., Buhler, D. R. & Cheeke, P. R. Species differences in the hepatic microsomal enzyme metabolism of the pyrrolizidine alkaloids. *Toxicology Letters* **99**, 127–137 (1998).

95. Cheeke, P. R. Natural toxicants in feeds, forages, and poisonous plants. *Natural toxicants in feeds, forages, and poisonous plants.* (1998).

96. Luo, J. *et al.* Sex difference in monocrotaline-induced developmental toxicity and fetal hepatotoxicity in rats. *Toxicology* **418**, 32–40 (2019).

97. Liang, Q. *et al.* The gender-dependent difference of liver GSH antioxidant system in mice and its influence on isoline-induced liver injury. *Toxicology* **280**, 61–69 (2011).

98. Cheeke, P. R. Nutritional implications of pyrrolizidine alkaloid toxicosis. *Poisoning by plants, mycotoxins and related toxins* 163–174 (2011) doi:10.1079/9781845938338.0163.

99. Aston, N., Morris, P. & Tanner, S. Retrorsine in breast milk influences copper handling in suckling rat pups. *J Hepatol* **25**, 748–755 (1996).

100. Buckmaster, G. W., Cheeke, P. R. & Shull, L. R. Pyrrolizidine alkaloid poisoning in rats: protective effects of dietary cysteine. *J Anim Sci* **43**, 464–473 (1976).

101. Swick, R. A., Cheeke, P. R., Miranda, C. L. & Buhler, D. R. The effect of consumption of the pyrrolizidine alkaloid-containing plant senecio jacobaea on iron and copper metabolism in the rat. *Journal of Toxicology and Environmental Health* **10**, 757–768 (1982).

102. Mattocks, A. R. *Chemistry and toxicology of pyrrolizidine alkaloids*. (Academic Press, 1986).

103. Culvenor, C. C. J. *et al.* Hepato- and pneumotoxicity of pyrrolizidine alkaloids and derivatives in relation to molecular structure. *Chemico-Biological Interactions* **12**, 299–324 (1976).

104. Chen, T., Mei, N. & Fu, P. P. Genotoxicity of pyrrolizidine alkaloids. *J Appl Toxicol* **30**, 183–196 (2010).

105. Widjaja, F., Alhejji, Y. & Rietjens, I. M. C. M. The Role of Kinetics as Key Determinant in Toxicity of Pyrrolizidine Alkaloids and Their N-Oxides. *Planta Med* **88**, 130–143 (2022).

106. Tu, M. *et al.* Organic cation transporter 1 mediates the uptake of monocrotaline and plays an important role in its hepatotoxicity. *Toxicology* **311**, 225–230 (2013).

107. Mattocks, A. R. & Legg, R. F. Antimitotic activity of dehydroretronecine, a pyrrolizidine alkaloid metabolite, and some analogous compounds, in a rat liver parenchymal cell line. *Chemico-Biological Interactions* **30**, 325–336 (1980).

108. Downing, D. & Peterson, J. Quantitative Assessment of the Persistent Antimitotic Effect of Certain Hepatotoxic Pyrrolizidine Alkaloids on Rat Liver. *Australian Journal of Experimental Biology and Medical Science* **46**, 493–502 (1968).

109. Hincks, J. R. *et al.* DNA cross-linking in mammalian cells by pyrrolizidine alkaloids: structure-activity relationships. *Toxicol Appl Pharmacol* **111**, 90–98 (1991).

110. Ames, M. M. *et al.* Pharmacokinetic study of indicine N-oxide in pediatric cancer patients. *Cancer Chemother Pharmacol* **10**, 43–46 (1982).

111. Kovach, J. S. *et al.* Toxicity and pharmacokinetics of a pyrrolizidine alkaloid, indicine N-oxide, in humans. *Cancer Res* **39**, 4540–4544 (1979).

112. Wang, C. *et al.* The comparative pharmacokinetics of two pyrrolizidine alkaloids, senecionine and adonifoline, and their main metabolites in rats after intravenous and oral administration by UPLC/ESIMS. *Anal Bioanal Chem* **401**, 275–287 (2011).

113. Williams, L. *et al.* Toxicokinetics of riddelliine, a carcinogenic pyrrolizidine alkaloid, and metabolites in rats and mice. *Toxicol Appl Pharmacol* **182**, 98–104 (2002).

114. Tu, M. *et al.* Involvement of organic cation transporter 1 and CYP3A4 in retrorsine-induced toxicity. *Toxicology* **322**, 34–42 (2014).

115. Fu, P. P., Xia, Q., Lin, G. & Chou, M. W. Pyrrolizidine Alkaloids—Genotoxicity, Metabolism Enzymes, Metabolic Activation, and Mechanisms. *Drug Metabolism Reviews* **36**, 1–55 (2004).

116. Xu, J. *et al.* Pyrrolizidine alkaloids: An update on their metabolism and hepatotoxicity mechanism. *Liver Research* **3**, 176–184 (2019).

117. Ruan, J., Yang, M., Fu, P., Ye, Y. & Lin, G. Metabolic Activation of Pyrrolizidine Alkaloids: Insights into the Structural and Enzymatic Basis. *Chem. Res. Toxicol.* **27**, 1030–1039 (2014).

118. Yang, Y. C. *et al.* Metabolic activation of the tumorigenic pyrrolizidine alkaloid, riddelliine, leading to DNA adduct formation in vivo. *Chem Res Toxicol* **14**, 101–109 (2001).

119. Allen, J. R. & Chesney, C. F. Effect of age on development of cor pulmonale in nonhuman primates following pyrrolizidine alkaloid intoxication. *Exp Mol Pathol* **17**, 220–232 (1972).

120. Allen, J. R. & Hsu, I. C. Antimitotic Effects of Dehydroretronecine Pyrrole. *Proceedings of the Society for Experimental Biology and Medicine* **147**, 546–550 (1974).

121. Huan, J. Y., Miranda, C. L., Buhler, D. R. & Cheeke, P. R. The roles of CYP3A and CYP2B isoforms in hepatic bioactivation and detoxification of the pyrrolizidine alkaloid senecionine in sheep and hamsters. *Toxicol Appl Pharmacol* **151**, 229–235 (1998).

122. Chung, W. G. & Buhler, D. R. Major factors for the susceptibility of guinea pig to the pyrrolizidine alkaloid jacobine. *Drug Metab Dispos* **23**, 1263–1267 (1995).

123. Strange, R. C., Jones, P. W. & Fryer, A. A. Glutathione S-transferase: genetics and role in toxicology. *Toxicol Lett* **112–113**, 357–363 (2000).

124. Winter, C. K., Segall, H. J. & Haddon, W. F. Formation of cyclic adducts of deoxyguanosine with the aldehydes trans-4-hydroxy-2-hexenal and trans-4-hydroxy-2-nonenal in vitro. *Cancer Res* **46**, 5682–5686 (1986).

125. Ma, J., Xia, Q., Fu, P. P. & Lin, G. Pyrrole-protein adducts - A biomarker of pyrrolizidine alkaloid-induced hepatotoxicity. *J Food Drug Anal* **26**, 965–972 (2018).

126. Lamé, M. W., Jones, A. D., Wilson, D. W., Dunston, S. K. & Segall, H. J. Protein targets of monocrotaline pyrrole in pulmonary artery endothelial cells. *J Biol Chem* **275**, 29091–29099 (2000).

127. Deleve, L. D. *et al.* Sinusoidal obstruction syndrome (veno-occlusive disease) in the rat is prevented by matrix metalloproteinase inhibition. *Gastroenterology* **125**, 882–890 (2003).

128. Nakayama Wong, L. S., Lamé, M. W., Jones, A. D. & Wilson, D. W. Differential Cellular Responses to Protein Adducts of Naphthoquinone and Monocrotaline Pyrrole. *Chem. Res. Toxicol.* **23**, 1504–1513 (2010).

129. Xia, Q., Ma, L., He, X., Cai, L. & Fu, P. P. 7-Glutathione Pyrrole Adduct: A Potential DNA Reactive Metabolite of Pyrrolizidine Alkaloids. *Chem. Res. Toxicol.* **28**, 615–620 (2015).

130. He, X., Ma, L., Xia, Q. & Fu, P. P. 7-N-Acetylcysteine-pyrrole conjugate-A potent DNA reactive metabolite of pyrrolizidine alkaloids. *J Food Drug Anal* **24**, 682–694 (2016).

131. Zhao, M. *et al.* Cytochrome P450 Enzymes and Drug Metabolism in Humans. *Int J Mol Sci* **22**, 12808 (2021).

132. Acland, H. M. *et al.* Toxic hepatopathy in neonatal foals. *Vet Pathol* **21**, 3–9 (1984).

133. *Jubb, Kennedy, and Palmer's pathology of domestic animals*. (Elsevier, 2016).

134. Edgar, J. A., Molyneux, R. J. & Colegate, S. M. Pyrrolizidine Alkaloids: Potential Role in the Etiology of Cancers, Pulmonary Hypertension, Congenital Anomalies, and Liver Disease. *Chem Res Toxicol* **28**, 4–20 (2015).

135. Oinonen, T. & Lindros, K. O. Zonation of hepatic cytochrome P-450 expression and regulation. *Biochem J* **329 (Pt 1)**, 17–35 (1998).

136. Means, S. A. & Ho, H. A spatial-temporal model for zonal hepatotoxicity of acetaminophen. *Drug Metab Pharmacokinet* **34**, 71–77 (2019).

137. Jago, M. V. The development of the hepatic megalocytosis of chronic pyrrolizidine alkaloid poisoning. *Am J Pathol* **56**, 405–421 (1969).

138. Allen, J. R., Carstens, L. A. & Norback, D. H. Ultrastructural and biochemical changes in the liver of monocrotaline intoxicated chickens. *Toxicology and Applied Pharmacology* **16**, 800–806 (1970).

139. Hayes, M. A., Roberts, E. & Farber, E. Initiation and Selection of Resistant Hepatocyte Nodules in Rats Given the Pyrrolizidine Alkaloids Lasiocarpine and Senecionine1. *Cancer Research* **45**, 3726–3734 (1985).

140. Phillips, D. H. & Arlt, V. M. Genotoxicity: damage to DNA and its consequences. *EXS* **99**, 87–110 (2009).

141. Fu, P. P., Xia, Q., Lin, G. & Chou, M. W. Genotoxic Pyrrolizidine Alkaloids — Mechanisms Leading to DNA Adduct Formation and Tumorigenicity. *International Journal of Molecular Sciences* **3**, 948–964 (2002).

142. Phillips, D. H. & Arlt, V. M. The 32P-postlabeling assay for DNA adducts. *Nat Protoc* **2**, 2772–2781 (2007).

143. Yang, Y.-C. *et al.* Development of a 32P-Postlabeling/HPLC Method for Detection of Dehydroretronecine-Derived DNA Adducts in Vivo and in Vitro. *Chem. Res. Toxicol.* **14**, 91–100 (2001).

144. Xia, Q., Chou, M. W., Kadlubar, F. F., Chan, P.-C. & Fu, P. P. Human liver microsomal metabolism and DNA adduct formation of the tumorigenic pyrrolizidine alkaloid, riddelliine. *Chem Res Toxicol* **16**, 66–73 (2003).

145. Xia, Q., Chou, M. W., Lin, G. & Fu, P. P. Metabolic formation of DHP-derived DNA adducts from a representative otonecine type pyrrolizidine alkaloid clivorine and the extract of Ligularia hodgsonnii hook. *Chem Res Toxicol* **17**, 702–708 (2004).

146. Xia, Q., Chou, M. W., Edgar, J. A., Doerge, D. R. & Fu, P. P. Formation of DHP-derived DNA adducts from metabolic activation of the prototype heliotridine-type pyrrolizidine alkaloid, lasiocarpine. *Cancer Lett* **231**, 138–145 (2006).

147. Chou, M. W. & Fu, P. P. Formation of DHP-derived DNA adducts in vivo from dietary supplements and chinese herbal plant extracts containing carcinogenic pyrrolizidine alkaloids. *Toxicol Ind Health* **22**, 321–327 (2006).

148. Hadi, N. S. A. *et al.* Genotoxicity of selected pyrrolizidine alkaloids in human hepatoma cell lines HepG2 and Huh6. *Mutat Res Genet Toxicol Environ Mutagen* **861–862**, 503305 (2021).

149. Brink, N. G. The mutagenic activity of the pyrrolizidine alkaloid heliotrine in Drosophila melanogaster II. Chromosome rearrangements. *Mutation Research/Fundamental and Molecular Mechanisms of Mutagenesis* **8**, 139–146 (1969).

150. Campesato, V. R., Graf, U., Reguly, M. L. & de Andrade, H. H. Recombinagenic activity of integerrimine, a pyrrolizidine alkaloid from Senecio brasiliensis, in somatic cells of Drosophila melanogaster. *Environ Mol Mutagen* **29**, 91–97 (1997).

151. Bruggeman, I. M. & van der Hoeven, J. C. M. Induction of SCEs by some pyrrolizidine alkaloids in V79 Chinese hamster cells co-cultured with chick embryo hepatocytes. *Mutation Research Letters* **142**, 209–212 (1985).

152. Candrian, U., Lüthy, J. & Schlatter, C. In vivo covalent binding of retronecine-labelled [3H]seneciphylline and [3H]senecionine to DNA of rat liver, lung and kidney. *Chem Biol Interact* **54**, 57–69 (1985).

153. Coulombe, R. A., Drew, G. L. & Stermitz, F. R. Pyrrolizidine alkaloids crosslink DNA with actin. *Toxicol Appl Pharmacol* **154**, 198–202 (1999).

154. Petry, T. W. & Sipes, I. G. Modulation of monocrotaline-induced hepatic genotoxicity in rats. *Carcinogenesis* **8**, 415–419 (1987).

155. Rutz, L., Gao, L., Küpper, J.-H. & Schrenk, D. Structure-dependent genotoxic potencies of selected pyrrolizidine alkaloids in metabolically competent HepG2 cells. *Arch Toxicol* **94**, 4159–4172 (2020).

156. Louisse, J. *et al.* Determination of genotoxic potencies of pyrrolizidine alkaloids in HepaRG cells using the γH2AX assay. *Food Chem Toxicol* **131**, 110532 (2019).

157. Hayashi, Y. Overview of genotoxic carcinogens and non-genotoxic carcinogens. *Experimental and Toxicologic Pathology* **44**, 465–471 (1992).

158. Lee, S. J. *et al.* Distinguishing between genotoxic and non-genotoxic hepatocarcinogens by gene expression profiling and bioinformatic pathway analysis. *Sci Rep* **3**, 2783 (2013).

159. Fu, P. P. Pyrrolizidine Alkaloids: Metabolic Activation Pathways Leading to Liver Tumor Initiation. *Chem Res Toxicol* **30**, 81–93 (2017).

160. Griffin, D. S. & Segall, H. J. Lipid peroxidation and cellular damage caused by the pyrrolizidine alkaloid senecionine, the alkenal trans-4-hydroxy-2-hexenal, and related alkenals. *Cell Biol Toxicol* **3**, 379–390 (1987).

161. Kim, H. Y., Stermitz, F. R. & Coulombe, R. A. Pyrrolizidine alkaloid-induced DNA-protein cross-links. *Carcinogenesis* **16**, 2691–2697 (1995).

162. National Toxicology Program. Toxicology and carcinogenesis studies of riddelliine (CAS No. 23246-96-0) in F344/N rats and B6C3F1 mice (gavage studies). *Natl Toxicol Program Tech Rep Ser* 1–280 (2003).

163. Molyneux, R. J. & Johnson, A. E. Extraordinary Levels of Production of Pyrrolizidine Alkaloids in Senecio riddellii. *J. Nat. Prod.* **47**, 1030–1032 (1984).

164. Hirono, I., Ueno, I., Aiso, S., Yamaji, T. & Haga, M. Carcinogenic activity of Farfugium japonicum and Senecio cannabifolius. *Cancer Letters* **20**, 191–198 (1983).

165. Harris, P. N. & Chen, K. K. Development of hepatic tumors in rats following ingestion of Senecio longilobus. *Cancer Res* **30**, 2881–2886 (1970).

166. Hirono, I., Mori, H., Yamada, K., Hirata, Y. & Haga, M. Carcinogenic activity of petasitenine, a new pyrrolizidine alkaloid isolated from Petasites japonicus Maxim. *J Natl Cancer Inst* **58**, 1155–1157 (1977).

167. Kuhara, K., Takanashi, H., Hirono, I., Furuya, T. & Asada, Y. CArcinogenic activity of clivorine, a pyrrolizidine alkaloid isolated from Ligularia dentata. *Cancer Lett* **10**, 117–122 (1980).

168. Hirono, I., Mori, H. & Culvenor, C. C. Carcinogenic activity of coltsfoot, Tussilago farfara l. *Gan* **67**, 125–129 (1976).

169. Schoental, R. & Cavanagh, J. B. Brain and spinal cord tumors in rats treated with pyrrolizidine alkaloids. *J Natl Cancer Inst* **49**, 665–671 (1972).

170. Peterson, J. E., Jago, M. V., Reddy, J. K. & Jarrett, R. G. Neoplasia and chronic disease associated with the prolonged administration of dehydroheliotridine to rats. *J Natl Cancer Inst* **70**, 381–386 (1983).

171. Schoental, R., Head, M. A. & Peacock, P. R. Senecio alkaloids; primary liver tumours in rats as a result of treatment with (1) a mixture of alkaloids from S. jacobaea Lin.; (2) retrorsine; (3) isatidine. *Br J Cancer* **8**, 458–465 (1954).

172. Schoental, R. & Head, M. A. Progression of Liver Lesions Produced in Rats by Temporary Treatment with Pyrrolizidine (Senecio) Alkaloids, and the Effects of Betaine and High Casein Diet. *Br J Cancer* **11**, 535–544 (1957).

173. Hirono, I., Mori, H. & Haga, M. Carcinogenic activity of Symphytum officinale. *J Natl Cancer Inst* **61**, 865–869 (1978).

174. Hirono, I. *et al.* Induction of hepatic tumors in rats by senkirkine and symphytine. *J Natl Cancer Inst* **63**, 469–472 (1979).

175. Brandänge, S., Lüning, B., Moberg, C. & Sjöstrand, E. Studies on orchidaceae alkaloids. XXIV. A pyrrolizidine alkaloid from Phalaenopsis cornu-cervi Rchb. f. *Acta Chem Scand* **25**, 349–350 (1970).

176. Cook, J. W., Duffy, E. & Schoental, R. Primary Liver Tumours in Rats following Feeding with Alkaloids of Senecio jacobaea. *Br J Cancer* **4**, 405-410.3 (1950).

177. Schoental, R. Pancreatic islet-cell and other tumors in rats given heliotrine, a monoester pyrrolizidine alkaloid, and nicotinamide. *Cancer Res* **35**, 2020–2024 (1975).

178. Schoental, R., Fowler, M. E. & Coady, A. Islet cell tumors of the pancreas found in rats given pyrrolizidine alkaloids from Amsinckia intermedia Fisch and Mey and from Heliotropium supinum L. *Cancer Res* **30**, 2127–2131 (1970).

179. Allen, J. R., Hsu, I. C. & Carstens, L. A. Dehydroretronecine-induced rhabdomyosarcomas in rats. *Cancer Res* **35**, 997–1002 (1975).

180. Campbell, J. G. VI.—An Investigation of the Hepatotoxic Effects in the Fowl of Ragwort (. *Proceedings of the Royal Society of Edinburgh, Section B: Biological Sciences* **66**, 111–130 (1956).

181. 15th Report on Carcinogens. *National Toxicology Program* https://ntp.niehs.nih.gov/whatwestudy/assessments/cancer/roc.

182. National Toxicology Program. Bioassay of lasiocarpine for possible carcinogenicity. *Natl Cancer Inst Carcinog Tech Rep Ser* **39**, 1–66 (1978).

183. Maura, F. *et al.* A practical guide for mutational signature analysis in hematological malignancies. *Nat Commun* **10**, 2969 (2019).

184. Van Hoeck, A., Tjoonk, N. H., van Boxtel, R. & Cuppen, E. Portrait of a cancer: mutational signature analyses for cancer diagnostics. *BMC Cancer* **19**, 457 (2019).

185. He, Y. *et al.* Mutational Signature Analysis Reveals Widespread Contribution of Pyrrolizidine Alkaloid Exposure to Human Liver Cancer. *Hepatology* **74**, 264 (2021).

186. Alexandrov, L. B. *et al.* Mutational signatures associated with tobacco smoking in human cancer. *Science* **354**, 618–622 (2016).

187. Saeidnia, S., Manayi, A. & Abdollahi, M. From in vitro Experiments to in vivo and Clinical Studies; Pros and Cons. *Curr Drug Discov Technol* **12**, 218–224 (2015).

188. Ebmeyer, J. *et al.* Hepatotoxic pyrrolizidine alkaloids induce DNA damage response in rat liver in a 28-day feeding study. *Arch Toxicol* **94**, 1739–1751 (2020).

189. Buchmueller, J. *et al.* Pyrrolizidine alkaloid-induced transcriptomic changes in rat lungs in a 28-day subacute feeding study. *Arch Toxicol* **95**, 2785–2796 (2021).

190. Zhan, T., Rindtorff, N. & Boutros, M. Wnt signaling in cancer. *Oncogene* **36**, 1461–1473 (2017).

191. Huang, Z., Chen, M., Zhang, J., Sheng, Y. & Ji, L. Integrative analysis of hepatic microRNA and mRNA to identify potential biological pathways associated with

monocrotaline-induced liver injury in mice. *Toxicol Appl Pharmacol* **333**, 35–42 (2017).

192. Chen, T., Li, Z., Yan, J., Yang, X. & Salminen, W. MicroRNA expression profiles distinguish the carcinogenic effects of riddelliine in rat liver. *Mutagenesis* **27**, 59–66 (2012).
193. Mei, N., Guo, L., Liu, R., Fuscoe, J. C. & Chen, T. Gene expression changes induced by the tumorigenic pyrrolizidine alkaloid riddelliine in liver of Big Blue rats. *BMC Bioinformatics* **8 Suppl 7**, S4 (2007).
194. Guo, L., Mei, N., Dial, S., Fuscoe, J. & Chen, T. Comparison of gene expression profiles altered by comfrey and riddelliine in rat liver. *BMC Bioinformatics* **8**, S22 (2007).
195. Wang, W. *et al.* A TMT-based shotgun proteomics uncovers overexpression of thrombospondin 1 as a contributor in pyrrolizidine alkaloid-induced hepatic sinusoidal obstruction syndrome. *Arch Toxicol* **96**, 2003–2019 (2022).
196. Abdelfatah, S. *et al.* Pyrrolizidine alkaloids cause cell cycle and DNA damage repair defects as analyzed by transcriptomics in cytochrome P450 3A4-overexpressing HepG2 clone 9 cells. *Cell Biol Toxicol* **38**, 325–345 (2022).

CHAPTER II RELATIVE TOXICITY AND COMPARATIVE PATHOLOGY OF SHORT-TERM EXPOSURE TO SELECT DEHYDRO-PYRROLIZIDINE ALKALOIDS (RIDDELLIINE, SENECIONINE, SENECIPHYLLINE, HELIOTRINE, LASIOCARPINE, RIDDELLIINE N-OXIDE, AND SENECIONINE N-OXIDE) IN MICE.

Abstract:

Dehydropyrrolizidine alkaloids (PAs) frequently poison livestock, wildlife, and humans and are arguably the most important plant-derived toxins. At least 600 individual PAs have been identified in approximately 3% of the world's flowering plants. PAs share a similar chemical structure but vary in toxic potential. In this study, male C57BL/6J mice were exposed to five PAs (riddelliine, senecionine, seneciphylline, heliotrine, lasiocarpine) and two PA N-oxides (riddelliine N-oxide, senecionine N-oxide) for ten days by oral gavage. There were three mice per dosing group and 24 mice per compound. Hepatic necrosis severity scores; serum ALT, ALP, and AST concentrations; and hepatic pyrrole concentrations were compared. Liver tissue bound pyrroles were quantified by high performance liquid chromatography and paired mass spectrometry. Riddelliine and

riddelliine N-oxide caused hepatocellular hypertrophy, swelling, and necrosis in centrilobular areas at low dose progressing to panlobular hepatocellular hypertrophy/swelling with multifocal necrosis as dose increased. Senecionine and senecionine N-oxide exposure resulted in similar hepatocyte lesions but initially affected midzonal and periportal areas. Seneciphylline exposure resulted in strictly midzonal hepatocyte hypertrophy/swelling at low doses. Lasiocarpine caused periportal hepatocyte hypertrophy/swelling and necrosis, only at the highest dose. Heliotrine was much less toxic as it only caused subtle centrilobular hepatocyte hypertrophy without necrosis at the highest dose. Hepatic necrosis scores, ALT and ALP, and liver pyrrole concentrations were positively correlated with dose for all compounds except heliotrine and lasiocarpine. Though acute PA poisoning has been previously reported to produce centrilobular hepatic necrosis, under these conditions, the hepatic lobular area initially affected, and production of PA pyrroles varies between compounds and was alkaloid specific.

Key words: Pyrrolizidine alkaloids, dehydropyrrolizidine alkaloids, riddelliine, senecionine, hepatotoxin, seneciphylline, heliotrine, lasiocarpine, riddelliine N-oxide, and senecionine N-oxide, hepatic degeneration, hepatic necrosis, mice.

Introduction:

Dehydropyrrolizidine alkaloid (PA) containing plants are distributed worldwide and estimated to be found in 3% of flowering plants. Livestock and wildlife are exposed either by grazing or by inadvertent contamination of hay or grain. The frequency of poisoning in livestock varies between locations, mainly determined by the presence of the

plants in the environment and the availability of alternative forages. In many countries, PA containing plants are invasive weeds that can contaminate crops.[1] Most are not palatable and subsequently poisoning is uncommon unless they contaminate more palatable feedstuffs. Some parts of the world have endemic populations of more palatable PA containing plants and, in these areas, toxicosis is common in livestock. For example, poisoning of cattle by *Senecio* spp. results in more than half of all plant poisonings in cattle in some areas in Brazil. [2] Human exposure to pyrrolizidine alkaloids occurs either by ingestion of contaminated grain, honey, milk, eggs or herbal products.[3–5] Additional intoxications are caused by intentional ingestion of medicinal or herbal products that may be used in making PA contaminated tinctures or teas.[6] More recently, it has been suggested that the most common source of exposure in people currently is through the ingestion of herbal teas though the morbidity of such exposures is difficult to determine.[7]

Chemistry:

PAs are composed of a necine base composed of two five carbon rings with a single nitrogen atom in the center. This base may be esterified at one or two binding sites at carbons one or seven to one or two necic acids forming monoesters, diesters or macrocyclic diesters. Figure 1 represents the basic PA structure. Stereochemistry of carbon 7 results in retronecine and heliotridine necine bases, characteristic of most toxic PAs. Variation in the necic acid/ester side chains further provide PA diversity and subsequent toxicity. The compounds evaluated in this study include three macrocyclic diesters (senecionine, seneciphylline, and riddelliine), two macrocyclic diester N-oxides (senecionine N-oxide and riddelliine N-oxide), one diester (lasiocarpine) and one monoester (heliotrine). See figure 2.2 for compound structures.

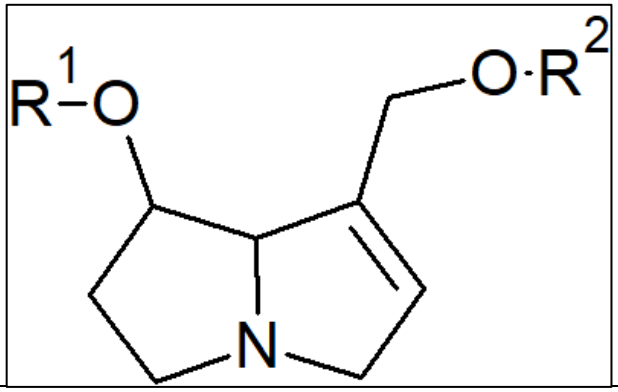

Figure 2.1: General chemical structure of a toxic pyrrolizidine alkaloid including the necine base and variable carboxylic acids (R1 and R2). Variation in both the base and the necic acids provide the diversity within this group of toxins. Though many pyrrolizidine alkaloids are not toxic, those that have a double bond between carbons 1 and 2 (dehydropyrrolizidine alkaloids) are toxic and have been associated with poisoning.

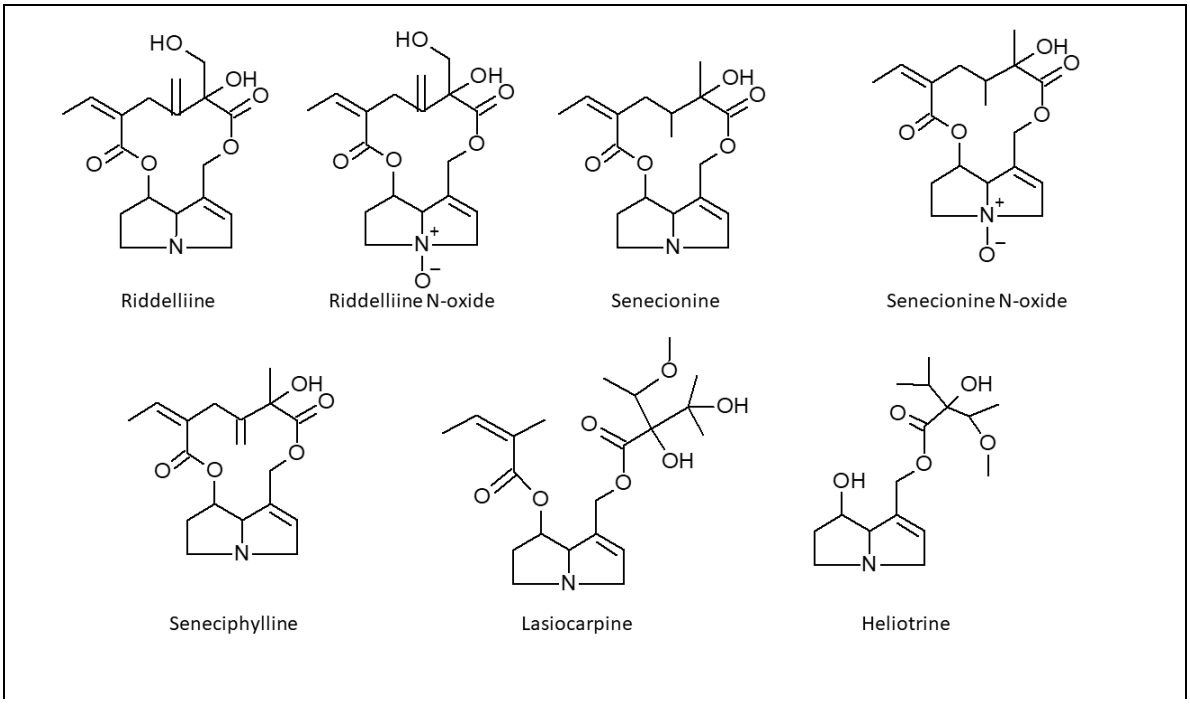

Figure 2.2: Chemical structure of the seven PAs evaluated in this study. Riddelliine, senecionine, and seneciphylline are macrocyclic diesters. Riddelliine and riddelliine N-oxide, and senecionine and senecionine N-oxide are identical aside from the oxygen that is bound to the nitrogen atom in the ring structure. Lasiocarpine is a diester and heliotrine is a monoester. Note the similarities in chemical structure.

Mechanism of Toxicity:

PAs are protoxins that, when bioactivated, are potent hepatotoxins which can also affect the kidneys and lungs. In addition to hepatotoxicity, these compounds are genotoxic and carcinogenic under some circumstances.[8] Bioactivation of the protoxins occurs mainly by interaction with the cytochrome p450 enzymes. The specific CYP450 enzyme responsible for bioactivation varies by species. In humans, CYP450 3A4 is thought to be the main enzyme responsible for bioactivation, whereas in rats it is CYP450 2B.[9,10] The bioactivation reaction is an oxidation reaction where the dehydropyrrolizidine alkaloid is converted to a didehydropyrrolizidine alkaloid. The didehydropyrrolizidine alkaloid, often referred to as a “pyrrole”, is a reactive electrophile and will readily interact with cellular macromolecules including nucleic acids and proteins.[11] This interaction results in a covalent bond between the toxic metabolite and a cellular protein or nucleic acid. This interaction with DNA results in the formation of DNA adducts and is also thought to be the main mechanism by which PAs act as carcinogens.[12] Certainly, this interaction with cellular proteins and nucleic acids results in hepatocellular degeneration and necrosis. This reaction takes place in hepatocytes and hepatic endothelial cells resulting in the liver being the first and most affected organ during toxicosis.[1] Within the liver, the site of metabolism should correspond with the distribution of the toxic insult. Concentrations of

CYP450 enzymes within the liver are reportedly 1.3 times greater in the centrilobular area (zone 3) when compared to periportal and midzonal areas (zone 1 and 2, respectively). [13,14] However, these reports were based on exposure to acetaminophen, which also requires CYP450 bioactivation, possibly involving different enzymes. Spatial distribution of CYP2B1/2 in rats was studied by Dail et al., (2007) and they observed differing increases of CYP2B1/2 after exposure to CYP450 inducers phenobarbital and dieldrin.[15] Phenobarbital induced greater CYP expression in midzonal hepatocytes, whereas dieldrin induced the greatest expression in centrilobular areas, followed by midzonal and last periportal zones. Spatial distribution of various CYP450 enzymes in the liver is likely more complex than the literature suggests, particularly when PA variation is considered.

Lesions:

When acute toxicity occurs, the hepatic lesions include hepatocellular hypertrophy, swelling, degeneration and necrosis. Affected hepatocytes become enlarged and have increased cytoplasmic eosinophilia in a specific area of the lobule. The cause of hepatocellular enlargement is most likely a continuum, starting with hypertrophy at lower doses and ending in cell swelling, degeneration and necrosis. The reported distribution of hepatic necrosis in acute toxicosis varies between sources. The pattern of necrosis for compounds that require metabolic activation by mixed function oxidase enzymes is generally described as centrilobular and multiple sources report that acute PA toxicosis results in centrilobular to massive or panlobular necrosis depending on the dose.[11,16–18] For example, California white chicks (*Gallus domesticus*) experimentally exposed to a variety of DHPAs consistently developed centrilobular to massive necrosis depending on

dose.[19] However, experimental poisoning in horses with *Cynoglossum officinale* (houndstongue) resulted in periportal necrosis and fibrosis.[20] The expected or assumed lesion distribution of toxicants requiring CYP450 bioactivation is based on a limited number of studies evaluating the lobular spatial distribution of the CYP450 enzymes or experimental exposure to few compounds.[13–15] The findings of this and previous experiments indicate that these generalizations are likely oversimplified.[20]

Chronic poisoning results in characteristic microscopic lesions including hepatic necrosis, ductular reaction (bile duct hyperplasia) and hepatic fibrosis and depending on the PA and duration may also produce hepatocellular megalocytosis. Fibrosis is typically periportal and may bridge with adjacent portal areas.[11,17,18] Karyomegaly has also been reported in renal tubular epithelial cells.[21] Veno-occlusive disease, also known as sinusoidal obstruction syndrome, with hepatic degeneration, portal hepatic fibrosis and portal vein hypertension occurs in some species.[11,22]

Hypothesis and Aims:

The experiments reported in this paper are a multipurpose study. The aims are to compare toxicosis in mice exposed to select PAs, characterize the lesions observed in mice following subacute toxicosis from these PAs, and to determine the appropriate dose for later carcinogenicity studies involving Pas in mice. We hypothesize that the five PAs and two PA N-oxides will cause dose dependent hepatocellular degeneration and necrosis. We further hypothesize that the PAs will differ in the severity of hepatocellular degeneration and necrosis. We expect that the PA N-oxides will cause less severe hepatic

necrosis when compared to their corresponding parent PAs. Also, the concentration of hepatic pyrroles is expected to correlate with the severity of hepatic necrosis.

Materials and Methods:

Animals:

Five- to thirteen-week-old, wild type C57BL/6J mice were used for this experiment. Mice were obtained from the United States Department of Agriculture Poisonous Plant Research Laboratory (USDA PPRL) breeding colony. Heterozygous B6.129S2 - Trp 53 ^{tm1Tyj}/J (JAX stock #002101) mice obtained from The Jackson Laboratory (Bar Harbor, Maine) were used to maintain a breeding colony at the United States Department of Agriculture Poisonous Plant Research Laboratory (USDA PPRL).[23] During breeding, heterozygous males were housed with heterozygous females, one of each per cage. Pups were weened at 4-5 weeks of age. After weening, a Trovan 100B/1.4 identification chip was implanted subcutaneously in the interscapular region, and a tail snip was obtained and frozen for genotyping. Genotyping was performed to determine whether mice were wild type, homozygous or heterozygous for the B6.129S2 - Trp 53 ^{tm1Tyj}/J mutation. DNA was isolated from mouse tail snips using the Gentra® Puregene® protocol according to the manufacturer's instructions (Qiagen, Germantown, MD). PCR primers for genotyping mice were obtained from *Integrated DNA Technologies*, Inc. (Coralville, IA). subcutaneously in the interscapular region, and a tail snip was obtained and frozen for genotyping. Genotyping was performed to determine whether progeny mice were wild type, homozygous or heterozygous for the B6.129S2 - Trp 53 ^{tm1Tyj}/J mutation according to the manufacturers.[24,25] PCR for genotyping were performed using the

protocol from Delidow et al. (1993).[26] Wild type mice did not carry the B6.129S2 - Trp 53 ^{tm1Tyj}/J mutation and will be referred to as wild type C57BL/6J mice, the genetic background for the B6.129S2 - Trp 53 ^{tm1Tyj}/J strain. All mice were acclimated to the cage environment for at least 7 days prior to treatment. Mice were housed in groups of five in Innovive cages (Innovive, San Francisco, CA) with Teklad ¼" corncob bedding (Envigo, Livermore, CA). The mouse facility has ambient light for 12 hours per day, and no ambient light overnight. Teklad Laboratory diet 8604 (Envigo, Livermore, CA). was fed ad libitum. Water was also provided ad libitum. Temperature and humidity were maintained at 70 degrees Fahrenheit and 30% respectively. This research was conducted with the approval of the Utah State University animal care and use committee (IACUC Protocol # 10065).

Purified Dehydropyrrolizidine Alkaloids:

PAs and PA N-oxides used were obtained from the USDA ARS Poisonous Plant Research Laboratory's collection that were previously isolated from various plant collections. Purity of 98% or greater was confirmed using liquid chromatography mass spectrometry and nuclear magnetic resonance (NMR).[27]

Experimental Design:

C57BL/6J male mice were randomly divided into groups of 24 for riddelliine, riddelliine N-oxide, senecionine, senecionine N-oxide, and heliotrine. Seneciphylline and lasiocarpine had groups of 25, with one more control mouse than the other compounds. Each dosing group included 3 mice. Mice were dosed as follows for each compound riddelliine 4, 8, 15, 30, 45 and 90 mg/kg/day, riddelliine N-oxide 15, 30, 45, 90, 180, 360

mg/kg/day, senecionine 2, 4, 8, 15, 30, 45 mg/kg/day, senecionine N-oxide 4, 8, 15, 30, 45, 90, and 180 mg/kg/day, seneciphylline 2, 4, 8, 15, 30, and 45 mg/kg/day, heliotrine 8, 15, 30, 45, 90, and 180 mg/kg/day, and lasiocarpine 1, 2, 4, 8, 15, and 30 mg/kg/day. Daily doses were divided in two. Mice were dosed for ten days. Differences in molecular weight between compounds are negligible, therefore milligram per kilogram dosing was used.

The dosing strategies used in these pilot studies were designed to follow a similar short-term PA exposure event as modeled by Brown et al. (2015).[28] They exposed heterozygous p53 knockout mice (B6.129S2 - Trp 53 ^{tm1Tyj}/J) to 5, 15 and 45 mg/kg/day riddelliine for ten days to determine if this mouse strain is an appropriate animal model for PA toxicity and carcinogenicity research. Brown et al. determined that mice were able to tolerate 45 mg/kg/day of riddelliine and that the heterozygous p53 knockout mouse has good potential for PA toxicity and carcinogenicity studies. Our aim was to identify the dose that results in clinical non-fatal intoxication over ten days of exposure, using Browns riddelliine dosing information as a guide. The range of doses used differed between compounds. Dosing ranges were selected based on published mouse or rat LD50 data as well as unpublished work performed at the USDA PPRL.[1,28–31] Mice did not tolerate more than 30 mg/kg/day of lasiocarpine in a previous unpublished pilot study performed at the USDA PPRL. Heliotrine has been well tolerated by mice and the dosing range of this compound was greater than all other PAs in the study. LD50 data was not available for the two NPA N-oxides. Most PA N-oxides are purportedly substantially less toxic than their parent PAs, therefore riddelliine N-oxide and senecionine N-oxide were

administered at dosing ranges of four times that of riddelliine and senecionine, respectively.[32]

During dosing, mice were evaluated daily for clinical signs suggestive of hepatotoxicity, including malaise, inappetence, or changes in mentation. Mice that developed clinical signs were immediately euthanized according to the IACUC guidelines. Mice were weighed using an Adventurer SL AS1502 scale (Ohaus, Parsippany, NJ) on Monday, Wednesday, and Friday, and again at the time of necropsy. Livers were weighed at the time of necropsy. Total weight loss was calculated using necropsy body weight subtracted by the weight from day 1 of exposure.

Mice were euthanized one day after the ten-day dosing period. Euthanasia was achieved using a CO2 chamber. Blood was collected during necropsy via cardiac puncture of the right ventricle for riddelliine, riddelliine N-oxide, senecionine N-oxide, and heliotrine. Blood was not collected for the earlier pilot studies including senecionine, seneciphylline, and lasiocarpine. Total blood volume collected ranged from 0.3-0.9 mL per mouse. Blood was centrifuged at 2500 rpm for 20 minutes, and serum concentrations of alanine aminotransferase (ALT), aspartate aminotransferase (AST), and alkaline phosphatase (ALP) were measured. The left liver lobe was collected and frozen for pyrrole quantification using high performance liquid chromatography and paired mass spectrometry (HPLC MS/MS). The remaining liver lobes along with the brain, heart, trachea, lungs, spleen, thyroid glands, kidneys, urinary bladder, adrenal glands, esophagus, stomach, duodenum, jejunum, ileum, colon, pancreas, and right testicle were placed in 10% neutral buffered formalin. After formalin fixation, tissues were processed and embedded in paraffin according to routine histologic techniques. Sections, 5-µm

thick, were stained with hematoxylin and eosin (H&E) stain according to standard methods and examined by light microscopy. Gross and microscopic lesions were recorded. Microscopic liver lesions were assigned a histologic grade for severity of hepatocellular necrosis.[33] Formalin-fixed liver was sectioned at 1-2 mm intervals and all 10-14 sections were evaluated and included in the hepatic necrosis score.

Hepatocellular Degeneration and Necrosis Scoring:

Microscopic grading of hepatocellular necrosis. A severity grade of minimal, mild, moderate, or severe was applied based on the amount of necrosis. These severity grades were each assigned a number between 0 and 4. In some of the lower dose groups, there were livers in which there was no necrosis, but hepatocyte hypertrophy and/or swelling was observed. In these cases, a necrosis score of zero was applied, but the lesion is described in the histopathology narrative.

Grade 0 = no microscopic evidence of hepatocellular necrosis.

Grade 1 = Minimal necrosis is defined as infrequent (less than 5 cells per 100X (3.14 square millimeters) field scattered individual cell necrosis.

Grade 2 = Mild necrosis is defined as frequent individual cell necrosis (5 or more necrotic cells per 100X field) and rare groups (one or less per 100X field) of necrotic cells.

Grade 3 = Moderate necrosis is defined as frequent groups of necrotic hepatocytes amounting to less than 3 groups of necrotic cells per 100X field.

Grade 4 = Severe necrosis is defined as groups of necrotic hepatocytes amounting to 3 or more groups per 100X field.

Figure 3 shows photomicrograph examples of each score.

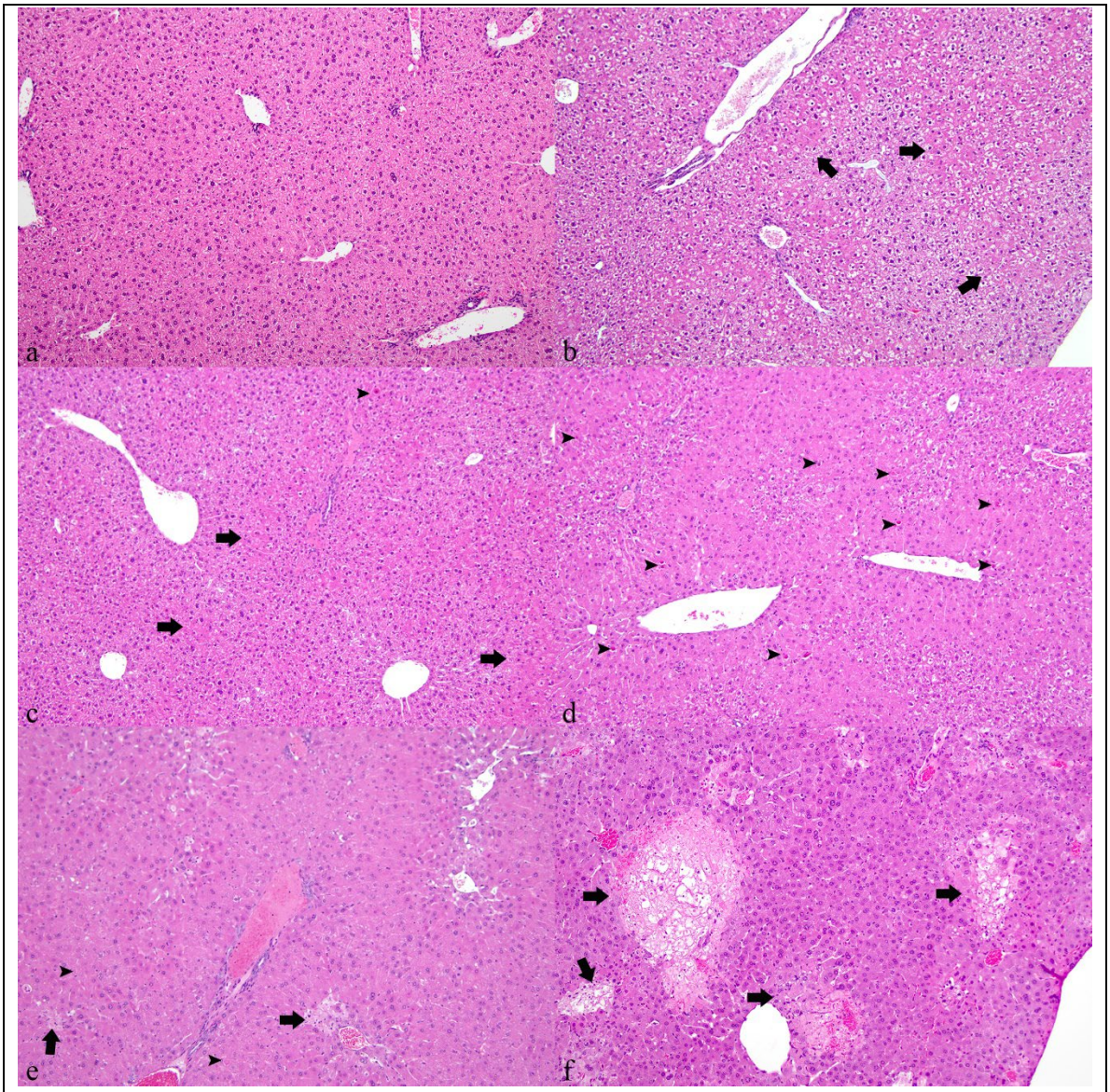

Figure 2.3: Images (a-f). Necrosis score examples. Mouse. Liver. a) liver from a control mouse. No microscopic changes are observed. Some control animals had rare minimal areas of lymphocytic and neutrophilic inflammation (not pictured). b) Necrosis score 0: liver from a mouse exposed to 8 mg/kg/day senecionine for 10 days. Hepatocytes were

multifocally enlarged (hypertrophy or cell swelling) (arrows) in midzonal and periportal areas, but no necrosis was observed. Hepatocyte enlargement (hypertrophy/swelling) without necrosis was given a score of zero. c) Necrosis score 1: liver of a mouse exposed to 8 mg/kg/day seneciphylline. The midzonal hepatocytes are hypertrophic/swollen (arrows) and rare individual hepatocytes undergo necrosis (arrowhead). d) Necrosis score 2: liver of a mouse exposed to 30 mg/kg/day riddelliine N-oxide for ten days. Hepatocyte hypertrophy/swelling in centrilobular to midzonal areas. Individual cell necrosis is frequently observed in areas of cell hypertrophy/swelling (arrowheads). e) Necrosis score 3: liver from a mouse exposed to 45 mg/kg/day senecionine for ten days. Small groups of contiguous hepatocytes undergo coagulative necrosis (arrows). These foci of necrosis are generally centrilobular and relatively rare, with 2 or fewer foci per 100X field. Individual cell necrosis (arrowheads) is also present in some but not all livers given this score. Mice with such necrosis had diffuse hepatocyte hypertrophy/swelling in periportal and midzonal areas. f) Necrosis score 4: liver from a mouse exposed to 90 mg/kg/day senecionine N-oxide. Frequent areas of coagulative necrosis (3 or more per 100X field) (arrows) are observed. Hepatocyte hypertrophy/swelling affects nearly all areas, sparing only some centrilobular hepatocytes.

Hepatic Pyrrole Detection:

The toxic metabolite was detected in liver using HPLC MS/MS. See Brown et al. (2015) for a complete description of this detection method. Solvents and reagents were purchased from Sigma-Aldrich (St. Louis, MO). Ethanolic silver nitrate was prepared by combining via sonication, 625 mg silver nitrate, 0.5 mL deionized water and 25 mL absolute ethanol. Ehrlichs reagent was prepared by combining 0.2 g ρ-Dimethylaminobenzaldehyde (DMABA), 10 mL absolute ethanol, and 2 mL BF_3O.

Briefly, liver was freeze-dried and pulverized into a powder using a Retsch MM301 ball mill (Verder Scientific, Newtown, PA), at a frequency of 20 revolutions per second, for 20 minutes with copper BBs (Crosman Corp., Bloomfield, NY). Approximately 50 mg of pulverized freeze-dried liver was mixed with 1.0 mL ethanolic silver nitrate and 0.01 mL of 0.1% trifluoroacetic acid and mixed on an auto rotator overnight (approximately 16 hours). The mixture was then centrifuged at 13000 G for ten minutes. Twenty uL of the supernatant was then combined with 170 uL absolute ethanol, and ten uL Ehrlich's reagent. Finally, this mixture was analyzed using an Agilent HPLC-esi(+) (Agilent, Santa Clara, CA) and Velos Pro LTQ mass spectrometer (Thermo Fisher Scientific, Waltham, MA). Quantification was achieved using an external calibration curve established from control standards. The calibration control standards were prepared using purchased monocrotaline (Sigma-Aldrich, St. Louis, MO), which is converted to dehydromonocrotaline as described by Brown et al. (2016).[19] Positive controls run alongside samples included an experimentally poisoned horse and pig from the USDA PPRL collection. The resulting pyrrole concentration (nmol/mL) of sample was converted to nmol/g of liver.

Statistical Analysis:

Statistical analysis of serum biochemistry analytes, liver pyrrole concentration, hepatic necrosis scores, and weights was performed using GraphPad prism version 9.3.1. Statistical comparisons were made within the same compound according to dose and among compounds at the same dose. Control animals not exposed to any compound, and vehicle control animals exposed to ethanol by oral gavage from each individual pilot study were combined. Serum biochemistry values, hepatic pyrrole concentrations, and

weight data were compared to the control values using ordinary one-way analysis of variance (ANOVA) tests. Post-hoc comparison between PAs was achieved using individual t-tests. Pearson correlations were used to determine the strength of correlation between dose of PA and serum biochemistry values (ALP, ALT, AST) and pyrrole concentrations. Spearman correlation was used to determine the strength of correlation between hepatic necrosis scores and dose, serum biochemistry values and hepatic pyrrole concentration. A students t-test was used to compare weights of the control groups to the vehicle groups. One way ANOVA was used to compare mean weight loss and liver weight to body weight ratios of all compounds of the same dose.[34]

Results:

Clinical Disease:

Clinical Signs:

Weight loss was observed in all compound groups except heliotrine and the control groups. Clinical signs which were rarely observed include general malaise, hunched posture, and lethargy. Mice in the 180 mg/kg/day senecionine N-oxide group did not survive the ten days of dosing. Two out of three mice became comatose one hour after being gavaged with the fourth dose and were then euthanized. The third mouse in this group was found dead on the morning of day 3 with no premonitory signs. Mice that were given 90 mg/kg/day senecionine N-oxide exhibited malaise, hunched posture and substantial weight loss and were euthanized after seven (1 out of 3) or ten (2 out of 3) doses at the onset of these signs. All three mice in the highest dose group of riddelliine N-

oxide (360 mg/kg/day) were found dead on the morning of day 3, after receiving four doses. Other than these animals, no clinical signs beyond weight loss were observed. Mice that did not survive ten days of exposure were not included in statistical analyses but were still necropsied and lesions were documented.

Weight Analysis:

Weight Loss:

The weight loss means of the combined control groups (0.21 +/- 0.54 g.) and the combined vehicle group (0.45 +/- 0.772 g.) were not significantly different. Minimal weight loss was observed in vehicle dosed animals in the seneciphylline, riddelliine, and senecionine N-oxide groups. For all compounds except seneciphylline and lasiocarpine, no significant difference between weight loss or liver to body weight ratios were present between the control and vehicle groups. Senecionine exposed mice exhibited minimal weight loss at doses as low as 8 mg/kg/day, but the weight loss was not statistically significant at any dose when compared to the combined control and vehicle groups. Mice exposed to seneciphylline exhibited weight loss at all doses and weight loss increased with dose. Weight loss was statistically significant only in the highest two dosing groups of 30 and 45 mg/kg/day amounting to 2.4 +/- 0.99 g and 4.14 +/- 1.9 g respectively. Mice dosed with the vehicle also lost a small amount of weight in this group (1.033 +/- 0.09 g). Riddelliine exposed mice exhibited weight loss in all dosed groups, but the difference was only statistically significant in the highest two dosing groups of 45 and 90 mg/kg/day, amounting to 2.23 +/- 0.37 g and 3.20 +/- 0.27 g respectively. The vehicle exposed mice had an average weight loss of 1.177 g +/- 0.3372. Average weight loss

increased with dose. Senecionine N-oxide exposed mice exhibited weight loss in all dosing groups. The weight loss was statistically significant when compared to the combined vehicle and control groups for all doses except 8 mg/kg/day. The vehicle dosed mice also lost a small amount of weight (0.6 g +/- 0.4384). Weight loss increased with dose until the 30 mg/kg/day dosing group and the 45, 90 and 180 mg/kg/day groups lost a similar amount of weight. Comparison with the highest two dosing groups (90 and 180 mg/kg/day) are imperfect given these mice did not survive the dosing period. Even so, these weights are included in discussion as they still represent a start and end point in the dosing period and these weights provide important information regarding severity of toxicity. Riddelliine N-oxide dosed mice exhibited weight loss in all dosed groups. Weight loss was significant in the groups exposed to 45, 90, and 180 mg/kg/day groups which lost 3.93 +/- 3.22 g, 4.39 +/- 0.13 g, and 5.10 +/- 1.18 g respectively. The 360 mg/kg/day group died after two days of dosing but lost an average of 2.17 +/- 0.44 g, which is likely significant but cannot be compared to other groups. Lasiocarpine exposure only caused weight loss in the highest dosing group (30 mg/kg/day), which lost an average of 4.31 g. Mice exposed to heliotrine did not lose significant amounts of weight in any dosing group.

Table 2.1: Total average weight loss (g.) ± standard deviation for each PA (rows). by dose (columns).

Dose (mg/kg/day)	4	8	15	30	45	90	180
Riddelliine	1.69 ± 0.41	1.29 ± 0.2	1.21 ± 0.14	1.35 ± 0.66	2.23 ± 0.37	3.20 ± 0.27	ND
Senecionine	0.003 ± 0.39	0.47 ± 0.38	0.55 ± 0.45	0.36 ± 0.75	1.77 ± 0.84	ND	ND
Seneciphylline	1.24 ± 0.11	1.44 ± 0.49	1.30 ± 0.47	2.40 ± 0.99	4.14 ± 1.94	ND	ND
Lasiocarpine	0.38 ± 0.19	0.66 ± 0.50	1.01 ± 0.37	4.31 ± 0.66	ND	ND	ND
Heliotrine	ND	0.76 ± 0.49	-0.12 ± 1.46	-0.32 ± 1.28	1.24 ± 0.17	1.29 ± 0.52	1.66 ± 0.69
Riddelliine N-oxide	ND	ND	0.94 ± 0.51	2.17 ± 0.48	3.96 ± 3.22	4.39 ± 0.13	5.10* ± 1.18
Senecionine N-oxide	ND	1.10 ± 0.31	2.69 ± 0.99	5.47 ± 1.30	3.72 ± 1.64	4.30* ± 1.74	3.61* ± 1.04
Control	0.21 ± 0.54	0.21 ± 0.54	0.21 ± 0.54	0.21 ± 0.54	0.21 ± 0.54	0.21 ± 0.54	0.21 ± 0.54
Vehicle	0.45 ± 0.77	0.45 ± 0.77	0.45 ± 0.77	0.45 ± 0.77	0.45 ± 0.77	0.45 ± 0.77	0.45 ± 0.77

*Mice exposed to 90 and 180 mg/kg/day of senecionine did not survive the complete ten days of dosing and are excluded from statistical analysis.

There was no significant difference between the mean liver to body weight ratios of the vehicle group and the control group. Weight loss values and liver to body weight ratios can be seen in tables 1 and 2, respectively. Liver to body weight ratios were calculated for mice using liver weight and body weight measured at necropsy. There was no statistically significant difference between the liver to body weight ratios of the control mice and the vehicle exposed mice ($p=0.055$) and these groups were combined for the purpose of determining which doses had statistically significant differences in liver to body weight ratios.

Microscopic evidence of cellular hypertrophy/swelling was observed in all groups with significant increases except for the group exposed to senecionine at 2 mg/kg/day. A significant increase ($p \leq 0.05$) in liver to body weight ratios was observed in mice exposed to riddelliine at doses of 30, 45, and 90 mg/kg/day compared to the combined control and vehicle exposed mice. Mice exposed to senecionine had significant increases in liver to body weight ratio in all groups except for the 4 mg/kg/day dosing group, when compared to the combined control and vehicle exposed mice ($p \leq 0.05$). Mice exposed to seneciphylline had significant increases in liver to body weight ratio in the 15, 30 and 45 mg/kg/day dosing groups ($p \leq 0.05$). Mice exposed to senecionine N-oxide had significant increases in liver to body weight ratios for all dosing groups except the 8 mg/kg/day dosing groups ($p \leq 0.05$). The 90 and 180 mg/kg dosing groups did not survive the ten days of dosing and are excluded from comparisons. Mice exposed to riddelliine N-oxide had significant increases in liver to body weight ratios for all dosing groups. Mice exposed to lasiocarpine and heliotrine had no significant increases in liver to body weight ratios.

Table 2.2. Percentage of liver to body weight ratio (%).

Dose (mg/kg/day)	4	8	15	30	45	90	180
Riddelliine	5.75 ± 0.31	5.45 ± 0.14	6.22 ± 0.33	8.12 ± 0.12	9.19 ± 0.55	9.32 ± 0.44	ND
Senecionine	6.31 ± 0.15	6.63 ± 0.33	7.06 ± 0.62	9.00 ± 0.43	9.34 ± 0.42	ND	ND
Seneciphylline	5.55 ± 0.64	5.85 ± 0.18	6.81 ± 0.55	9.17 ± 0.48	8.69 ± 0.20	ND	ND
Lasiocarpine	5.73 ± 0.15	5.96 ± 0.36	5.27 ± 0.15	4.62 ± 0.30	ND	ND	ND
Heliotrine	ND	5.45 ± 0.76	5.67 ± 0.17	6.17 ± 0.52	6.00 ± 0.37	6.30 ± 0.06	6.28 ± 0.43
Riddelliine N-oxide	ND	ND	7.32 ± 0.35	8.19 ± 0.43	10.11 ± 0.21	10.75 ± 0.13	9.30 ± 0.13
Senecionine N-oxide	ND	5.96 ± 0.14	6.85 ± 0.59	7.36 ± 0.94	8.54 ± 0.24	*6.50 ± 0.10	*7.15 ± 0.36
Control	5.42 ± 0.59	5.42 ± 0.59	5.42 ± 0.59	5.42 ± 0.59	5.42 ± 0.59	5.42 ± 0.59	5.42 ± 0.59
Vehicle	5.77 ± 0.53	5.77 ± 0.53	5.77 ± 0.53	5.77 ± 0.53	5.77 ± 0.53	5.77 ± 0.53	5.77 ± 0.53

*Mice exposed to 90 and 180 mg/kg/day of senecionine did not survive the complete ten days of dosing and are excluded from statistical analysis.

Serum Biochemistry:

Serum volumes were limited, and priority was given to biochemistry analytes relating to liver disease including alanine aminotransferase (ALT), aspartate aminotransferase

(AST), alkaline phosphatase (ALP), and gamma glutamyl transferase (GGT). Serum creatinine kinase (CK) was measured to differentiate muscle induced elevations in ALT and AST from hepatic elevation in groups exposed to senecionine N-oxide, riddelliine N-oxide and heliotrine. Serum AST concentrations were not statistically correlated with dose or with CK concentrations and the value of measuring AST in this study is unclear. Mean serum concentrations of ALP, ALT, and AST with standard deviations are presented in table 2.3, 2.4 and 2.5, respectively.

Correlations Between Liver Necrosis Score, Serum Biochemistry Parameters, and Pyrrole Concentration by Compound:

Riddelliine:

Dose of riddelliine correlated positively with serum concentrations for ALT ($r = 0.9241$, $p < 0.0001$), ALP ($r = 0.9302$, $p < 0.0001$), AST ($r = 0.4601$, $p = 0.0208$) and GGT ($r = 0.6297$, $p = 0.0158$). Microscopic necrosis score also correlated positively with ALT ($r_s = 0.8434$, $p < 0.0001$), ALP ($r_s = 0.8020$, $p < 0.0001$), AST ($r_s = 0.6121$, $p = 0.0015$), and GGT ($r_s = 0.6290$, $p = 0.0165$) for riddelliine. Liver pyrrole concentration correlated positively with ALT ($r = 0.6340$, $p = 0.0009$), ALP ($r = 0.5373$, $p = 0.0146$), AST ($r = 0.5582$, $p = 0.0046$) and GGT ($r = 0.5380$, $p = 0.0472$).

Riddelliine N-oxide:

Dose of riddelliine N-oxide correlated positively with serum concentrations of ALT ($r = 0.5398$, $p < 0.0001$), ALP (r 0.9375, $p < 0.0001$), AST ($r = 0.5562$, $p = 0.0088$) and GGT ($r = 0.7679$, $p < 0.0001$). Microscopic necrosis score correlated positively with ALT ($r_s = 0.8852$, $p = 0.0001$), ALP ($r_s = 0.8706$, $p < 0.0001$), AST ($r_s = 0.6703$, $p = 0.0009$), and

GGT (r_s = 0.6399, p < 0.0018). Liver pyrrole concentration correlated positively with ALT (r = 0.5743, p = 0.0065), ALP (r = 0.4909, p = 0.0238), and AST (r = 0.5124, p = 0.0176) but not GGT (r = 0.2887, p = 0.2).

Senecionine N-oxide:

Mice dosed with 90 and 180 mg/kg/day of senecionine N-oxide died or were euthanized early due to malaise and weight loss. The mice that did not complete the ten-day dosing period were excluded from statistical analysis. Doses of senecionine N-oxide correlated positively with serum concentrations of ALT (r = 0.6139, p = 0.0024), and AST (r = 0.8381, p < 0.0001) but not for ALP (r = 0.025, p = 0.9105). GGT concentration was not measured for senecionine N-oxide. Microscopic necrosis score correlates positively with concentrations of ALT (r_s = 0.8332, p = 0.0001), and AST (r_s = 0.7465, p = 0.001), and ALP (r_s = 0.6467, p = 0.0064). Liver pyrrole concentration did not have statistically significant Pearson correlations with ALT, AST, or ALP.

Heliotrine:

Concentrations of serum ALT, ALP, AST and GGT were not significantly different for mice exposed to heliotrine at any dose when compared to controls. Dose of heliotrine did not correlate with any of the serum biochemistry analyte concentrations. Pearson correlation coefficients are as follows; ALT (r = -0.2029, p = 0.3417), ALP (r = -0.3102, p = 0.1401), AST (r = -0.2445, p = 0.2496), GGT (r = -0.1914, p = 0.3702). Microscopic necrosis score and pyrrole concentration did not correlate with ALT, ALP, AST or GGT.

Serum Biochemistry Comparison Between Compounds:

Comparison between compounds will be presented for doses 15, 30, and 45 mg/kg/day as these are the doses shared by the four compounds with serum biochemistry data.

Alkaline Phosphatase:

Table 2.3: Serum ALP (Unit/Liter) by dose (mean ± standard deviation):

Dose (mg/kg/day)	Riddelliine	Riddelliine N-oxide	Senecionine N-oxide	Heliotrine
Control	186.9 ± 81.58	186.9 ± 81.58	186.9 ± 81.58	186.9 ± 81.58
8	138.7 ± 45.5	ND	188.7 ± 212.0	158.0 ± 81.2
15	209.7 ± 40.3	175.0 ± 13.0	1528.7 ± 1057.3	203.7 ± 58.3
30	323.7 ± 119.9	186.0 ± 30.1	3033.0 ± 1141.3	212.3 ± 61.3
45	307.5 ± 20.5	370.7 ± 112.2	1189.0 ± 598.4	170.0 ± 23.1
90	935.0 ± 68.8	516.0 ± 169.5	*628.3 ± 593.1	173.7 ± 27.5

*Mice exposed to 90 mg/kg/day senecionine N-oxide did not survive the ten-day dosing period and are therefore excluded from statistical comparisons. ND = not dosed, mice were not exposed to 8 mg/kg/day of riddelliine N-oxide.

Serum ALP Comparisons by Dose:

At 15 mg/kg/day only senecionine N-oxide had an ALP concentration that was significantly different than the control group ($p = 0.0145$). At 30 mg/kg/day, significant differences between ALP concentration means and the control group were observed for riddelliine ($p = 0.0154$) and senecionine N-oxide ($p<0.0001$). Serum ALP concentrations of riddelliine and senecionine N-oxide were not significantly different. At 45 mg/kg/day, mean ALP concentrations of riddelliine N-oxide ($p = 0.0017$) and senecionine N-oxide ($p < 0.0001$) were significantly different than the control group. Significant differences in ALP concentrations were present between riddelliine and heliotrine ($p = 0.066$),

riddelliine N-oxide and heliotrine ($p = 0.0386$), and senecionine N-oxide and heliotrine ($p = 0.0360$). At 90 mg/kg/day, significant differences existed between ALP means of riddelliine ($p < 0.0001$) and riddelliine N-oxide ($p < 0.0001$) when compared to the control group. Significant differences between the ALP concentration means of riddelliine and heliotrine ($p < 0.0001$), riddelliine and riddelliine N-oxide (0.0166), and heliotrine and riddelliine N-oxide ($p = 0.026$) were noted.

Table 2.4. Serum ALT (Units/Liter) by dose (mean ± standard deviation).

Dose (mg/kg /day)	Riddelliine	Riddelliine N-oxide	Senecionine N-oxide	Heliotrine
Contr.	87.75 ± 79.42	87.75 ± 79.42	87.75 ± 79.42	87.75 ± 79.42
8	66.0 ± 21.7	ND	188.7 ± 212.0	317.3 ± 177.1
15	95.7 ± 23.7	147.7 ± 28.2	1528.7 ± 1057.3	135.3 ± 134.8
30	661.3 ± 272.9	463.7 ± 127.8	3033.0 ± 1144.3	60.67 ± 24.4
45	2127.7 ± 353.2	1779.3 ± 528.6	1869.0 ± 598.4	53.0 ± 10.58
90	2642.3 ± 440.8	3621.3 ± 2960.6	*628.3 ± 593	189.3 ± 244.1

*Mice exposed to 90 mg/kg/day senecionine N-oxide did not survive the ten-day dosing period and are therefore excluded from statistical comparisons. ND = not dosed, mice were not exposed to 8 mg/kg/day of riddelliine N-oxide.

Serum ALT Comparisons by Dose:

At doses of 15 mg/kg/day, significant differences were observed between ALT concentration means of the control group and senecionine N-oxide ($p >0.0001$). At 30, 45 and 90 mg/kg/day, there were significant differences in ALT concentrations between the control group and riddelliine ($p < 0.0001$), riddelliine N-oxide ($p < 0.0001$), and

senecionine N-oxide ($p < 0.0001$, excluding the 90 mg/kg/day group). Heliotrine exposure did not result in significant differences in ALT concentrations compared to the control group. Mice exposed to riddelliine, riddelliine N-oxide, and senecionine N-oxide had elevations in ALT concentrations that correlated well with histopathologic findings. At 30 mg/kg per day, significant differences were observed between the ALT concentrations means of riddelliine and heliotrine ($p = 0.0192$), and riddelliine and senecionine N-oxide ($p = 0.0335$). At 45 mg/kg/day, there were significant differences between the ALT concentration means of riddelliine and heliotrine ($p = 0.0005$). At 90 mg/kg/day there were significant differences between the ALT concentration means of riddelliine and heliotrine ($p = 0.0011$).

Table 2.5. Serum AST (Units/Liter) by dose (mean ± standard deviation).

Dose (mg/kg /day)	Riddelliine	Riddelliine N-oxide	Senecionine N-oxide	Heliotrine
Contr.	669.3 ± 776.3	669.3 ± 776.3	669.3 ± 776.3	669.3 ± 776.3
8	514.7 ± 286.4	ND	333.3 ± 240.6	2219.0 ± 2309.2
15	421.7 ± 186.4	540.0 ± 325.6	1962.7 ± 2077.0	1591.7 ± 2115.4
30	748.7 ± 302.0	626.0 ± 394.5	3787.0 ± 1750.8	368.7 ± 151.3
45	3043.0 ± 2269.2	1589.3 ± 1188.0	2270.3 ± 779.3	343.0 ± 92.3
90	1939.3 ± 572.5	2297.7 ± 1160.7	*2380.0 ± 109.2	1208.0 ± 1686.2

*Mice exposed to 90 mg/kg/day senecionine N-oxide did not survive the full ten-day dosing period and are therefore excluded from statistical comparisons. ND = not dosed, mice were not exposed to 8 mg/kg/day of riddelliine N-oxide.

Serum AST Comparisons by Dose:

At doses of 15 mg/kg/day, there were no significant differences between AST concentration means and the control group. At 30 mg/kg/day, significant differences

between the AST concentration means of the control group and senecionine N-oxide ($p < 0.0001$), and riddelliine and senecionine N-oxide ($p = 0.0494$) were observed. At 45 mg/kg/day, there were significant differences between the AST concentration means of riddelliine and the control ($p = 0.006$), senecionine N-oxide and the control ($p = 0.0025$, and senecionine N-oxide and heliotrine ($p = 0.0131$). At 90 mg/kg/day, significant differences between the AST means of riddelliine ($p = 0.006$) and the control group were noted.

Microscopic Findings:

Characterization of Microscopic Lesions by Compound:

The lesions induced by all compounds included hepatocellular hypertrophy, swelling, degeneration and necrosis. Hepatocellular necrosis was always accompanied by hepatocyte enlargement. Hepatocyte hypertrophy and cell swelling occurred in PA specific lobular zonal distribution at lower doses and for riddelliine, riddelliine N-oxide, senecionine, senecionine N-oxide, and seneciphylline. The distribution of cell swelling progressed to include additional zones or became panlobular, with scattered foci of necrosis as dose was increased. Hepatocyte hypertrophy/swelling and increased cytoplasmic eosinophilia was interpreted as a continuum starting with hepatocyte hypertrophy at the dose in which the lowest observed effect level was observed, and progressing to cell swelling, a degenerative change, as dose was increased. Hepatocyte hypertrophy is characterized by zonal increases in hepatocyte size with increased cytoplasmic eosinophilia, as is observed in the lower doses of the macrocyclic diester PAs tested in this experiment, and the highest dose of lasiocarpine (30 mg/kg/day).[35] The

compounds can be placed into three groups, greatest, intermediate, and least hepatotoxic based on the microscopic lesions. The group with the greatest hepatotoxicity included senecionine N-oxide, senecionine and seneciphylline. Riddelliine and riddelliine N-oxide comprised the group with intermediate hepatotoxicity. Lasiocarpine and heliotrine were the least hepatotoxic. There were not significant differences between the mean necrosis scores of senecionine N-oxide, senecionine and seneciphylline; between riddelliine and riddelliine N-oxide; or between heliotrine and lasiocarpine. Within the least toxic group, lasiocarpine was more hepatotoxic than heliotrine, as heliotrine did not cause necrosis at any dose. Extrahepatic lesions were not observed for any of the PAs or PA N-oxides. Microscopic lesions for each compound at specific doses are described below.

Seneciphylline:

Mice that were exposed to seneciphylline by gastric gavage exhibited multifocal midzonal hepatocyte hypertrophy/swelling at doses as low as 8 mg/kg/day (3/3 mice). One of these mice had infrequent individual hepatocellular necrosis within areas of hypertrophy/swelling. Hepatocyte hypertrophy/swelling was more widespread at higher doses affecting midzonal and periportal hepatocytes, and then progressing to panlobular. At doses of 15 mg/kg/day or greater, diffuse midzonal hepatocellular hypertrophy/swelling with necrosis affected individual hepatocytes and groups of contiguous hepatocytes (3/3 mice). Mice exposed to 30 mg/kg/day had hepatocyte hypertrophy/swelling in midzonal and periportal to panlobular areas (3/3 mice), with frequent groups of contiguous necrotic hepatocytes. The 45 mg/kg/day dosing group had panlobular hepatocellular hypertrophy/swelling, degeneration, and necrosis affecting

individual hepatocytes and groups of necrotic cells (3/3 mice). Dose had a strong positive correlation with hepatic necrosis score ($r = 0.09047$, $p < 0.0001$). See figure 2.4.

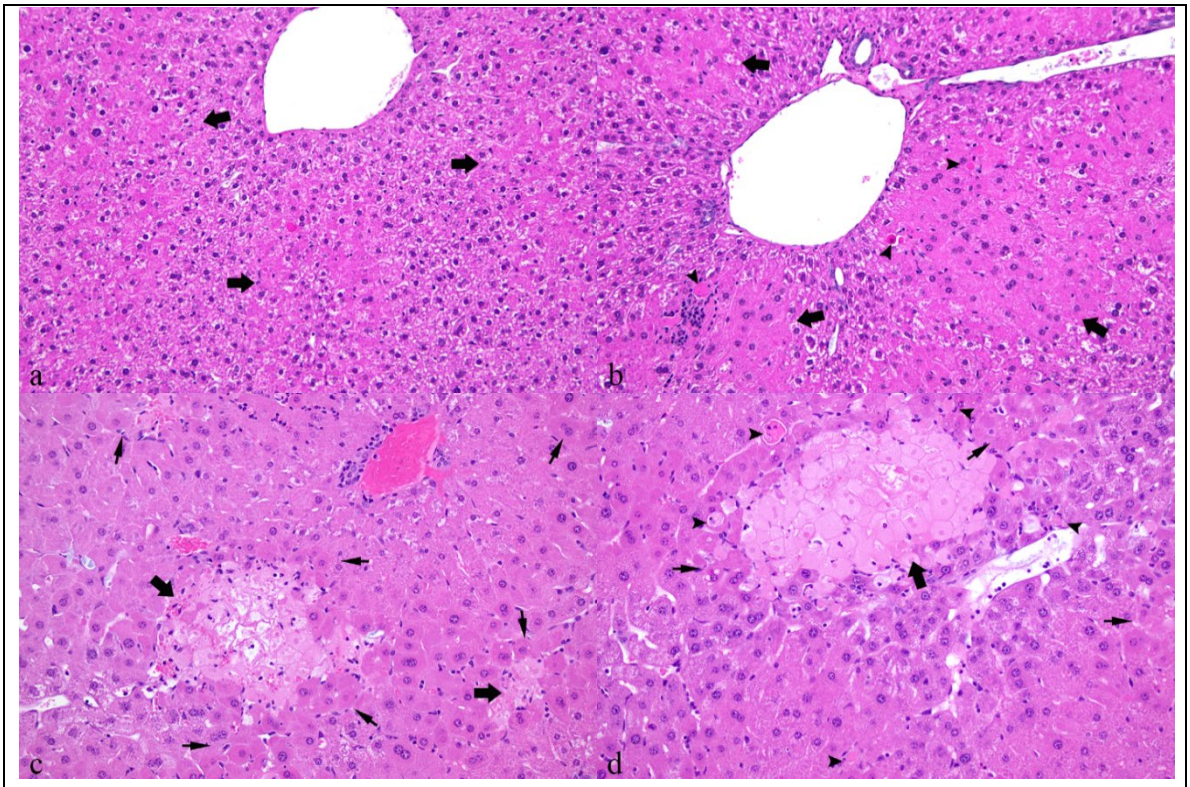

Figure 2.4. Images a-d.Liver of mice exposed to seneciphylline for ten days at various doses. a) 8 mg/kg/day. Contiguous hepatocytes in midzonal areas are multifocally hypertrophic/swollen (arrows). b) 15 mg/kg/day. Midzonal hepatocytes are diffusely affected by hypertrophy/swelling (arrows). Areas of hepatocellular hypertrophy/swelling are highlighted by the lack of small clear cytoplasmic vacuoles (glycogen) which are observed in the hepatocytes of control animals and low dose groups. Within areas of hepatocellular hypertrophy/swelling, individual hepatocytes are small and shrunken with pyknotic nuclei and hypereosinophilic cytoplasm (necrosis) multifocally (arrowheads). c) 30 mg/kg/day. Panlobular hepatocellular hypertrophy/swelling with multiple foci of coagulative necrosis (arrows). Hepatocytes adjacent to areas of necrosis are enlarged or shrunken with hypereosinophilic cytoplasm (degeneration) (small arrows). Individual hepatocellular necrosis is also observed (not pictured). d) 45 mg/kg/day. Microscopic changes are similar but more severe than those observed in the 8, 15 and 30 mg/kg/day dosing groups. Foci of coagulative necrosis (arrow) are frequent. Hepatocytes adjacent

to areas of necrosis are hypereosinophilic, enlarged or shrunken, sometimes with clear cytoplasmic vacuoles (small arrows). Individual hepatocellular necrosis is observed (arrowheads). Hematoxylin and eosin stain. 200X.

Senecionine:

One of three mice dosed with 4 mg/kg/day had a single, 0.5 mm diameter focus of coagulative necrosis. Mice exposed to 8 mg/kg/day had multifocal midzonal and periportal hepatocellular hypertrophy/swelling (3/3 mice) and one of these mice had infrequent foci of individual cell necrosis. 15 mg/kg/day exposure resulted in multifocal to coalescing hepatocellular hypertrophy/swelling in midzonal and periportal areas with infrequent individual cell necrosis (2/3 mice) or 2-6 foci of necrotic hepatocytes per 100X field (1/3 mice). The 30 mg/kg/day dosing group had multifocal to coalescing midzonal and periportal hepatocellular hypertrophy/swelling and degeneration with individual hepatocytes and foci of necrosis (3/3 mice). Mice exposed to 45 mg/kg/day had panlobular hepatocellular hypertrophy/swelling, degeneration and individual and groups of necrotic cells (3/3 mice). Severity of necrosis increased with dose. Dose had a strong positive correlation with hepatic necrosis score ($r = 0.8841$, $p < 0.0001$). See figure 2.5.

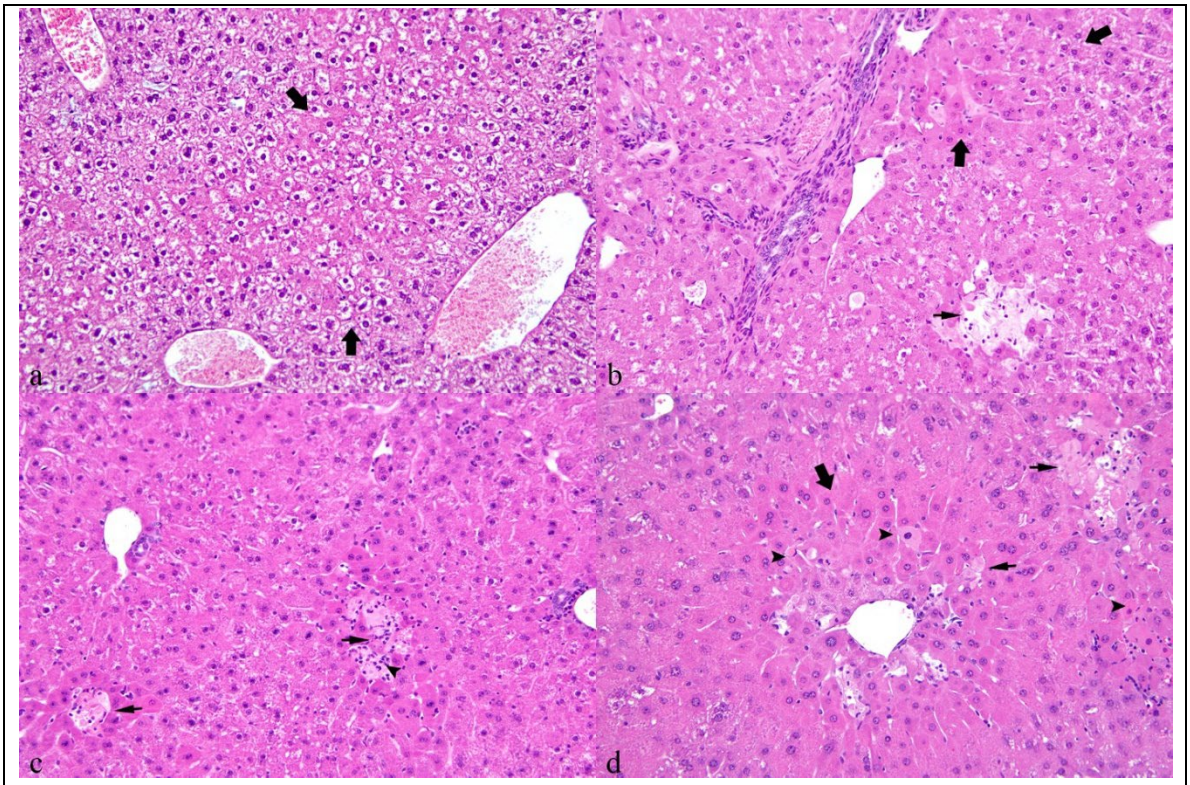

Figure 2.5. Images a-d. Livers of mice exposed to senecionine for ten days at various doses. a) Mouse dosed with 8 mg/kg/day: Hepatocytes in midzonal and periportal areas are multifocally enlarged (hypertrophy/cell swelling) (arrows). Notice the prominent cytoplasmic vacuolation (glycogen type) in nearly all hepatocytes as in control mice. This vacuolation is easily contrasted with hepatocyte enlargement and degenerative swelling (arrows). b) Mouse dosed with 15 mg/kg/day: Coalescing hepatocyte hypertrophy/swelling (arrows) and a focus of coagulative necrosis (small arrow). c) 30 mg/kg/day: Hepatocyte hypertrophy/swelling is panlobular. Foci of coagulative necrosis are in the midzonal area in this image (arrows) but could be found in periportal, midzonal and centrilobular hepatocytes. Small numbers of neutrophils infiltrate areas of necrosis (arrowheads). d) 45 mg/kg/day: Panlobular hepatocyte hypertrophy/swelling, most prominently affecting midzonal and periportal hepatocytes (arrow). Multiple foci of coagulative necrosis (small arrows) and individual cell necrosis (arrowheads) are present. Microscopic changes are similar to those observed in the 30 mg/kg/day dosing group. Hematoxylin and eosin stain. 200X.

Senecionine N-oxide:

exposed to doses as low as 8 mg/kg/day had multifocal midzonal to periportal hepatocyte hypertrophy/swelling with individual cell necrosis (3/3 mice). Doses of 15 mg/kg/day induced diffuse midzonal and periportal hepatocellular hypertrophy/swelling with individual cell and foci of coagulative hepatocellular necrosis (3/3 mice). In one of the three mice exposed to 30 mg/kg/day, all lobular zones were affected, and the other two mice had midzonal and periportal necrosis and hepatocyte enlargement. Mice exposed to 45 mg/kg/day had diffuse midzonal and periportal (1/3 mice) to panlobular (2/3 mice) hepatocyte hypertrophy/swelling with frequent groups of necrotic hepatocytes (3/3 mice). In the dosing groups given 90 mg/kg (3/3 mice) and 180 mg/kg (3/3 mice), the distribution of hepatocyte hypertrophy/swelling was panlobular with multifocal areas of necrosis located in all parts of the lobule. The 90 and 180 mg/kg/day dosing groups did not tolerate a full ten days of dosing, and either died or were euthanized early, hence these groups were excluded from statistical analyses. Mice that were exposed to 180 mg/kg/day only survived for 4 out of 20 doses. Mice that were given 90 mg/kg/day exhibited malaise and substantial weight loss and were euthanized after 4 to 5 days of dosing. Severe coalescing areas of necrosis affecting 50% or more of the liver sections were observed in all mice in the 90 and 180 mg/kg/day groups. Dose had a strong positive correlation with hepatic necrosis score ($r = 0.8286$, $p < 0.0001$). See figure 2.6.

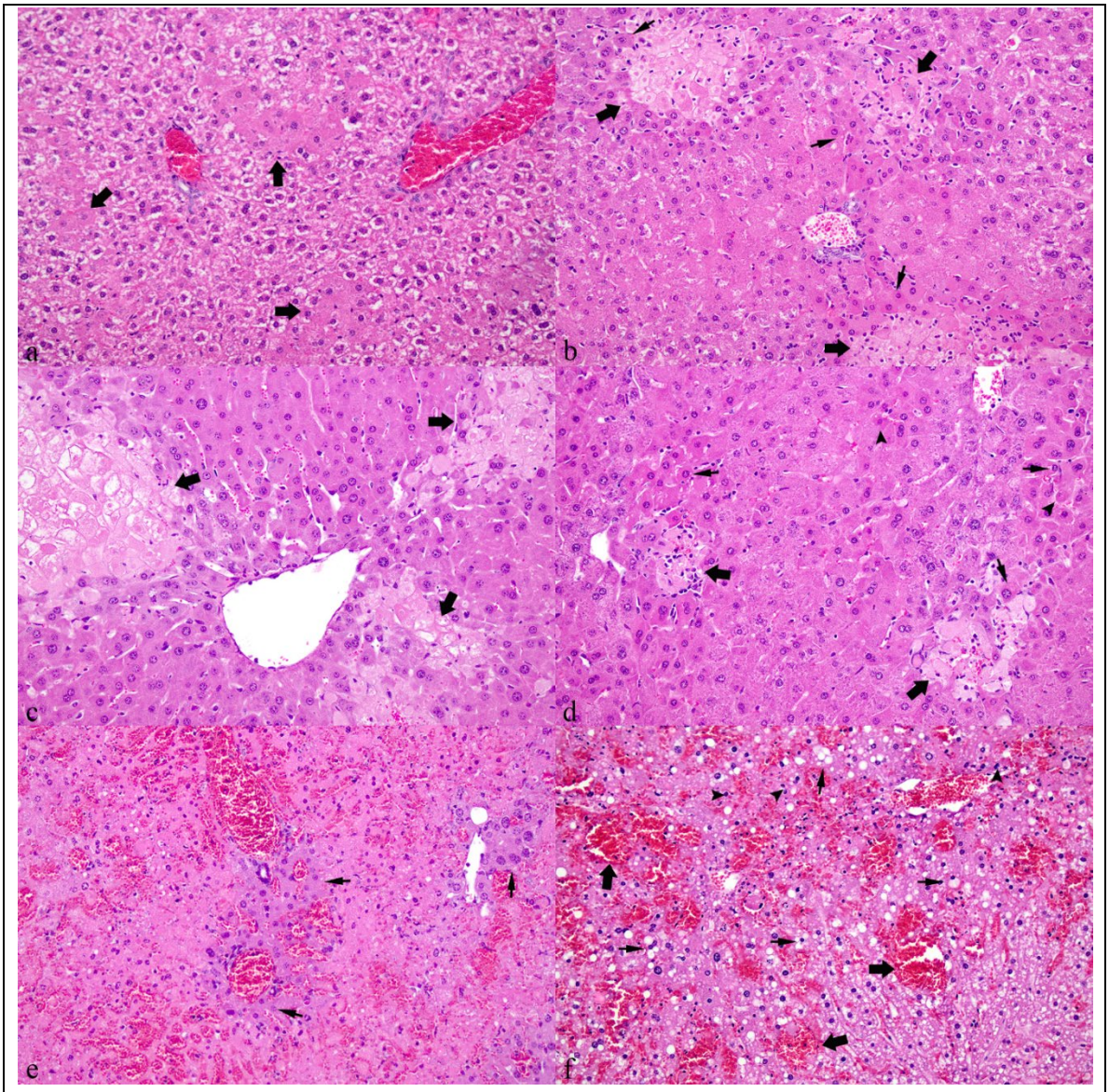

Figure 2.6. Images a-f. Liver of mice exposed to senecionine N-oxide for ten days at various doses. a) 8 mg/kg/day: Midzonal hepatocytes are multifocally hypertrophic/swollen (arrows). b) 15 mg/kg/day: Hepatocyte hypertrophy/swelling affects midzonal and periportal hepatocytes but spares centrilobular areas. Multiple foci of coagulative necrosis are present (large arrows). Hepatocytes adjacent to areas of coagulative necrosis are frequently hypereosinophilic, enlarged or shrunken, sometimes with nuclear pyknosis (degeneration and necrosis) (small arrows). c) 30 mg/kg/day: Hepatocyte hypertrophy/swelling is panlobular. Foci of coagulative necrosis are observed in all portions of the lobule (arrows). d) 45 mg/kg/day: Microscopic changes are similar to those seen in the 30 mg/kg/day dosing group. Panlobular hepatocellular

enlargement and foci of coagulative necrosis (large arrows). Hepatocytes adjacent to areas of necrosis are hypereosinophilic, enlarged or shrunken, sometimes with nuclear pyknosis or have clear variably sized cytoplasmic vacuoles (vacuolar degeneration) (small arrows). Individual cell necrosis is observed (arrowheads). e) 90 mg/kg/day. Lytic and coagulative necrosis replaces most of the lobules. Few enlarged centrilobular hepatocytes are spared (small arrows). These mice only received 7 to 9 of the 20 planned doses and were euthanized due to malaise and weight loss. f) 180 mg/kg/day: Panlobular necrosis. Nearly all remaining hepatocytes have clear cytoplasmic vacuoles (vacuolar degeneration) (small arrow) some with nuclear pyknosis (arrowhead). Spaces created by hepatocellular loss are filled with extravasated erythrocytes (arrow). These mice only received 4 of the 20 planned doses and either died or were euthanized due to malaise and weight loss. Hematoxylin and eosin stain. 200X.

Riddelliine:

Multifocal centrilobular hepatocellular hypertrophy/swelling was observed at doses as low as 15 mg/kg/day (3/3 mice). Mice exposed to 30 mg/kg/day had diffuse centrilobular hepatocellular hypertrophy/swelling with individual necrotic hepatocytes (3/3 mice). The 45 mg/kg/day dosing groups (3/3 mice) had diffuse centrilobular hepatocellular hypertrophy/swelling with individual cell necrosis. Mice exposed to 90 mg/kg/day had panlobular hepatocellular hypertrophy/swelling and degeneration with 1to 4 clusters of necrotic hepatocytes per 100X field (3/3 mice). Dose of riddelliine had a strong positive correlation with necrosis score ($r = 0.9495$, $p < 0.0001$). See figure 2.7.

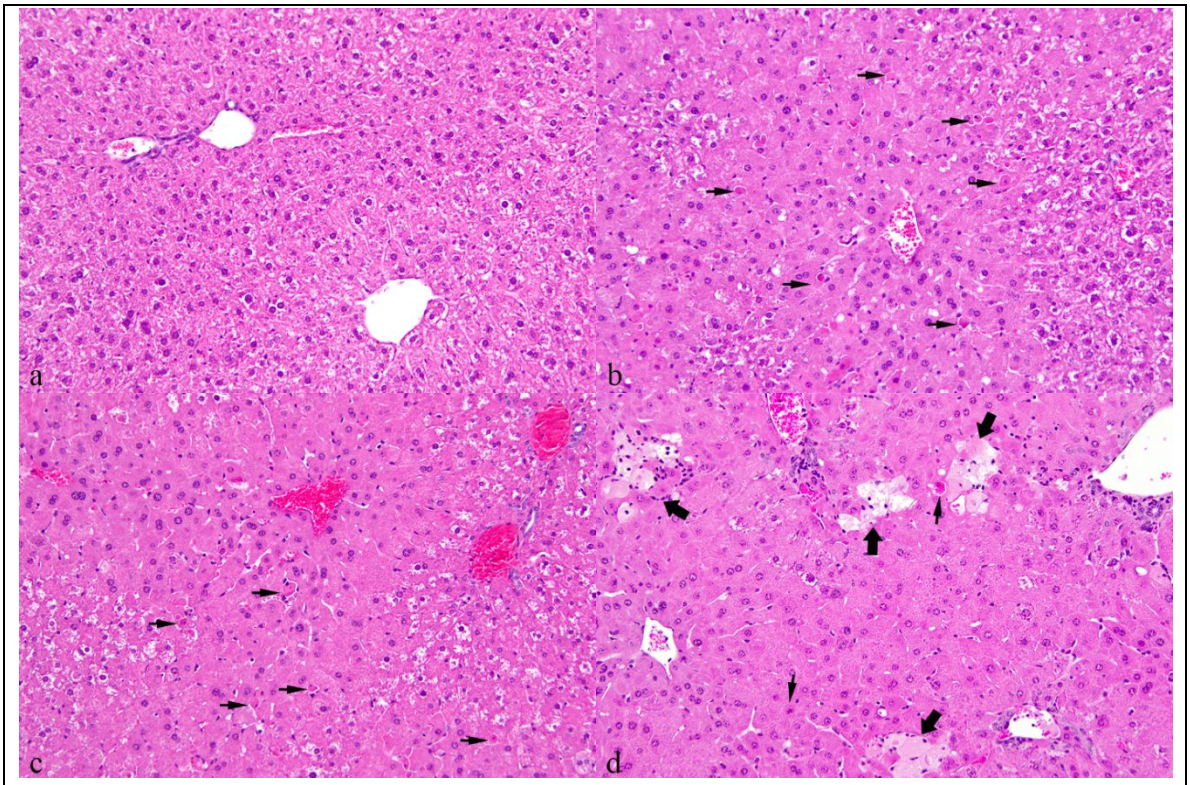

Figure 2.7. Images (a-d). Liver of mice exposed to riddelliine for ten days at various doses. a) 15 mg/kg/day: No significant microscopic lesions are observed. b) 30 mg/kg/day: Centrilobular hepatocytes are diffusely hypertrophic/swollen with scattered individual necrotic hepatocytes (arrows). c) 45 mg/kg/day: Microscopic changes are similar to those seen at 30 mg/kg/day. Centrilobular to midzonal hepatocellular hypertrophy/swelling and degeneration with individual hepatocelluar necrosis (arrows). d) 90 mg/kg/day: Panlobular hepatocellular hypertrophy/swelling is observed. Multiple foci of coagulative necrosis are observed in midzonal, periportal and centrilobular areas (large arrows). Occasional individual hepatocellular necrosis is present (small arrows). Hematoxylin and eosin stain. 200X.

Riddelliine N-oxide:

Mice exposed to riddelliine N-oxide developed multifocal centrilobular hepatocyte hypertrophy/swelling at doses as low as 15 mg/kg/day (3/3 mice). Mice given 30 mg/kg/day (3/3 mice) had diffuse centrilobular hypertrophy/swelling with individual cell

necrosis. The mice exposed to 45 mg/kg/day (3/3 mice) had diffuse centrilobular hypertrophy/swelling sometimes affecting midzonal (2/3 mice) or panlobular (1/3 mice) areas with individual cell necrosis (1/3 mice) or foci of necrosis (2/3 mice). The group given 90 mg/kg/day had hypertrophy/swelling affecting centrilobular and midzonal to panlobular hepatocytes with individual hepatocyte necrosis (3/3 mice). The group given 180 mg/kg/day had diffuse panlobular hepatocyte hypertrophy/swelling with frequent, variably large areas of hepatocellular necrosis (3/3 mice). The highest dosing group for this compound was 360 mg/kg/day, and all three mice died after receiving 4 doses. In the 360 mg/kg/day, severe panlobular hepatocellular necrosis with hemorrhage, affecting up to 70% of liver sections was observed. The 360 mg/kg/day dosing group was excluded from statistical analysis as they did not tolerate ten days of dosing. Dose had a strong positive correlation with hepatic necrosis score ($r = 0.8879$, $p < 0.0001$). See figure 2.8.

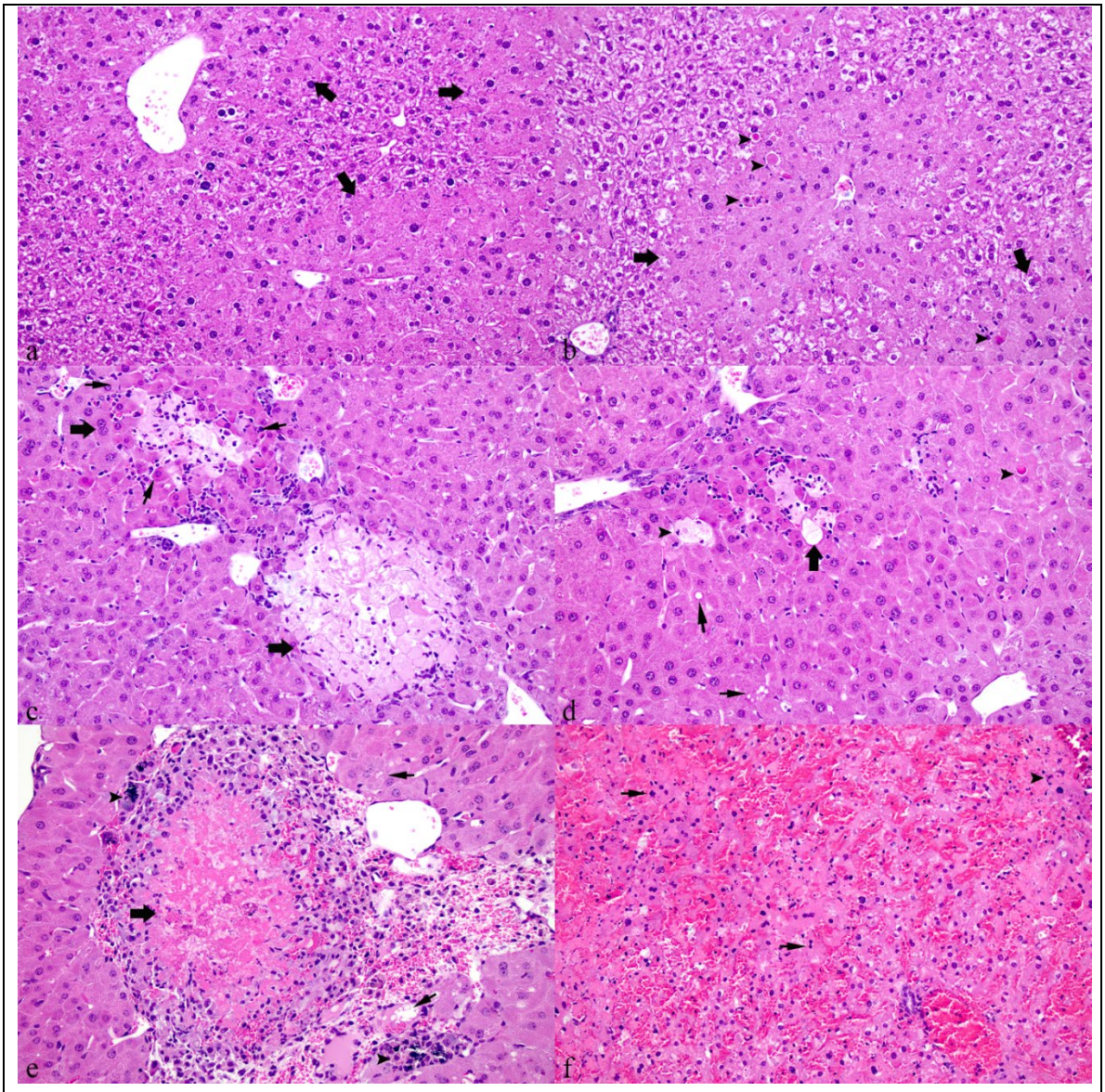

Figure 2.8. Images a-f: Liver of mice exposed to riddelliine N-oxide for ten days at various doses. a) 15 mg/kg/day: Centrilobular hepatocytes are hypertrophic/swollen (arrows). b) 30 mg/kg/day: Centrilobular hepatocellular hypertrophy/swelling becomes more pronounced (arrows). Individual hepatocellular necrosis (arrowheads) occurs within areas of hepatocellular hypertrophy/swelling. c) 45 mg/kg/day: Hepatocellular hypertrophy/swelling is panlobular and foci of coagulative necrosis are present (arrows). Small numbers of neutrophils infiltrate areas of hepatocellular necrosis. Individual hepatocytes adjacent to areas of coagulative necrosis are frequently necrotic (small arrows) d) 90 mg/kg/day: Panlobular hepatocellular hypertrophy/swelling with occasional cytoplasmic vacuolation (small arrows) (vacuolar degeneration). Individual hepatocellular

necrosis is occasionally observed (arrowheads). Groups of hypereosinophilic enlarged or shrunken hepatocytes (degeneration) surround small numbers of necrotic hepatocytes (arrow). e) 180 mg/kg/day: An area of lytic necrosis surrounded by macrophages (arrow). Diffuse panlobular hepatocellular hypertrophy/swelling affects remaining hepatocytes. Occasional hepatocytes contain multiple clear cytoplasmic vacuoles (small arrows) (vacuolar degeneration). Multiple foci of dystrophic mineralization (arrowheads) are adjacent to the area of necrosis. f) 360 mg/kg/day: Panlobular hepatocellular necrosis. Hepatocytes in all portions of the lobule are necrotic (small arrows), or replaced by lytic necrosis (arrowhead). Hematoxylin and eosin stain. 200X.

Lasiocarpine:

Mice exposed to lasiocarpine exhibited mild hepatocellular hypertrophy/swelling in periportal hepatocytes with rare individual hepatocellular necrosis, but only in the highest dosing group, which was 30 mg/kg/day (3/3 mice). Mice did not tolerate doses greater than 30 mg/kg/day and exhibited weight loss and severe malaise. A cause of these clinical signs was not determined after microscopic evaluation of all major organs. Although there was a strong positive correlation between dose and hepatic necrosis score ($r = 0.8871$, $p < 0.0001$), this correlation is based on a necrosis score of one for the high dose (30 mg/kg/day) group and zero for all other groups. See figure 2.9.

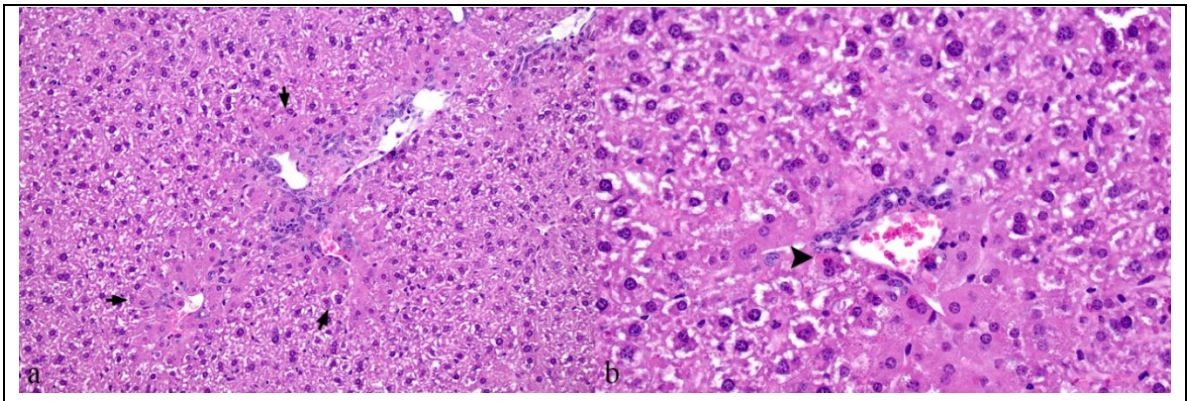

Figure 2.9. Images a-b. Liver of mice exposed to 30 mg/kg/day lasiocarpine for ten days. a) Periportal hepatocyte hypertrophy/swelling (arrows). b) Higher magnification of enlarged periportal hepatocytes with individual hepatocellular necrosis (arrowhead). Hematoxylin and eosin stain. 200X.

Heliotrine:

Mice exposed to heliotrine exhibited hepatocellular enlargement in centrilobular hepatocytes only in the highest dosing group, which was 180 mg/kg/day. Hepatocellular necrosis was not observed in any dosing group. Dose had no correlation with hepatic necrosis score, and all mice exposed to heliotrine received a necrosis score of zero. See figure 2.10.

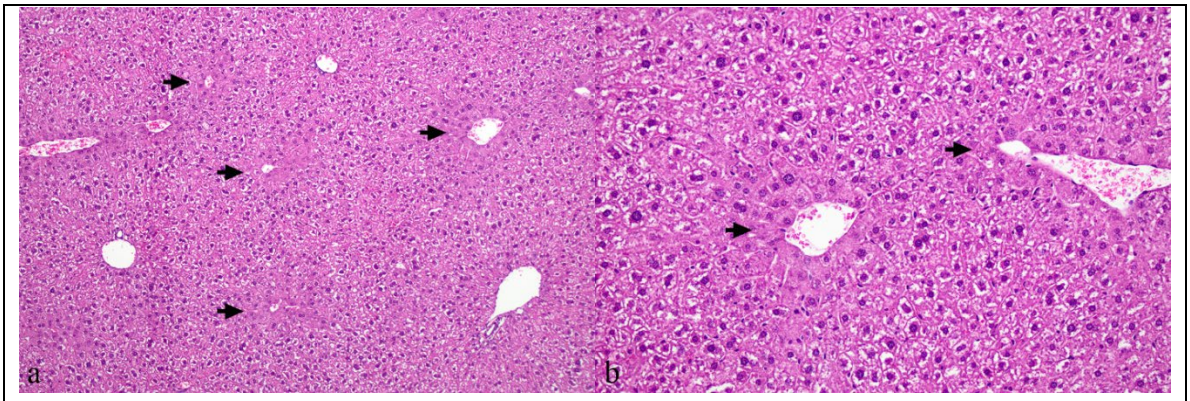

Figure 2.10 Images a-b. Liver of mice exposed to 180 mg/kg/day of heliotrine for ten days. a) Hypertrophy/swelling of centrilobular hepatocytes (arrows). b) Higher magnification showing subtle centrilobular hepatocyte hypertrophy/ swelling. Hematoxylin and eosin stain. 200X.

Compound Toxicity Severity Comparison by Dose:

Mean necrosis scores were compared between compounds at similar doses. Kruskal-Wallis and Mann-Whitney tests were used for statistical comparisons. Because of the variability in dosing range between compounds, comparative data will be presented for the 4, 8, 15, 30, 45 and 90 mg/kg/day dose groups. The 1, 2, 180 and 360 mg/kg data is not used in comparison as these doses were not given for all compounds.

For the 4 mg/kg/day dose, senecionine was the only compound with microscopic evidence of hepatocellular necrosis (1 out of 3 mice). This was the only compound with a statistically significant difference when compared to the control group ($p < 0.0001$). Riddelliine, seneciphylline, and lasiocarpine were the other compounds with 4 mg/kg/day dosing groups and no microscopic lesions were observed for these compounds at this dose.

For the 8 mg/kg/day dosing groups, the order of necrosis score from most to least severe is senecionine N-oxide (1.333 +/-0.577), seneciphylline (0.333 +/- 0.577) and senecionine (0.3333 +/- 0.577), and last are riddelliine (0), lasiocarpine (0) and heliotrine (0). Mice were not exposed to riddelliine N-oxide at this dose. Senecionine N-oxide ($p < 0.0001$) was significantly different than the control group.

For the 15 mg/kg/day dosing groups, the order of necrosis score from most to least severe is senecionine N-oxide (2.667 +/- 1.155), senecionine (2 +/- 1.732) and seneciphylline (2), riddelliine N-oxide (1), and last are riddelliine (0), lasiocarpine (0) and heliotrine (0). There were significant differences ($p < 0.0001$) compared to control groups for senecionine N-oxide, senecionine, seneciphylline, riddelliine N-oxide.

For the 30 mg/kg dosing groups, the order of necrosis score from most to least severe is seneciphylline (3.667 +/- 0.577), senecionine (3 +/- 1), senecionine N-oxide (2.667 +/- 1.528), riddelliine (1.667 +/- 0.577), riddelliine N-oxide (1.333 +/- 0.577), lasiocarpine (1), and last is heliotrine (0). Differences were statistically significant ($p < 0.0001$) for all compounds except heliotrine when compared to the control group.

For the 45 mg/kg dosing groups, the order of necrosis score from most to least severe is senecionine (3.667 +/- 0.577) and senecionine N-oxide (3.667 +/- 0.577), seneciphylline (3.333 +/- 1.155) and riddelliine (2) and riddelliine N-oxide (2), and last heliotrine (0). Lasiocarpine was not included in this comparison because mice did not tolerate dosing of lasiocarpine at 45 mg/kg/day. Differences with the control group were statistically significant ($p < 0.0001$) for all compounds except heliotrine.

For the 90 mg/kg/day dosing groups, the order of necrosis score from most to least severe is riddelliine (3.333 +/- 0.577), riddelliine N-oxide (2), and last is heliotrine (0). Senecionine, seneciphylline and lasiocarpine were not given at this dose. Compared to the control group, riddelliine and riddelliine N-oxide were significantly different ($p < 0.0001$).

Table 2.6 Hepatic necrosis scores (4,8,15,30,40, and 90 mg/kg/day): The highest necrosis score for each dose is highlighted (mean ± standard deviation).

Dose (mg/kg/day)	4	8	15	30	45	90
Riddelliine	0	0	0	1.67 +/- 0.58	2	3.3 +/- 0.58
Senecionine	0.33 +/- 0.58	0.33 +/- 0.58	2 +/- 1.7	3 +/- 1	3.67 +/- 0.58	ND
Seneciphylline	0	0.33 +/- 0.58	2 0	3.67 +/- 0.58	3.33 +/- 1.16	ND
Lasiocarpine	0	0	0	1	ND	ND
Heliotrine	ND	0	0	0	0	0
Riddelliine N-oxide	ND	ND	1	1.33 +/- 0.58	2.33 +/- 0.58	2
Senecionine N-oxide	ND	2.67 +/- 1.16	2.67 +/- 1.16	2.67 +/- 1.53	3.67 +/-0.58	*4
Control	0	0	0	0	0	0
Vehicle	0	0	0	0	0	0

*Mice exposed to 90 and 180 mg/kg senecionine N-oxide did not survive the complete dosing period and are excluded from statistical comparisons.

Lowest Observed Effect Level (LOEL): Microscopic Changes

Table 2.7. Lowest observed effect levels (LOEL).

Lowest observed effect levels (LOEL)		
	Lowest dose resulting in hepatocellular hypertrophy	Lowest dose resulting in hepatic necrosis
Riddelliine	15 mg/kg/day	30 mg/kg/day
Riddelliine N-oxide	*15 mg/kg/day	*15 mg/kg/day
Senecionine	8 mg/kg	4 mg/kg/day
Senecionine N-oxide	*8 mg/kg/day	* 8 mg/kg/day
Seneciphylline	8 mg/kg/day	8 mg/kg/day
Lasiocarpine	30 mg/kg/day	30 mg/kg/day
Heliotrine	**180 mg/kg/day	NA

*Hepatocyte swelling and necrosis were observed in the lowest dosing groups of riddelliine N-oxide (15 mg/kg/day) and senecionine N-oxide (8 mg/kg/day). Additional studies are needed to determine the LOEL for these PAs in mice.

**Mice exposed to 180 mg/kg/day of heliotrine had subtle increases in size and cytoplasmic eosinophilia of centrilobular hepatocytes. This change may simply be a histologic artifact. Heliotrine did not result in hepatic necrosis at any dose.

Pyrrole Analysis:

Pyrrole concentration was positively correlated with dose for each compound using a Pearson's correlation ($P \leq 0.05$, riddelliine $R = 0.6567$, senecionine $R = 0.6861$, seneciphylline $R = 0.6888$, heliotrine $R = 0.7407$, riddelliine N-oxide $R = 0.6876$, senecionine N-oxide $R = 0.5839$, lasiocarpine $R = 0.9432$). Pyrrole concentration is presented on a dry matter basis in nmol/g. Though seneciphylline and senecionine N-oxide pyrrole concentrations also tended to have a positive correlation with dose, those results were variable and not statically significant (see table 8). Dose comparisons are presented for the 8, 15, 30, 45 and 90 mg/kg/day dosing groups. At 8 mg/kg/day,

senecionine N-oxide induced the greatest concentration of liver pyrroles (36.37 +/- 5.359 nmol/g) but was only slightly greater than riddelliine (25.27 +/- 7.778 nmol/g), followed by seneciphylline (19.4 +/- 13.17 nmol/g), senecionine (8.567 +/- 1.724 nmol/g), lasiocarpine (7.7 +/- 3.315 nmol/g) and last heliotrine (0.1667 +/- 0.1528 nmol/g). Riddelliine N-oxide is not included in this comparison, as the lowest dose for this compound was 15 mg/kg/day.

At 15 mg/kg/day pyrrole concentrations in riddelliine exposed mice increased dramatically to 122.1 +/-16.95 nmol/g. Senecionine N-oxide induced the next greatest liver pyrrole concentration (39.23 +/- 23.87 nmol/g), followed by seneciphylline (25.27 +/- 6.897 nmol/g), riddelliine N-oxide (22.03 +/- 2.003 nmol/g), senecionine (18.8 +/- 9.395 nmol/g), lasiocarpine (7.933 +/- 3.066 nmol/g), and last heliotrine (0.5 +/- 0.2 nmol/g). Pyrrole concentrations induced by riddelliine remained substantially greater than all other compounds for all remaining common doses.

At 30 mg/kg/day riddelliine induced the greatest concentrations of pyrroles at 97 +/- 27.4 nmol/g, followed by riddelliine N-oxide (47.8 +/- 18.18 nmol/g), senecionine N-oxide (33.23 +/- 27.73 nmol/g), seneciphylline (33.17 +/- 10.13), senecionine (25.37 +/- 2.928 nmol/g), lasiocarpine (18.4 +/- 1.587 nmol/g) and last heliotrine (0.4667 +/- 0.2517 nmol/g).

At 45 mg/kg/day riddelliine induced the greatest concentrations of pyrroles at 154.6 +/- 84.68 nmol/g, followed by senecionine N-oxide (43.87 +/- 25.27 nmol/g), riddelliine N-oxide (29.27 +/- 14.93 nmol/g), seneciphylline (29 +/- 24.63), senecionine (13.43 +/- 1.589 nmol/g), and last heliotrine (1.1 +/- 0.3606 nmol/g). Lasiocarpine was not included in this comparison as mice did not tolerate doses as high as 45 mg/kg/day.

At 90 mg/kg/day riddelliine induced the greatest concentrations of pyrroles at 124.3 +/- 56.67 nmol/g, followed by riddelliine N-oxide (77.3 +/- 43.76 nmol/g), senecionine N-oxide (54.7 +/- 31.89 nmol/g) and last heliotrine (3.13 +/- 1.53 nmol/g). Senecionine, seneciphylline and lasiocarpine were not included in this comparison because mice were not given doses this high for any of these compounds. Mean hepatic pyrrole concentrations can be seen in table 2.8.

Table 2.8. Hepatic pyrrole concentration (nmol/g), by PA (rows) and dose (columns), mean ± standard deviation.

Dose (mg/kg/day)	4	8	15	30	45	90	Pearson correlation with dose (P ≤ 0.05)
Riddelliine	17.0 ± 0.2	25.27 ± 7.78	122.1 ± 16.95	97 ± 27.4	154.6 ± 84.68	124.3 ± 56.67	0.66
Senecionine	5.53 ± 2.83	8.57 ± 1.72	18.8 ± 9.39	25.37 ± 2.93	13.43 ± 1.59	ND	0.69
Seneciphy.	12.43 ± 2.37	19.4 ± 13.17	25.27 ± 6.90	33.17 ± 10.13	29 ± 24.63	ND	0.69
Lasio.	2.83 ± 2.37	7.7 ± 3.32	7.93 ± 3.07	18.4 ± 1.59	ND	ND	0.3
Helio.	ND	0.17 ± 0.15	0.5 ± 0.2	0.47 ± 0.25	1.1 ± 0.36	3.13 ± 1.53	0.74
Rid. N-ox.	ND	ND	22.03 ± 2.0	47.8 ± 18.18	29.27 ± 14.93	77.3 ± 43.76	0.69
Sen. N-ox.	ND	36.37 ± 5.36	39.23 ± 23.87	33.23 ± 27.73	43.87 ± 25.27	54.7 ± 31.89	0.58
Control	0.21 ± 0.46	0.21 ± 0.46	0.21 ± 0.46	0.21 ± 0.46	0.21 ± 0.46	0.21 ± 0.46	NA

Riddelliine induced greater concentrations of hepatic pyrroles than all other compounds in all dosing groups except 8mg/kg/day. At 8 mg/kg/day, the mean pyrrole concentration induced by senecionine N-oxide (36.37 +/- 5.36 nmol/g) was slightly greater than riddelliine (25.27 +/- 7.78 nmol/g). It is noteworthy that riddelliine induces greater concentrations of hepatic pyrroles than compounds which induce more severe necrosis at any given dose, namely senecionine, senecionine N-oxide and seneciphylline.

Table 2.9. 30 mg/kg/day PA toxicity ranking using hepatic necrosis score (column 2), hepatic pyrrole concentration (column 3), Mean ALT (column 4), Mean ALP (column 5), compared to published LD50 data (column 6). Comparisons between PAs are made using the greatest dose, which was shared by all PAs, 30 mg/kg/day.

1. Dehydro-pyrrolizidine alkaloid	2. Necrosis score rank (mean necrosis score)	3. Pyrrole concentration Rank (mean concentration, nmol/g)	4. Serum ALT Rank (mean conc., U/L)	5. Serum ALP Rank (mean conc., U/L)	6. LD50 Rank, mg/kg (route, species)[29]
Seneciphylline	1 (3.6 +/- 0.58)	4 (33.17 +/- 10.13)	Not measured	Not measured	2, 77 mg/kg (rat, IP) 90 mg/kg (IV, mouse)[29,30]
Senecionine	2 (3 +/- 1)	5 (25.37 +/- 2.93)	Not measured	Not measured	1, 57 mg/kg (oral, mouse) [29]
Senecionine N-oxide	3 (2.67 +/- 1.5)	3 (33.23 +/- 27.73)	1 (3033 +/- 1144.3)	1 (3318 +/- 3550)	No reference found
Riddelliine	4 (1.67 +/- 0.58)	1 (97.0 +/- 27.4)	2 (661.3 +/- 272.9)	2 (323.7 +/- 119.9) *	3, 80 mg/kg (oral, rat) [29]

Riddelliine N-oxide	5 (1.33 +/- 0.58)	2 (47.8 +/- 18.18)	3 (463.7 +/- 127.8)	4 (186.0 +/- 30.12) *	No reference found
Lasiocarpine	6 (1)	6 (18.4 +/- 1.59)	Not measured	Not measured	4, 110 mg/kg (oral, rat)[29]
Heliotrine	7 (0)	7 (0.47 +/- 0.25) *	4 (60.67 +/- 24.4) *	3 (212.3 +/- 61.33) *	5, 510 mg/kg (oral, rat)[29]
Control	0	(0.21 +/- 0.46)	87.75 +/- 79.42	186.9 +/- 81.58	

Numbers marked with an asterisk were not significantly different than control values. Note that riddelliine and riddelliine N-oxide induced hepatic pyrrole concentrations that were greater than expected based on microscopic necrosis score. Aside from the inordinate hepatic pyrrole concentration, hepatic pyrrole concentration and serum ALT were relatively consistent with hepatic necrosis score in terms of ranking the compounds hepatotoxicity. Serum ALP was not significantly increased compared to controls for any compound except senecionine N-oxide. Our ranking closely matches the published LD50 values, the exception is the riddelliine and seneciphylline are reversed in order. These LD50 values vary in species and route of administration and may not be relevant to this experiment.

Discussion:

The aims of this experiment were to compare the toxicity of five PAs and two PA N-oxides, to characterize the microscopic lesions caused by acute PA exposure in mice, and to determine suitable doses for future studies comparing the relative carcinogenicity of PAs in mice. The results have demonstrated differences in the toxic effects of PAs in mice. This study provided a ranking of severity of toxicity between these PAs in mice. The retronecine macrocyclic diesters appear to be the most potent hepatotoxins in this experiment. Another important and novel finding is the observed differences in the

distribution of hepatocyte hypertrophy, degeneration, and necrosis between these PAs. The finding that PAs affect different areas of the hepatic lobule indicates that there are differences in bioactivation and/or toxic metabolites produced by bioactivation, or differences in phase II metabolism. This work also demonstrated great disparities in the production of the hepatic pyrrole between the PAs tested. Riddelliine induced far greater pyrrole concentrations than all other PAs. Notably, senecionine, seneciphylline, and senecionine N-oxide caused more severe hepatic necrosis than riddelliine but had lower hepatic pyrrole concentrations. ALT and ALP were shown to be useful biomarkers as indicators of PA induced hepatic injury. These findings demonstrate that regardless of chemical similarity, individual PAs differ in biologically important ways. Further studies are needed to determine if PAs also differ in their carcinogenic potential. Comparison of microscopic changes is useful in trying to determine which PAs are more toxic relative to one another. Detection and quantification of the toxic metabolite in the liver, and serum ALT and ALP values are also valuable to support histopathologic findings.

Ranking of Hepatotoxicity:

Extrahepatic lesions were not observed; therefore, comparison of toxicity refers strictly to comparison of hepatotoxicity. Hepatotoxicity rankings in this study (see table 9) were based on hepatic necrosis score (column 2), hepatic pyrrole concentration (column 3), mean serum ALT concentration (column 4), and mean serum ALP concentration (column 5). The most hepatotoxic PAs in this study were senecionine, senecionine N-oxide, and seneciphylline. The group with intermediate hepatotoxicity included riddelliine and riddelliine N-oxide. Macrocyclic diester PAs have been shown to induce greater quantities of pyrrole-protein adducts in vitro, compared to monoester PAs.[36] The results

of our study are in agreement with this statement, as heliotrine and lasiocarpine induced the lowest concentrations of hepatic pyrroles. The least toxic compounds were lasiocarpine and heliotrine. Lasiocarpine is a heliotridine type diester PA and heliotrine is a heliotridine type monoester. The five most hepatotoxic PAs in this study, namely senecionine, senecionine N-oxide, seneciphylline, riddelliine and riddelliine N-oxide, are all macrocyclic diester PAs. This may indicate a structurally specific order of hepatotoxicity for PAs in mice. Differences in toxicity may indicate that the general mechanism of toxicity which is presumably shared by toxic PAs is oversimplified. The most toxic group includes senecionine and its N-oxide and seneciphylline. Studies of the toxic mechanism of senecionine have demonstrated that at least one additional hepatotoxic metabolite, trans-4-hydroxy-2-hexenal is produced by its bioactivation.[37] Senecionine has also been shown to cause compromises in bile acid homeostasis in rats.[38] Senecionine was also shown to cause loss of mitochondrial membrane potential in cultured human hepatocytes.[39] Wang et al. (2020) demonstrated that seneciphylline induces apoptosis in mouse hepatocytes via mitochondrial damage as well.[40] These mechanisms represent possible reasons that senecionine, senecionine N-oxide and seneciphylline were the most toxic PAs in this study, even though riddelliine induced far greater concentrations of hepatic pyrroles.

The group of PAs with intermediate toxicity includes riddelliine and riddelliine N-oxide. Chou et al. (2003) demonstrated that riddelliine N-oxide has similar genotoxic potential to its parent PA riddelliine.[41] Our experiments show that riddelliine N-oxide is also equally or even more hepatotoxic than riddelliine. Riddelliine and riddelliine N-oxide most likely share a metabolic pathway for bioactivation.

The least hepatotoxic group included lasiocarpine and heliotrine. Although lasiocarpine is in the least hepatotoxic group, this PA is among the most toxic when considering clinical signs. Previous unpublished work performed at the USDA PPRL determined that mice could not tolerate ten days of exposure at doses greater than 30 mg/kg/day, making this the lowest dosing range in the study. Mice exposed to 45 mg/kg/day exhibited severe malaise, lethargy and weight loss and were removed from the experiment. The cause of these clinical signs was not determined. Additional research with extrahepatic biomarkers is needed to clarify the toxic effects of lasiocarpine in mice. Heliotrine did not cause any clinical signs, microscopic lesions, or significant increases in ALT, ALP, or hepatic pyrrole concentration. Mice were exposed to doses as high as 180 mg/kg/day, which is a greater dose than was tolerated for any other PA or PA N-oxide evaluated. Heliotrine has been shown to be teratogenic to rats and to induce pancreatic islet cell tumors.[42,43] However, these studies are decades old and have not been replicated. This further illustrates species variability in susceptibility to PAs. Caution is warranted when extrapolating reported toxicity of PAs to other species, particularly considering the many purported homeopathic benefits attributed to ingestion of PAs in people.

Comparisons to Experimental Exposure in California White Chicks (*Gallus domesticus*):

In 1974, in Victoria, Australia several flocks of chickens and ducks were exposed to feed contaminated with *Heliotropium europaeum*. The main PAs present in the contaminated feed were lasiocarpine and heliotrine. Exposed birds developed ill-thrift and ascites. Necropsy findings included hepatic degeneration, necrosis, sometimes with

fibrosis. Necrosis mainly affected midzonal and centrilobular hepatocytes.[44] This outbreak indicated that chickens are sensitive to PA poisoning and may be a good animal model for research. Brown et al. (2015) experimentally exposed California white chicks to eleven PAs, including those which were used in this experiment. The rank of toxicity from most toxic to least in California white chicks was heliotrine, senecionine, riddelliine, senecionine N-oxide, seneciphylline, riddelliine N-oxide, lasiocarpine, echimidine, lasiocarpine N-oxide, and lycopsamine. Notable differences between the current study and the chick study include the greater toxicity of heliotrine, and lasiocarpine in chicks.[28] Heliotrine was virtually nontoxic, and lasiocarpine was less toxic than all other PAs and PA N-oxides in this study. California white chicks most likely have the cytochrome p450 enzyme necessary for bioactivation of heliotrine, and C57BL6/j mice lack this enzyme. Less likely possibilities include differences in absorption or phase II metabolism.

Comparisons to In Vitro Studies:

There are many studies involving in vitro exposure of hepatocytes, endothelial cells, and other cell lines to various PAs. It is possible that such in vitro studies do not accurately mimic the events that occur following ingestion, however these studies are relatively simple to carry out when compared to in vivo work. In vitro studies also enable better control of external factors such as individual animal variability than can be achieved in vivo. Stegelmeier et al. (2016) incubated chicken hepatocarcinoma cells (CRL-2118) with various PAs to compare cytotoxicity. Lasiocarpine was the most cytotoxic, followed in descending order of cytotoxicity by seneciphylline, senecionine, heliotrine and riddelliine. Senecionine N-oxide and riddelliine N-oxide were among the

group tested that was significantly less cytotoxic.[1] Notable differences in our study include the lack of hepatotoxicity observed from heliotrine and lasiocarpine exposure, as well as the relatively greater ranking of senecionine N-oxide and riddelliine N-oxide observed in C57BL6/j mice. Field et al. (2015) similarly compared cytotoxicity of the same selected PAs using different cell lines (Hep G2, HEK 293, CCL-22, and CRL-2118) and found a ranking of cytotoxicity similar to Stegelmeier (2016).[1,45] Lasiocarpine and heliotrine were again placed in the group with the greatest cytotoxicity, along with senecionine and seneciphylline while senecionine N-oxide and riddelliine N-oxide were placed in the least cytotoxic group. These differing results illustrate the importance of in-vivo testing to validate toxicity data that are determined using in vitro methods.

Relative Toxicity of Dehydropyrrolizidine Alkaloids and Dehydropyrrolizidine Alkaloid N-oxides:

Some N-oxides are equally or even more toxic than their parent compounds. This finding supports the possibility that alternative metabolic pathways may contribute to toxicity and that these pathways may be compound specific, resulting in variation of the lesion severity and distribution. Further work is needed to determine which mechanisms are responsible for the variation in distribution of cell swelling and necrosis. Compound specific affinity to different CYP450 enzymes is the most likely explanation.

Differences within the most toxic group were not statistically significant, but the overall hepatic necrosis score tended to be greater for senecionine N-oxide than senecionine and seneciphylline. Similarly, riddelliine N-oxide had slightly greater necrosis scores compared to riddelliine, though not statistically significant. These

differences are noteworthy given previous writings that stated that PA N-oxides are less toxic than their parent compounds.[22,32] PA N-oxides often coexist with their parent compounds in the PA containing plant.[22] Differences in toxicity between PAs and PA N-oxides may be the result of differences in absorption, metabolism, or reactivity of metabolic products. Yang et al. (2020) compared absorption of PAs and their corresponding PA N-oxides in Sprague-Dawley rats by measuring plasma concentrations following single dose exposure. That work determined that absorption of PA N-oxides was consistently lower when compared to the corresponding parent compound, concluding that reduced absorption is one of the reasons for the purportedly lesser toxic potential of PA N-oxides.[40] Their findings regarding relative toxic potential between PAs and PA N-oxides (Yang et al., 2017) are contrary to those reported in this experiment.[46] Yang et al. (2019) also demonstrated intestinal and hepatic conversion of PA N-oxides to their parent compounds by rat liver microsomes.[22] The rate and site of conversion of PA N-oxides to corresponding PAs is an additional possible reason for species differences and even individual animal differences in hepatotoxicity. These compounds coexist as an equilibrium depending on rates of N-oxidation and reduction, which may be affected by pH and other physiologic parameters in the intestinal tract, the blood and liver. Intestinal conversion of PA N-oxides to PAs could explain why in vitro studies such as that performed by Field et al. (2015) find PA N-oxides to be among the least toxic, contrary to our findings.[45] Additional studies in mice and rats are needed to determine whether these converse findings represent a species difference between rats and mice, a difference in endpoint comparisons, or experimental variability.

Lethal Dose (LD50) Data:

Much of the published LD50 data (see table 2.9) for PAs was obtained using rats. Rats are more sensitive to PA toxicosis than mice, therefore using LD50 data from rats for mice in this study is inadequate.[8] Published LD50 values in rats and mice ranked from lowest to greatest are as follows: 1) senecionine (57 mg/kg, oral, mouse), 2) seneciphylline (77 mg/kg oral, rat, 90 mg/kg IV mouse), 3) riddelliine (80 mg/kg, oral, rat), 4) lasiocarpine (110 mg/kg, oral, rat) and 5) heliotrine (510 mg/kg, oral, rat).[29,30] LD50 data was not available for riddelliine N-oxide or senecionine N-oxide. Ranking these compounds by LD50 would also place the macrocyclic diester retronecine type PAs in the most toxic group, although the order of seneciphylline and riddelliine differs depending on whether we compare the LD50 for IV exposure in mice or oral exposure in rats. Lasiocarpine and heliotrine, the two heliotridine type PAs, both of which lack secondary ring structures in the necic acids, are ranked lowest in toxicity by each method used. This data suggests that mice, and possibly rats, are not as susceptible to poisoning from non-macrocyclic heliotridine type PAs (such as heliotrine and lasiocarpine) compared to the macrocyclic diester retronecine type (such as riddelliine, senecionine, and seneciphylline).

Weight Analysis:

Weight Loss:

Weight loss was a good indicator of toxicosis in this study. Weight loss was observed in every compound that caused significant microscopic hepatic necrosis. Riddelliine, riddelliine N-oxide, senecionine, senecionine N-oxide and seneciphylline caused weight

loss at doses that resulted in hepatic necrosis. The weight loss did not necessarily correlate with microscopic hepatic necrosis severity. For example, at 15 mg/kg/day, riddelliine caused more weight loss but milder hepatic necrosis when compared to seneciphylline and senecionine. Lasiocarpine only caused significant weight loss at the highest dose. This high dose (30 mg/kg/day) was the only dose of lasiocarpine for which microscopic necrosis was observed, but the necrosis was minimal and is unlikely to be the sole cause of weight loss. Heliotrine did not cause hepatic necrosis and did not cause significant weight loss at any dose.

Liver to Body Weight Ratios:

Increases in liver to body weight ratio were observed in mice with microscopic evidence of hepatocellular hypertrophy/swelling, and degeneration and necrosis. In our study, mice with significant increases in liver to body weight ratio consistently had microscopic evidence of hepatocellular hypertrophy/swelling, except for the mice exposed to 2 mg/kg/day of senecionine. In this group, the increase in liver to body weight ratio was thought to be spurious. Liver to body weight ratio is an excellent objective measurement that can be used to assess changes in the composition of the liver. These measurements must be viewed alongside the gross and microscopic appearance of the liver, and body weight loss must be taken into consideration.[47] Total liver weight is typically a useful measurement, but the mice used in this study are from a breeding colony and range from five to thirteen weeks of age so the value must be normalized by presenting it as a ratio over body weight. Increases in liver weight may indicate treatment related changes such as hepatocellular hypertrophy.[47] Liver weights must be interpreted in within the context of the entire data set for any given study. In this case, increases in liver to body weight

ratio occurred in conjunction with zonal to panlobular hepatocellular enlargement. Necrosis and hepatocellular loss may also influence liver weight, but in the mice that survived the dosing period liver to body weight ratios were consistently increased even in mice with severe hepatic necrosis. Weight loss will affect the liver to body weight ratio as well and must be considered while interpreting this measurement.

Serum Biochemistry Findings:

Clinical pathology, including serum biochemistry analyses are commonly employed in evaluations of toxicity. There are differences between species and even among strains of mice when it comes to the expected reference range of clinical pathology values.[48,49] Even collection method can affect these values. In an experimental setting, appropriate controls are critical for comparison and published reference ranges are less important. In this study there were limitations based on the available volume of blood and the specific serum biochemistry analyzer used. These limitations only allowed for consistent testing of 4-5 analytes, and less in cases where the blood draw was not ideal. For most mice the amount of whole blood collected ranged from 0.25-0.5 mL, and approximately half of this volume was obtained as serum after centrifugation. In some cases, dilution was needed to obtain the desired liver enzyme values. Priority was given to serum biochemistry values that are associated with liver damage because of these limitations.

Wang et al. (2020) showed that mice exposed to seneciphylline had severe liver injury, which had a positive correlation with elevations in serum ALT, AST, total bilirubin (TBIL), and total bile acid (TBA).[40] Yang et al. (2017) demonstrated elevations in serum ALT following senecionine exposure in mice.[39] Limitations imposed by sample

size and analyzer requirements did not enable us to evaluate TBIL and TBA in this experiment. Alanine aminotransferase (ALT) and alkaline phosphatase (ALP) were the most valuable measures of liver damage in this experiment. Aspartate aminotransferase (AST) did not correlate with the microscopic lesions. The cause of AST elevations in is not known. AST is typically an indicator of either liver damage or muscle injury.[50] Microscopic evaluation of skeletal muscle (right hind limb) was consistently unremarkable. ALT is considered one of the primary measures for detecting liver disease, and in this study ALT had strong correlations with microscopic changes of hepatic degeneration and necrosis.[51] ALT seems to be a good measure of liver damage caused by PA induced liver disease in mice. ALP also had strong correlations with microscopic hepatic necrosis. Increased serum concentrations of ALP are commonly used to indicate cholestasis which can be associated with liver damage.[52,53]

Hepatic Pyrrole Detection:

Detection of pyrroles in liver or other organs is the most specific marker of exposure to PAs available. The findings of zonal hepatocellular hypertrophy/swelling, degeneration and necrosis are nonspecific lesions. As is true with any toxicant, proving exposure does not necessarily prove intoxication as the cause of death, and detection of a toxicant must be interpreted in conjunction with the entire data set. Detection of microscopic lesions compatible with the toxicant detected is of paramount importance. Other biomarkers of hepatocellular injury such as serum concentrations of ALT and ALP are also helpful. In suspected natural intoxication cases, field studies inspecting the environment and feed sources are critically important and enable diagnosticians to determine the source of intoxication and make the correct diagnosis. Detection with HPLC MS-MS is the most

frequently utilized means of detection of PAs.[36] While HPLC MS-MS is the optimal test to confirm poisoning, it is not perfect. The toxic metabolite is volatile and can potentially be lost during processing. Additionally, the time frame in which the pyrrole persists within the liver following poisoning is not known, and may vary depending upon species, sex, nutritional status, and other variables. These factors provide challenges particularly for diagnostic cases, whereas in research where the time of exposure is known, HPLC MS-MS is a reliable method of pyrrole detection. In research detection of pyrrole is necessary to prove that the microscopic lesions and other endpoint changes are induced by the PAs evaluated.

There are multiple methods of detection for tissue bound pyrroles. In general, detection methods start by adding a chemical to cleave the pyrrole from the tissue product to which it is bound. This is typically accomplished using silver nitrate. After cleavage occurs, Ehrlich's reagent is added to the reaction to form a product that can be detected by high-performance liquid chromatography (HPLC) and mass spectrometry (MS). A recent study showed promise in detection of pyrrole-protein adducts using monoclonal antibodies, although this has not been widely used to this point.[54]

Riddelliine is particularly noteworthy in terms of hepatic pyrrole concentration. Riddelliine induced far greater concentrations of liver "pyrroles" than all other compounds at comparable doses except 8 mg/kg/day. Hepatic pyrrole concentrations in riddelliine exposed mice were up to eleven times greater than those of senecionine and seneciphylline. This information is disparate with the histopathologic findings in this study which indicate that senecionine, senecionine N-oxide and seneciphylline caused more severe hepatic necrosis than riddelliine at comparable doses. Concentrations of

hepatic pyrroles in riddelliine-exposed mice formed a somewhat sigmoidal curve when charted by dose, which may indicate enzymatic saturation of the mixed function oxidases responsible for bioactivation. Riddelliine is an important PA and an abundance of research has been performed using riddelliine. Several PAs have been associated with the development of various neoplasms, but riddelliine is the only pyrrolizidine alkaloid to be proven carcinogenic to the standards of the national toxicology program (NTP). (https://ntp.niehs.nih.gov/ntp/roc/content/listed_substances_508.pdf). Stegelmeier et al. (2016) observed that riddelliine induced liver pyrrole concentrations in chicks that were consistently greater than other PAs with similar hepatotoxicity and in some cases produced pyrrole concentrations that were ten times greater.[1] These results, in addition to the results of the current study suggest that hepatotoxicity is not directly related to pyrrole concentration for some PAs. The finding that pyrrole concentration did not necessarily coincide with severity of hepatocellular necrosis is noteworthy. This observation is difficult to explain given the current understanding of the toxic mechanisms by which PAs cause cellular damage. The production of toxic metabolites with different affinities for cellular constituents including DNA, RNA, proteins, etc., could explain this disparity. Said otherwise, if riddelliine produces greater concentrations of pyrroles that are more likely to damage DNA than those produced by senecionine or seneciphylline, this disparity could be explained. Similarly, senecionine and seneciphylline may produce toxic metabolites that are more likely to interact with vital cellular components and cause degeneration and necrosis.

Within compound groups, the relationship between pyrrole concentration and hepatic necrosis was mostly as expected. For example, riddelliine had a sharp increase in

pyrrole concentration which plateaued at the highest doses. Similarly, the histopathologic changes in the liver increased from multifocal centrilobular cell swelling to panlobular cell swelling with necrosis, but the higher doses were microscopically similar. Senecionine and seneciphylline had linear increases in pyrrole concentration as dose and severity of hepatic necrosis increased. In mice exposed to senecionine N-oxide hepatic pyrrole concentration changed very little as dose was increased but the severity of necrosis increased sometimes markedly with each successive dosing group. This result is somewhat unexpected given the need for enzymatic bioactivation to form the toxic metabolite. As discussed earlier, senecionine has been shown to have additional mechanisms of hepatotoxicity. Lasiocarpine induced lower concentrations of hepatic pyrroles than riddelliine, senecionine and seneciphylline. The only dose of lasiocarpine that induced hepatocellular necrosis was 30 mg/kg/day and the pyrrole concentration at this dose was similar to the pyrrole concentrations of riddelliine, senecionine and seneciphylline at which hepatic necrosis was first observed. Heliotrine induced minimal hepatic pyrrole concentrations at all doses. Heliotrine and lasiocarpine were the least toxic of these compounds by all measures. These two compounds differ from the remaining compounds in chemical structure. All the other five are retronecine macrocyclic diester, heliotrine is a monoester and lasiocarpine is an open diester and both are heliotridine type PAs. Riddelliine N-oxide induced 51-82% less of the pyrrole compared to its parent compound riddelliine. This is expected as PA N-oxides are thought of as less toxic and more water soluble than their parent compounds and hence more easily eliminated by excretion.[22] Unlike riddelliine N-oxide, senecionine N-oxide unexpectedly induced 1.31-4.24 times the concentration of hepatic pyrroles as its parent

compound senecionine. This work provides evidence that some PA N-oxides may be as toxic or even more toxic than their parent compounds in mice. Further work is needed to determine if this is true in other species and to evaluate additional PA N-oxides in direct comparison to their parent compounds.

Histopathologic Findings:

The hepatic lesion caused by all PAs evaluated (except heliotrine) included zonal hepatocyte hypertrophy/swelling followed by individual cell necrosis and/or foci of coagulative necrosis. Hepatocyte hypertrophy/swelling is zonal at lower doses and progresses to panlobular necrosis in the highest doses except for lasiocarpine. The severity and distribution of hepatocyte hypertrophy/swelling, degeneration and necrosis varied between PAs.

Hepatocyte hypertrophy has been associated with enzyme induction following exposure to various xenobiotics.[55] Gordon et al. (2000) demonstrated that retrorsine, a macrocyclic diester PA similar to those evaluated in this study, is an inducer of various CYP450 enzymes in rats.[56] They detected increased expression of hepatic CYPs 1A1, 1A2, 2B1/2 and 2E1 with little morphologic correlation such as altered cellular ultrastructure. Hepatocellular hypertrophy and cell swelling (enlargement) may look similar microscopically, particularly in the early stage of the lesion.[35] Degeneration is a more appropriate interpretation when there is clear progression from cell enlargement to necrosis indicated by organelle swelling and cellular vacuolation.[57,58] Hepatocyte hypertrophy likely precedes degeneration and necrosis after exposure to PAs. There are multiple illustrative examples in this study. For example, seneciphylline at doses of 8

mg/kg/day induced cellular enlargement and eosinophilia specifically in midzonal hepatocytes. Increases in cellular size and cytoplasmic eosinophilia, affecting specific lobular zones are characteristic of hepatocellular hypertrophy.[35] At this dose, one of the three mice had individual cell necrosis of swollen midzonal hepatocytes. As dose increased, hepatocytes in additional areas became enlarged with increased cytoplasmic eosinophilia and the frequency and severity of necrosis increased. These lesions demonstrate a progression starting with hepatocellular hypertrophy and ending with degeneration and necrosis. Ultrastructural research performed by Afzelius and Schoental (1967) concluded that rats had enlarged hepatocytes one month after exposure to retrorsine, and that the morphologic changes in these enlarged cells were not indicative of degeneration. Rather, they found that the changes indicated increased metabolic activity (hypertrophy).[59] Allen et al. (1970) showed that there was ultrastructural evidence of degeneration in the hepatocytes of chickens following a single dose of monocrotaline.[60] Our findings indicate a progression from hypertrophy to degeneration and necrosis, however we have also shown that PAs differ, and retrorsine and monocrotaline may have unique metabolic and toxic profiles which differ from the PAs in our study. Their studies also differed in the timing of sample collection, where we euthanized immediately after a ten-day exposure, they gave a single dose and performed necropsies 20 or 30 days later.

Alkaloid Specific Differences in Lobular Distribution:

In discussions of PA toxic mechanism, the toxic members of this group of compounds are lumped together under one mechanism of action. If the mechanism of action that results in hepatocellular damage in the liver is common, it is noteworthy that the distribution of hepatocellular hypertrophy, degeneration and necrosis differs between PAs. Differences

in lobular zonal distribution between individual PAs and PA N-oxides are demonstrated in this experiment. This difference in lobular lesion distribution supports differences in the site of bioactivation between different PAs. Multiple sources state that PAs induce degeneration and necrosis mainly in centrilobular hepatocytes.[16–18,28] One experimental study described periportal necrosis in horses following PA exposure.[20] The findings of our experiments indicate that generalizations regarding distributions of PAs and possibly other xenobiotics requiring CYP450 bioactivation are oversimplified. Heterogeneity exists between periportal and centrilobular hepatocytes in biotransformation, protection from oxidative damage, oxidative metabolism, glucose uptake and output, and other functional aspects.[61] Hailfinger et al. (2006) characterized gradated differences in gene expression along the portal to central axis, attributing these differences to gradients of opposing signaling molecules along this axis. The specific signaling pathways mentioned were β-catenin, presumably initiated by central vein endothelial cells, and a Ras-dependent pathway generated by blood-borne molecules. In this work, they used immunohistochemical staining to determine that CYP2C and CYP2E1 were preferentially expressed in centrilobular hepatocytes of mice. Using gene expression analysis, they showed an approximately 5-fold increase in expression of CYP1A1 in centrilobular hepatocytes. They also assert that CYPs involved in drug metabolism are almost exclusively expressed by centrilobular hepatocytes.[62] Multiple additional sources also state that the CYP450 enzymes responsible for bioactivation of PAs are in their greatest concentration in centrilobular areas.[13–16] The results of our studies suggest that the spatial distribution of CYP450 enzymes responsible for bioactivation of DHPAs may not be the main factor which determines distribution of necrosis following PA exposure.

Many studies evaluating CYP450 enzyme activity evaluate a small number of CYP450 enzymes. Information regarding greater concentrations of CYP450 enzymes in centrilobular areas explains why previous publications expected the distribution of DHPA induced hepatocellular injury to be centrilobular. Much of the literature regarding heterogeneity of hepatocytes discusses differences in periportal and pericentral (aka centrilobular) hepatocytes and leaves midzonal hepatocytes out.[61] This study demonstrates significant differences in the lobular distribution of the toxin induced lesion in mice between different PAs. Differences in distribution of hepatic necrosis between PAs may result from structurally specific preferential location of bioactivation, differences in phase II metabolism, or production of additional unique toxic metabolites.

Senecionine and its N-oxide similarly affected midzonal and periportal areas at lowest toxic doses, and riddelliine and its N-oxide affected centrilobular areas. Lasiocarpine specifically affected periportal hepatocytes. Heliotrine did not induce necrosis at any dose, and it is possible that the enlarged centrilobular hepatocytes observed in these mice represents a lesion of hypertrophy and not degeneration (see figure 2.9). Hypertrophy alone would not account for the elevations in ALT and ALP, which indicate hepatocellular and cholestatic injury respectively.[63]

For all the hepatotoxic macrocyclic diester retronecine type PAs, distribution of affected hepatocytes progressed to panlobular at higher doses. As dose increased, hepatocytes in other zones became affected until all hepatocytes were eventually affected by hepatocyte enlargement, with interspersed foci of necrosis and some individual cell necrosis. The progression of hepatocellular hypertrophy/swelling, degeneration, and

necrosis from zonal to panlobular observed in the five macrocyclic diester PAs illustrates another key concept, that dose determines lesion distribution in hepatic lobules.

Additional research is needed to determine the mechanism(s) responsible for producing PA specific lobular distributions. The toxic metabolite for pyrrolizidine alkaloids, typically referred to as a pyrrole, tends to be lumped together for all compounds and the mechanism is characterized as held in common for these compounds. If this is true, the reason for variability in lesion distribution may be based on spatial differences in distribution of specific CYP450 enzymes needed for bioactivation within the hepatic lobule. Other proposed explanations for the variation in lesion distribution include differences in phase II metabolism of the toxic metabolites, differing susceptibilities to toxicosis due to differences in blood flow across the lobule, alternative metabolic pathways or additional toxic metabolites that have not been discovered. Phase II metabolism of PAs occurs mainly by glutathione conjugation, but glucuronidation also participates minimally.[64,65] Heterogeneity in expression of protective molecules such as glutathione could explain the difference in zonal distribution between PAs. Jungermann (1986) notes that periportal hepatocytes have greater concentrations of glutathione and glutathione peroxidase.[61] Lobular differences in glutathione S transferase (GST) induction in rats has been documented, with three-fold greater concentrations in centrilobular hepatocytes than in periportal.[66] Differences in GST concentrations could affect which lobule is most susceptible to toxic insult. But this does not explain differences in distribution of individual PAs, unless different PAs could induce varying concentrations of GST in different areas of the lobule. Differences in blood flow across

the lobule would not account for differences in distribution between compounds within the same species either.

Previously undiscovered PA-specific toxic metabolites and alternative PA-specific metabolic pathways are interesting possibilities and considered the most likely cause of PA-specific differences in lobular distribution. Previous studies on senecionine discovered unique toxic metabolites and metabolic pathways. Griffin and Segall (1986) discovered an additional toxic metabolite, trans-4-hydroxy-2-hexenal, formed after bioactivation of senecionine.[37] Trans-4-hydroxy-2-hexenal has been shown induce hepatic necrosis although the distribution was not discussed. An additional enzymatic pathway in the metabolism of senecionine was discovered in which flavin-containing monooxygenases catalyzed N-oxidation of the compound.[67] It is possible that other PAs also produce additional undiscovered toxic metabolites which contribute to hepatotoxicity. Geburek et al. (2020) characterized metabolic products for several PAs including senecionine and lasiocarpine.[64] They determined that senecionine dehydrogenation reactions created ten different metabolites and lasiocarpine metabolism resulted in the production of 48 different metabolites. It is feasible that other PAs also have unique metabolic products and pathways that could result in differences in their toxic effects.

Pyrrolizidine alkaloid poisoning continues to be an important topic in human and animal health. This study highlights differences in toxic potential between the seven compounds evaluated. Important findings from this experiment include the ranking of hepatotoxicity from most to least toxic of senecionine, senecionine N-oxide and seneciphylline; followed by riddelliine and riddelliine N-oxide; and last, lasiocarpine and

heliotrine. We also showed that the acute hepatic lesion distribution from short-term PA exposure in mice is PA specific. This study also demonstrated that some PA N-oxides are equally or more toxic than their corresponding PAs. The results of this study should be viewed considering species differences in susceptibility to poisoning but provides valuable information regarding the mechanism of PA toxicity and the microscopic lesions from PA exposure.

References:

1. Stegelmeier, B. L., Colegate, S. M. & Brown, A. W. Dehydropyrrolizidine Alkaloid Toxicity, Cytotoxicity, and Carcinogenicity. *Toxins (Basel)* 8, 356 (2016).
2. Panziera, W., Pavarini, S. P., Sonne, L., Barros, C. S. L. & Driemeier, D. Poisoning of cattle by Senecio spp. in Brazil: a review. *Pesq. Vet. Bras.* 38, 1459–1470 (2018).
3. Edgar, J. A., Colegate, S. M., Boppré, M. & Molyneux, R. J. Pyrrolizidine alkaloids in food: a spectrum of potential health consequences. *Food Addit Contam Part A Chem Anal Control Expo Risk Assess* 28, 308–324 (2011).
4. Schrenk, D. *et al.* Pyrrolizidine alkaloids in food and phytomedicine: Occurrence, exposure, toxicity, mechanisms, and risk assessment - A review. *Food Chem Toxicol* 136, 111107 (2020).
5. Brugnerotto, P. *et al.* Pyrrolizidine alkaloids and beehive products: A review. *Food Chem* 342, 128384 (2021).
6. Neuman, M. G., Cohen, L., Opris, M., Nanau, R. M. & Hyunjin, J. Hepatotoxicity of Pyrrolizidine Alkaloids. *J Pharm Pharm Sci* 18, 825–843 (2015).
7. Dusemund, B. *et al.* Risk assessment of pyrrolizidine alkaloids in food of plant and animal origin. *Food Chem Toxicol* 115, 63–72 (2018).

8. Stegelmeier, B. L. *et al.* Pyrrolizidine alkaloid plants, metabolism and toxicity. *J Nat Toxins* 8, 95–116 (1999).

9. Lin, G., Cui, Y.-Y., Liu, X.-Q. & Wang, Z.-T. Species differences in the in vitro metabolic activation of the hepatotoxic pyrrolizidine alkaloid clivorine. *Chem Res Toxicol* 15, 1421–1428 (2002).

10. Ebmeyer, J. *et al.* Human CYP3A4-mediated toxification of the pyrrolizidine alkaloid lasiocarpine. *Food Chem Toxicol* 130, 79–88 (2019).

11. Haschek, W. M., Rousseaux, C. G. & Wallig, M. A. Toxicologic Pathology: An Introduction. in *Haschek and Rousseaux's Handbook of Toxicologic Pathology* 1–9 (Elsevier, 2013). doi:10.1016/B978-0-12-415759-0.00094-7.

12. Chen, T., Mei, N. & Fu, P. P. Genotoxicity of pyrrolizidine alkaloids. *J Appl Toxicol* 30, 183–196 (2010).

13. Oinonen, T. & Lindros, K. O. Zonation of hepatic cytochrome P-450 expression and regulation. *Biochem J* 329 (Pt 1), 17–35 (1998).

14. Means, S. A. & Ho, H. A spatial-temporal model for zonal hepatotoxicity of acetaminophen. *Drug Metab Pharmacokinet* 34, 71–77 (2019).

15. Dail, M. B. *et al.* Spatial distribution of CYP2B1/2 messenger RNA within the rat liver acinus following exposure to the inducers phenobarbital and dieldrin. *Toxicol Sci* 99, 35–42 (2007).

16. Brown, D. L., Van Wettere, A. J. & Cullen, J. M. Hepatobiliary System and Exocrine Pancreas. in 412-470.e1 (Elsevier, 2017). doi:10.1016/B978-0-323-35775-3.00008-4.

17. Acland, H. M. *et al.* Toxic hepatopathy in neonatal foals. *Vet Pathol* 21, 3–9 (1984).

18. *Jubb, Kennedy, and Palmer's pathology of domestic animals*. (Elsevier, 2016).

19. Brown, A. W. *et al.* The comparative toxicity of a reduced, crude comfrey (Symphytum officinale) alkaloid extract and the pure, comfrey-derived pyrrolizidine alkaloids, lycopsamine and intermedine in chicks (Gallus gallus domesticus). *J Appl Toxicol* 36, 716–725 (2016).

20. Stegelmeier, B. L., Gardner, D. R., James, L. F. & Molyneux, R. J. Pyrrole detection and the pathologic progression of Cynoglossum officinale (houndstongue) poisoning in horses. *J Vet Diagn Invest* 8, 81–90 (1996).

21. Harding, J. D. J., Lewis, G., Done, J. T. & Allcroft, R. Experimental Poisoning by Senecio jacobaea in Pigs. *Pathologia veterinaria* 1, 204–220 (1964).

22. Yang, M. *et al.* Intestinal and hepatic biotransformation of pyrrolizidine alkaloid N-oxides to toxic pyrrolizidine alkaloids. *Arch Toxicol* 93, 2197–2209 (2019).

23. Jacks, T. *et al.* Tumor spectrum analysis in p53-mutant mice. *Curr Biol* 4, 1–7 (1994).

24. Protocol 37953 - Trp53<tm1Tyj>-Probe. https://www.jax.org/Protocol?stockNumber=002101&protocolID=37953.

25. Protocol 27521 - Trp53<tm1Tyj> Alternate2. https://www.jax.org/Protocol?stockNumber=002101&protocolID=27521.

26. Delidow, B. C., Lynch, J. P., Peluso, J. J. & White, B. A. Polymerase chain reaction : basic protocols. *Methods Mol Biol* 15, 1–29 (1993).

27. Culvenor, C., Edgar, J., Smith, L. & Tweeddale, H. Dihydropyrrolizines. III. Preparation and reactions of derivatives related to pyrrolizidine alkaloids. *Aust. J. Chem.* 23, 1853 (1970).

28. Brown, A. Relative Toxicity of Select Dehydropyrrolizidine Alkaloids and Evaluation of a Heterozygous P53 Knockout Mouse Model for Dehydropyrrolizidine Alkaloid Induced Carcinogenesis. *All Graduate Theses and Dissertations* (2015) doi:https://doi.org/10.26076/7997-d859.
29. World Health Organization and Food and Agriculture Organization of the United Nations. Safety evaluation of certain food additives and contaminants: supplement 2: pyrrolizidine alkaloids, prepared by the eightieth meeting of the Joint FAO/WHO Expert Committee on Food Additives (JECFA). https://www.who.int/publications-detail-redirect/9789240012677.
30. *Sax's Dangerous Properties of Industrial Materials*. (Wiley, 2004). doi:10.1002/0471701343.
31. Mattocks, A. R. *Chemistry and toxicology of pyrrolizidine alkaloids*. (Academic Press, 1986).
32. Yang, M. *et al.* Absorption difference between hepatotoxic pyrrolizidine alkaloids and their N-oxides - Mechanism and its potential toxic impact. *J Ethnopharmacol* 249, 112421 (2020).
33. Maronpot, R. R. Liver - Necrosis - Nonneoplastic Lesion Atlas. https://ntp.niehs.nih.gov/nnl/hepatobiliary/liver/necrosis/index.htm.
34. Kim, H.-Y. Analysis of variance (ANOVA) comparing means of more than two groups. *Restor Dent Endod* 39, 74–77 (2014).
35. Hall, A. P. *et al.* Liver Hypertrophy: A Review of Adaptive (Adverse and Non-adverse) Changes—Conclusions from the 3rd International ESTP Expert Workshop. *Toxicol Pathol* 40, 971–994 (2012).

36. Ma, J., Xia, Q., Fu, P. P. & Lin, G. Pyrrole-protein adducts - A biomarker of pyrrolizidine alkaloid-induced hepatotoxicity. *J Food Drug Anal* 26, 965–972 (2018).

37. Griffin, D. S. & Segall, H. J. Genotoxicity and cytotoxicity of selected pyrrolizidine alkaloids, a possible alkenal metabolite of the alkaloids, and related alkenals. *Toxicol Appl Pharmacol* 86, 227–234 (1986).

38. Xiong, A. *et al.* Metabolomic and genomic evidence for compromised bile acid homeostasis by senecionine, a hepatotoxic pyrrolizidine alkaloid. *Chem Res Toxicol* 27, 775–786 (2014).

39. Yang, X. *et al.* Inhibition of Drp1 protects against senecionine-induced mitochondria-mediated apoptosis in primary hepatocytes and in mice. *Redox Biol* 12, 264–273 (2017).

40. Wang, W. *et al.* Seneciphylline, a main pyrrolizidine alkaloid in Gynura japonica, induces hepatotoxicity in mice and primary hepatocytes via activating mitochondria-mediated apoptosis. *Journal of Applied Toxicology* 40, 1534–1544 (2020).

41. Chou, M. W. *et al.* Riddelliine N-oxide is a phytochemical and mammalian metabolite with genotoxic activity that is comparable to the parent pyrrolizidine alkaloid riddelliine. *Toxicol Lett* 145, 239–247 (2003).

42. Peterson, J. E. & Jago, M. V. Comparison of the toxic effects of dehydroheliotridine and heliotrine in pregnant rats and their embryos. *J Pathol* 131, 339–355 (1980).

43. Schoental, R. Pancreatic islet-cell and other tumors in rats given heliotrine, a monoester pyrrolizidine alkaloid, and nicotinamide. *Cancer Res* 35, 2020–2024 (1975).

44. Pass, D. A. *et al.* Poisoning of chickens and ducks by pyrrolizidine alkaloids of Heliotropium europaeum. *Aust Vet J* 55, 284–288 (1979).

45. Field, R. A., Stegelmeier, B. L., Colegate, S. M., Brown, A. W. & Green, B. T. An in vitro comparison of the cytotoxic potential of selected dehydropyrrolizidine alkaloids and some N-oxides. *Toxicon* 97, 36–45 (2015).

46. Yang, M. *et al.* First evidence of pyrrolizidine alkaloid N-oxide-induced hepatic sinusoidal obstruction syndrome in humans. *Arch Toxicol* 91, 3913–3925 (2017).

47. Sellers, R. S. *et al.* Society of Toxicologic Pathology position paper: organ weight recommendations for toxicology studies. *Toxicol Pathol* 35, 751–755 (2007).

48. Matsuzawa, T., Nomura, M. & Unno, T. Clinical pathology reference ranges of laboratory animals. Working Group II, Nonclinical Safety Evaluation Subcommittee of the Japan Pharmaceutical Manufacturers Association. *J Vet Med Sci* 55, 351–362 (1993).

49. McClure, D. E. Clinical pathology and sample collection in the laboratory rodent. *Vet Clin North Am Exot Anim Pract* 2, 565–590, vi (1999).

50. Panteghini, M. Aspartate aminotransferase isoenzymes. *Clin Biochem* 23, 311–319 (1990).

51. Senior, J. R. Alanine aminotransferase: a clinical and regulatory tool for detecting liver injury-past, present, and future. *Clin Pharmacol Ther* 92, 332–339 (2012).

52. Tang, G. *et al.* Comparing distress of mouse models for liver damage. *Sci Rep* 10, 19814 (2020).

53. Xu, Q., Lu, Z. & Zhang, X. A novel role of alkaline phosphatase in protection from immunological liver injury in mice. *Liver* 22, 8–14 (2002).

54. Li, N. *et al.* Immunoassay approach for diagnosis of exposure to pyrrolizidine alkaloids. *J Environ Sci Health C Environ Carcinog Ecotoxicol Rev* 35, 127–139 (2017).

55. Maronpot, R. R. *et al.* Hepatic enzyme induction: histopathology. *Toxicol Pathol* 38, 776–795 (2010).

56. Gordon, G. J., Coleman, W. B. & Grisham, J. W. Induction of cytochrome P450 enzymes in the livers of rats treated with the pyrrolizidine alkaloid retrorsine. *Exp Mol Pathol* 69, 17–26 (2000).

57. Thoolen, B. *et al.* Proliferative and Nonproliferative Lesions of the Rat and Mouse Hepatobiliary System. *Toxicol Pathol* 38, 5S-81S (2010).

58. Majno, G. & Joris, I. Apoptosis, oncosis, and necrosis. An overview of cell death. *Am J Pathol* 146, 3–15 (1995).

59. Afzelius, B. A. & Schoental, R. The ultrastructure of the enlarged hepatocytes induced in rats with a single oral dose of retrorsine, a pyrrolizidine (Senecio) alkaloid. *Journal of Ultrastructure Research* 20, 328–345 (1967).

60. Allen, J. R., Carstens, L. A. & Norback, D. H. Ultrastructural and biochemical changes in the liver of monocrotaline intoxicated chickens. *Toxicology and Applied Pharmacology* 16, 800–806 (1970).

61. Jungermann, K. Functional heterogeneity of periportal and perivenous hepatocytes. *Enzyme* 35, 161–180 (1986).

62. Hailfinger, S., Jaworski, M., Braeuning, A., Buchmann, A. & Schwarz, M. Zonal gene expression in murine liver: lessons from tumors. *Hepatology* 43, 407–414 (2006).

63. Amacher, D. E. A toxicologist's guide to biomarkers of hepatic response. *Hum Exp Toxicol* 21, 253–262 (2002).

64. Geburek, I., Schrenk, D. & These, A. In vitro biotransformation of pyrrolizidine alkaloids in different species: part II-identification and quantitative assessment of the metabolite profile of six structurally different pyrrolizidine alkaloids. *Arch Toxicol* 94, 3759–3774 (2020).

65. He, Y.-Q. *et al.* Glucuronidation, a new metabolic pathway for pyrrolizidine alkaloids. *Chem Res Toxicol* 23, 591–599 (2010).

66. Selim, N., Branum, G. D., Liu, X., Whalen, R. & Boyer, T. D. Differential lobular induction in rat liver of glutathione S-transferase A1/A2 by phenobarbital. *Am J Physiol Gastrointest Liver Physiol* 278, G542-550 (2000).

67. Miranda, C. L. *et al.* Flavin-containing monooxygenase: a major detoxifying enzyme for the pyrrolizidine alkaloid senecionine in guinea pig tissues. *Biochem Biophys Res Commun* 178, 546–552 (1991).

CHAPTER III RELATIVE CARCINOGENICITY OF FIVE DEHYDROPYRROLIZIDINE ALKALOIDS; RIDDELLIINE, SENECIONINE, SENECIPHYLLINE, LASIOCARPINE AND HELIOTRINE IN MALE HETEROZYGOUS P53 KNOCKOUT MICE.

Abstract:

Dehydropyrrolizidine alkaloids (PAs) are a large group of plant derived toxins. Though liver toxicity is recognized as the primary effect of poisoning, there has long been evidence that some PAs are carcinogenic. Exposure to PA containing plants occurs in both humans and animals. Human exposure occurs through ingestion of foods containing PAs. PAs can be present in foods either as natural components of the food, (i.e., herbal teas), by animal exposure to PAs followed by transfer into food products (i.e., milk, honey, or eggs), or grain contamination with PA-containing plants. Animal exposure occurs through contamination of hay or grain, or by grazing. Over 600 PAs have been identified though only half are purportedly toxic. Of the toxic PAs, only Riddelliine has been designated a potential human carcinogen by the standards of the National Toxicology Program (NTP). As similar mechanisms have been hypothesized for toxicity and carcinogenicity, additional work is needed to correlate toxic and carcinogenic effects in a suitable comparative model. In this work heterozygous male p53 knockout mice were exposed to riddelliine, senecionine, seneciphylline and heliotrine for ten days at doses of 0.129 mmol/kg/day for ten days. Lasiocarpine was administered at 0.086 mmol/kg/day, and a vehicle control group was exposed to ethanol. The mice were necropsied one year later, and the incidence of neoplasia was compared between these groups. A variety of neoplasms were detected in various organs in all groups, including the vehicle control.

The most common tumors observed were hemangiosarcomas, bronchioloalveolar tumors, lymphoma, and soft tissue sarcomas. Hemangiosarcoma was the tumor of interest as this was the main neoplasm observed in the National Toxicology Program (NTP) rodent riddelliine studies. Due to relatively high neoplastic transformation in all groups, there were no statistical differences in the incidence of neoplasia between the control group and any compound group. Although not statistically significant, riddelliine-exposed mice developed the greatest number of tumors and the greatest number of hemangiosarcomas. Based on these results, senecionine, seneciphylline, lasiocarpine and heliotrine are not carcinogenic in mice under the conditions of exposure used in this study. These results also indicate the short-term PA exposure is less likely to induce neoplasia when compared to long-term exposure.

Key words: Pyrrolizidine alkaloids, dehydropyrrolizidine alkaloids, riddelliine, senecionine, carcinogen, mice.

Introduction:

In the previous chapter C57BL6/j mice were exposed to riddelliine, senecionine, seneciphylline, lasiocarpine and heliotrine at varying doses for ten days to compare the toxic potencies of these dehydropyrrolizidine alkaloids (PAs). In this chapter, carcinogenic potential between five PAs from that group is compared. One of the purposes of the study described in the previous chapter was to determine a suitable dose for this year long carcinogenicity experiment. The PA with the strongest evidence of carcinogenicity is riddelliine, hence this compound is used as a positive control in these

comparisons. To remove dose as a variable, a common molar dose was used for the PAs in this study except lasiocarpine. Lasiocarpine was not tolerated at the same dose, and a reduced dose equal to 2/3 of the molar dose used for the other PAs was used. The ranking of toxicity determined in the pilot study, from most toxic to least was senecionine, seneciphylline, riddelliine, lasiocarpine and heliotrine. The highest dose of the most toxic PAs was selected for use in this study. The pilot studies demonstrated that mice would tolerate this dose for the ten-day dosing period. Because riddelliine is the standard of carcinogenicity the other PAs are being measured against, 45 mg/kg/day of riddelliine was used to calculate the molar dose of 0.129 mmol/kg/day used for all PAs in this study. This short-term dosing strategy was selected to replicate the type of exposure that a livestock animal in North America may be exposed to. Livestock exposure in North America occurs mainly through contamination of hay as fields are invaded by PA containing plants. Consequently, most livestock have periodic exposures that occur when they are fed contaminated feeds. It is unlikely that chronic low dose exposures would occur in this setting. However, such chronic lifespan exposures were the methods used in long-term carcinogenicity studies. Using such chronic exposures, the National Toxicology Program (NTP) established riddelliine as a known carcinogen in rats and mice. In the NTP riddelliine studies, rodents were dosed daily for two years.[1] Such chronic exposures are unlikely in livestock even in areas were PA containing plants are endemic.

Background:

Dehydropyrrolizidine alkaloids (PAs) are a large group of plant derived toxins classified by a common chemical base structure. Ingestion of several PA containing plants and

some isolated PAs have been associated with the development of various neoplasms in rodents[2–10]. Given that PAs are known to vary in toxic potential, we aimed to evaluate the differences in carcinogenic and genotoxic potential between select PAs. Using dosing data from Brown and Stegelmeier's work (2015), and the pilot studies performed in chapter 2, carcinogenicity of five PAs in male heterozygous p53 knockout mice was compared.[4] We hypothesize that hepatotoxic PAs are likely to be carcinogenic. We suppose that the ranking of carcinogenicity will be similar to the hepatotoxicity ranking obtained in chapter one. In other words, senecionine and seneciphylline will induce neoplasia at the greatest frequency followed by riddelliine, lasiocarpine and heliotrine.

Dehydropyrrolizidine Alkaloid Toxicity:

Please refer to these chapters 1 and 2 for details regarding the mechanism of toxicity, metabolism, chemistry, and occurrence in plants. PAs require metabolic bioactivation by the cytochrome p450 (CYP450) enzymes to exert toxicity. As such, toxic effects are largely directed at the liver because the liver has the greatest tissue concentrations of CYP450 enzymes.[9] Some PAs are also pneumotoxic, but pneumotoxic affects require greater doses and are generally specific to certain PAs such as monocrotaline.[11–13] The PAs used in this study are primarily hepatotoxins and as detailed in chapter 2, pulmonary lesions were not observed following ten-day exposure to various doses of PAs, while hepatic degeneration and necrosis was marked.

Genotoxicity:

Genotoxicity is the ability of an agent to cause DNA or chromosomal damage. Genotoxicity may result in mutagenicity and carcinogenicity. Genotoxicity studies often

precede studies involving carcinogenicity and are important in characterizing the mechanism by which chemical-induced carcinogenicity may occur.[14] Metabolic formation of pyrrolic esters is considered the main mechanism by which the genotoxic and carcinogenic effects of PAs occurs.[15] These pyrrolic esters exhibit multiple mechanisms of genotoxicity including formation of covalent bonds to DNA, DNA cross-linking, and DNA-protein cross-linking.[15,16] Some early genotoxicity studies involving PAs operated under the assumption that all PAs are equally genotoxic. Relative genotoxicity between individual PAs is an understudied area of this field of research. It is hypothesized that the same mechanisms that contribute to hepatotoxic potential of individual PAs (chemical structure and species-specific metabolism) also determine their genotoxic potential. If this is the case formation of pyrroles, reactive toxic metabolites which can bind to proteins and nucleic acids, should correlate with both toxicity and carcinogenicity.[9] Hadi et al. (2021) demonstrated differences in genotoxicity of seven PAs in human hepatoma cells, finding that lasiocarpine and riddelliine were the most genotoxic; retrorsine and echimidine were intermediate; and seneciphylline, europine and lycopasamine were the least.[17] These results do not correlate with our individual PA toxicitiy findings discussed in chapter two. We found that mice dosed with purified lasiocarpine had minimal affects, and seneciphylline was among the most toxic compounds. This difference in ranking of in vitro genotoxicity to human cells and hepatotoxicity to mice highlight a major challenge in PA research. This challenge is the fact that in vitro studies do not necessarily correspond to in vivo studies, and neither do in vivo studies in one species necessarily correspond with other species.

Carcinogenicity:

The mechanism responsible for PA induced neoplasia, as well as genotoxicity is thought to be due to the formation of pyrrole-DNA adducts, DNA-DNA crosslinks and DNA-protein crosslinks.[9,15,16] This damage often results in nucleic acid mutations. Molecularly these have been characterized as: G:C > T:A transversions and GG > TT and GG > AT base substitutions.[17,18] Riddelliine has been shown to have the greatest affinity for guanine but were capable of binding to adenine, and thymine as well.[19] Mei et al., (2004) found that more protein DNA adducts were generated in hepatic sinusoidal endothelial cells compared to hepatocytes, which may explain why hemangiosarcomas occur when mice and rats were treated with riddelliine [1,2,18] Molecular studies of riddelliine-induced mutations showed that nearly all mutations were base pair substitutions.[20]

The carcinogenic potential of PAs has been understood, or at least purported for many decades. The strongest evidence of the carcinogenic potential was published by Chan et al. (2003) in a large group of experiments conducted by the National Toxicology Program (NTP) using riddelliine in mice and rats. The NTP performed multiple studies on riddelliine, exposing male and female mice and rats to the compound for two years. They reported clear evidence of carcinogenicity in male and female rats and mice. The most frequent tumors observed in male mice were hemangiosarcomas of the liver. Female mice mainly developed lung tumors. Rats exposed to riddelliine developed liver tumors, including hemangiosarcomas, hepatomas and hepatocellular carcinomas. As a result of this work, riddelliine was classified as a "potential human carcinogen" by the NTP [1,2] Rats exposed to riddelliine developed liver tumors, including hemangiosarcomas, hepatomas and hepatocellular carcinomas. Male mice developed similar liver tumors,

whereas female mice mainly developed lung tumors. Leukemia was also increased in riddelliine exposed mice. [1] Additional publications have also reported carcinogenesis due to PA exposure. Allen et al. (1975) demonstrated that rats would develop rhabdomyosarcomas at the injection site when monocrotaline or dehydroretronecine were injected biweekly for one year. Some of these rats also developed metastatic lesions including myelogenous leukemias. [21] Johnson et al. (1978) demonstrated that female swiss mice would develop skin tumors after topical and injectable exposure to dehydroretronecine, the toxic metabolite of retronecine PAs. Most tumors were basal cell tumors or squamous cell carcinomas.[22] Mattocks and Cabral (1982) provided similar evidence that topical dehydromonocrotaline and dehydroretronecine induced integumentary malignancies in LACA mice.[23]

Rats have been shown to develop hemangiosarcomas, hepatic adenomas, carcinomas or other liver tumors following exposure to multiple PA containing plants, including *Tussilago farfara*, *Senecio jacobea*, *Symphytum officinale*, *Senecio longilobus*, *Farfugium japonicum*, and *Senecio cannabifolius*.[5,7,24–26] Rats have also been shown to develop liver tumors from exposure to individual PAs such as senkirkine, symphytine, riddelliine, lasiocarpine, clivorine and petasitene. [1,3,6,8,10,27] . Kuhara et al. (1980) also induced liver neoplasms in inbred rats by adding the PA clivorine into drinking water.[8] Some of these studies used injection as the method of exposure, whereas natural exposure occurs through ingestion.

Experimental Design:

Aims and Hypothesis:

Previous studies have demonstrated that individual PAs differ in their hepatotoxic, genotoxic and cytotoxic potential. We aim to characterize the frequency and type of neoplasia that develops in heterozygous male p53 knockout mice (following short-term exposure to senecionine, seneciphylline, riddelliine, lasiocarpine and heliotrine. We hypothesize that PA-induced hyperplasia, dysplasia and carcinogenicity differ as does toxicity according to PA base and ester structures. Considering the ranking of hepatotoxicity obtained in chapter one, we hypothesize that seneciphylline and senecionine will induce carcinogenesis more frequently when compared to riddelliine, a known carcinogen. Lasiocarpine and heliotrine are unlikely to induce carcinogenesis.

Dehydropyrrolizidine Alkaloids Used in This Experiment:

Five PAs were compared in this experiment. The initial work included a pilot study to determine a dose that would produce non-fatal poisoning during a relatively short ten-day exposure by gastric gavage. The results of this study were reported in chapter 2. The PAs selected were riddelliine, senecionine, seneciphylline, lasiocarpine and heliotrine. Each of which were compared against both a negative and positive control. The negative control group was gavaged with carrier, 10% ethanol and water. Riddelliine was selected as a positive control because of its established status as a carcinogen in rats and mice. The NTP performed multiple studies on riddelliine, exposing male and female mice and rats to the compound for two years. They reported clear evidence of carcinogenicity in male and female rats and mice. The most frequent tumors observed in male mice were

hemangiosarcomas of the liver.[1,2] Senecionine and seneciphylline are selected as they are similar structurally to riddelliine and they produce similar hepatic necrosis in other animals and in mice .[28–31] Lasiocarpine and heliotrine are used as examples of PAs that are less toxic in mice when compared to senecionine, seneciphylline and riddelliine. Lasiocarpine caused minimal hepatic necrosis in the pilot study, while in mice heliotrine had no effect on the liver or any other organ. Other studies have shown that lasiocarpine can cause hepatic necrosis when doses of 80-110 mg/kg when administered intravenously to mice.[32] Lasiocarpine is also toxic in other species including rats.[10,33]

Mouse Model:

Five- to thirteen-week-old, heterozygous B6.129S2-Trp53tm1Tyj/J male mice were used for this experiment. Long-term rodent carcinogenicity studies are usually lifetime studies that generally last two years. Exposure to the candidate carcinogen often occurs for the duration of the experiment, i.e., two full years. Exposure routes vary as many agents allow easy addition to feed or water. This has been attempted by mixing PA containing plant material into rodent chow; however, with the exception of riddelliine most PA are difficult to isolate and purify. Riddelliine is unique as it is the primary alkaloid in *Senecio riddellii* and is often in concentrations of nearly 18% of the plant dry weight.[34] Dosing purified PAs is also problematic as most are insoluble requiring acidic solvents that complicate dosing. Typical variable response studies require groups of 50 male and 50 female mice or rats chronically dosed for more than 700 days which requires kg. amounts of purified PAs. A more sensitive model is needed for a direct in-vivo comparisons of carcinogenicity using the small amounts of purified PAs that are available. Genetically modified mice have been proposed as such a model.[35,36] Brown, et al., (2015)

investigated the use of heterozygous p53 knockout male mice in the study of dehydropyrrolizidine alkaloid induced carcinogenicity. In this work, they exposed mice to riddelliine at various doses by oral gavage or in pelleted feed and observed an increased incidence and dose-related trend of liver tumors compared to non-exposed heterozygous p53 knockout control mice. Brown's work demonstrated the utility of this animal model in the study of dehydropyrrolizidine alkaloid induced carcinogenicity.[4] Male mice were used exclusively to eliminated variability in response due to sex. Males were preferable to females based on the NTP study on carcinogenesis from riddelliine in rats and mice, which determined that male mice were more susceptible than females to liver carcinogenesis following exposure to riddelliine.[1,2] With these facts in mind, our study aims to perform carcinogenicity studies on hepatotoxic PAs in a shorter period than the typical two years by using riddelliine as a positive control in a p53 knockout mouse model. The number of variables is reduced by using only male mice and using an equivalent molar dose. Jacks et al. (1994) developed this p53 knockout mutation via deletion of 40% of the coding reason for the p53 gene.[37] Homozygous mice have a complete lack of the p53 protein and develop neoplasms at three to six months of age. Mice that are heterozygous for the mutation also developed neoplasms at an increased frequency. Heterozygous mice had similar viability to wild type mice until nine months of age, but by seventeen months 28% of these mice had died or had to be euthanized. These heterozygous animals developed a variety of tumors, but sarcomas were the most frequent. They measured the concentration of the p53 protein in fibroblasts and determined that heterozygous mice had approximately half the concentration when compared to wild type mice.[37] The exposure method used in the current study differs

from a typical long-term carcinogenicity study. The United States Department of Agriculture Poisonous Plant Research Laboratory's mission is "to investigate poisonous plants and their toxins, determine how the plants poison animals, develop and prognostic procedures, identify the conditions under which poisoning occurs, and develop management strategies and treatments for ranchers to reduce livestock losses". The majority of livestock exposure occurs through ingestion of contaminated feedstuffs as livestock typically avoid these nonpalatable plants.[38,39] The ten-day dosing regimen used in this study is meant to replicate the exposure that a livestock animal may be exposed to from a one-time exposure to a crop of contaminated feed. This type of exposure is also comparable to human exposure resulting from ingestion of contaminated grain, as has occurred in large-scale outbreaks in developing countries, or from short term use of PA containing medicinal plants or other herbal products.[40–44]

Materials and Methods

Animals:

Mice used for this experiment were heterozygous for the B6.129S2 - Trp 53 ^{tm1Tyj}/J mutation, a mutation which knocks out the p53 gene. Heterozygous B6.129S2-Trp53tm1Tyj/J (p53 knockout) male mice were sourced from the United States Department of Agriculture Poisonous Plant Research Laboratory (USDA PPRL) breeding colony. Heterozygous B6.129S2 - Trp 53 ^{tm1Tyj}/J (JAX stock #002101) mice obtained from The Jackson Laboratory (Bar Harbor, Maine) were used to maintain the breeding colony at the USDA PPRL.[37] During breeding, heterozygous males were housed with heterozygous females, one of each per cage. Pups were weened at 4-5 weeks. After

weening, a Trovan 100B/1.4 identification chip was implanted subcutaneously in the interscapular region, and a tail snip was obtained and frozen for genotyping. Genotyping was performed to determine whether progeny mice were wild type, homozygous or heterozygous for the B6.129S2 - Trp 53 ^{tm1Tyj}/J mutation according to the manufacturers (The Jackson Laboratory) guidelines.[45,46] DNA was isolated from mouse tail snips using the Gentra Puregene protocol according to the manufacturer's instructions (Qiagen, Germantown, MD). PCR for genotyping were performed using the protocol from Diledow et al. (1993).[47] All mice were acclimated to the cage environment for at least 7 days prior to treatment. Mice were housed in groups of five in Innovive cages (Innovive, San Francisco, CA) with Teklad ¼" corncob bedding (Envigo, Livermore, CA). The mouse facility has ambient light for 12 hours per day, and no ambient light overnight. Teklad Laboratory diet 8604 (Envigo, Livermore, CA). was fed ad libitum. Water was also provided ad libitum. Temperature and humidity were maintained at 70 degrees Fahrenheit and 30% respectively. This research was conducted with the approval of the Utah State University animal care and use committee (IACUC Protocol # 12195).

Purified Dehydropyrrolizidine Alkaloids:

PAs and PA N-oxides used were obtained from the USDA ARS Poisonous Plant Research Laboratory's collection that were previously isolated from various plant collections. Purity of 98% or greater was confirmed using liquid chromatography mass spectrometry (LC-MS) and nuclear magnetic resonance (NMR).[48]

Animal Groups and Dosing:

Fifty heterozygous male p53 knockout (B6.129S2-*Trp53*^{tm1Tyj}/J) mice were exposed to one of five compounds as well as a control group which was exposed to the vehicle (ethanol). Each PA group and the control consists of two groups of 25, with a total sample size of 50 mice. Experiments were completed in two groups of 25 mice each for riddelliine, senecionine, seneciphylline and lasiocarpine. In the groups exposed to heliotrine, there were three groups, composed of 25, 23 and 2 mice due to a lack of sufficient numbers of heterozygous mice from the breeding colony. The order with which the experiments were completed was control, lasiocarpine, riddelliine, seneciphylline, senecionine, and last was heliotrine. The dates of the experiments can be seen in table 3.1 below. Mice were exposed by oral gavage to each PA for ten days. Each PA dose was 0.129 mmol/kg/day except lasiocarpine. Lasiocarpine was given at the lower dose of 0.073 mmol/kg, as mice could not tolerate ten days of dosing at 0.129 mmol/kg/day in a previous unpublished experiment performed at the USDA PPRL. Doses in mg/kg/day are as follows: riddelliine 45 mg/kg/day, lasiocarpine 30 mg/kg/day, senecionine 43.2 mg/kg/day, seneciphylline 42.9 mg/kg/day and heliotrine 40.36 mg/kg/day. Vehicle control mice were gavaged with 1.38 mL/kg absolute ethanol, the same volume riddelliine-exposed mice were given in the riddelliine solution. PAs in solution and the vehicle (absolute ethanol) were diluted in water prior to gavage making a total volume of approximately 0.5 mL. The order of compounds tested was randomly selected. Doses were selected based on data obtained from the short-term pilot studies described in chapter two and on Brown et al.'s (2015).[4]

During dosing, mice were evaluated daily for clinical signs suggestive of hepatotoxicity, including malaise, inappetence, or changes in mentation. After dosing mice were observed on weekdays. Mice were weighed using an Adventurer SL AS1502 scale (Ohaus, Parsippany, NJ) on Monday, Wednesday and Friday, during dosing. After dosing, mice were weighed weekly and again at the time of necropsy. Livers were weighed at the time of necropsy.

Mice were euthanized and necropsied one year after dosing was completed. Mice that developed significant weight loss or other clinical signs were euthanized early according to the IACUC guidelines. Weight loss was considered significant if it amounted to 20 percent or more of their body weight in one week, or if the weight loss was persistent over 2-4 weeks, depending on severity of weight loss and concurrent clinical signs such as malaise or lethargy. Euthanasia was achieved using a CO2 chamber. During necropsy, gross evaluation of all major organs was performed. The brain, liver, heart, trachea, lungs, spleen, thyroid glands, kidneys, urinary bladder, adrenal glands, esophagus, stomach, duodenum, jejunum, ileum, colon, pancreas, and right testicle were placed in 10% neutral buffered formalin. After formalin fixation, tissues were processed and embedded in paraffin according to routine histologic techniques. Sections, 5-µm thick, were stained with hematoxylin and eosin (H&E) stain according to standard methods and examined by light microscopy. An Olympus BX-53 microscope (Shinjuku, Tokyo, Japan) was used for microscopy. Gross and microscopic lesions were recorded. Tumors were diagnosed based on microscopic evaluation of H&E-stained sections.

Table 3.1. Dates of experiments

PA		Dosing	Necropsy date
Vehicle control	group 1 (n=25)	7/16/2018-7/25/2018	7/17/2019
	group 2 (n=25)	8/20/2018-8/20/2018	8/21/2019
Lasiocarpine	group 1 (n=25)	9/24/2018-10/3/2018	9/24/2019
	group 2 (n=25)	11/5/2018-11/14/2018	11/06/2019
Riddelliine	group 1 (n=25)	6/3/2019-6/12/2019	6/2/2020
	group 2 (n=25)	6/10/2019-6/19/2019	6/9/2020
Senecionine	group 1 (n=25)	9/23/2019-10/2/2019	9/21/2020
	group 2 (n=25)	10/21/2019-10/30/2019	10/20/2020
Seneciphylline:	Group 1 (n=25)	12/4/2019-12/13/2019	12/3/2020
	Group 2 (n=25)	1/6/2020-1/15/2020	1/5/2021
Heliotrine	Group 1 (n=25)	11/16/2020-11/25/2020	11/15/2021
	Group 2(n=23)	4/12/2021-4/12/2021	4/12/2022
	Group 3 (n=2)	9/14/2021-9/23/2021	9/14/2022

Microscopic Tissue Evaluation:

Sections of brain, trachea, esophagus, thyroid gland, heart, lungs, liver, kidneys, adrenal gland, spleen, stomach, small and large intestine, skeletal muscle (right hind limb), testicle, and urinary bladder were microscopically evaluated. The International Harmonization of Nomenclature and Diagnostic Criteria (INHAND) guides were referenced for morphologic diagnosis of lesions.[49–54]

Statistical Analysis:

Statistical Comparisons of Neoplasm Development:

The poly-k test was performed to correct for differences in mortality between groups.[55] The R package MCPAN was used to perform this test using R version 4.2.[56] The Dunnett

test was used to compare proportions of mice affected by different neoplasms and total mice that developed neoplasia. When comparing proportions of neoplasms to the control group, a one tail (upper-tail) test was used. The tumors for which this statistical testing was performed include hemangiosarcomas, hepatic adenomas, bronchioloalveolar adenoma/carcinoma, lymphoma, histiocytic sarcoma, and soft tissue sarcomas not suspected to be the microchip related. Bronchioloalveolar adenomas and carcinomas were combined in this statistical analysis mainly because differentiation of these two tumors is somewhat subjective. Statistical testing was not performed for neoplasms that were only observed in single mice per group, including osteosarcoma, seminal vesicle adenoma, seminoma, and papilloma. Lastly, comparisons were performed for total neoplasms per PA, which included the sum of all neoplasms, even those that were only observed in single mice. The poly-k test adjusts the denominator of the total affected mice in a group to correct for mice that did not survive for the entire 365 days. A mouse that dies or is euthanized early is corrected to a fraction of one in the denominator. The calculation is that mouse equals (days of life / total days of the study) to the power of k. The standard value of k used is 3, which was determined based on the distribution of tumor onset times.[57] Mice that were euthanized for a microchip tumor that had an additional neoplasm found incidentally at necropsy were included and no mortality-weighted adjustment was made.

Statistical Analysis of Non-neoplastic Lesions:

Statistical analysis was performed using GraphPad prism version 9.3.1. Chi-squared tests were used to compare proportions of mice affected by various nonneoplastic lesions between each PA group and the control. Follow up tests were performed using Fishers

exact test. Survival curves were calculated using a Log-rank (Mantel-Cox) test, a Log-rank test for trend, and a Gehan-Breslow-Wilcoxon test ($p < 0.0001$).

Results:

Clinical Disease:

After dosing was completed, mice were monitored daily for clinical signs of disease. Body weights were measured and recorded weekly. Mice were euthanized prior to the study termination date (365 days) for any evidence of clinical disease. The most common reason a mouse was euthanized early was because of substantial reduction in body weight. Weight loss was considered substantial if it was persistent over 2-4 weeks depending on amount of weight lost and the presence of concurrent lethargy or malaise, or if 20% of the previous week's body weight was lost. Other observations of clinical disease included the development of visible or palpable tumors, lethargy, or difficulty ambulating. Occasionally, mice were found dead without preceding clinical signs. Table 2 shows mortality information for each group. Table 3 shows mortality data for mice that were euthanized only because of microchip induced tumors. Description of lifespan and mortality for each compound group is detailed below. A common reason for early euthanasia was the development of non-treatment-related tumors around the identification microchip. These tumors clearly developed as a result of the microchip.

Table 3.2. Mortality for each PA group in days. The following table shows the number of mice that were euthanized early due to observed clinical signs or significant weight loss.

Time interval	Rid.	Senecio.	Seneciph.	Lasio.	Helio.	Control
0-182 d.	1	2	2	1	3	1

183-273 d.	6	20	9	6	4	2
274-364 d.	7	15	15	7	10	6
Study termination (365 days)	36	13	24	36	33	41

Abbreviations: d. = days, Rid. = riddelliine, Seneciph = seneciphylline, Lasio. = lasiocarpine, Helio. = heliotrine.

Table 3.3. Mortality for each PA group after excluding mice euthanized early due to microchip induced tumors.

Mortality in days	Rid.	Senecio.	Seneciph.	Lasio.	Helio.	Control
0-182 d.	1	2	2	1	2	1
183-273 d.	4	17	6	6	2	1
274-364 d.	4	13	12	0	3	6
Study termination (365 d.)	36	13	24	36	33	40
Total mice euthanized early due to microchip induced tumors	5	5	6	7	10	2

Abbreviations: d. = days, Rid. = riddelliine, Seneciph = seneciphylline, Lasio. = lasiocarpine, Helio. = heliotrine.

Survival Data:

Kaplan-Meier survival analysis was performed. Mice that were euthanized early due to visible tumors that were obviously caused by their microchips were censored from survival analysis. Tumors obviously caused by microchips were typically located in the subcutis of the dorsal scapular area, and many had the microchip embedded within the

neoplasm. Figure 1 shows the Kaplan-Meier survival curve. Senecionine exposed mice had the poorest survival, with a median survival of 291 days and a mean survival of 292.8 ± 61.78. The remaining groups in order from lowest to greatest survival times are as follows: seneciphylline (mean = 321.1 ± 81.31 days), riddelliine (mean = 341.4 ± 54.75 days), lasiocarpine (mean = 345.6 ± 50.72 days), heliotrine (mean = 344.1 ± 54.8 days) and last was the control group (mean = 352.5 ± 46.49 days).

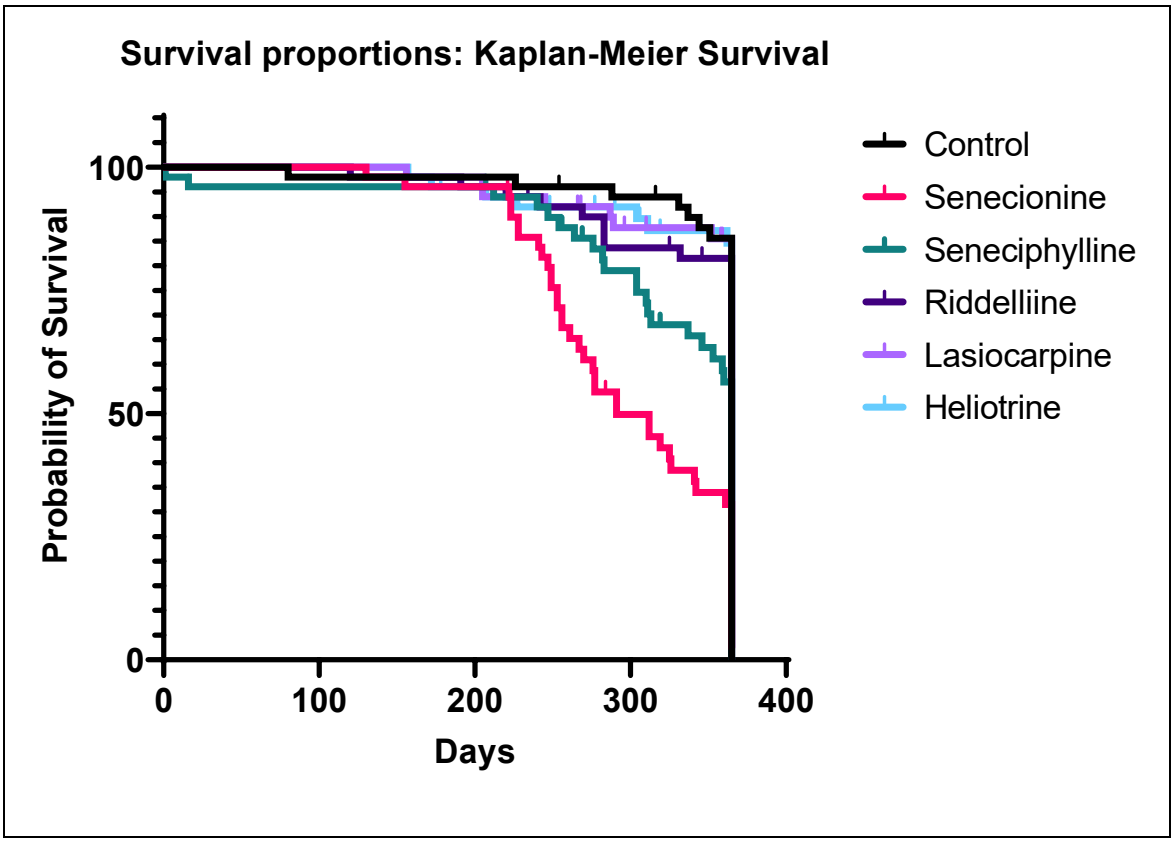

Figure 3.1: Kaplan-Meier survival curve. Mice were not included in this analysis if they were euthanized early because of tumors around their microchips. The graph clearly shows that survival was lowest for mice exposed to senecionine, followed by seneciphylline, riddelliine, and lasiocarpine and heliotrine appear similar.

Kaplan-Meier Survival Analysis.

Survival curves were significantly different using a Log-rank (Mantel-Cox) test ($p < 0.0001$), a Log-rank test for trend ($p = 0.0027$) and a Gehan-Breslow-Wilcoxon test ($p < 0.0001$).

Clinical Signs:

Control:

Forty one out of 50 control mice survived until study termination at 365 days. Two mice were euthanized early (day 254 and 316) due to visible microchip induced tumors. Other mice in the control group were euthanized early due to the following clinical signs: Abdominal distention (1 mouse at day 337), paraparesis/paraplegia (1 mouse at day 344), weight loss and lethargy (six mice at day 80, 226, 254, 288, 331, 351).

Senecionine:

Thirteen out of fifty senecionine exposed mice survived for the entire 365 days. Five mice were euthanized early due to observed microchip induced tumors (days 221, 284, 256, 256, and 342). Four mice were found dead without preceding clinical signs at day 155, 228, 241, 253. Twenty-seven mice were euthanized due to substantial weight loss sometimes accompanied by a hunched posture and lethargy (day 130, 222, 223, 223, 228, 228, 243, 247, 249, 249, 256, 256, 261, 267, 270, 276, 277, 277, 291, 291, 312, 312, 325, 326, 341, 342, and 361). One mouse had a 18x20x20 mm mass (soft tissue sarcoma) in the inguinal area. Although similar in type, this neoplasm was not associated with the microchip (day 319).

Seneciphylline:

One mouse was found dead on the ninth day of dosing and had subcutaneous icterus. (3 in group 2). Two mice were found dead on days six and 237 respectively days after dosing with no gross lesions. A mouse was found dead on day 313 and had a 12 x 10 x 10 mm dark red mass (hemangiosarcoma) in the left medial liver lobe. Seven mice were euthanized early due to microchip induced tumors (days 207, 240, 256, 269, 282, 319, 337). Fourteen mice were euthanized early due to substantial weight loss sometimes accompanied by a hunched posture and lethargy: (days 212, 240, 247, 254, 264, 283, 304, 304, 310, 346, 337, 353, 359, 360). The remaining twenty-four mice exhibited no clinical signs and were euthanized and necropsied at the terminal date of the study.

Riddelliine:

Two riddelliine-exposed mice were found dead (day 120 and 332). Seven mice were euthanized due to substantial weight loss sometimes accompanied by a hunched posture and lethargy (day, 191, 220, 269, 283, 283, 283, 332). Five mice were euthanized early due to a microchip induced tumor (day 234, 269, 325, 332, 346). The remaining thirty-six mice exhibited no clinical signs and were euthanized and necropsied at the terminal date of the study.

Lasiocarpine:

Five mice were euthanized early due to observed microchip induced tumors (day 296, 310, 358, 359, 266). Three mice were found dead (day 287, 245, 268), the mouse found dead at day 268 had a microchip-induced tumor. Six mice were euthanized early due to substantial weight loss sometimes accompanied by a hunched posture and lethargy (day

156, 205, 205, 245, 289, 352). The remaining Forty-three mice survived until the study termination and displayed no clinical signs.

Heliotrine:

Ten mice were euthanized early due microchip-induced tumors (day 178, 227, 248, 277, 277, 277, 290, 306, 319, 345). One mouse was euthanized due to hindlimb paresis with no deep pain at day 207. An osteosarcoma located in the lumbar vertebrae is suspected to be the cause of paresis and lack of hind limb deep pain. One mouse was euthanized at day 157 when a mass (osteosarcoma) surrounding proximal aspect of the left femur was observed. Five mice were euthanized early due to substantial weight loss sometimes accompanied by a hunched posture and/or lethargy (day 227, 172, 304, 31, 362). The remaining thirty-three mice exhibited no clinical signs and were euthanized at the study termination date.

Necropsy Results:

Gross Lesions:

Control Group:

Gross lesions observed in control mice (n = 50 mice) include masses in the abdominal cavity adjacent to the urinary bladder (soft tissue sarcomas) (2 mice). Additional gross lesions included mild to moderate splenomegaly (6 mice), a splenic mass (one mouse) (lymphoma), hemothorax (one mouse), and emaciation (1 mouse). Microchip induced tumors were observed grossly as subcutaneous masses (soft tissue sarcomas) ranging from 3x3x5 mm to 25x20x10 mm located in adjacent to or surrounding the microchip in various anatomic sites including adjacent to the prepuce (1 mouse), the interscapular area

(2 mice), axilla (1 mouse), adjacent to the vertebral column (1 mouse), dorsal pelvic (1 mouse). Thirty-seven control mice had no gross lesions.

Senecionine:

Gross lesions observed in senecionine-exposed mice (n=50 mice) included white to tan, or red pinpoint foci disseminated throughout multiple liver lobes (13 mice) (Osseous metaplasia). Splenomegaly was observed in 10 mice. Twenty-three mice were emaciated or in poor body condition. Two mice were icteric. Two mice had a diffusely enhanced reticular appearance of the liver. Circular red raised masses (hemangiosarcomas) on one or more liver lobes were present in two mice. One mouse had lymphadenomegaly (submandibular 5x3x2 mm, superficial cervical 6x4x2 mm, mesenteric (8x3x2 to 4x3x2 mm) and a white thoracic mass in the location of the thymus (1 mouse) (multicentric lymphoma). A single mouse had unilateral testicular enlargement (right testicle 10X6X6 mm compared to left 6X4X4 mm) (infiltrative seminoma). One mouse had a mass surrounding the proximal right hind limb (hemangiosarcoma). Microchip induced tumors were observed grossly as subcutaneous masses that often surrounded the microchip, ranging from 6 mm diameter (spherical) to 30x20x15 mm located in various anatomic sites including interscapular (5 mice) or caudal to the right ear (1 mouse) (soft tissue sarcomas). Gross lesions were not observed in eight mice in the senecionine-exposed group.

Seneciphylline:

Gross lesions observed in mice exposed to seneciphylline (n=50 mice) included white to tan, or red pinpoint foci disseminated throughout multiple liver lobes observed in nine mice (osseous metaplasia). Sixteen mice were emaciated or in poor body condition or

emaciation) One mouse was icteric. One mouse had unilateral nephromegaly. Seven mice had splenomegaly. Two mice had splenic masses (40x8x12 mm, 5x12x6 mm) (hemangiosarcomas). One mouse had a shrunken, nodular liver. Dark red spherical liver masses were present in two mice (hemangiosarcomas). Two mice had thymic masses (1 lymphoma and 1 osteosarcoma). Two mice had abdominal masses (soft tissue sarcomas). Microchip induced tumors were observed grossly as subcutaneous masses ranging from 25x15x15 to 18x14x14 mm located in various anatomic sites including interscapular (3 mice), superficial to the right shoulder (1 mouse), the dorsal thoracolumbar area (1 mouse), or caudal to the right ear (1 mouse). Five of the microchip-induced tumors were soft tissue sarcomas and one was a histiocytic sarcoma. Twenty seneciphylline-exposed mice had no gross lesions at necropsy.

Riddelliine:

Gross lesions observed in mice exposed to riddelliine (n=50 mice) included dark red, circular areas on liver lobes ranging from 1.2 x 2 to 6 x 4 mm (5 mice) (hemangiosarcomas). White to tan pinpoint foci disseminated throughout multiple liver lobes (osseous metaplasia) were present in one mouse. One mouse was emaciated. Six mice had splenomegaly. Two mice had abdominal masses (soft tissue sarcomas). White thymic masses were present in two mice. Single mice had ascites, a renal mass (lymphoma) and mesenteric lymphadenomegaly (lymphoma). Subcutaneous masses were observed on the ventral thorax of one mouse (hemangiosarcoma) or surrounding the right hind proximal limb (soft tissue sarcoma), or on the lateral dorsal right hip (soft tissue sarcoma). Microchip induced tumors were observed grossly as subcutaneous masses (soft tissue sarcomas) ranging from 10x8x8 to 23x15x14 mm located in various anatomic sites

including dorsal midline between ears (1 mouse), caudal to the right ear (1 mouse), over the left shoulder (1 mouse), dorsal interscapular (1 mouse). Twenty-eight riddelliine-exposed mice had no gross lesions at necropsy.

Lasiocarpine:

Gross lesions observed in mice exposed to lasiocarpine (n=50) include single or multiple, red or tan nodules in liver lobes (3 mice), splenomegaly (7 mice), poor body condition or emaciation (2 mice). Masses encompassing the pelvis (1 mouse) (soft tissue sarcoma) or surrounding the proximal right hind limb (1 mouse) (osteosarcoma) were also observed. Microchip induced tumors were observed grossly as subcutaneous masses ranging from 15x10x5 to 25x24x18 mm located in various anatomic sites including the superficial to the right or left scapulae (5 mice), caudal to the right ear (1 mouse), dorsal interscapular area (2 mice). Thirty-four of the lasiocarpine-exposed group did not have gross lesions. All microchip-induced tumors were soft tissue sarcomas.

Heliotrine:

Gross lesions observed in mice exposed to heliotrine (n=50) included splenomegaly (5 mice), poor body condition or emaciation (4 mice) and a diffuse enhanced reticular pattern on the liver (2 mice). One mouse had a subcutaneous mass surrounding the proximal left hind limb (soft tissue sarcoma). White masses in the mediastinum (20x10x10 mm), both kidneys (1 mm diam, 3 mm diam), and diffuse hepatomegaly (lymphoma) were present in one mouse. One mouse had axillary lymphadenomegaly and a single 10x6x4 mm subcutaneous white mass over the medial aspect of the proximal left hind limb (lymphoma). One mouse had a 1 mm diameter dark red circular area on the left liver lobe. Three cholelithes, ranging from 0.2-1 mm in diameter were present in one

mouse. One mouse had a distended abdomen with diffuse mesenteric lymphadenomegaly (lymphoma). Microchip induced tumors (soft tissue sarcomas) were observed grossly as subcutaneous masses ranging from 15x10x10 to 25x18x19 mm located in various anatomic sites including superficial to left or right scapulae (5 mice), dorsal interscapular area (5 mice), right lateral ventral thorax (1 mouse). Twenty-nine of the heliotrine exposed mice had no gross lesions.

Histopathologic Findings:

Neoplasms Observed:

Table 3.4 shows a summary of neoplasms observed in each PA group and the vehicle control group. Figures 2-7 include photomicrographs with examples of the neoplasms observed in this experiment.

Table 3.4. Neoplasms observed in each PA group

Tumor	Con.	Sen.	Sph.	Rid.	Lasio.	Helio.
Hemangiosarcoma	1 (liver)	2 (1 liver, 1 skeletal muscle)	3 (1 liver and spleen, 1 spleen, 1 heart)	6 (5 liver, 1 skel. m.)	3 (2 liver, 1 liver and spleen)	n.d.
Hepatic adenoma(s)	n.d.	3	1	n.d.	n.d.	n.d.
Bronchioloalveolar adenoma/carcinoma	3 (ad.)	6 (4 ad., 2 carc.)	1 ad.	1 ad.	1 ad.	n.d.
Lymphoma	3	3	4	3	2	6

Soft tissue sarcoma (not assoc. w/ microchip)	3 (1 urinary bladder, 1 abdominal cavity, 1 cutaneous)	n.d.	1 (pancreas, mesentery skel. musc.)	4 (2 urinary bladder, 1 skel. m., 1 heart)	1 (skel m.)	1 (skel. m., LH limb)
Histiocytic sarcoma	1 (skin)	n.d.	n.d.	2	1	n.d.
Osteosarcoma	n.d.	1 (vertebral)	1 (liver)	n.d.	1 (RH limb)	1 (vertebral)
Pars distalis carcinoma	1	n.d.	n.d.	n.d.	n.d.	n.d.
Seminal vesicle adenoma	n.d.	n.d.	1	n.d.	n.d.	n.d.
Seminoma	n.d.	n.d.	n.d.	1	n.d.	n.d.
papilloma	1	n.d.	n.d.	n.d.	n.d.	n.d.
Total neoplasms	13	15	12	17	9	8
Total mice with neoplasms	12	15	9	17	9	8

Abbreviations: Con. = control, Sen. = senecionine, Sph. = seneciphylline, Rid. = riddelliine, Lasio. = lasiocarpine, Helio. = heliotrine, HSA = hemangiosarcoma, Bronch. = bronchioloalveolar, ad. = adenoma, carc. = carcinoma, n.d. = not detected.

Control Group:

Three mice in the control group (n=50 mice) had bronchioloalveolar adenomas. There were three mice with lymphoma affecting the spinal cord, spleen, liver, and lungs. The mouse with the spinal lymphoma had a 9 mm in diameter neoplasm that surrounded several vertebrae. The second mouse had neoplasms in the liver, spleen and a mesenteric

lymph node and the third mouse had splenic lymphoma. Three mice had soft tissue sarcomas not suspected to be related to microchip implantation. Soft tissue sarcomas were located within the wall of the urinary bladder (1 mouse), the abdominal cavity (1 mouse) and the subcutis (1 mouse). Additional neoplasms observed in the control group include one hemangiosarcoma of the liver, one pars distalis carcinoma, one dermal histiocytic sarcoma, and one cutaneous papilloma. There was a total of thirteen neoplasms detected in twelve mice.

Riddelliine:

In mice exposed to riddelliine (n=50 mice), six hemangiosarcomas were observed. Five were in the liver and one was found in skeletal muscle. Four soft tissue sarcomas which were not thought to be related to microchip implantation were observed. Soft tissue sarcomas were in skeletal muscle (1 mouse), urinary bladder wall (2 mice), and in the heart (1 mouse). Three mice had lymphoma. In two, lymphoma created a mediastinal mass that infiltrated the lungs, heart, and spleen. The third lymphoma infiltrated both kidneys. Histiocytic sarcoma was detected in two mice, one in the liver and lungs and the other in skeletal muscle. Additional neoplasms included a bronchioloalveolar adenoma and a seminoma. Seventeen neoplasms were detected in seventeen mice.

Senecionine:

Senecionine exposed mice (n=50 mice) developed a variety of neoplasms. There were three mice with multiple hepatocellular adenomas. In these mice, there was multifocal hyperplasia and dysplasia characterized by coalescing nodules of moderate to severe anisocytosis and anisokaryosis. These nodules were classified as hepatic adenomas based

on disorganization of hepatocellular cords, lack of portal tracts, and production of expansile masses Though nodular hyperplasia would be a differential diagnosis, the dysplasia makes adenoma more likely. Four mice in this group had bronchioloalveolar tumors (3 adenomas, 1 carcinoma). Three mice had lymphoma. Lymphoma was detected in the liver, stomach, small intestine, and mesenteric lymph nodes (2 mice), and a single mesenteric lymph node (1 mouse). Two hemangiosarcomas were observed, one was in the liver and the other was in skeletal muscle. There was a single vertebral osteosarcoma. Fifteen neoplasms were observed in fifteen mice.

Seneciphylline:

In mice exposed to seneciphylline (n = 50 mice), a single mouse had multiple hepatocellular adenomas. These nodules were composed of neoplastic hepatocytes that formed spherical nodules which expanded the capsule and replaced normal liver. The neoplastic nodules lacked portal tracts and had occasional disorganization of cords. Nodular hyperplasia was a less likely differential considering the disorganization. Three hemangiosarcomas were found in the heart (1 mouse), liver and spleen (1 mouse), and spleen (1 mouse) (See figure 2, hemangiosarcomas). Four mice had lymphomas that were detected in the thymus, heart, and lungs (1 mouse), brain (1 mouse), liver and spleen (1 mouse), and thymus, lungs, liver, and bilaterally in kidneys and adrenal glands (1 mouse). Additional neoplasms included a seminal vesicle adenoma, a bronchioloalveolar carcinoma, a hepatic osteosarcoma, and a soft tissue sarcoma of the mesentery, pancreas, and gastric wall. There were twelve neoplasms observed in nine mice.

Lasiocarpine:

Mice exposed to lasiocarpine (n=50 mice) developed three hemangiosarcomas, two of which were in the liver and a third was found in the liver and spleen. Two mice had lymphoma. Lymphoma was detected in the heart, lungs, liver, spleen, mesenteric lymph node, and bilateral kidneys and adrenal glands (1 mouse), and a single mesenteric lymph node (1 mouse). Additional neoplasms observed include a bronchioloalveolar adenoma, an osteosarcoma (right femur), and histiocytic sarcoma (liver and lungs). Nine neoplasms were observed in nine mice.

Heliotrine:

Six mice exposed to heliotrine (n=50) developed lymphomas that involved the mediastinum, lungs, heart, liver, kidneys, spleen (1 mouse); the lungs, liver, kidneys, mesenteric lymph nodes, and spleen (1 mouse); the lung, heart, abdominal cavity, skeletal muscle, pancreas and gastrointestinal tract (1 mouse); lungs (1 mouse); and spleen (2 mice). Additional neoplasms observed include an osteosarcoma in skeletal muscle and a vertebral osteosarcoma. Eight neoplasms were observed in eight mice.

Table 3.5. Tumor status and day of death for all groups: The number indicates the days of life. The presence of an asterisk indicates the presence of a tumor in that mouse. Numbers in parentheses indicate numbers of mice that died on that specific day.

Control:	226*, 254*, 288*, 316, 331, 337*, 344, 351*, 365(35), 365*(6), 80*
Senecionine:	130, 155, 221, 222*, 223*(2), 228(2), 241, 243*, 247, 249(2), 253, 253*, 256(3), 256*, 261*, 267, 270, 276*, 277, 277*, 284, 291(2), 312, 312*, 319*, 325, 326, 341, 342, 342*, 361, 365(10), 365*(3)

Seneciphylline:	16, 169*, 207, 212, 240, 240*, 247*, 254, 256, 264, 269, 276, 282, 283, 304, 304*, 310*, 311*, 313, 319, 337(2), 346*, 353, 359*, 360, 365(23), 365*
Riddelliine:	120*, 191*, 220*, 234, 242, 269(2), 283*(3), 325*, 332, 332*, 346, 365(27), 365*(9)
Lasiocarpine:	156*, 205*(2), 245, 266, 268(2), 287, 289, 296, 310, 352*, 358, 359, 365(31), 365*(5)
Heliotrine:	157*, 172*, 178, 207*, 227, 227*, 248, 277(3), 290, 304*, 306, 311*, 319, 345, 362*, 365(32), 365*

Figures 3.2 to 3.7: Photomicrographs Showing Examples of Neoplasms Observed in This Experiment.

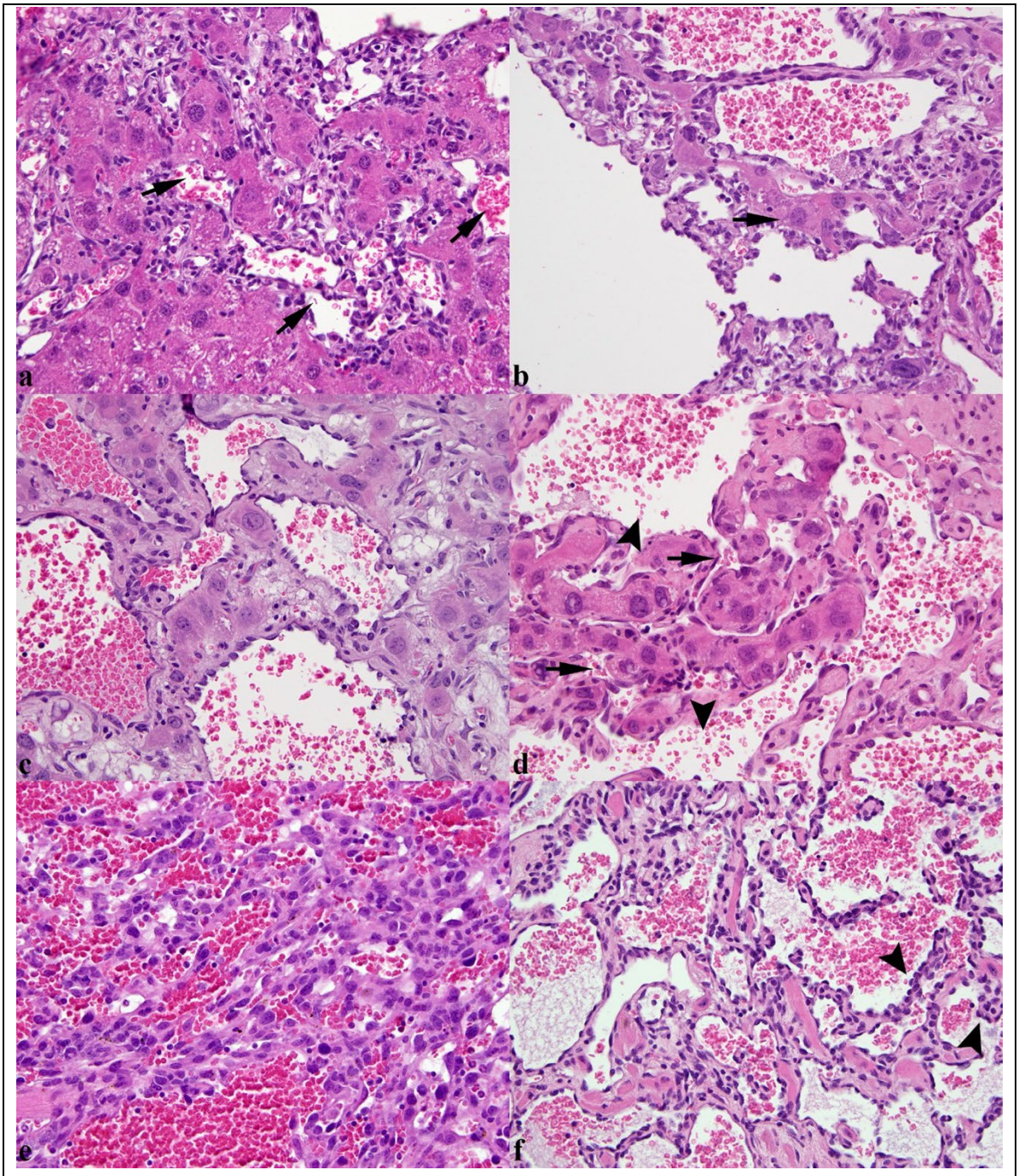

Figure 3.2. Hemangiosarcomas observed in control and various PA groups. In each image, neoplastic endothelial cells line variably sized, erythrocyte-filled spaces. Neoplastic endothelial cells vary from well differentiated, flat cells that mildly protrude

into spaces to poorly differentiated plump cells with moderate to severe anisokaryosis and anisocytosis. Image (a): Liver from a control mouse. Neoplastic spindle cells form tortuous channels (arrows) which contain erythrocytes. Image (b): Liver from a riddelliine-exposed mouse. Neoplastic endothelial cells are well-differentiated and resemble normal endothelial cells. Blood-filled spaces separate few remaining hepatocytes (arrow) Image c) Liver from a riddelliine-exposed mouse. Neoplastic endothelial cells are well-differentiated. Image (d): Liver from a senecionine-exposed mouse. Blood-filled spaces are open and vary from thin (arrows) to wide (arrowheads). Image (e): Liver from a seneciphylline-exposed mouse. Neoplastic cells exhibit moderate anisocytosis and anisokaryosis. Image (f): Heart (left ventricular lumen) from a seneciphylline exposed mouse. Neoplastic cells sometimes have prominent nuclei which protrude into the spaces (arrowheads).

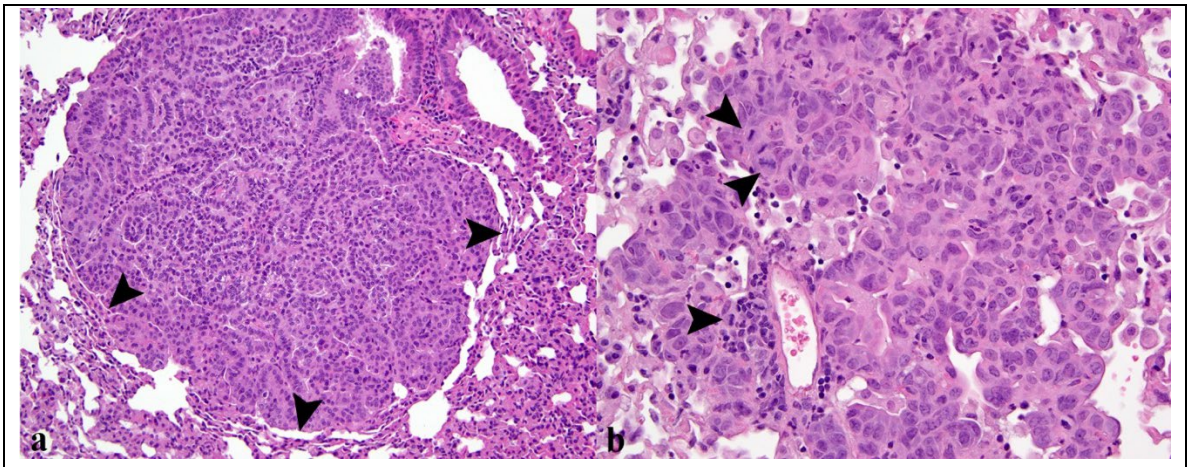

Figure 3.3. images (a) and (b). Bronchioalveolar neoplasms.

Image (a): Lung from a control mouse with a bronchioloalveolar adenoma. Neoplastic epithelial cells form palisading cords (arrow). The neoplasm multifocally compresses adjacent alveolar spaces (arrows). Image (b): Lung from a senecionine-exposed mouse with a bronchioloalveolar carcinoma. Neoplastic epithelial cells exhibit moderate anisocytosis and anisokaryosis and form a mass. Three mitotic figures are present (arrowheads.

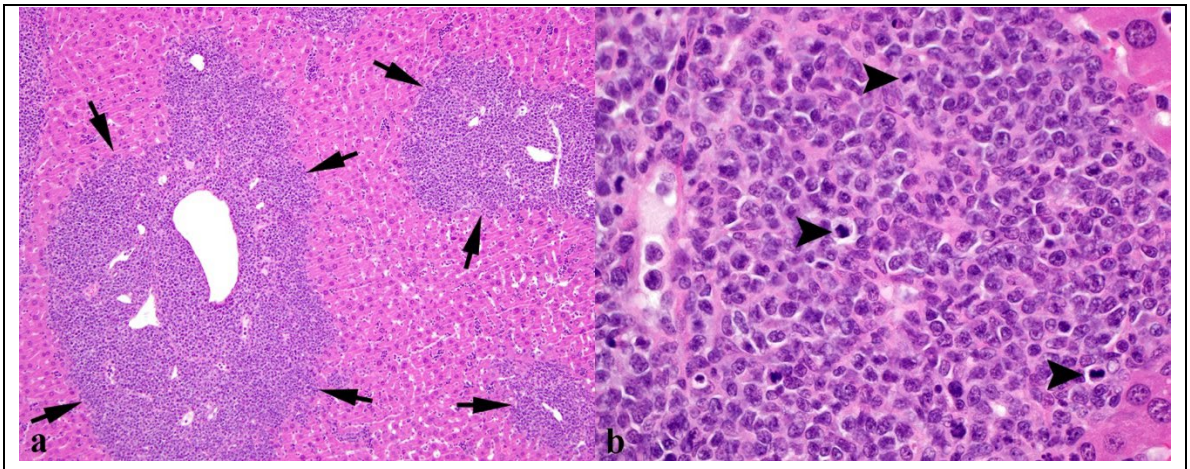

Figure 3.4. Images (a) and (b). Lymphoma in the liver from a heliotrine-exposed mouse. Image (a): Low magnification view shows neoplastic round cells (lymphocytes) infiltrating around centrilobular veins (arrows). Image (b): High magnification image of neoplastic round cells (lymphocytes) shows several mitotic figures (arrowheads).

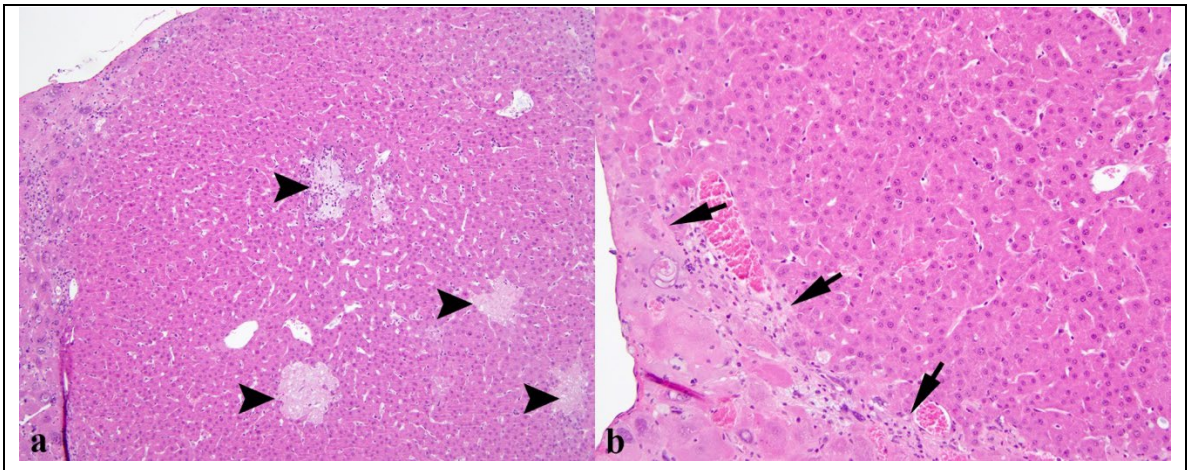

Figure 3.5. Liver from a seneciphylline-exposed mouse with a hepatoma. Image (a): The mass is composed of well-differentiated neoplastic hepatocytes. The adjacent liver is

composed of hepatocytes that exhibit moderate cellular and nuclear atypia. Multiple foci of necrosis (arrowheads) are within the neoplasm Image (b): The border of the neoplasm shows compression of the adjacent hepatocytes (arrows). Nodular hyperplasia is a differential, but was not favored because this mass had marked peripheral compression of adjacent hepatocytes, disorganized chords, and elevated the capsule prominently.

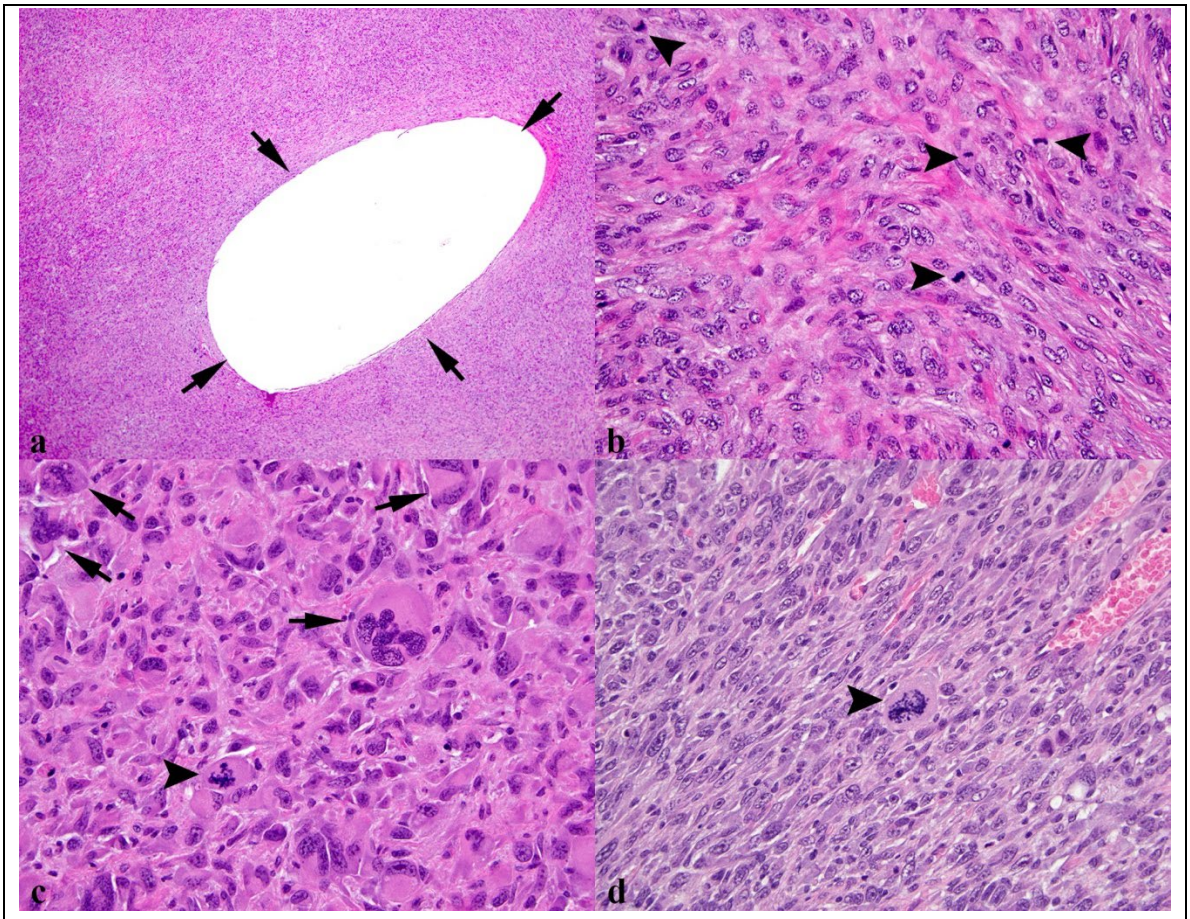

Figure 3.6. Images a-d. Neoplasms that developed around the microchips of mice from various PA groups. Image (a): Soft tissue sarcoma from the dorsal subcutis of a control mouse. Low magnification view of neoplastic spindle cells forming interlacing bundles and streams. The clear space (arrows) is the area that was occupied by the microchip. Image (b): Soft tissue sarcoma from the dorsal subcutis of a heliotrine-exposed mouse. Neoplastic spindle cells form interlacing streams and bundles admixed with eosinophilic fibrillar matrix material (collagen). Several mitotic figures are present (arrowheads). Image (c): Round cell neoplasm from the dorsal subcutis of a control mouse. Neoplastic

round cells are arranged in haphazard sheets and exhibit severe anisocytosis and anisokaryosis. Multinucleated giant cells (arrows) were frequently observed. A single bizarre mitotic figure is pictured (arrowhead). Image (d): Soft tissue sarcoma from the dorsal subcutis of a seneciphylline-exposed mouse. Neoplastic spindle cells form interlacing streams. A single giant cell with a bizarre mitotic figure (arrowhead) is present.

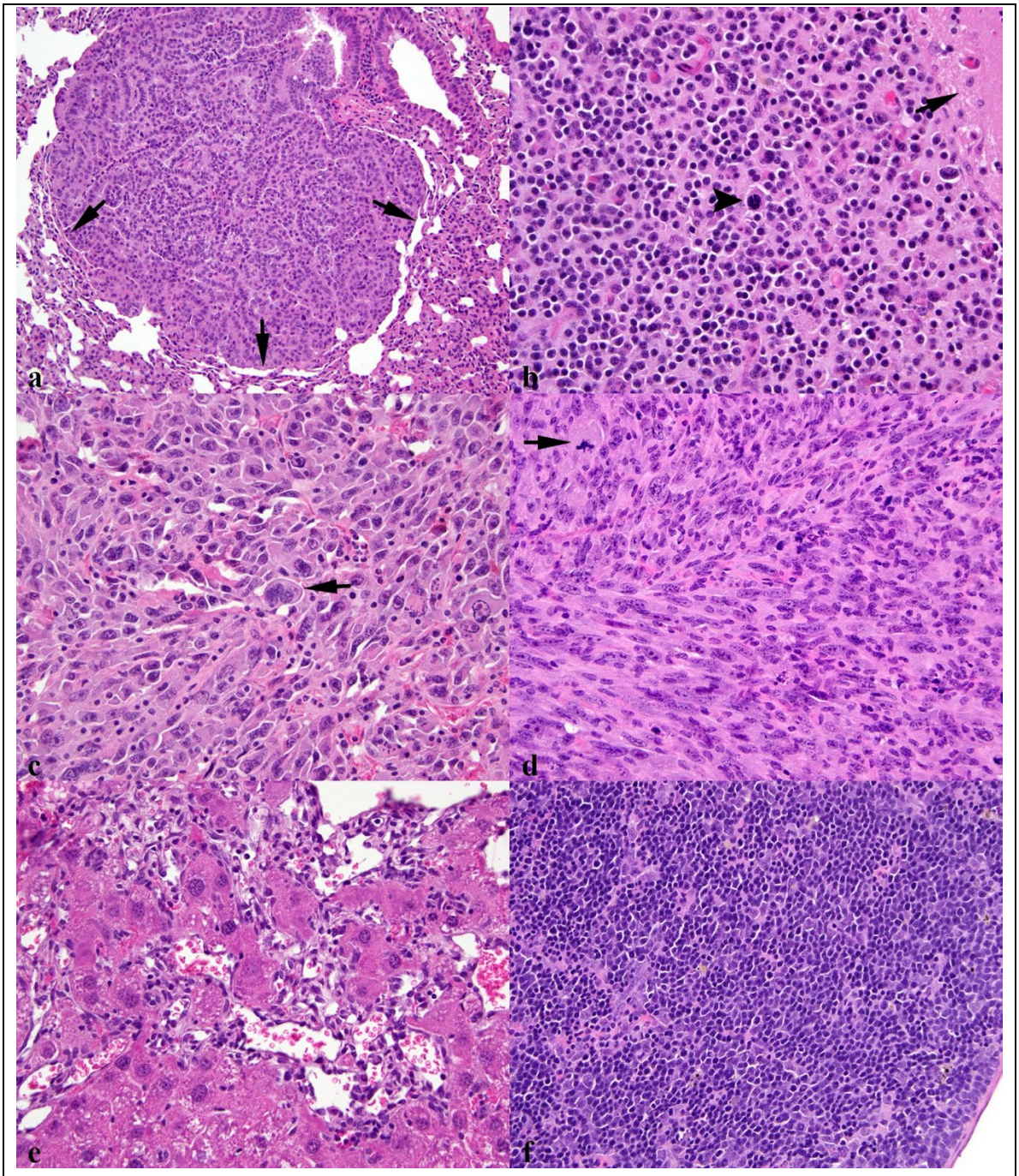

Figure 3.7. Images a-e. Neoplasms observed in control mice. Image (a): lung from a control mouse. Bronchioloalveolar adenoma. Palisading neoplastic epithelial cells arranged in wandering cords produce a spherical mass which compresses adjacent alveoli (arrows). Image (b): brain from a control mouse. Pituitary adenocarcinoma. Neoplastic cells resembling chromophobe cells create a mass that extends into the midbrain neuropil (arrow). A single mitotic figure is observed (arrowhead). Image (c):

Soft tissue sarcoma from the abdominal cavity of a control mouse. Neoplastic spindle-shaped or round cells are arranged in short bundles. Neoplastic giant cells are observed (arrow). Image (d): Soft tissue sarcoma from the urinary bladder wall of a control mouse. Neoplastic spindle-shaped cells are arranged in interlacing streams and bundles. A single mitotic figure is pictured (arrow). Image (e): Liver from a control mouse. Hemangiosarcoma. Neoplastic spindle cells produce variably sized blood-filled spaces. Image (f): Spleen from a control mouse. Neoplastic lymphocytes are arranged in solid sheets that replace fill sinuses and expand the capsule.

Nonneoplastic Lesions:

Nonneoplastic lesions were observed in all groups including controls. Unlike neoplastic lesions, non-neoplastic lesions do not require corrections for differences in mortality during statistical analysis, particularly background lesions that are also observed in the control group. Scoring systems are defined for three of the non-neoplastic lesions which were observed frequently and in multiple groups. These lesions included heterotopic bone in the liver, hepatocellular necrosis, and hydronephrosis. A brief description of the general microscopic appearance of these lesions is provided.

Heterotopic bone within the liver was a frequent lesion in mice exposed to riddelliine, senecionine, and seneciphylline. Foci of bone varied from hemispherical or irregularly shaped nodules, or branching trabeculae of laminated eosinophilic, or basophilic (mineralized), material. Other foci were composed of an outer rim of amphophilic to basophilic laminated material, surrounding a central lumen (medulla) containing a mixture of adipocytes and erythroid and myeloid precursor cells (bone marrow). Small numbers of osteoblasts frequently lined the surface. Lacunae containing

osteocytes were occasionally observed. Heterotopic bone in the liver (interpreted as osseous metaplasia) was classified as mild if there were less than five foci, moderate for 5-10 foci and severe if greater than 10 foci were observed. Foci of heterotopic bone varied in size, from less than 1 um for small foci and up to 1 mm in the largest foci. Hepatocytes adjacent to foci of heterotopic bone were generally microscopically unremarkable, and there was typically not inflammation or fibrosis associated with bone.

Hepatic necrosis was occasionally observed in all groups. Foci of necrosis were either groups of pale eosinophilic contiguous hepatocytes which maintained cellular architecture but lost nuclear and cytoplasmic detail (coagulative necrosis), or individual hepatocytes that were enlarged and hypereosinophilic with pyknotic or absent nuclei (individual cell necrosis). The majority of necrotic foci were approximately 1 um in diameter, but occasional mice had foci which were greater in size, even up to multiple millimeters, and affecting up to 50% of the liver. However, these large areas of necrosis were rarely observed in any group. Hepatic necrosis was classified as mild if less than 10 foci were observed, moderate for 10-20 foci, and severe is more than 20 foci were present. If foci of necrosis were large, severity score was adjusted accordingly.

Pulmonary alveolar histiocytosis was frequently observed in all groups. Alveolar histiocytosis varied from focal minimal to severe multifocal to coalescing areas of macrophages in alveolar spaces. Alveolar macrophages contained cytoplasmic clear vacuoles (lipid) or eosinophilic acicular structures (eosinophilic crystalline pneumonia). In some cases of moderate or severe alveolar histiocytosis, alveolar histiocytes were accompanied by low to moderate numbers of neutrophils, or lymphocytes which infiltrated perivascular areas (interstitial pneumonia). In some cases, this lesion was

accompanied by bronchiolar or alveolar epithelial hyperplasia, with or without cellular atypia in the hyperplastic cells. These areas of hyperplasia with atypia were considered preneoplastic. Mild alveolar histiocytosis was considered incidental, while moderate to severe alveolar histiocytosis was possibly related to the cause of death or the cause of early euthanasia.

Hydronephrosis varied from mild dilation of the renal pelvis to severe dilation resulting in expansion of the capsule and severe loss of both cortex and medulla. Mild hydronephrosis is defined as dilation of the renal pelvis that does not markedly enlarge the overall size of the kidney or result in thinning of the medulla and cortex. Moderate hydronephrosis is dilation of the renal pelvis resulting in less than fifty percent enlargement of the kidney. Severe hydronephrosis is defined as marked renal pelvis dilation resulting in severe thinning of the cortex and medulla resulting in greater than 50% reduction of the cortical and medullary thickness.[58] Interstitial edema or inflammation did not typically accompany hydronephrosis.

Nonneoplastic Lesions by Group:

Control Group:

Mice in the control group (n=50 mice) had the following nonneoplastic lesions. Multifocal centrilobular or midzonal hepatocyte vacuolation with multiple clear cytoplasmic vacuoles that did not displace nuclei (glycogen vacuoles) was observed in six mice. Two mice had multifocal to coalescing foci of hepatocyte hyperplasia with anisokaryosis and anisocytosis interpreted as non-regenerative hepatocellular hyperplasia. Focal or multifocal, mild to moderate sinusoid angiectasis (also known as peliosis hepatica or telangiectasia) was present in five mice. One mouse had multifocal mild

lymphocytic hepatitis. Aggregates of lymphocytes were multifocally observed in the livers (5 mice), kidneys (9 mice) and lungs (1 mouse). Three mice had alveolar histiocytosis with multifocal intracellular acicular eosinophilic structures (eosinophilic crystalline pneumonia). A single mouse had a minimal focus of myocardial mineralization. Six mice had mild to severe extramedullary hematopoiesis in the spleen.

Senecionine:

In the group exposed to senecionine (n=50 mice), nonneoplastic lesions were observed in the liver, lungs, kidneys and spleen. Multiple foci of heterotopic bone (osseous metaplasia) were observed in the liver of all mice exposed to senecionine (50 mice). Foci of bone ranged from 0.1 um up to 1.3 mm in diameter, and sometimes had medullary cavities which contained megakaryocytes and erythroid and myeloid progenitor cells resembling bone marrow. Hepatic osseous metaplasia was focal in two mice, and 48 mice had multiple foci. Classification of severity of heterotopic bone formation as defined previously senecionine-exposed mice categorized classified 18 mice as mild, 19 as moderate and 13 severe. Two mice had non-regenerative hepatocellular hyperplasia with multifocal to coalescing areas of hepatocyte anisokaryosis and anisocytosis. Two mice had mild, focal or multifocal hepatocellular necrosis, and one mouse had multifocal individual hepatocyte necrosis. Six mice had focal or multifocal, mild to moderate bile duct hyperplasia. Centrilobular to midzonal hepatocellular vacuolation, with glycogen type cytoplasmic vacuoles was seen in seven mice. Focal or multifocal, minimal to mild sinusoidal angiectasis was observed in three mice. Aggregates of lymphocytes, which were mild to moderate, focal or multifocal occurred in two mice in the liver. Five mice had multifocal to coalescing hepatocyte anisocytosis and anisokaryosis with no mass

formation. In the lungs of senecionine-exposed mice, alveolar histiocytosis was observed in 41 of the 50 mice. Alveolar histiocytosis was accompanied by mild to severe lymphocytic and sometimes neutrophilic interstitial pneumonia in eight of these cases. Bronchial or alveolar epithelial hyperplasia was seen in conjunction with alveolar histiocytosis in 17 of these mice. Hyperplastic bronchial epithelial cells sometimes exhibited anisocytosis and anisokaryosis (4 mice). In two mice, alveolar histiocytes contained acicular eosinophilic cytoplasmic structures (eosinophilic crystalline pneumonia). Renal lesions observed in senecionine-exposed mice included multifocal, mild to moderate, interstitial lymphocyte infiltration (6 mice), mild to moderate, unilateral or bilateral hydronephrosis (3 mice), and focal cortical and medullary loss (chronic infarct) (1 mouse). Thirty mice had mild to severe splenic extramedullary hematopoiesis.

Seneciphylline Group:

In the group exposed to seneciphylline (n=50 mice), hepatic osseous metaplasia was observed in 45 mice. This lesion was focal in four mice and multifocal in 41. Hepatic osseous metaplasia was mild in 24 mice, moderate in 16 and severe in five. Thirty-two of the seneciphylline-exposed mice had foci hepatic of necrosis. Hepatic necrosis was focal in four of these mice and multifocal in twenty-eight. Severity of necrosis, determined by the number of observed foci and defined in the introductory paragraph to nonneoplastic lesions, was mild in twenty-three mice, moderate in four mice and severe in five mice. Mild to moderate, focal or multifocal lymphocyte infiltration was observed in seven mice. Multifocal centrilobular to midzonal, glycogen-type hepatocellular vacuolation was present in four mice. Three mice had focal or multifocal bile duct hyperplasia. Four mice

had focal minimal to mild sinusoid angiectasis. Multifocal to coalescing areas of hepatocyte cytomegaly and karyomegaly with no mass formation was observed in five mice. Within the lungs, focal or multifocal, alveolar histiocytosis was present in 32 mice. The lesion was classified in severity based on the portion of lung affected. Alveolar histiocytosis was mild in 12 mice, moderate in 13 mice and severe in 7 mice. Mild alveolar histiocytosis was considered incidental, while moderate to severe alveolar histiocytosis was possibly related to the cause of death or the cause of early euthanasia. Lymphocytic and neutrophilic interstitial pneumonia accompanied alveolar histiocytosis in 16 of these mice. Bronchial or alveolar epithelial hyperplasia was present in 21 mice, and in four of these mice there was anisocytosis and anisokaryosis in the hyperplastic epithelial cells. In two cases alveolar histiocytes contained cytoplasmic eosinophilic acicular structures (eosinophilic crystalline pneumonia). Within the kidneys, mild to moderate, focal or multifocal interstitial lymphocyte infiltration was observed in 21 mice. Hydronephrosis was observed in 13 mice. Hydronephrosis was bilateral in two mice and unilateral in eleven, mild in one mouse, moderate in 6 and severe in 6. Cardiac lesions included focal lymphocyte infiltration in three mice. Mild to severe splenic extramedullary hematopoiesis was present in 24 mice.

Riddelliine Group:

In mice exposed to riddelliine (n=50 mice), hepatic osseous metaplasia was observed in 38 mice. Thirteen mice focal hepatic osseous metaplasia, and twenty-five had multiple foci. Classification of severity based on the number of observed foci of bone in the liver was mild in 30 mice and moderate in 8. None of the riddelliine-exposed mice had severe osseous metaplasia in the liver, as defined previously. Rather, foci of heterotopic bone

were generally less than 0.1 mm in diameter for riddelliine-exposed mice. Seven mice had mild hepatic necrosis, three of these mice had single foci, and four had multiple foci. In four additional mice there was mild focal subcapsular hepatocyte loss, interpreted as necrosis. Multifocal centrilobular to midzonal hepatocellular vacuolation (glycogen type) was observed in five mice. Mild to moderate, focal or multifocal lymphocyte infiltration was observed in the liver of three mice. Sinusoid angiectasis, which was focal or multifocal, and minimal to mild was observed in two mice. One mouse had multifocal to coalescing foci of non-regenerative hepatocellular hyperplasia with hepatocyte anisocytosis and anisokaryosis. Within the lungs, focal or multifocal, mild to severe? alveolar histiocytosis was observed in 24 mice. Alveolar histiocytosis was accompanied by minimal lymphocytic and neutrophilic interstitial pneumonia in 11 of these mice. Six mice had occasional foci of bronchial or alveolar epithelial hyperplasia and in four of these mice the hyperplastic cells exhibited multifocal anisocytosis and anisokaryosis. In six mice alveolar histiocytes contained cytoplasmic eosinophilic acicular structures (eosinophilic crystalline pneumonia). In the kidneys there was mild to moderate, focal or multifocal lymphocyte infiltration in 18 mice. Seven mice had hydronephrosis, which was classified as mild in three and moderate in four cases. Hydronephrosis was unilateral in five of these mice and bilateral in the other two. Two mice had focal cortical and medullary loss (chronic infarction) involving the cranial or caudal pole, resulting in loss of 30-50 percent of renal mass. Mild to severe splenic extramedullary hematopoiesis was present in 12 mice. Two mice had neutrophilic and lymphocytic pancreatitis with fibrosis.

Lasiocarpine Group:

In mice expose to lasiocarpine (n=50 mice), one mouse had a single focus of osseous metaplasia, which was classified as mild. Seven mice had livers with mild to moderate, focal or multifocal lymphocyte infiltration distributed in pericentral or subcapsular areas. Multifocal midzonal or centrilobular hepatocellular vacuolation (glycogen type) was present in five mice. Hepatic necrosis or loss was observed in five mice, two of these mice had a single focus of necrosis. and the remaining three had multiple foci. Foci of necrosis were less than 1 um in diameter. In two of these mice, hepatic necrosis was accompanied by mild neutrophilic inflammation. Minimal to mild, focal or multifocal sinusoid angiectasis was observed in four mice. Neutrophilic hepatitis was observed in two mice, one of these mice also had lymphocytic hepatitis. Two mice had multifocal to coalescing areas of nodular hepatocyte hyperplasia with minimal anisocytosis and anisokaryosis. In one mouse, rare mitotic figures were present in hepatocytes. Pulmonary alveolar histiocytosis was observed in eight mice. Three of these mice also had lymphocytic and neutrophilic interstitial pneumonia. Bronchiolar or alveolar epithelial hyperplasia was present in two mice in addition to alveolar histiocytosis. In seven of the mice with alveolar histiocytosis, alveolar macrophages contained cytoplasmic eosinophilic acicular structures (eosinophilic crystalline pneumonia). Within the kidneys, nine mice had focal or multifocal, mild to moderate interstitial lymphocyte infiltration. Two mice had moderate hydronephrosis, which was unilateral in one and bilateral in the other. One mouse had a focus of cortical and medullary renal loss (chronic infarction). One mouse had multifocal, necrotizing and fibrosing, global glomerulonephritis. Eleven mice had mild to severe, splenic extramedullary hematopoiesis. One mouse had neutrophilic, lymphocytic and fibrosing pancreatitis.

Heliotrine Group:

In mice exposed to heliotrine (n=50), hepatic necrosis was observed in six mice. Hepatic necrosis was multifocal and severe with neutrophilic inflammation in 2 mice. Three mice had rare individual cell necrosis (3 mice), and one mouse had a single focus of necrosis. Lung lesions included alveolar histiocytosis with cytoplasmic eosinophilic acicular material (eosinophilic crystalline pneumonia) in one mouse, and focal or multifocal mild lymphocyte infiltration in four mice. Hydronephrosis was observed in 15 mice. Hydronephrosis was bilateral in four mice and unilateral in 11, and classified as mild in four mice, moderate in four mice and severe in seven mice. Mild to moderate, focal or multifocal, Interstitial lymphocyte infiltration of the kidneys was observed in 12 mice. Moderate to severe splenic extramedullary hematopoiesis was present in four mice.

Tables 3.6-3.8: Severity Grades for Frequently Observed Nonneoplastic Lesions by Group.

Table 3.6. Hepatic Osseous Metaplasia Observed in Each PA Group

Osseous metaplasia	Mild (≤ 5 foci)	Moderate (5-10 foci)	Severe (≥ 10 foci)
Control (n=50)	n.d.	n.d.	n.d.
Senecionine (n=50)	18	19	13
Seneciphylline (n=50)	24	16	5
Riddelliine (n=50)	33	5	0
Lasiocarpine (n=50)	1	0	0
Heliotrine (n=50)	n.d.	n.d.	n.d.

n.d. = not detected.

Table 3.7. Hepatic necrosis observed in each PA group

Hepatic necrosis	Mild (≤ 10 foci)	Moderate (10-20 foci)	Severe (≥ 20 foci)
Control (n=50)	n.d.	n.d.	n.d.
Senecionine (n=50)	12	0	0
Seneciphylline (n=50)	23	4	5
Riddelliine (n=50)	7	0	0
Lasiocarpine (n=50)	3	1	0
Heliotrine (n=50)	4 (3 have rare ind. cell necrosis)		2

*Foci of necrosis were generally less than 1 um in diameter unless otherwise noted. n.d. = not detected.

Table 3.8. Hydronephrosis observed in each PA group

Hydronephrosis	Mild	Moderate	Severe
Control (n=50)	n.d.	n.d.	n.d.
Senecionine (n=50)	1 (bilat.)	2 (unilat.)	0
Seneciphylline (n=50)	2 (1 unilat. 1 bilat.)	7 (5 unilat. 2 bilat.)	4 unilat.
Riddelliine (n=50)	3 (1 bilat. 2 unilat.)	4 (1 bilat. 3 unilat.)	0
Lasiocarpine (n=50)	1 bilat.	1 unilat.	0
Heliotrine (n=50)	3 (2 unilat. 1 bilat.)	5 (3 unilat. 2 bilat.)	7 (6 unilat. 1 bilat)

n.d. = not detected, unilat. = unilateral, bilat. = bilateral.

Figures 3.8-3.10: Photomicrographs Showing Examples of Select Nonneoplastic Lesions.

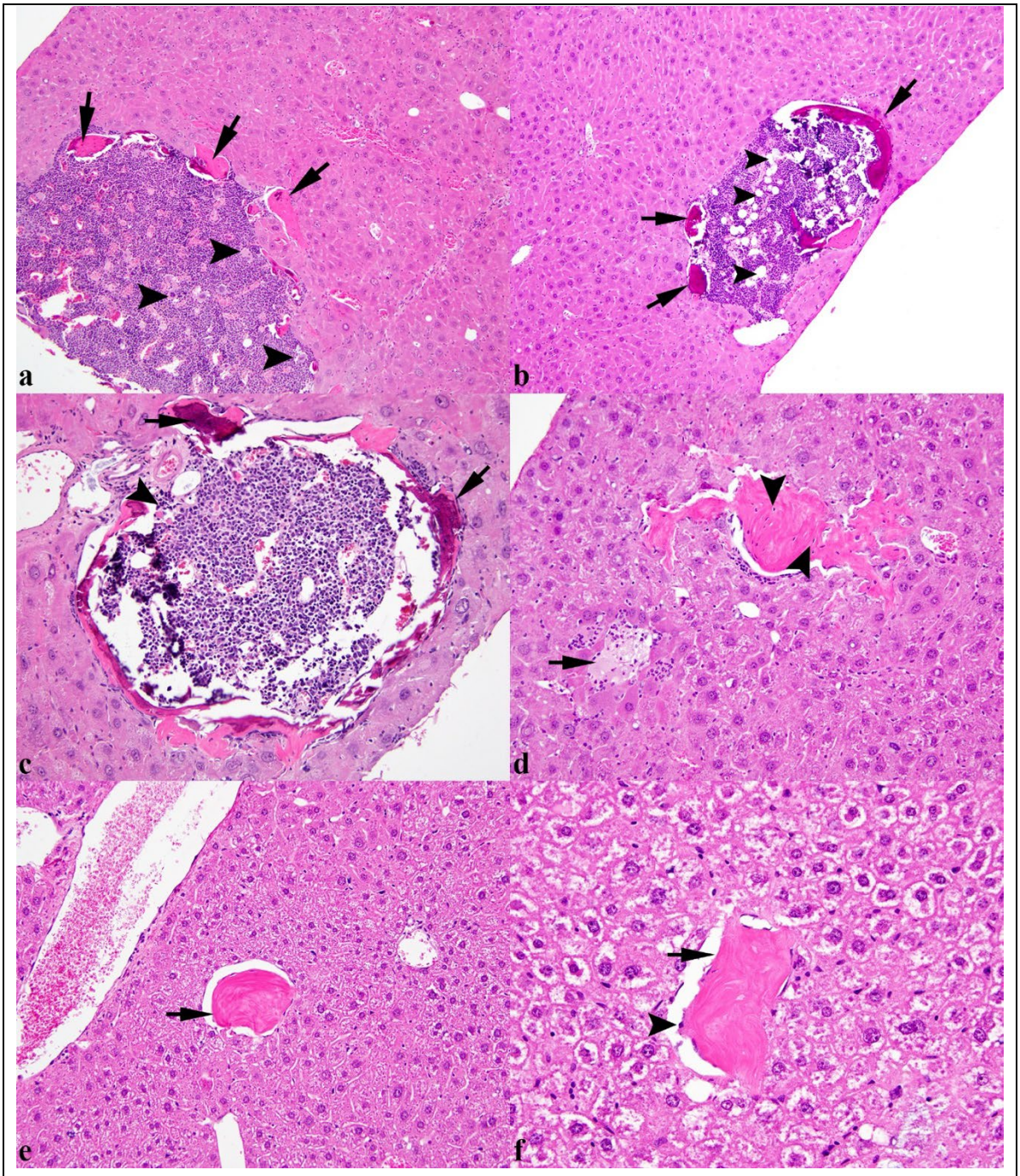

Figure 3.8. Images a-f. Heterotopic bone replaces hepatocytes in the livers of PA exposed mice from multiple PA groups. Image (a): Liver from a senecionine-exposed mouse. Spicules of eosinophilic bone (arrows) surround a central area composed of bone marrow admixed with numerous small blood vessels. Megakaryocytes (arrowheads) are present within bone marrow. Image (b): Liver from a senecionine-

exposed mouse. Eosinophilic bone spicules are mineralized (arrows). Bone marrow and adipocytes (arrowheads) are in the center of the focus of bone. Adjacent hepatocytes are occasionally compressed Image (c): Liver from a seneciphylline-exposed mouse. Bone is mineralized (arrows) and forms a circular cavity surrounding a center composed of bone marrow (arrowhead). Hepatocyte hypertrophy and/or swelling with dysplasia, fibrosis, and minimal inflammation. Image (d): Liver from a seneciphylline-exposed mouse. A focus of eosinophilic bone replaces hepatocytes. Multiple lacunae containing osteocytes (arrowheads) are within the osteoid. A single focus of hepatocellular necrosis (arrow) with moderate numbers of infiltrating neutrophils is near to the osteoid. Images (e): Liver from a riddelliine-exposed mice. A focus of bone (arrow) multifocally replace hepatocytes. Image (f): Liver from a riddelliine-exposed mice. A focus of bone (arrow) multifocally replace hepatocytes. Osteoblasts (arrowhead) multifocally line the osteoid.

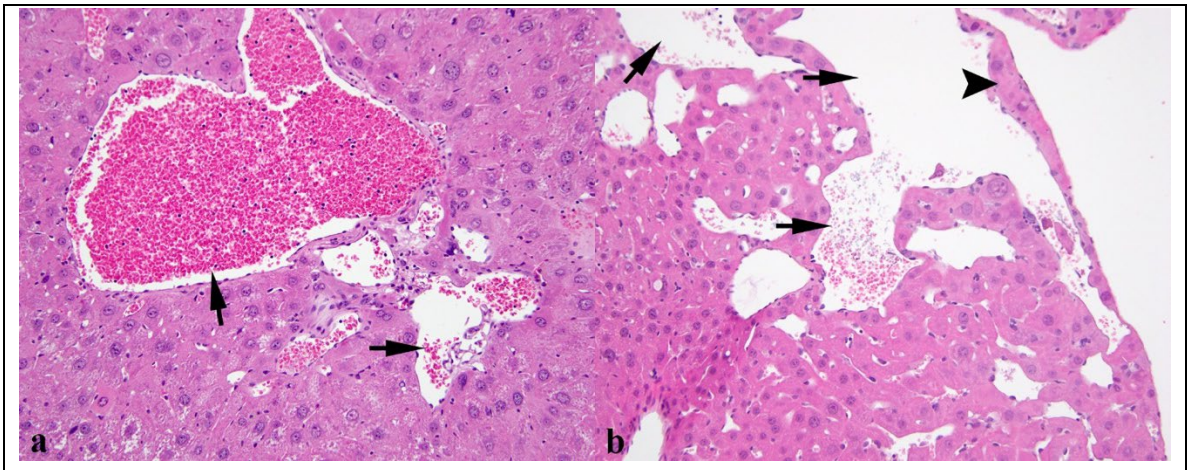

Figure 3.9. Images a and b: Liver angiectasis (also referred to as peliosis hepatis or telangiectasia). Image (a): liver from a senecionine-exposed mouse. Focal dilation of sinusoids creates cavernous, blood-filled spaces (arrows) lined by endothelial cells. Image (b): liver from a seneciphylline-exposed mouse. Dilated sinusoids create variably sized spaces (arrows) that are lined by endothelial cells. Spaces can result in loss of hepatocytes leaving only a thin layer of hepatocytes (arrowhead) adjacent to the capsule.

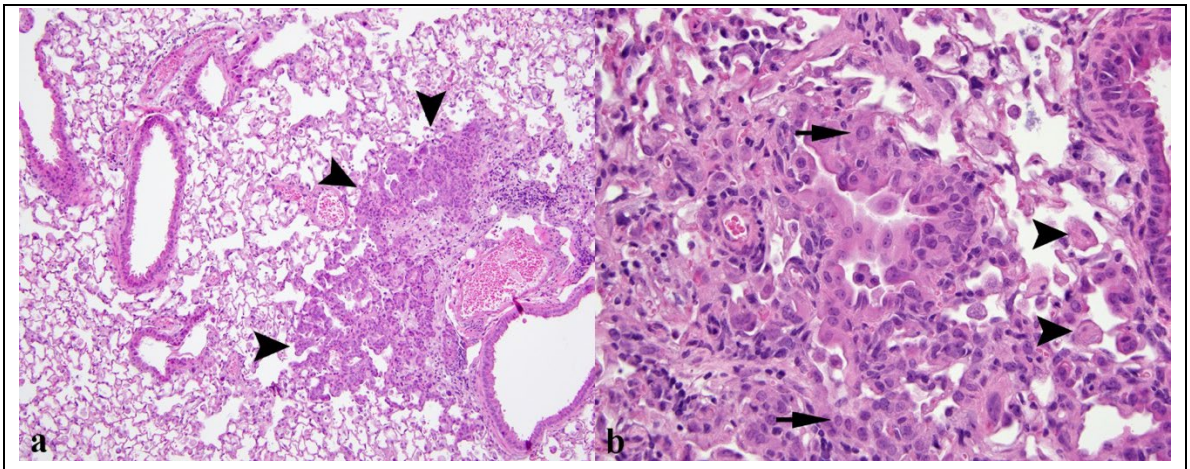

Figure 3.10. Images (a) and (b), Lung with alveolar epithelial hyperplasia from a senecionine-exposed mouse. Image (a): low magnification view showing increased numbers of cuboidal pneumocytes (arrowheads). Image (b): High magnification of the cuboidal epithelial cells shows variation in cell size and nuclear size (arrows) in these pneumocytes. Small numbers of macrophages (arrowheads) are in alveolar spaces.

Statistical Comparison of Neoplasms Between Groups:

Dunnett's Test and Poly-k Adjustment Results for Neoplasms:

Tables including the poly-k (poly-3) adjusted proportion can be seen in supplemental material. Also seen in supplemental material are tables including the test statistic and lower bound from the Dunnett tests. Adjusted p-values are listed below. These statistical tests were run for proportions of mice with tumors and for individual tumor types. There was no statistically significant difference between any PA and the control group for any of these comparisons. For numbers of mice with neoplasia, adjusted p-values are 0.158 for senecionine, 0.907 for seneciphylline, 0.313 for riddelliine, 0.952 for lasiocarpine and 0.974 for heliotrine. For hemangiosarcomas, adjusted p-values are 0.5363 for

senecionine, 0.4239 for seneciphylline, 0.1037 for riddelliine, 0.4850 for lasiocarpine and 0.9842 for heliotrine. For hepatocellular adenomas adjusted p-values are 0.1667 for senecionine, 0.5777 for seneciphylline, 0.8895 for riddelliine, 0.8913 for lasiocarpine and 0.8838 for heliotrine. For bronchioloalveolar tumors adjusted p-values are 0.1785 for senecionine, 0.9573 for seneciphylline, 0.9694 for riddelliine, 0.9705 for lasiocarpine and 0.9960 for heliotrine. For lymphoma adjusted p-values are 0.6246 for senecionine, 0.6175 for seneciphylline, 0.8345 for riddelliine, 0.9356 for lasiocarpine and 0.3607 for heliotrine. For soft tissue sarcomas not attributed to the microchip adjusted p-values are for 0.9876 senecionine, 0.9439 for seneciphylline, 0.6056 for riddelliine, 0.9618 for lasiocarpine and 0.9935 for heliotrine. For histiocytic sarcomas adjusted p-values are 0.9249 for senecionine, 0.9484 for seneciphylline, 0.6032 for riddelliine, 0.8025 for lasiocarpine and 0.9544 for heliotrine.

Chi-squared and Fisher's Exact Test Comparison of Nonneoplastic Lesions:

There were significant differences in the frequency of osseous metaplasia between groups ($p < 0.0001$). Fisher's exact text comparisons to the control determined that senecionine, seneciphylline, and riddelliine ($p <0.0001$). Chi-squared testing detected significant differences in the frequency of hepatic necrosis between groups ($p < 0.0001$). Fisher's exact tests comparisons with the control group detected significant differences for senecionine ($p = 0.0004$), seneciphylline ($p < 0.0001$), riddelliine ($p = 0.0125$), and heliotrine ($p = 0.0267$). Chi-squared tests detected differences in the frequency of pulmonary alveolar histiocytosis between groups ($p < 0.0001$). Fisher's exact test detected differences between the control group and senecionine, seneciphylline, and riddelliine ($p < 0.0001$). The frequency for senecionine was significantly greater than

riddelliine and seneciphylline ($p < 0.0001$). Regarding the frequency of hydronephrosis, Chi-squared testing detected significant differences between groups ($p > 0.0001$). Fisher's exact tests comparisons with the control group detected significant differences for seneciphylline ($p < 0.0001$), riddelliine ($p = 0.0125$), and heliotrine ($p < 0.0001$).

Discussion:

Neoplasms:

The results of this study indicate that senecionine, seneciphylline, lasiocarpine and heliotrine are not carcinogenic mice at the dose and exposure length used in this model. Our hypothesis was that PAs with similar hepatotoxicity to riddelliine, will have similar carcinogenic potential. However, under these conditions, there was no statistically significant difference between the control and any of the treatment groups in the frequency of neoplasia. Similarly, there was no significant difference in the frequency of lesions interpreted as preneoplastic. Although not statistically different, riddelliine-exposed mice developed the greatest number of neoplasms and the greatest number of hemangiosarcomas. The aim of this research was to characterize the type and frequency of neoplastic development in heterozygous p53 knockout male mice, and to determine if selected PAs which vary in their hepatotoxic potential have similar carcinogenic potential in mice. Riddelliine was used as a positive control because it is proven carcinogenic in rats and mice and has been classified as a potential human carcinogen in humans.[59] Riddelliine also increased neoplastic incidence in a similar experiment performed in P53 knockout mouse by Brown et al. (2015). They exposed a similar P53 knockout mouse model to various doses of riddelliine and observed a dose related trend in the

development of liver hemangiosarcomas.[4,60] Though the P53 knockout mouse model used in our experiment was similar to the one used by Brown, we did not observed statistically significant differences in the frequency of neoplasia development between the control group and of the treatment groups.

The experiment performed by Brown et al. (2015) demonstrating the utility of a heterozygous p53 knockout mouse model for carcinogenicity studies in PAs provides important context for the experimental design used in this experiment.[1,4,60] Brown's work was a pilot for the experimental design we used, with some important differences. These differences may provide possible reasons for the lack of statistical significance in our study, and potential ways in which our experimental model could be strengthened. The key differences were a different laboratory source for mice, mice obtained by breeding in our study, a larger sample size in our study, and in our study, experiments were staggered and completed over a period of years. In Brown's work, mice were obtained from a different source (Techronic), all the animals were the same age, and all were dosed at once. As the strain used by Brown was not available, we used Jackson Laboratory's p53 knockout mouse (B6.129S2-Trp53^{tm1Tyj}/J) to develop a breeding colony to provide the 300 heterozygous p53 knockout male mice for this study. Though the mice are supposed to be of similar genetics, there may have been some genetic drift. As even commercial supplier with large breeding colonies have difficulty supplying small groups of male heterozygous mice, the cost and lack of supply required that we develop our own colony and spread the exposures over multiple years. PCR testing was performed in our study to confirm heterozygous males but genetic variation from breeding could have gone undetected.

In addition to potential genetic variation, there were small variations in the ages of mice during dosing. Age is a key determinant in susceptibility to PA poisoning, due to differences in both bioactivation and phase 2 metabolism and excretion of the toxic pyrroles.[38,61]. Young animals are generally more susceptible to PA poisoning, which may potentially skew comparisons within groups and between PA groups.

Another key difference between Brown's study and the current one was that the number of mice in Brown's study was comparatively small. In Brown et al.'s work, the groups were composed of ten mice each. In his control group, only one mouse developed neoplasia in the form of a round cell tumor. Our control group included 50 mice, and 13 tumors of varying types developed in 12 of these mice. One of these control mouse tumors happened to be a liver hemangiosarcoma, which resulted in our comparison of this tumor type being non-significant even for the riddelliine group which had six hemangiosarcomas. Brown's experiment also used three different doses of riddelliine, 0.014, 0.043, or 0.129 mmol/kg/day for ten days and observed an increased odds ratio of tumor development with increasing dose. The odds ratio was 2.05 with Wald 95% confidence limits between 1.2 and 3.4. Additionally, they exposed a fourth group to a lower dose (0.003 mmol/kg/day) for the entire year long course of the experiment. The low dose group with year-long exposure had the largest number of liver hemangiosarcomas. The year-long exposure group also had the same number of all tumors as the high dose (0.129 mmol/kg/day for ten days) group.

The exposure method used by Brown in the year-long low dose group resembles the exposure method used by the NTP in their long-term carcinogenicity studies of riddelliine which established riddelliine as a carcinogen. Brown's group only exposed

mice for one year, but the mice were heterozygous p53 knockouts and will more readily develop neoplasia. The NTP study exposed rats and mice to riddelliine five days a week for 105 weeks.[2] The difference in duration of exposure is another way that dosing might be changed to increase the chance of tumorigenicity. Our study was designed to represent short periods of exposure, such as may occur with intermittent herbal use or contaminated food or feed.

In our experiment, we used the highest riddelliine dose from Brown et al. as a common molar dose for all PAs. As purified PAs are difficult to purify in quantities needed for extended dosing, and there was similar neoplastic transformation in Brown's high dose 10-day treatment, we used a short duration of exposure. It is possible that our results could have differed if a longer duration of exposure was used.

Another key difference between these studies has to do with statistical tests used and differences in mortality between groups. Browns work did not have substantial differences in mortality between dosing groups. They also had different doses, enabling the use of a trend test for statistical analysis. In our study there were significant differences in early mortality rates between groups. Mice exposed to senecionine had the lowest survival, followed by seneciphylline, riddelliine, lasiocarpine and heliotrine. When performing statistical analysis in long-term carcinogenicity studies, early mortality must be accounted. Failing to perform this adjustment for mortality could result in a test articles carcinogenicity being underestimated if exposure to that agent results in early mortality.[57,62,63] With this adjustment, we were limited by availability of software which will support a mortality adjustment and the Dunnett's test with the poly-k mortality

adjustment was our best option. Dunnett's test is known to be somewhat conservative and found no statistical significance between any PA and the control group.[64]

Our strategy to run these 50 mouse group studies in groups of 25 could also have created variation and affected statistical outcomes. This variation could result from genetic variation in the breeding colony, varying environmental conditions, or simply random chance. The order with which the experiments were completed was control, lasiocarpine, riddelliine, seneciphylline, senecionine, heliotrine and lastly a repeat of riddelliine. The greatest to least number of mice with neoplasia was riddelliine, senecionine, seneciphylline, control, lasiocarpine, heliotrine, so it does not appear that the order of experiments trended up or down with the incidence of neoplasia. For statistical purposes it would be preferable to run the entire experiment at once, but this is not feasible due to limitations in facility size and staff to dose, monitor and necropsy mice.

Lastly, use of a different animal model may provide improved results. Due to their heterozygous p53 knockout mutation, and reduced tumor suppressor gene function, a substantial number of mice in the control group developed various neoplasms. More mice in the control group had tumors than the lasiocarpine, seneciphylline, and heliotrine. The presence of neoplasms in the control group is likely the reason for a lack of statistically significant differences.

In summary, some areas of potential improvement for our experimental design include use of mice from the same generation of breeding and the same age, including different dosing groups, increasing the duration of exposure, performing all mouse experiments at once, and using a different animal model. These changes could be easily

achieved given the necessary facility space for animal housing as well as staffing for dosing, animal care and necropsy.

Hemangiosarcomas:

Hemangiosarcomas of the liver are the main neoplasm of interest based on the NTP carcinogenicity study of riddelliine. In the control group, there was one mouse with a hepatic hemangiosarcoma. In riddelliine-exposed mice (n=50), six hemangiosarcomas were identified, one in skeletal muscle and five in the liver. Six was the greatest number of any group although not statistically significant than the control using Dunnett's test. Three hemangiosarcomas were detected in the seneciphylline group, as well as the lasiocarpine group, which was not significantly different than the control group. Senecionine-exposed mice developed two hemangiosarcomas and heliotrine-exposed mice had none. When comparing riddelliine to the other PA groups using a two-tail test, only riddelliine and heliotrine were significantly different.

In the NTP riddelliines carcinogenicity study, liver hemangiosarcomas were the main neoplasm observed in male mice. Liver hemangiosarcomas were also the primary neoplasm observed in Brown et al.'s study when mice were exposed to the lowest dose (0.0003 mmol/kg/day) for a full year.[4,59] Mice in Browns ten-day exposure groups also developed liver hemangiosarcomas, but there was a lower number, and a variety of other neoplasms were observed in Brown's study. It is worth noting that the other neoplasms seen in the high dose group were also observed in the original publication which characterized the neoplasms seen in p53 knockout mice.[37] In our study the incidence of hemangiosarcoma in riddelliine-exposed mice at least doubled every other PA group. The

finding of a single liver hemangiosarcoma in a control mouse resulted in a lack of statistically significant difference between the control group and all PAs. It is possible, but unlikely that in mice riddelliine is not carcinogenic when given short durations as in this study. This is unlikely because the significant trend and increased odds ratio of tumor development observed by Brown.

The results of this study do not call into question the established fact that long-term exposure to riddelliine is carcinogenic to mice and is a reasonably anticipated to be a human carcinogen, nor do they negate the statistically significant trend in neoplasia demonstrate.[2] [1,3,60]

Hepatic Angiectasis:

Hepatic angiectasis (also known as peliosis hepatis or telangiectasia) was observed in mice in the control group (6/50 mice), senecionine (2/50 mice), seneciphylline (4/50 mice), riddelliine (2/50 mice), lasiocarpine (6/50 mice), and heliotrine (3/50 mice). Angiectasis has been documented to occur following a variety of hepatic insults, including exposure to PAs.[4,49,65] This lesion was characterized by dilation of sinusoids, resulting in enlarged blood filled spaces. Blood-filled spaces varied from widened sinusoids to larger cavernous spaces, sometimes reaching 0.5 mm in diameter. In some of these cases, hepatic angiectasis closely resembled hemangioma or a hemangiosarcoma. Differentiating these lesions was based on the cellular appearance and organization of the lining endothelial cells. This is difficult as many invasive and metastatic hemangiosarcomas had minimal endothelial cell atypia in this study. Hemangiosarcomas were characterized by enlarged endothelial cells that protruded into spaces and sometimes had anisocytosis and anisokaryosis. The similarity of these lesions suggests a

spectrum and that angiectasis may precede the development of hemangiosarcomas in the liver. Brown et al. (2015) reported this lesion and suggested that it may be preneoplastic.[4] Brugerra et al. (1978) reported that sinusoidal dilation may be associated with the presence of a neoplasm or granulomatous disease, either in the liver or in extrahepatic sites.[66] Detection of this lesion in the control and heliotrine exposed groups suggests that is may also be incidental.

Additional Neoplasms Observed:

Additional tumors observed in multiple mice include hepatocellular adenomas (hepatomas), bronchioloalveolar adenomas/carcinomas, lymphoma in various organs, undifferentiated soft tissue sarcomas, histiocytic sarcomas, and osteosarcomas. There was also a single pars distalis carcinoma, one seminal vesicle adenoma, one seminoma and a cutaneous papilloma. All of the tumors that were observed in multiple mice are also described by Jacks et al (1996) in heterozygous p53 knock out mice.[37] In addition to the single liver hemangiosarcoma, control mice had three bronchioloalveolar adenomas, three lymphomas, three soft tissue sarcomas at various anatomic sites, one histiocytic sarcoma, one pars distalis carcinoma, and one papilloma were observed. Given the lack of statistically significant differences between groups, and the incidence of these tumors in control mice these neoplasms should not attributed to PA exposure. The tumors which were only observed in single animals are also likely the result of chance and the p53 mutation.

Hepatocellular adenomas (hepatomas) were observed in rats that were fed riddelliine in water in the NTP study, but in mice there was a negative dose-related trend in the incidence of these tumors.[2] In our study, the appearance of the liver of mice in

which this lesion was observed was abnormal. Hepatocytes not involved with the hepatocellular neoplasm exhibited moderate to severe anisocytosis and anisokaryosis. There was also heterotopic bone in these livers. Hepatocellular adenomas can be difficult to distinguish from nonregenerative and regenerative foci of hepatocellular hyperplasia, as is the case with these neoplasms. Nonregenerative and regenerative foci of hepatocellular hyperplasia remain differentials for these neoplasms. It seems unlikely that these neoplasms are directly due to PA exposure. It is possible that PA exposure could result in hepatic necrosis and subsequent repair processes could result in hyperplasia or neoplasia.

Bronchioalveolar tumors were observed in female mice exposed to riddelliine in the NTP study.[2] The largest number of bronchioloalveolar adenomas and carcinomas in our study was in the senecionine exposed mice at 6, followed by the control group at 3. One bronchioloalveolar adenoma/carcinoma was observed in each of the seneciphylline, riddelliine and lasiocarpine groups. The difference between proportion of senecionine-exposed mice and the control group was not significantly different. Comparisons between all other groups were not statistically significant. In the previous chapter, acute lesions in the lung were not observed. Given the incidence of these tumors in the control group, these neoplasms should not be attributed to PA exposure.

Lymphoma was not observed with statistical significance in the NTP study.[2] Brown et al. detect lymphomas in some of the riddelliine-exposed mice.[60] Heliotrine-exposed mice had the largest number of lymphoma cases (6), followed by seneciphylline (4), riddelliine (3), senecionine (3) and the control groups (3), and lasiocarpine was last (2 cases). Two-tail tests were used for comparisons with the control group, as the control

had as many or more cases than all other groups except heliotrine. None of the comparisons between any of the compound groups and the control group were significantly different. It is unlikely that PA exposure could lead to the development of lymphoproliferative disease, given the need for metabolic activation by CYP450 enzymes. Lymphoma in our study is most likely a consequence of the reduced p53 function in these mice.

The undifferentiated soft tissue sarcomas were differentiated from hemangiosarcomas by the lack of erythrocyte-filled spaces lined by neoplastic endothelial cells. The largest number of soft tissue sarcomas (4/50) was observed in the mice exposed to riddelliine. The next largest number was in the control group (3/50), followed by seneciphylline (1), lasiocarpine (1), and heliotrine (1). There were no soft tissue sarcomas in the senecionine group aside from those that were thought to be related to microchip implantation. Two-tail Chi-squared comparisons and Fisher's exact tests were used, as the control group had the second greatest number of this particular tumor type. There was no significant difference between any of the PAs and the control group. Jacks et al. (1994) describes a variety of soft tissue sarcomas in mice heterozygous for p53 knockout mutations.[37] These tumors are likely related to the animal model and not to PA exposure. Riddelliine-exposed mice had the largest number of histiocytic sarcomas (2/50). Lasiocarpine-exposed mice and the control group each had one mouse with histiocytic sarcoma. There were no statistically significant differences between these affected groups.

Alveolar/Bronchiolar Epithelial Hyperplasia:

Alveolar and/or bronchiolar epithelial hyperplasia was also observed in mice in the control (3/50 mice), senecionine (5/50 mice), seneciphylline (3/50 mice), riddelliine (6/50 mice), and lasiocarpine (2/50 mice) groups. Bronchiolar/alveolar epithelial hyperplasia can be caused by exposure to pulmonary irritants or respiratory viral infections.[50] In rare cases, hyperplastic epithelial cells exhibited mild to moderate atypia characterized by anisokaryosis and anisocytosis. Cellular atypia is also common feature of neoplasia.[50] Differentiating hyperplasia from bronchioloalveolar neoplasia was based on the presence of mass production, compression of surrounding alveoli, cellular atypia and mitotic activity.[50] Given the similarity between this lesion and neoplasia bronchial and alveolar hyperplasia preceded development of tumors. Multistage carcinogenesis in bronchioloalveolar neoplasms has been proven, therefore hyperplasia of bronchiolar and alveolar epithelium with anisocytosis and anisokaryosis may be a preneoplastic lesion.[67] It is unlikely that this lesion developed from PA exposure but could be due to decreased p53 tumor suppressor gene function.[68]

Nonneoplastic Lesions:

When evaluating frequency of non-neoplastic lesions in this study, it is important to remember that regardless of statistical significance, these lesions may not be caused by exposure to the select PA. It is possible that the lesions developed incidentally, or because of genetic variation within the breeding colony. The temporal order of the groups from earliest to latest is vehicle control, lasiocarpine, riddelliine, senecionine, seneciphylline, and last heliotrine. The control group developed fewer non-neoplastic lesions when compared to mice exposed to senecionine, seneciphylline, riddelliine, and

less so lasiocarpine. The mechanism of PA toxicity must be considered before attempting to attribute these lesions to exposure. In this study, statistical significance was observed when comparing lesion frequency to the control group for the following non-neoplastic lesions: Hepatic osseous metaplasia, pulmonary alveolar histiocytosis, hepatic necrosis, and hydronephrosis. We will consider each of these lesions individually and discuss the possibility that they are the result of exposure to PAs in this study.

Heterotopic Bone (Osseous Metaplasia):

Among the most common nonneoplastic lesions observed was the presence of heterotopic bone within the liver. Foci of heterotopic bone were variably mineralized, lined by osteoblasts, often had lacunae containing osteocytes, and sometimes had medulla-like centers filled with myeloid and erythroid precursors resembling bone marrow. Osseous metaplasia, also referred to as heterotopic ossification, ectopic bone, or metaplastic bone, is defined as "pathologic bone formation in soft tissues".[69] This lesion is described as "an uncommon incidental finding" by the International Harmonization of Nomenclature and Diagnostic Criteria for Lesions in Rats and Mice, hematolymphoid system reference for mice and rats.[51] Additional references to this lesion occurring in the liver of mice are few. Heterotopic bone can form secondary to degeneration and/or neoplasia which stimulate production of bone morphogenetic proteins (BMPs). [51] BMPs are a group of proteins belonging to the transforming growth factor-beta superfamily that have a variety of functions, the most notable of which is inducing production of bone, cartilage, ligament and tendon formation.[70] Heterotopic ossification can also occur secondary to trauma or can be inherited.[69] Inherited heterotopic ossification is associated with multiple characterized mutations including ACVR1 resulting in fibrodysplasia ossificans

progressive, and GNAS resulting in progressive osseous heteroplasia or Albright inherited osteodystrophy.[69,71,72] Heterotopic ossification in humans has also been described in association with central nervous system injuries, burns, sickle cell anemia, poliomyelitis, multiple sclerosis, tetanus, and toxic epidermal necrolysis. [73] Osseous metaplasia can also develop from foci of mineralization.[51] In the acute hepatotoxicosis lesions seen in the previous chapter, mineralization is not typically observed in foci of necrosis.

We speculate that osseous metaplasia developed in our study as a response to PA-induced hepatic necrosis. Brown et al. (2015) observed this lesion in the six out of ten mice in the high dose group (45 mg/kg/day) of riddelliine exposed mice.[4] The mice used by Brown were a similar genetic strain as those described in this current study. The largest proportion of affected mice occurred in the group exposed to senecionine, followed by seneciphylline, and then riddelliine. One of the lasiocarpine-exposed mice had a single focus of bone in the liver, and none of the heliotrine-exposed mice or the control mice had this lesion. The order of this frequency mirrors the order of severity of necrosis observed in our earlier work which ranked severity of hepatotoxicity immediately after exposure the same PAs used in this study. This assertion is strengthened by the fact that none of the heliotrine-exposed mice or control mice had this lesion, and these mice were the last group temporally, and the control group was the first group tested. It is likely that this lesion is a unique response to PA-induced hepatic necrosis, related to the genetic alteration in the B6.129S2-Trp53^{tm1Tyj}/J mice. This can be stated because mouse studies of PA toxicosis using other mouse strains have not detected the development of hepatic osseous metaplasia. These mice likely have an aberrant

response to PA-induced hepatic necrosis. An additional possibility is that these nodules of heterotopic bone were the result of a neoplastic process. Osseous metaplasia is associated with various neoplasms including mammary tumors in dogs and people and various other tumors.[74–76] This seems unlikely based on the histologic appearance of the lesion and lack of association with neoplasms. Many other rodent studies have been performed on PA toxicosis, and the only reference to this lesion was in Brown's work, also using a heterozygous p53 knockout mouse, hence the lesion is specific to this mouse model.

Hepatic Necrosis:

Hepatic necrosis was observed in all groups except the vehicle control group. Senecionine ($p = 0.0004$), seneciphylline ($p < 0.0001$), riddelliine ($p = 0.0125$), and heliotrine ($p = 0.0267$) were significantly different than the control group. Hepatic necrosis is known to be caused by exposure to various PAs in virtually all species to varying degrees.[9,9,77] Hepatic necrosis is also a frequently observed background lesion in mice.[51] Retrorsine, a representative PA was shown to persist in liver for at least 8-weeks in mice. This study showed that multiple doses led to prolonged retention in tissues.[78,79] Half-life varies between PAs and it is not known if the PAs evaluated in our study could persist for a full year. It is possible that PA-induced pyrrole-protein adducts or DNA-adducts could be recycled and cause hepatic necrosis long after exposure. In this study, measurement of hepatic pyrrole concentration was not performed as this testing uses too much of the liver, and histopathology was the main endpoint of interest. Given the time elapsed between exposure and necropsy, ranging from 223 to 365 days, it is unlikely that this necrosis is caused by PA exposure. Hepatic necrosis was observed at the greatest

frequency (32 of 50 mice) in the seneciphylline group, followed by senecionine (12 of 50 mice) and riddelliine (7 of 50 mice) and lastly heliotrine (6 of 50 mice). Lasiocarpine was not statistically different than the control. Heliotrine having a significantly greater incidence of hepatic necrosis than the control group is most likely due to a background of necrosis. This is true, because in our earlier work, mice did not develop necrosis even at doses four times greater than the dose of heliotrine that these mice were exposed to. On the other hand, the large proportion of seneciphylline and senecionine exposed mice may indicate ongoing necrosis, possibly due to recycling of pyrroles or persistence of these PAs.[39] These two PAs caused the most severe hepatic necrosis among this group in wildtype mice from the same breeding colony but lacking the p53 knockout mutation. It may be the case that seneciphylline has more potential to cause latent hepatic necrosis than other PAs, followed by senecionine. Further studies are needed to confirm this.

Alveolar Histiocytosis:

Pulmonary alveolar histiocytosis was observed in all groups with varying frequency. The distribution and severity ranged from mild focal areas of macrophages up to multifocal to coalescing severe histiocytic inflammation. Perivascular lymphocytic inflammation and/or aggregates of neutrophils sometimes accompanied the alveolar macrophages. The frequency of this lesions greatest in mice exposed to senecionine (44 of 50 mice), followed by seneciphylline (32 of 50 mice), riddelliine (25 of 50 mice), lasiocarpine (9 of 50 mice). Three of the control mice had this lesion and one of the heliotrine exposed mice. PAs are mainly hepatotoxic, but to a lesser extent they can also result in pulmonary lesions. The primary PA with evidence of pulmonary toxicity is monocrotaline. It is thought that this PA produces more stable toxic metabolites that are able to reach the lung

following bioactivation in the liver.[13,80] Song et al. (2020) demonstrated that the liver is the main site of bioactivation for PAs, although Clara cells within the lung also have the capability to metabolically activate PAs using CYP450 enzymes.[13] They detected pyrrole-protein adducts within the lungs of rats following PA exposure, and suggested that pulmonary injury may be a common outcome of PA exposure. In chapter 2, we microscopically examined lung, in addition to other tissues, in mice directly following exposure to five PAs and two PA N-oxides at varying doses. The doses in Chapter 2. were four to eight times the dose used in this year-long study. There was no microscopic evidence of pulmonary toxicity in any of these experiments. While it is possible that pulmonary injury occurred without leaving microscopic evidence, this is unlikely given the doses used. Alveolar histiocytosis is a common lesion in aged mice.. [81] Differences in frequency of this lesion between groups are most likely not related to PA exposure. In a small number of the cases observed, alveolar macrophages contained cytoplasmic eosinophilic crystalline material, consistent with eosinophilic crystalline pneumonia. C57BL6/j mice are commonly affected by this lesion, and this is the background strain for these p53 knockout mice.[81,82] Differences in the frequency of pulmonary alveolar histiocytosis between groups may be due to secondary effects of PA hepatotoxicity. Liver disease has been shown to increase risk for certain pulmonary diseases, in part because the liver is responsible for metabolic inactivation of endogenous inflammatory mediators.[83] Statistically significant differences withstanding, attribution of the lesion to PA exposure would require additional research.

Hydronephrosis:

Hydronephrosis is a common background lesion in certain strains of mice.[81] Spontaneous hydronephrosis has been described in C57BLKsJ mice, a strain that is similar to the background strain of the mice used in this experiment. This lesion is considered incidental in this study, despite the statistical significance between groups. The order of frequency from greatest to least is heliotrine (15 of 50), seneciphylline (13 of 50), riddelliine (7 of 50), senecionine (3 of 50), lasiocarpine (2 of 50), and no cases were observed in the control group. This order is similar to the temporal order that the experiments were carried out. Heliotrine and seneciphylline, the compounds with the greatest frequencies of this lesion, are the most recent studies to be completed, which indicates that this lesion may have increased because of our mouse breeding program. Hydronephrosis should be considered incidental to studies in which breeding programs for B6.129S2-Trp53^{tm1Tyj}/J mice are employed.

Statistical Analysis:

Dunnett's test with the poly-k mortality adjustment did not detect statistically significant differences in the proportions of mice with neoplasms when compared to the control group. These tests were performed individually for total affected mice, hemangiosarcomas, hepatocellular adenomas, lymphoma, bronchioloalveolar adenomas, histiocytic sarcomas, and soft tissue sarcomas. These tests did not detect significant differences between control group and the PA group for any of these neoplasms. Poly-3 test adjusted sample sizes and adjusted p-values can be seen in supplemental data (word document "All R output"). The poly-k test is currently the standard used by the NTP for mortality correction in long-term carcinogenicity studies.[62] The poly-k test adjusts the

weight of mice euthanized early for causes other than the neoplasms of interest, weight meaning the denominator in the proportion of mice affected. Stated otherwise, mice that do not survive to study termination due to causes besides the neoplasm (s) of interest are not considered as a whole mouse, rather a fraction based on the time they survived. The calculation is (time of life/time to study terminal sacrifice) to the power of k. Comparisons between compound groups and controls use a one tail test to determine statistical significance. The purpose of the poly-k adjustment for mortality is to avoid underestimating the carcinogenic potential of a group of animals, if the group had shorter lifespans.

When comparing proportions of neoplasms to the control group and upper-tail test was used, because it is not reasonable to expect PAs to reduce the risk of neoplasia development. When comparing proportions with tumors between PA exposed groups, a two tail Chi-squared test was used. Schaarschmidt et al. (2008) state that two-tail tests in carcinogenicity studies are likely to produce more false negative results and should therefore be avoided. [63]

Heterozygous p53 Knockout Mice as a Model for Chemical Carcinogenicity Studies:

The mouse model selected for this experiment was validated as a potentially useful model for this research by Brown et al.[4] In this work, they exposed p53 knockout male mice (B6.129S2-Trp53^{tm1Tyj}/J) to four doses of riddelliine, with groups consisting of 10 mice per dose group. Their control group of ten only had a single mouse that developed a round cell neoplasm. In this work, we had groups of fifty male mice per group. The control group had a total of 12 mice develop 12 different neoplasms. One of the control

mice developed a hemangiosarcoma of the liver. The incidence of neoplasia in the control group is the most likely reason for the lack of statistically significant differences in this study. Jack et al. (1996) reported that heterozygous p53 mutant mice mainly developed lymphomas, osteosarcomas, and soft tissue sarcomas with fewer lung adenocarcinomas, hemangiosarcomas, hepatomas, hair matrix tumors and brain tumors.[37] Therefore attempting to attribute any of these neoplasms to a test article is ill-advised. Further in vivo studies on carcinogenicity of PAs should consider using other strains of mice, without genetic alterations that increase the chance of neoplasia.

Conclusions:

In summary, this work indicates that a ten-day exposure by gastric gavage to 0.129 mmol/kg/day of senecionine, seneciphylline, and heliotrine, and 0.086 mmol/kg/day lasiocarpine is not carcinogenic in mice. This exposure mimics the type of exposure a livestock animal would be exposed to from a batch of contaminated hay. Human exposure from contaminated grain would be similar to the exposure method used in this study. Two-year, dose-dependent long-term carcinogenicity studies should be performed on these PAs to assess their carcinogenic potential during long-term exposure.

References:

1. National Toxicology Program. Toxicology and carcinogenesis studies of riddelliine (CAS No. 23246-96-0) in F344/N rats and B6C3F1 mice (gavage studies). *Natl Toxicol Program Tech Rep Ser* 1–280 (2003).

2. Chan, P. C., Haseman, J. K., Prejean, J. D. & Nyska, A. Toxicity and carcinogenicity of riddelliine in rats and mice. *Toxicology Letters* 144, 295–311 (2003).

3. Chan, P. C., Mahler, J., Bucher, J. R., Travlos, G. S. & Reid, J. B. Toxicity and carcinogenicity of riddelliine following 13 weeks of treatment to rats and mice. *Toxicon* 32, 891–908 (1994).

4. Brown, A. Relative Toxicity of Select Dehydropyrrolizidine Alkaloids and Evaluation of a Heterozygous P53 Knockout Mouse Model for Dehydropyrrolizidine Alkaloid Induced Carcinogenesis. *All Graduate Theses and Dissertations* (2015) doi:https://doi.org/10.26076/7997-d859.

5. Hirono, I., Mori, H. & Culvenor, C. C. Carcinogenic activity of coltsfoot, Tussilago farfara l. *Gan* 67, 125–129 (1976).

6. Hirono, I., Mori, H., Yamada, K., Hirata, Y. & Haga, M. Carcinogenic activity of petasitenine, a new pyrrolizidine alkaloid isolated from Petasites japonicus Maxim. *J Natl Cancer Inst* 58, 1155–1157 (1977).

7. Hirono, I., Ueno, I., Aiso, S., Yamaji, T. & Haga, M. Carcinogenic activity of Farfugium japonicum and Senecio cannabifolius. *Cancer Letters* 20, 191–198 (1983).

8. Kuhara, K., Takanashi, H., Hirono, I., Furuya, T. & Asada, Y. CArcinogenic activity of clivorine, a pyrrolizidine alkaloid isolated from Ligularia dentata. *Cancer Lett* 10, 117–122 (1980).

9. Stegelmeier, B. L., Colegate, S. M. & Brown, A. W. Dehydropyrrolizidine Alkaloid Toxicity, Cytotoxicity, and Carcinogenicity. *Toxins (Basel)* 8, 356 (2016).

10. Rao, M. S. & Reddy, J. K. Malignant neoplasms in rats fed lasiocarpine. *Br J Cancer* 37, 289–293 (1978).

11. Culvenor, C. C. J. *et al.* Hepato- and pneumotoxicity of pyrrolizidine alkaloids and derivatives in relation to molecular structure. *Chemico-Biological Interactions* 12, 299–324 (1976).

12. Huxtable, R. J. Activation and pulmonary toxicity of pyrrolizidine alkaloids. *Pharmacology & Therapeutics* 47, 371–389 (1990).

13. Song, Z., He, Y., Ma, J., Fu, P. P. & Lin, G. Pulmonary toxicity is a common phenomenon of toxic pyrrolizidine alkaloids. *Journal of Environmental Science and Health, Part C* 38, 124–140 (2020).

14. Phillips, D. H. & Arlt, V. M. Genotoxicity: damage to DNA and its consequences. *EXS* 99, 87–110 (2009).

15. Chen, T., Mei, N. & Fu, P. P. Genotoxicity of pyrrolizidine alkaloids. *J Appl Toxicol* 30, 183–196 (2010).

16. Fu, P. P., Xia, Q., Lin, G. & Chou, M. W. Genotoxic Pyrrolizidine Alkaloids — Mechanisms Leading to DNA Adduct Formation and Tumorigenicity. *International Journal of Molecular Sciences* 3, 948–964 (2002).

17. Hadi, N. S. A. *et al.* Genotoxicity of selected pyrrolizidine alkaloids in human hepatoma cell lines HepG2 and Huh6. *Mutat Res Genet Toxicol Environ Mutagen* 861–862, 503305 (2021).

18. Mei, N., Chou, M. W., Fu, P. P., Heflich, R. H. & Chen, T. Differential mutagenicity of riddelliine in liver endothelial and parenchymal cells of transgenic big blue rats. *Cancer Lett* 215, 151–158 (2004).

19. Chou, M. W. *et al.* Identification of DNA adducts derived from riddelliine, a carcinogenic pyrrolizidine alkaloid. *Chem Res Toxicol* 16, 1130–1137 (2003).

20. Mei, N., Heflich, R. H., Chou, M. W. & Chen, T. Mutations Induced by the Carcinogenic Pyrrolizidine Alkaloid Riddelliine in the Liver cII Gene of Transgenic Big Blue Rats. *Chem. Res. Toxicol.* 17, 814–818 (2004).

21. Allen, J. R., Hsu, I. C. & Carstens, L. A. Dehydroretronecine-induced rhabdomyosarcomas in rats. *Cancer Res* 35, 997–1002 (1975).

22. Johnson, W. D., Robertson, K. A., Pounds, J. G. & Allen, J. R. Dehydroretronecine-induced skin tumors in mice. *J Natl Cancer Inst* 61, 85–89 (1978).

23. Mattocks, A. R. & Cabral, J. R. P. Carcinogenicity of some pyrrolic pyrrolizidine alkaloid metabolites and analogues. *Cancer Letters* 17, 61–66 (1982).

24. Cook, J. W., Duffy, E. & Schoental, R. Primary Liver Tumours in Rats following Feeding with Alkaloids of Senecio jacobaea. *Br J Cancer* 4, 405-410.3 (1950).

25. Hirono, I., Mori, H. & Haga, M. Carcinogenic activity of Symphytum officinale. *J Natl Cancer Inst* 61, 865–869 (1978).

26. Harris, P. N. & Chen, K. K. Development of hepatic tumors in rats following ingestion of Senecio longilobus. *Cancer Res* 30, 2881–2886 (1970).

27. Hirono, I. *et al.* Induction of hepatic tumors in rats by senkirkine and symphytine. *J Natl Cancer Inst* 63, 469–472 (1979).

28. Chen, K. K., Harris, P. N. & Rose, C. L. The Action and Toxicity of Platyphylline and Seneciphylline. *J Pharmacol Exp Ther* 68, 130–140 (1940).

29. Wang, W. *et al.* Seneciphylline, a main pyrrolizidine alkaloid in Gynura japonica, induces hepatotoxicity in mice and primary hepatocytes via activating

mitochondria-mediated apoptosis. *Journal of Applied Toxicology* 40, 1534–1544 (2020).

30. Ghallab, A. Pyrrolizidine alkaloids act by toxicity to sinusoidal endothelial cells of the liver. *Arch Toxicol* 93, 3639–3640 (2019).
31. Hessel-Pras, S. *et al.* The pyrrolizidine alkaloid senecionine induces CYP-dependent destruction of sinusoidal endothelial cells and cholestasis in mice. *Arch Toxicol* 94, 219–229 (2020).
32. Chen, K. K., Harris, P. N. & Schulze, H. A. The Toxicity of Lasiocarpine. *J Pharmacol Exp Ther* 68, 123–129 (1940).
33. Svoboda, D. J. & Reddy, J. K. Malignant Tumors in Rats Given Lasiocarpine1. *Cancer Research* 32, 908–913 (1972).
34. Molyneux, R. J., Gardner, D. L., Colegate, S. M. & Edgar, J. A. Pyrrolizidine alkaloid toxicity in livestock: a paradigm for human poisoning? *Food Addit Contam Part A Chem Anal Control Expo Risk Assess* 28, 293–307 (2011).
35. Toxicology/Carcinogenicity. *National Toxicology Program* https://ntp.niehs.nih.gov/whatwestudy/testpgm/cartox.
36. Chhabra, R. S., Huff, J. E., Schwetz, B. S. & Selkirk, J. An Overview of Prechronic and Chronic Toxicity/Carcinogenicity Experimental Study Designs and Criteria Used by the National Toxicology Program. *Environmental Health Perspectives* 86, 313–321 (1990).
37. Jacks, T. *et al.* Tumor spectrum analysis in p53-mutant mice. *Curr Biol* 4, 1–7 (1994).

38. Stegelmeier, B. L. *et al.* Pyrrolizidine alkaloid plants, metabolism and toxicity. *J Nat Toxins* 8, 95–116 (1999).

39. Stegelmeier, B. L. Pyrrolizidine Alkaloid–Containing Toxic Plants (Senecio, Crotalaria, Cynoglossum, Amsinckia, Heliotropium, and Echium spp.). *Veterinary Clinics: Food Animal Practice* 27, 419–428 (2011).

40. Kakar, F. *et al.* An Outbreak of Hepatic Veno-Occlusive Disease in Western Afghanistan Associated with Exposure to Wheat Flour Contaminated with Pyrrolizidine Alkaloids. *J Toxicol* 2010, 313280 (2010).

41. Mohabbat, O. *et al.* AN OUTBREAK OF HEPATIC VENO-OCCLUSIVE DISEASE IN NORTH-WESTERN AFGHANISTAN. *The Lancet* 308, 269–271 (1976).

42. Tandon, B. N., Tandon, H. D., Tandon, R. K., Narndranathan, M. & Joshi, Y. K. An epidemic of veno-occlusive disease of liver in central India. *Lancet* 2, 271–272 (1976).

43. Letsyo, E., Jerz, G., Winterhalter, P. & Beuerle, T. Toxic pyrrolizidine alkaloids in herbal medicines commonly used in Ghana. *J Ethnopharmacol* 202, 154–161 (2017).

44. Bodi, D. *et al.* Determination of pyrrolizidine alkaloids in tea, herbal drugs and honey. *Food Addit Contam Part A Chem Anal Control Expo Risk Assess* 31, 1886–1895 (2014).

45. Protocol 37953 - Trp53<tm1Tyj>-Probe. https://www.jax.org/Protocol?stockNumber=002101&protocolID=37953.

46. Protocol 27521 - Trp53<tm1Tyj> Alternate2. https://www.jax.org/Protocol?stockNumber=002101&protocolID=27521.

47. Delidow, B. C., Lynch, J. P., Peluso, J. J. & White, B. A. Polymerase chain reaction : basic protocols. *Methods Mol Biol* 15, 1–29 (1993).

48. Culvenor, C., Edgar, J., Smith, L. & Tweeddale, H. Dihydropyrrolizines. III. Preparation and reactions of derivatives related to pyrrolizidine alkaloids. *Aust. J. Chem.* 23, 1853 (1970).

49. Thoolen, B. *et al.* Proliferative and Nonproliferative Lesions of the Rat and Mouse Hepatobiliary System. *Toxicol Pathol* 38, 5S-81S (2010).

50. Renne, R. *et al.* Proliferative and Nonproliferative Lesions of the Rat and Mouse Respiratory Tract. *Toxicol Pathol* 37, 5S-73S (2009).

51. Willard-Mack, C. L. *et al.* Nonproliferative and Proliferative Lesions of the Rat and Mouse Hematolymphoid System. *Toxicol Pathol* 47, 665–783 (2019).

52. Berridge, B. R. *et al.* Non-proliferative and Proliferative Lesions of the Cardiovascular System of the Rat and Mouse. *J Toxicol Pathol* 29, 1S-47S (2016).

53. Creasy, D. *et al.* Proliferative and Nonproliferative Lesions of the Rat and Mouse Male Reproductive System. *Toxicol Pathol* 40, 40S-121S (2012).

54. Frazier, K. S. *et al.* Proliferative and Nonproliferative Lesions of the Rat and Mouse Urinary System. *Toxicol Pathol* 40, 14S-86S (2012).

55. Research, C. for D. E. and. Statistical Aspects of the Design, Analysis, and Interpretation of Chronic Rodent Carcinogenicity Studies of Pharmaceuticals. *U.S. Food and Drug Administration* https://www.fda.gov/regulatory-information/search-

fda-guidance-documents/statistical-aspects-design-analysis-and-interpretation-chronic-rodent-carcinogenicity-studies (2021).

56. Bolker, B., Piaskowski, J., Tanaka, E., Alday, P. & Viechtbauer, W. CRAN Task View: Mixed, Multilevel, and Hierarchical Models in R. https://CRAN.R-project.org/view=MixedModels (2022).
57. Rahman, M. A. & Lin, K. K. A comparison of false positive rates of peto and poly-3 methods for long-term carcinogenicity data analysis using multiple comparison adjustment method suggested by Lin and Rahman. *J Biopharm Stat* 18, 949–958 (2008).
58. Babu, R., Venkatachalapathy, E. & Sai, V. Hydronephrosis severity score: an objective assessment of hydronephrosis severity in children-a preliminary report. *J Pediatr Urol* 15, 68.e1-68.e6 (2019).
59. Chan, P. NTP technical report on the toxicity studies of Riddelliine (CAS No. 23246-96-0) Administered by Gavage to F344 Rats and B6C3F1 Mice. *Toxic Rep Ser* 27, 1-D9 (1993).
60. Heterozygous p53 knockout mouse model for dehydropyrrolizidine alkaloid-induced carcinogenesis. *J Appl Toxicol* 35, 1557–1563 (2015).
61. He, Y., Zhu, L., Ma, J. & Lin, G. Metabolism-mediated cytotoxicity and genotoxicity of pyrrolizidine alkaloids. *Arch Toxicol* 95, 1917–1942 (2021).
62. Gebregziabher, M. & Hoel, D. Applications of the Poly-K Statistical Test to Life-Time Cancer Bioassay Studies. *Hum Ecol Risk Assess* 15, 858–875 (2009).

63. Schaarschmidt, F., Sill, M. & Hothorn, L. A. Poly-k-trend tests for survival adjusted analysis of tumor rates formulated as approximate multiple contrast test. *J Biopharm Stat* 18, 934–948 (2008).

64. Hothorn, L. A. & Hasler, M. The Dunnett procedure with possibly heterogeneous variances. Preprint at https://doi.org/10.48550/arXiv.2303.09222 (2023).

65. Ruebner, B. H., Watanabe, K. & Wand, J. S. Lytic necrosis resembling peliosis hepatis produced by lasiocarpine in the mouse liver. A light and electron microscopic study. *Am J Pathol* 60, 247–271 (1970).

66. Bruguera, M., Aranguibel, F., Ros, E. & Rodés, J. Incidence and clinical significance of sinusoidal dilatation in liver biopsies. *Gastroenterology* 75, 474–478 (1978).

67. BETTIO, D., VENCI, A., ACHILLE, V., ALLOISIO, M. & SANTORO, A. Lung cancer in which the hypothesis of multi-step progression is confirmed by array-CGH results: A case report. *Exp Ther Med* 11, 98–100 (2016).

68. Jackson, E. L. *et al.* The Differential Effects of Mutant p53 Alleles on Advanced Murine Lung Cancer. *Cancer Research* 65, 10280–10288 (2005).

69. Xu, R., Hu, J., Zhou, X. & Yang, Y. Heterotopic ossification: Mechanistic insights and clinical challenges. *Bone* 109, 134–142 (2018).

70. Xiao, Y.-T., Xiang, L.-X. & Shao, J.-Z. Bone morphogenetic protein. *Biochemical and Biophysical Research Communications* 362, 550–553 (2007).

71. Mantovani, G. *et al.* Pseudohypoparathyroidism and GNAS Epigenetic Defects: Clinical Evaluation of Albright Hereditary Osteodystrophy and Molecular Analysis

in 40 Patients. *The Journal of Clinical Endocrinology & Metabolism* 95, 651–658 (2010).

72. Happle, R. Progressive osseous heteroplasia is not a Mendelian trait but a type 2 segmental manifestation of GNAS inactivation disorders: A hypothesis. *Eur J Med Genet* 59, 290–294 (2016).
73. Gibson, C. J. & Poduri, K. R. Heterotopic ossification as a complication of toxic epidermal necrolysis. *Arch Phys Med Rehabil* 78, 774–776 (1997).
74. Dantas Cassali, G. *et al.* Canine Mammary Mixed Tumours: A Review. *Vet Med Int* 2012, 274608 (2012).
75. Saad, E. S. *et al.* Canine Mixed Mammary Tumour as a Model for Human Breast Cancer with Osseous Metaplasia. *J Comp Pathol* 156, 352–365 (2017).
76. Byard, R. W. & Thomas, M. J. Osseous metaplasia within tumours. A review of 11 cases. *Ann Pathol* 8, 64–66 (1988).
77. Xu, J. *et al.* Pyrrolizidine alkaloids: An update on their metabolism and hepatotoxicity mechanism. *Liver Research* 3, 176–184 (2019).
78. Zhu, L., Xue, J., Xia, Q., Fu, P. P. & Lin, G. The long persistence of pyrrolizidine alkaloid-derived DNA adducts in vivo: kinetic study following single and multiple exposures in male ICR mice. *Arch Toxicol* 91, 949–965 (2017).
79. Moreira, R., Pereira, D. M., Valentão, P. & Andrade, P. B. Pyrrolizidine Alkaloids: Chemistry, Pharmacology, Toxicology and Food Safety. *Int J Mol Sci* 19, 1668 (2018).

80. Xiao, R. *et al.* Monocrotaline pyrrole induces pulmonary endothelial damage through binding to and release from erythrocytes in lung during venous blood reoxygenation. *Am J Physiol Lung Cell Mol Physiol* 316, L798–L809 (2019).

81. Taylor, I. Chapter 4 - Mouse. in *Background Lesions in Laboratory Animals* (eds. McInnes, E. F. & Mann, P.) 45–72 (W.B. Saunders, 2012). doi:10.1016/B978-0-7020-3519-7.00004-8.

82. Klug, J. J. & Snyder, J. M. Eosinophilic crystalline pneumonia, an age-related lesion in mice. *Aging Pathobiol Ther* 2, 232–233 (2020).

83. Herrero, R. *et al.* Liver–lung interactions in acute respiratory distress syndrome. *Intensive Care Medicine Experimental* 8, 48 (2020).

CHAPTER IV COMPARISON OF DELAYED AND IMMEDIATE CHANGES IN HEPATIC GENE EXPRESSION FOLLOWING EXPOSURE TO THREE DEHYDROPYRROLIZIDINE ALKALOIDS, RIDDELLIINE, SENECIONINE AND HELIOTRINE, IN C57BL/6 MALE MICE.

Abstract:

Dehydropyrrolizidine alkaloids (PAs) are a large group of plant derived protoxins that frequently poison people and animals. Human exposure results either from purposeful ingestion of herbal products containing DHPAs, or from contamination of products such as grain, tea, honey, eggs, etc. Animal exposure occurs from contamination of feedstuffs or from grazing. After bioactivation by the cytochrome p450 enzymes, PA metabolites are hepatotoxic, pneumotoxic, genotoxic, cytotoxic, and carcinogenic. Fifteen C57BL6/j mice were exposed to 0.129 mmol/kg of riddelliine, senecionine, and heliotrine for eight days by oral gavage. Hepatic gene expression necropsy, histopathology, serum chemistries, and hepatic pyrrole concentrations were compared. Comparisons were made between compounds, as well as within compounds at two time points, immediately post-exposure and 28-days post-exposure. Five mice from each PA group were necropsied immediately after dosing and the remaining ten mice were necropsied 28-days after dosing. Hepatic gene expression was performed on all five mice from each PA in the immediate post-exposure group, and five of the ten mice from the 28-day post-exposure group. All other endpoints were performed on all mice. Senecionine and riddelliine exposure caused weight loss, while only senecionine-exposed mice exhibited malaise. Alanine aminotransferase, alkaline phosphatase, and aspartate aminotransferase were increased in mice exposed to riddelliine and senecionine immediately post-exposure.

After the recovery period, liver enzymes were not significantly different than the controls. Microscopic findings immediately after exposure included midzonal to panlobular hepatocyte enlargement with multifocal moderate to severe hepatic necrosis in senecionine-exposed mice. Riddelliine-exposed mice had hepatocellular hypertrophy in centrilobular areas with scattered individual cell degeneration and necrosis. After the recovery period, senecionine-exposed mice had occasional foci of hepatocellular necrosis, while riddelliine-exposed mice had no lesions. Heliotrine-exposed mice had no lesions at either time point. Mice exposed to senecionine and riddelliine had similar changes in gene expression. Senecionine exposure led to the greatest number of differentially expressed genes (DEGs; $Log_2FC > 1$, $FDR < 0.05$) with 3,006 DEGs immediately post-exposure and 341 DEGs after recovery, followed by riddelliine with 2,017 DEGs immediately post-exposure and 179 after recovery. Both senecionine and riddelliine affected genetic pathways related to metabolism and cancer development. Mice exposed to heliotrine had 112 DEGs immediately after exposure and 111 after recovery, and these genes were mostly unrelated to pathways expected to be involved in cell injury and neoplasia. Based on the similarity of gene expression effects to riddelliine, a known carcinogen, senecionine is most likely carcinogenic in mice.

Introduction:

Dehydropyrrolizidine alkaloids (PAs) are a large group of plant-derived protoxins that share a common chemical base. These toxins require metabolic activation by the cytochrome p450 enzymes. Following bioactivation, PAs are hepatotoxic, pneumotoxic, genotoxic and, under some circumstances carcinogenic. The liver has the greatest concentration of CYP450 enzymes, therefore is the main target organ.[1,2]. PAs are

composed of a necine base, and one or two side chains called necic acids. The necine base is composed of two five membered carbon rings with a single nitrogen at the center. PAs are classified as either platynecine, otonecine, retronecine or heliotridine based on the necine structures double bonds and steric conformation. Toxic PAs have a double bond between carbons 1 and 2, and fall into either the retronecine, otonecine or heliotridine categories. The necic acid side chains vary greatly and define the over 600 identified PAs. Based on the side chains, PAs can also be classified as either macrocyclic diesters, diesters or monoesters.[3,4] In this study, senecionine and riddelliine are retronecine macrocyclic diesters and heliotrine is a heliotridine monoester. Previous work has shown that senecionine and riddelliine are hepatotoxic and genotoxic.[5] Heliotrine on the other hand apparently has little to no effect on mice at doses similar to hepatotoxic doses of other PAs. Riddelliine is unique among PAs, as it is classified by the National Toxicology Program as a proven carcinogen in mice and rats, and a likely human carcinogen.[6] Senecionine has been proven genotoxic and there are some rodent studies demonstrating carcinogenicity, but more research is needed to determine whether senecionine is a carcinogen, and compare to other PAs especially riddelliine which is a known carcinogen.[7] The focus of this experiment was to determine the changes in gene expression in mice induced by ingestion of 3 PAs, riddelliine, senecionine and heliotrine.

Genotoxicity:

A genotoxin is an agent that has the ability to damage genetic material, or to cause DNA or chromosomal damage.[8–10] Chemical carcinogens are classified as either genotoxic or non-genotoxic. Genotoxic carcinogens induce neoplasia by causing mutations, whereas non-genotoxic carcinogens use other mechanisms such as hormonal effects, cytotoxicity,

cell proliferation, or epigenetic changes.[11] Mori et al. (1985) demonstrated genotoxicity in seventeen isolated PAs using the hepatocyte primary culture/DNA repair test. That study determined that PAs are genotoxic carcinogens.[12–14] Genotoxic carcinogens are thought to be a risk factor for cancer regardless of dose.[11] In other words, there is no safe exposure threshold and these substances should be avoided when possible. The ability of PAs to induce DNA damage has now been demonstrated in several studies using multiple methods of genotoxicity testing. In vivo and in vitro methods including ^{32}P-postlabeling with HPLC, in vivo covalent binding analysis using ^{3}H labeling, in vitro alkaline elution, in vitro cross-linking assays, and others have been used to characterize the types of DNA damage PAs can cause. PAs cause DNA damage via DNA adducts, DNA cross-linking, DNA strand breakage, and unscheduled DNA synthesis. Chromosomal damage caused by PAs has been proven using multiple in vivo and in vitro assays in multiple cell lines and in mouse tissues.[5] Chou et al. (2003) identified specific types of DNA adducts induced by PA exposure through the development and application of a ^{32}P-postlabeling/HPLC assay.[15,16] Yang et al. determined that exposure to dehydroretronecine, a common DHPA metabolite, leads to the formation two enantiomers of DHR-3'-dGMP and six other unidentified DNA adducts. A follow-up study by the same research group determined that the six unidentified DNA adducts were PA-modified dinucleotides. Guanine was determined as the nucleotide most likely to bind to the PA metabolites. PA metabolites have two functional groups, at the C7 and the C9 positions which can bind to DNA, resulting in DNA cross-linking. These groups can bind to cellular constituents including nucleic acids and proteins. This covalent binding is thought to be the mechanism by

which the anti-mitotic effects occur. These mechanisms are also though to contribute to the toxic and carcinogenic effects of PAs.[5]

Mutagenicity:

While genotoxicity encompasses mutagenicity, not all genotoxins are mutagenic.[10] The mutagenic potential of PAs was initially demonstrated by exposing *Drosophila melanogaster* to heliotrine.[17] Further studies using multiple PAs in *Drosophila melanogaster* demonstrated mutagenicity in some but not all PAs tested.[18] Mutagenicity was also proven in *Aspergillus nidulans*.[19] A variety of PAs were tested for mutagenicity using the Ames test, and the salmonella/mammalian microsome test.[20–22] These studies found that some PAs had the potential to induce mutations. Additionally, PAs only induced mutations in the presence of liver S9 fraction (the 9000*g* supernatent of a liver homogenate), which contains various phase I and phase II metabolism enzymes, including CYP450 enzymes necessary for bioactivation of PAs.[23] Mei et al. (2004) exposed female big blue Fisher transgenic rats to riddelliine and detected spontaneous mutations in the liver cII gene via DNA sequencing.[24] The same group exposed big blue rats to comfrey (*Symphytum officinal*e), a pyrrolizidine alkaloid containing plant. Comfrey induced a greater number of mutations when compared to riddelliine alone.[25] Comfrey has been touted as holistic cure for numerous ailments that is consumed as an herbal tea or remedy, and was banned for sale in the US in the early 2000's.[26] In addition to proving that PAs can be mutagenic, these studies demonstrated that PAs differ in their mutagenic potential. These differences indicate that PAs should be studied as individual toxins. Given the large number of documented PAs, many studies are needed.

Toxicogenomics in Dehydropyrrolizidine Alkaloid Research:

Gene expression profile analysis in toxicology (toxicogenomics) is an emerging method of evaluating mechanism of toxicity for chemical carcinogens.[27] Toxicogenomic studies are a useful tool for predicting toxic effects and determining safe exposure concentrations of phytotoxins such as PAs by detecting changes in gene expression that may precede phenotypic or morphologic changes.[28] Mei et al. (2007) exposed big blue fisher rats to riddelliine and comfrey root for 12 weeks and then used microarray analysis to compare gene expression. They observed a larger number of differentially expressed genes (DEGs) in comfrey exposed rats (1841) compared to riddelliine exposed rats (639 DEGs) with 273 DEGs in common. G:C → T:A transversion was the major mutation type. They also observed that both riddelliine and comfrey caused dysregulation of genes involved in metabolism, cancer, cell death, and others. This study concluded that comfrey and riddelliine likely use shared mechanisms to exert their hepatotoxic, genotoxic and carcinogenic effects.[29,30] Abdelfatah et al. (2022) performed transcriptomics on CYP3A4 transfected HepG2 cells after incubation with five PAs, one of which was riddelliine. They found dysregulation in pathways related to DNA damage and repair, and cell cycle regulation in all PAs tested, concluding that this may explain the carcinogenic effects of PAs. They also demonstrated that dysregulation of these pathways was concentration dependent, with monocrotaline requiring the greatest concentration, followed by riddelliine and lasiocarpine required the lowest to exert genotoxic effects.[31] Ebmeyer et al. (2020) exposed rats to doses ranging from 0.1-3.3 mg/kg of heliotrine, echimidine, lasiocarpine, senecionine, senkirkine, and platyphylline for 28 days. They found that dysregulation of genes associated with DNA damage response occurred in all PAs except

platyphylline.[32] Wang et al. (2022) exposed mice to a single dose of 50 mg/kg senecionine and then used proteomics to determine that gene ontology domains including cellular process, metabolic process, biological regulation, response to stimulus, and localization were affected. They noted that TSP1 and MMP9 were overexpressed. They attempted to relate this overexpression to the development of hepatic sinusoidal obstruction syndrome (HSOS).[33] Li et al. (2018) similarly used proteomics to demonstrate differential protein expression in rats following exposure to 140 mg/kg of retrorsine. They found dysregulation of seven proteins related to "VEGF signaling", "epithelial adherens junctions", and "cellular effects of sildenafil", which corresponded with hepatic sinusoidal endothelial cell damage.[34] Luckert et al. used whole genome transcriptome analysis to measure gene expression changes in human hepatocytes following exposure to four PAs, echimidine, heliotrine, senecionine, and senkirkine. They found that common pathways related to cell cycle regulation, cell death and cancer development were dysregulated.[35] In this study, gene expression analysis utilizing total RNA expression from the livers of C57BL6/j mice exposed to three PAs was performed. Gene expression results were interpreted alongside clinical findings, serum biochemical assays, and necropsy findings. Results are presented further in this chapter.

Carcinogenicity:

There are multiple reports characterizing and documenting the carcinogenic potential of PAs in mice and rats.[36–40,40–44] Riddelliine is the PA with the strongest evidence of carcinogenicity. A large study performed by the National Toxicology Program (NTP) determined that there was "clear evidence of carcinogenicity in mice and rats" and established riddelliine as "reasonably anticipated to be a human carcinogen".[6,45]

Riddelliine is frequently used in research as a model of a carcinogenic PA, as it was used in this study. In our previous chapter we exposed male heterozygous p53 knockout mice to riddelliine, senecionine, seneciphylline, lasiocarpine and heliotrine for ten days, and necropsied these mice one year later to compare the incidence of neoplasia between these PAs and a control group. The results of this experiment indicated that short-term exposure (ten days in this case) to various PAs may not be carcinogenic, as there was no significant difference between and of the PA groups and the vehicle control group. Notwithstanding the lack of statistical significance in this experiment using p53 knockout mouse, there is still a body of literature documenting carcinogenic effects of other PAs besides riddelliine in mice and rats to consider. Under certain conditions, PAs are generally considered to be carcinogenic.

Aims and Hypothesis:

The aims of this study are to characterize the immediate and delayed (28-days post-exposure) genetic, histopathologic, serum biochemical and clinical effects of short-term (eight day) exposure by gastric gavage of three different PAs, riddelliine, senecionine, and heliotrine, in male C57BL6/j mice. As it is likely that the mechanism of PA toxicity also results in carcinogenic effects, we hypothesize that riddelliine and senecionine will result in similar effects on hepatic gene expression and the other endpoints compared. It is expected that riddelliine and senecionine will cause changes in hepatic gene expression related to neoplastic development and xenobiotic metabolism. We also expect that heliotrine will differ from senecionine and riddelliine in its effects on these endpoints. Heliotrine is expected to have gene expression profiles similar to controls, reflecting heliotrine's lack of hepatotoxicity in mice.

Materials and Methods:

Animals:

Seven-week-old male C57BL/6J mice were purchased from Jackson laboratory's (Sacramento, CA). Mice were randomly placed into groups of fifteen, and randomly assigned to riddelliine, senecionine, heliotrine, or the control group. Mice were acclimated to the cage environment for at least 7 days prior to treatment. Mice were housed in groups of five in Innovive cages (Envigo, Livermore, CA) with Teklad ¼" corncob bedding The mouse facility has ambient light for 12 hours per day, and no ambient light overnight. Teklad Laboratory diet 8604 and water were provided ad libitum. Food and bedding were produced by Envigo (Livermore, CA). Temperature and humidity were maintained at 70 degrees Fahrenheit and 30% respectively. This research was conducted with the approval of the Utah State University animal care and use committee (IACUC Protocol #12439).

Purified Dehydropyrrolizidine Alkaloids:

Riddelliine, senecionine and heliotrine were obtained from the USDA ARS Poisonous Plant Research Laboratory's collection and were previously isolated from various plant collections. Purity of 98% or greater was confirmed using liquid chromatography mass spectrometry (LC-MS) and nuclear magnetic resonance (NMR).[46]

Experimental Design:

Mice were randomly divided into groups of 15. Each group was randomly assigned to riddelliine, senecionine, and heliotrine or the control group. Mice were exposed by oral

gavage to 0.129 mmol/kg/day of riddelliine, senecionine, or heliotrine. Doses of PA were measured using an Eppendorf Reference 100 ul pipette, then diluted in water to a total volume of 0.5 ml. The control group was exposed by gastric gavage to 1.37 mL/kg ethanol diluted in water to a total volume of 0.5 mL twice daily. Ethanol is the vehicle in which the PAs dissolved, and the ethanol dose for the control group was calculated to be an equal volume of ethanol to the riddelliine group. Daily doses of PA were divided in two and administered eight hours apart, twice daily for eight days. The dosing strategies used in this experiment were selected based on information obtained from a pilot study (see chapter 2). In the pilot study mice were exposed to various doses of the senecionine (2, 4, 8, 15, 30 and 45 mg/kg/day), riddelliine (4, 8, 15, 30, 45, and 90 mg/kg/day), and heliotrine (8, 15, 30 45, 90, and 180 mg/kg/day). The aim of the pilot studies was to find a common molar dose that induced hepatocellular hypertrophy/swelling, degeneration, and necrosis. Heliotrine is the exception to the dosing strategy, as mice in the heliotrine pilot study did not develop hepatic necrosis at doses as high as 0.574 mmol/kg/day (180 mg/kg/day). Following dosing mice were necropsied at two timepoints. The first group was necropsied the day after dosing, and the second group was necropsied 28 days later.

Weight Measurements:

Mice were weighed using an Adventurer SL AS1502 scale (Ohaus Corporation, Pine Brook, NJ, USA) every other day starting on day 1 of exposure during dosing, and every 1-4 days during the 28-day recovery period. Livers were weighed at the time of necropsy using the same scale. Total weight loss was calculated using necropsy body weight subtracted by the weight at day 1 of exposure.

Euthanasia and Necropsy:

Mice in the senecionine group had substantial weight loss (up to 32% or 7.6 g of bodyweight) necessitating reducing the exposure period was from the initially planned ten days to eight days. Eight of the senecionine-exposed mice (n=15) lost between 17.1% and 19.4% of their original body weight, 4 lost between 22.3% and 24.7%, and 3 lost between 25.2 and 32.3%.

Five mice from each exposure group and the control group were euthanized and necropsied on day 9, one day after the eight-day exposure period, and the remaining 10 mice (9 mice for the control group) were euthanized 28 days after the eight-day exposure period (day 37). The groups that were euthanized first, one day after dosing (day 9) will be referred to as the immediate post-exposure group and the group that was euthanized 28 days after exposure (day 37) will be referred to as the 28-day post exposure or delayed group. Mice from each exposure group were randomly selected for euthanasia via the list randomizer tool on random.org. During the 28-day post-exposure period, mice were monitored daily for clinical signs including malaise or inappetence. Clinical signs were not observed in any mice after dosing in the 28-day post exposure group, and no mice were euthanized early. Body weights were measured every 1-4 days and the percentage of weight loss was calculated. The liver from all five mice in each immediate post exposure groups and from five mice in the 28-days post-exposure groups were used RNA expression analysis. The five mice in the 28-days post-exposure groups on which liver RNA expression was performed were randomly selected. Other endpoints, including serum biochemistry, histopathology, and liver pyrrole detection by HPLC-MSMS, were performed on all mice in the study.

Necropsy Procedure:

Euthanasia was achieved using a CO2 chamber. Mice were necropsied immediately after euthanasia. Blood was collected in serum separator tube during necropsy via cardiac puncture of the right ventricle. Total blood volume collected ranged from 0.3-0.9 mL per mouse. The left liver lobe was collected and frozen for pyrrole quantification using high performance liquid chromatography and paired mass spectrometry (HPLC MSMS). The right liver lobe was divided in two, placed in 0.8-1 mL RNAlater solution, ensuring that the solution to tissue volume ratio was at least five to one. The remaining liver lobes and the brain, heart, trachea, lungs, thyroid glands, kidneys, urinary bladder, adrenal glands, esophagus, stomach, duodenum, jejunum, ileum, colon pancreas, and right testicle were placed in 10% neutral buffered formalin at room temperature. After formalin fixation, tissues were processed and embedded in paraffin according to routine histologic techniques. Sections, 5-µm thick, were stained with hematoxylin and eosin (H&E) stain according to standard methods and examined by light microscopy. Blood was centrifuged at 2500 rpm for 20 minutes using an Eppendorf 5810 centrifuge (Eppendorf, Hamburg, Germany). Serum chemistry panels with 20 assays were completed using a DiaSys respons910 vet (DiaSys Diagnostic Systems, USA, LLC, Wixom, Michigan) when sufficient serum allowed. In mice where serum volume was limited, priority was placed on assays evaluating liver enzymes, and liver function including alanine aminotransferase (ALT), aspartate aminotransferase (AST), alkaline phosphatase (ALP), total bilirubin (TBIL), albumin (ALB) and glucose (GLUC). Gross and microscopic lesions were recorded. Microscopic liver lesions were assigned a histologic grade for severity of

hepatocellular necrosis. Formalin-fixed liver was sectioned at 1-2 mm intervals and all tissues were evaluated and included in the hepatic necrosis score.

Hepatocellular Necrosis Scoring:

Microscopic grading of hepatocellular necrosis. A severity grade of minimal (1), mild (2), moderate (3), or severe (4) was applied based on the amount of necrosis. Hepatocellular necrosis was always accompanied by hepatocyte hypertrophy/swelling. If hepatocyte hypertrophy/swelling was observed without evidence of degeneration (vacuolation), and necrosis, a necrosis grade of zero was applied.

- Grade 0 = no microscopic evidence of hepatocellular degeneration and necrosis.
- Grade 1 = Minimal degeneration and necrosis is defined as infrequent (less than 5 cells per 10X field) scattered individual cell necrosis.
- Grade 2 = Mild degeneration and necrosis is defined as frequent individual cell necrosis (5 or more necrotic cells per 10X field) and rare groups (one or less per 10X field) of necrotic cells.
- Grade 3 = Moderate degeneration and necrosis is defined as frequent groups of necrotic hepatocytes amounting to less than 3 groups of necrotic cells per 10X field.
- Grade 4 = Severe necrosis is defined as groups of necrotic hepatocytes amounting to 3 or more groups per 10X field.

Hepatic Pyrrole Detection:

The toxic metabolite was detected in liver using high performance liquid chromatography and paired mass spectrometry (HPLC MS/MS). See Brown et al. (2015) for a complete description of this detection method.[47,48] Solvents and reagents were purchased from Sigma-Aldrich (St. Louis, MO). Ethanolic silver nitrate was prepared by combining via sonication, 625 mg silver nitrate, 0.5 mL deionized water and 25 mL absolute ethanol. Ehrlich's reagent was prepared by combining 0.2 g ρ-Dimethylaminobenzaldehyde (DMABA), 10 mL absolute ethanol, and 2 mL BF_3O.

Briefly, the left liver lobe was freeze-dried and pulverized into a powder using a Retsch MM301 ball mill (Haan, Germany), at a frequency of 20 revolutions per second, for 20 minutes with copper BBs. Approximately 50 mg. of pulverized freeze-dried liver was mixed with 1.0 mL ethanolic silver nitrate and 0.01 mL of 0.1% trifluoroacetic acid and mixed on an auto rotator overnight (approximately 16 hours). The mixture was then centrifuged at 13000 G for ten minutes. Twenty uL of the supernatant was then combined with 170 uL absolute ethanol, and ten uL Ehrlich's reagent. Finally, this mixture was analyzed using an Agilent HPLC-esi(+) and Velos Pro LTQ mass spectrometer (Agilent, Santa Clara, CA, USA). Quantification was achieved using an external calibration curve established from control standards. The calibration control standard was prepared using purchased monocrotaline (Sigma-Aldrich, St. Louis, MO), which was converted to dehydromonocrotaline.[48] Positive controls ran alongside samples included an experimentally poisoned horse and pig from the USDA PPRL collection. The resulting pyrrole concentration (nmol/mL) of sample was converted to nmol/g of liver.

RNA Extraction:

RNAlater solution was used to preserve the right liver lobe at the time of necropsy. RNA extraction was achieved using the RNeasy minikit (Qiagen, Hilden, Germany) following the manufacturer's directions. Thirty mg of liver was placed in Buffer RLT with β-Mercaptoethanol (lysis buffer) in an RNase free 1.0 mL eppendorf tube with a single 3 mm stainless steel bead. Tissue in lysis buffer was lysed on a Qiagen TissueLyser II, at a frequency of 20 Hz for 3 minutes. The lysate was then centrifuged at 15,000 RPM for 3 minutes, and then the solution was transferred to a new micro centrifuge tube. An equal volume of 70% ethanol was added to the solution, which was then centrifuged through a spin column at 10,000 RPM for 15 seconds and the flow through was discarded. Buffer RW1 was then added to the spin column, which was centrifuged at 10,000 RPM for 15 seconds and the flowthrough is discarded. DNase digestion was not performed. Buffer RPE was added to the spin column, which was centrifuged for 15 seconds at 10,000 RPM and the flowthrough is discarded. Buffer RPE was added again, and the spin column was centrifuged at 10,000 RPM for 2 minutes. 50 uL of RNAse-free water was then added to the spin column and centrifuged for 1 minute at 10,000 RPM, this step was repeated. RNA concentration and quality were analyzed using a NanoDrop Lite spectrophotometer (Thermofisher Scientific, Madison, WI) followed by TapeStation electrophoresis (Agilent Technologies, Santa Clara, CA). All samples had RNA integrity numbers (RIN) greater than or equal to 7. The samples were then stored at -80° C until RNA sequencing was performed. RNAlater was purchased from Thermofisher (Invitrogen, Thermofisher, Vilnus, Lithuania). The RNeasy minikit was purchased from Qiagen (Hilden, Germany).

RNA Sequencing:

After extraction from liver, total RNA was sequenced. The NEBnext Ultra II Directional Library Prep Kit from NEB was used for library preparation.[49,50] Sequencing was performed with the Illumina NextSeq 500 using the 75-cycle kit (Illumina inc., La Jolla, CA).[51]

RNA Expression Bioinformatics:

The samples undergo gene expression analysis by first aligning them to the reference genome and then analyze the expression of the genes to compare the differences among each group. FastQC (https://www.bioinformatics.babraham.ac.uk/projects/fastqc/) is a quality control analysis tool created to identify potential issues in high throughput sequencing datasets, and we utilized it for the initial quality check.[52] Then, using Trim Galore (https://www.bioinformatics.babraham.ac.uk/projects/trim_galore/), read trimming and adaptor removal was carried out.[53] The trimmed fastq reads were aligned with the reference genome using the STAR aligner. STAR (https://github.com/alexdobin/STAR) is an aligner designed to specifically address many of the challenges of RNA-Seq data mapping using a strategy to account for spliced alignments.[54] After the alignment step, we performed feature counts analysis for each sample by using FeatureCounts (http://subread.sourceforge.net/).[55] DESeq2 included in the pySeqRNA pipeline (https://bioinfo.usu.edu/pyseqrna/) was used to normalize the expression values across all samples.[56] Principal component analysis (PCA) was used to assess the clustering of normalized data using the expression levels of the top 50 most expressed genes. DESeq2 was used to perform differential gene expression analysis,

making pairwise comparisons of normalized read counts between treatments using a likelihood ratio test (LRT), for a total of 10 comparisons: 9C-9S, 9C-9R, 9C-9H, 37C-37H, 37C-37R, 37C-37S, 9H-37H, 9R-37R, 9S-37S, 9C-37C. The LRTs' *p*-values were modified using the false discovery rate (FDR). A gene is said to be differentially expressed (DEG) when its FDR in a treatment comparison was lower than 0.05. Venn diagrams were obtained using pySeqRNA to see if the overlapping number of DEGs between different DEG sets was statistically greater than expected. Further, the gene ontology (GO) terms associated with each gene identifier were identified. The genes expressed in the experiment were utilized to create a GO term and GO term enrichment analysis was performed for the biological process, molecular function, and cellular component ontologies for the up-regulated and down-regulated DEG sets. If the weighted Fisher's exact test *p*-value was less than 0.05, the GO term was declared enriched.

Randomization of Animals:

RANDOM.ORG was used to randomize groups of mice whenever randomization was possible Mice were housed in groups of five. Housing groups were randomly selected prior to microchipping. Groups of 15 for riddelliine, senecionine, heliotrine or the control were randomly assigned to a compound.

Statistical Analysis:

Bioinformatics analysis is performed using DESeq2 version: 1.34.0 by the department of bioinformatics at Utah State University.[56] Statistical analysis of serum biochemistries, liver pyrroles, hepatic necrosis scores, and liver and body weights was performed using GraphPad prism version 9.3.1 (GraphPad Software, Boston, MA, USA). Serum

biochemistry values, hepatic pyrrole concentrations, and weight data were compared to the control values using ordinary one-way analysis of variance (ANOVA) tests. Post-hoc comparison between PAs was achieved using individual t-tests. Kruskal-Wallis and Mann-Whitney tests were used to compare average hepatic necrosis scores between compound groups and the control group. Pearson correlation was also used to determine the strength of correlation between hepatic necrosis scores and serum biochemistry values or hepatic pyrrole concentrations. A students t-test was used to compare weights of the control groups to the vehicle groups. One way ANOVA was used to compare mean weight loss and liver weight to body weight ratios of all compounds of the same dose.[57]

Results:

Clinical Signs:

Body Weights:

Weight loss was observed in all compound groups and the control group during dosing. Weight loss during dosing is calculated for all mice, meaning the immediate post-exposure and 28-day post exposure groups are combined. Body weights are discussed for each group separately in the paragraphs below. No additional clinical signs were observed. The means of the initial body weights prior to exposure were only significantly different between the control group (mean = 22.35 g.) and the heliotrine group (mean = 23.55 g.) ($p \leq 0.05$). The mean starting body weights for the senecionine group was 22.63 g. and 22.66 g. for riddelliine.

Control animals exposed to the vehicle lost a small amount of weight during dosing (mean weight loss = 0.44 ± 0.54 g.). Weight loss during dosing is calculated by subtracting the weight on day eight from the weight on day zero the (day before dosing was started). Weight loss was calculated by subtracting the weight on day eight or the weight on day 37 from the weight on day zero (day before dosing was started). Weight loss during dosing for each compound group was significantly different than the control group ($p \leq 0.05$). Mice exposed to senecionine lost the greatest amount of weight (mean weight loss = 4.95 ± 1.05 g), followed by riddelliine (mean weight loss= 2.67 ± 0.65 g) and the smallest amount of weight lost was in the heliotrine (mean weight loss = 1.13 ± 0.4 g.) group. Weight loss in the senecionine group became unacceptable, with one mouse losing 32.3% of its original body weight, and two others losing over 25% of their body weight. Because of concern for welfare, survival and sample loss, the decision was made to shorten the dosing period from the initially planned ten days to eight days. After dosing was completed, body weights were monitored for animals that were not euthanized the day after exposure ended (day 9). Each compound group ceased losing weight following dosing and eventually gained weight (see figure 2, 28-day post-exposure weights).

Immediate Post-Exposure Body Weights:

Weight change during dosing for the entire group was calculated differently because necropsy body weights were only available for the five randomly selected mice from each group. Necropsy body weights are more accurate due to lack of movement while on the scale. Weight loss in the immediate post-exposure group was calculated by

subtracting the weight taken at necropsy (after euthanasia) from the weight taken on day zero (the day before dosing was started).

Weight loss in the immediate post-exposure groups were statistically significant for senecionine and riddelliine, compared to the control group ($p \leq 0.05$), but not for heliotrine. Senecionine caused the greatest amount of weight loss (mean weight loss = 5.77 ± 1.403), followed by riddelliine (mean weight loss = 2.53 ± 0.76) and last was heliotrine (mean weight loss = 0.96 ± 0.29).

28-Day Post-Exposure Body Weights:

Weight gains in the 28-day post-exposure groups were significantly different for senecionine and riddelliine compared to the control group ($p \leq 0.05$), but not for heliotrine. Mice exposed to riddelliine gained the smallest amount of weight (mean weight gain= 0.91 ± 0.44 g.), followed by senecionine (mean weight gain = 0.95 ± 0.82 g.), and the means of these two groups were not significantly different. Mice exposed to heliotrine gained the most weight (mean weight gain = 2.1 ± 0.74g.), and control mice gained the second most (mean weight gain =1.86 ± 0.3).

Table 4.1. Average weight loss/gain data for all groups. Average liver weights are also listed (Mean weight ± standard deviation).

Group	Control (vehicle)	Senecionine	Riddelliine	Heliotrine
Mean weight loss during dosing, all mice (g.) ± SD	0.44 ± 0.54	4.95 ± 1.05	2.67 ± 0.65	1.13 ± 0.4
Weight loss in immediate	0.31 ± 0.51	5.77 ± 1.4	2.53 ± 0.76	0.96 ± 0.29[a]

post-exposure group (g.) (day 0 weight – necropsy weight) ± SD				
Immediate post-exposure group mean liver weights (g.)	1.02 ± 0.04	1.22 ± 0.16	1.5 ± 0.06	0.95 ± 0.09 [a]
28-day post-exposure group mean liver weights (g.) ± SD	1.29 ± 0.11	1.24 ± 0.1	1.19 ± 0.08	1.3 ± 0.15
Mean weight gain in long term group (necropsy weight – day 0 weight) g. ± SD	1.86 ± 0.3	0.95 ± 0.82	0.91 ± 0.44	2.1 ± 0.74 [a]
Mean liver to BW ratios in short term group	0.046 ± 0.001	0.073 ± 0.006	0.074 ± 0.004	0.044 ± 0.003 [a]
Mean liver to BW ratios in 28-day post-exposure group	0.053 ± 0.003	0.052 ± 0.002 [a]	0.051 ± 0.003 [a]	0.050 ± 0.006 [a]

Abbreviations: SD = standard deviation. BW = body weight.

a) Not significantly different than the control group mean.

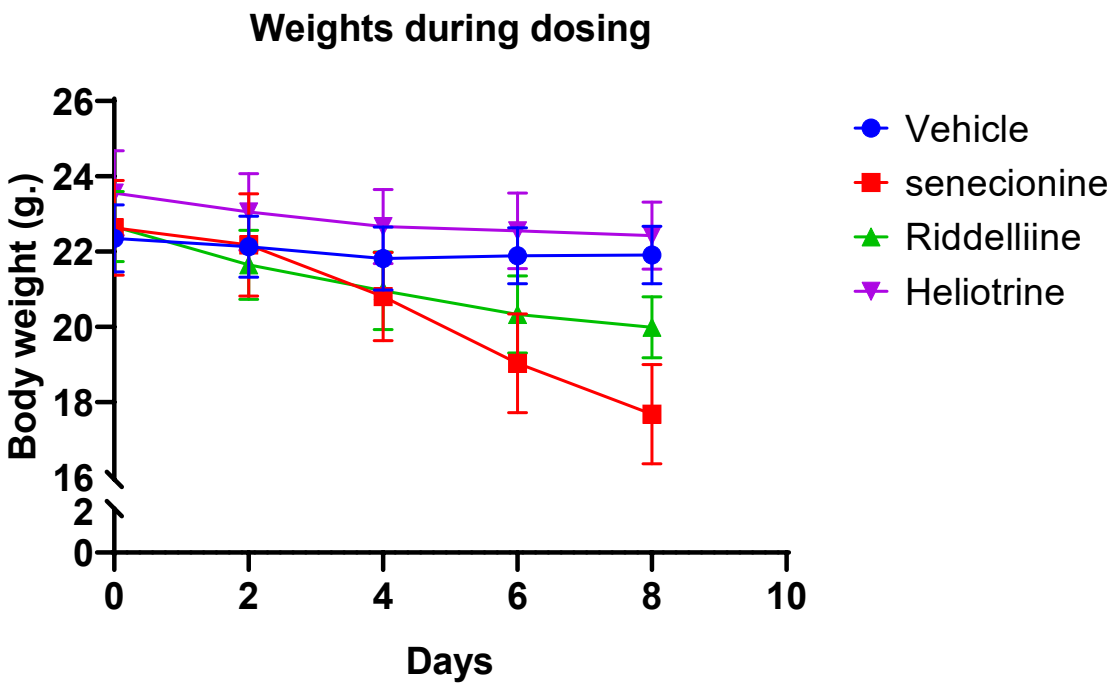

Figure 4.1. Average body weights by compound during dosing. There is a negative slope for each group. Control mice were exposed to the vehicle by oral gavage. Mice exposed to senecionine lost the most weight, followed by riddelliine and then heliotrine caused the smallest amount of weight loss.

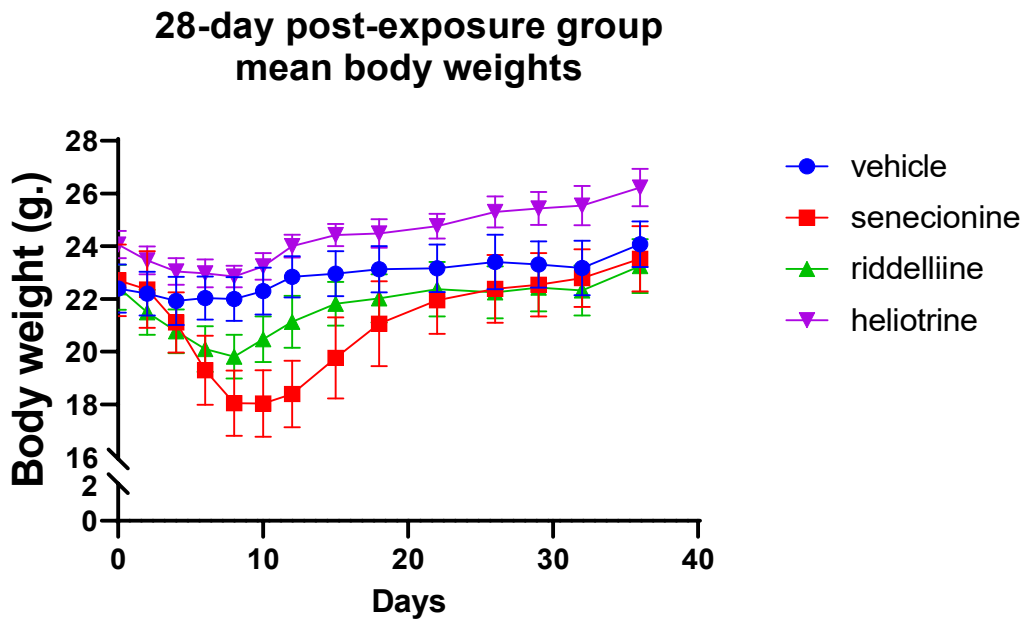

Figure 4.2. Average body weights in 28-day post exposure groups. The period with negative slopes for all groups is the dosing period. When the dosing period ended, weight loss ceased, and all groups eventually gained weight.

Liver Weights:

Comparison of liver weights is a valid metric because these mice were age matched to within 1-2 days. Additionally, mice were randomly placed into their compound groups, and then randomly selected for immediately post-exposure euthanasia (day 9), or 28-day-post-exposure euthanasia (day 37). Comparison of body weights on day 0, the day before dosing was started found the only significant difference between group mean body weights was between the control group (mean starting weight = 22.35 g.), and the heliotrine group (mean starting weight = 23.55 g.) ($p \leq 0.05$).

Mean liver weights can be seen in table 1. Regarding the immediate post-exposure group, the riddelliine and senecionine groups had liver weights that were significantly different than the control group ($p \leq 0.05$). The riddelliine group had the largest average liver weight (1.5 ± 0.06 g), followed by senecionine (1.22 ± 0.16 g.), the vehicle control group (1.02 ± 0.04 g.), and last was heliotrine (0.95 ± 0.09 g.). There were no statistically significant differences between liver weights or liver to body weight ratios in all four 28-day post-exposure compound groups.

Liver to Body Weight Ratios:

Liver to body weight ratios can be seen in table 4.1. At the immediate post-exposure time point, significant differences in liver to body weight ratio were detected between the control group and the senecionine and riddelliine groups ($p<0.0001$), but not heliotrine. Riddelliine-exposed mice had the greatest liver to body weight ratios with a mean of 0.074 ± 0.004. Senecionine-exposed mice were in close second with a mean liver to body weight ratio of 0.073 ± 0.006. Heliotrine-exposed mice had the lowest mean liver to body weight ratios at 0.044 ± 0.003. Senecionine and riddelliine were not significantly different in liver to body weight ratio.

At the 28-day-post-exposure time-point, liver to body weight ratios were not significantly different than the control group for any PA.

Serum Biochemistry Data:

When serum biochemistry assays are referred to as “increased” or “decreased”, this refers to analysis of variance comparisons to the control group. Significantly increased or

decreased values are in comparison to the control group. Significantly different values have a p-value less than or equal to 0.05.

Immediate post-exposure Serum Biochemistry Data:

Mean albumin concentration was significantly decreased ($p \leq 0.05$) for mice exposed to senecionine and riddelliine in the immediate post-exposure groups. Mean glucose concentration was significantly decreased for the senecionine and riddelliine groups. Mean cholesterol concentration was significantly increased for senecionine exposed mice, but this assay was only measured in two out of five of the senecionine-exposed mice because of limited serum volumes.

One mouse in the short term senecionine group had severely elevated concentrations of total bilirubin (7.5 mg/dL) and ALP (1178 U/L). While these are considered valid results for this mouse, they were classified as outliers using the robust outlier (ROUT) method and thus removed from statistical analysis. After removing the outliers, mean total bilirubin and ALP were significantly increased in the riddelliine and senecionine groups. Mean ALT was significantly increased for mice exposed to senecionine and riddelliine. Mean ALT was greatest for senecionine exposed mice, nearly doubling that of riddelliine. Mean AST concentration was significantly increased for mice exposed to senecionine. See table 2 for mean serum concentrations in the immediate post-exposure (day 9) group. Because of limited serum volume in the immediate post-exposure senecionine group, AST was only measured in three mice; total protein, globulin, albumin, phosphorous, calcium, cholesterol, potassium, and sodium were only measured in two of five mice; and chloride was only measured in one mouse. In the control group, total protein, globulin, phosphorous, calcium, magnesium,

cholesterol, chloride, potassium, and sodium were only measured for three out of five mice.

28-day post-exposure Serum Biochemistry Data:

Mean total protein and albumin were significantly increased in the heliotrine exposed group. Mean BUN was significantly decreased for the senecionine and heliotrine groups. Mean cholesterol was significantly decreased for the riddelliine group. Mean ALP and ALT were significantly different than the control group for senecionine exposed mice, but not for riddelliine and heliotrine. Mean sodium was significantly decreased for the heliotrine group. See table 3 for mean serum concentrations in the 28-day post-exposure group. In the 28-day post-exposure group there were nine control animals and ten mice for each compound group. One control mouse died during dosing. Because of limited serum volume some mice had fewer analytes available. In the 28-day post-exposure senecionine group (n=10), globulin, calcium, magnesium, chloride, and sodium were measured in six mice; total protein, phosphorous, cholesterol, and potassium were measured in seven mice; albumin, and BUN were measured in eight mice; and total bilirubin, and AST were measured in nine mice. For 28-day post-exposure riddelliine (n=10), total protein, globulin, phosphorous, calcium, magnesium, cholesterol, chloride, potassium, and sodium were measured in six mice. For the 28-day post-exposure heliotrine group (n=10) magnesium and chloride were measured in six mice; total protein, globulin, albumin, phosphorous, calcium, cholesterol, potassium, and sodium were measured in seven mice.

Table 4.2. Immediate post-exposure serum biochemistry data. Mean concentration ± standard deviations are listed. Values that are not significantly different than the control are marked with an asterisk.

Analyte	Vehicle Control (n=5)	Senecionine (n=5)	Riddelliine (n=5)	Heliotrine (n=5)
Total protein (g/dL)	5.8 ± 0.2	5.15 ± 0.07	5.54 ± 0.27[a]	5.98 ± 0.08[a]
Albumin (g/dL)	3.88 ± 0.08	3.02 ± 0.11	3.48 ± 0.08	3.8 ± 0.1[a]
Globulin (g/dL)	1.93 ± 0.15	2.15 ± 0.07[a]	2.06 ± 0.23[a]	2.18 ± 0.13[a]
Total Bilirubin (mg/dL)	0.14 ± 0.14	0.56 ± 0.15	0.3 ± 0.07	0.22 ± 0.04[a]
Blood Urea Nitrogen (mg/dL)	27.0 ± 1	26.0 ± 2.45[a]	25.4 ± 3.65[a]	27.8 ± 5.12[a]
Glucose (mg/dL)	372.6 ± 40.5	147.4 ± 51.99	251.8 ± 59.03	363.6 ± 75.2[a]
Phosphorous (mg/dL)	11.37 ± 1.35	10.25 ± 1.06[a]	10.6 ± 0.69[a]	10.84 ± 1.1[a]
Calcium (mg/dL)	11.3 ± 0.26	10.75 ± 0.35[a]	10.86 ± 0.438[a]	10.72 ± 0.36[a]
Magnesium (mg/dL)	4.0 ± 0.46	4.2 ± 0.14[a]	4.0 ± 0.45[a]	3.6 ± 0.2[a]
Cholesterol (mg/dL)	94.0 ± 18.73	282.5 ± 57.28	96.2 ± 11.19[a]	75.6 ± 5.9[a]
Alkaline Phosphatase (U/L)	105.0 ± 34.76	430.3 ± 31.44	289.0 ± 52.71	138.6 ± 28.87[a]
Alanine aminotransferase (U/L)	30.8 ± 10.52	1415 ± 226.8	715.0 ± 119.3	25.6 ± 4.83[a]
Aspartate aminotransferase (U/L)	263 ± 212.9	1693 ± 473.6	522.4 ± 151.3[a]	202.8 ± 81[a]
Chloride (mmol/L)	117.7 ± 2.52	124.0[a]	122.2 ± 2.59[a]	120.6 ± 5.46[a]
Potassium (mmol/L)	8.33 ± 0.65	10.35 ± 2.62[a]	9.320 ± 1.98[a]	9.740 ± 1.89[a]
Sodium (mmol/L)	145.0 ± 2.65	141.0 ± 1.41[a]	148.6 ± 2.97[a]	149.8 ± 3.96[a]

b) Not statistically different than the control group mean.

Table 4.3. Long term serum biochemistry data. Mean values ± standard deviations are listed. Values that are not significantly different than the control are marked with an asterisk.

Analyte	Vehicle Control (n=10)	Senecionine (n=10)	Riddelliine (n=10)	Heliotrine (n=10)
Total protein (g/dL)	6.09 ± 0.18	*5.87 ± 0.19 [a]	*5.8 ± 0.18 [a]	5.73 ± 0.35
Albumin (g/dL)	3.81 ± 0.09	*3.75 ± 0.22 [a]	*3.69 ± 0.1 [a]	3.56 ± 0.16
Globulin (g/dL)	2.28 ± 0.14	*2.18 ± 0.08 [a]	*2.13 ± 0.18[a]	*2.23 ± 0.21 [a]
Total Bilirubin (mg/dL)	0.14 ± 0.09	*0.22 ± 0.07 [a]	*0.18 ± 0.06[a]	*0.18 ± 0.1[a]
Blood Urea Nitrogen (mg/dL)	34.89 ± 1.9	31.75 ± 2.19	32.5 ± 2.92[a]	31.2 ± 2.57
Glucose (mg/dL)	236.4 ± 21.84	193.9 ± 35.77[a]	218.9 ± 35.66[a]	245.1 ± 50.22[a]
Phosphorous (mg/dL)	11.42 ± 0.82	11.3 ± 0.78[a]	10.7 ± 0.38[a]	10.77 ± 0.65[a]
Calcium (mg/dL)	10.98 ± 0.37	11.3 ± 0.39[a]	11.25 ± 0.45[a]	11.17 ± 0.35[a]
Magnesium (mg/dL)	4.16 ± 0.16	4.22 ± 0.16[a]	3.92 ± 0.23[a]	3.85 ± 0.36[a]
Cholesterol (mg/dL)	97.33 ± 6.75	86.29 ± 7.83[a]	82.67 ± 7.71	85.14 ± 12.99
Alkaline Phosphatase (U/L)	152.4 ± 27.12	199.0 ± 54.98	157.6 ± 14.54[a]	132.3 ± 22.31[a]
Alanine aminotransferase (U/L)	45.56 ± 12.01	142.4 ± 105.5	59.2 ± 14.56[a]	45.1 ± 11.77[a]

Aspartate aminotransferase (U/L)	228.0 ± 113.3	493.1 ± 324.8[a]	436.9 ± 304.3[a]	359.8 ± 269.5[a]
Chloride (mmol/L)	118.2 ± 3.27	115.5 ± 3.94[a]	117.0 ± 5.1[a]	116.5 ± 3.67[a]
Potassium (mmol/L)	7.69 ± 0.61	7.4 ± 0.72[a]	7.17 ± 0.45[a]	8.43 ± 1.33[a]
Sodium (mmol/L)	151.1 ± 2.89	151.2 ± 3.125[a]	152.5 ± 2.88[a]	145.3 ± 3.04

a) Not statistically different than the control group mean.

Spearman Correlations Between Hepatic Necrosis Scores and Serum Biochemistry Analytes in the Immediate Post-Exposure Group:

In the immediate post-exposure group, there were strong positive correlations between hepatic necrosis score and ALP, ALT, AST, and total bilirubin ($p < 0.0001$), and a moderate positive correlation between necrosis score and cholesterol ($p = 0.02$). Strong negative correlations were present between hepatic necrosis score and albumin and glucose ($p < 0.0001$). In the 28-day post-exposure group correlations between serum biochemistry values and hepatic necrosis score were weak or non-existent.[58]

Table 4.4. Spearman correlation of serum biochemistry concentrations with hepatic necrosis score for immediate post-exposure group.

	ALP	ALT	AST	T. Bili	Albumin	Glucose	Cholesterol
R	0.93	0.91	0.82	0.85	-0.93	-0.88	0.60
95% CI	0.8197 to 0.9724	0.7732 to 0.9666	0.5657 to 0.9333	0.6405 to 0.9434	-0.9712 to -0.8122	-0.9535 to -0.7115	0.1103 to 0.8554
P value (two tailed)	<0.0001	<0.0001	<0.0001	<0.0001	<0.0001	<0.0001	0.02

Abbreviations: ALP = alkaline phosphatase, ALT = alanine aminotransferase, AST = aspartate aminotransferase, T. Bili = total bilirubin, CI = confidence interval.

Spearman Correlations Between Hepatic Necrosis Scores and Serum Biochemistry Analytes in the 28-Day Post-Exposure Group: In the 28-day post-exposure groups, there were moderate positive correlations between hepatic necrosis score and ALP and ALT ($p < 0.0001$). Other correlations were not statistically significant.[58]

Table 5: Spearman correlation of serum biochemistry concentrations with hepatic necrosis score for 28-day post-exposure group

Table 4.5. Spearman correlation of serum biochemistry concentrations with hepatic necrosis score for 28-day post-exposure group.

	ALP	ALT	AST	T. Bili	Albumin	Glucose	Cholesterol
R	0.5532	0.6379	0.2353	0.1784	0.3092	-0.2105	0.1529
95% CI	0.2790 to 0.7439	0.3955 to 0.7972	-0.1010 to 0.5233	-0.1593 to 0.4788	-0.02643 to 0.5821	-0.5041 to 0.1267	-0.2370 to 0.5004
P value (two tailed)	0.0003	<0.0001	0.1551	0.2838	0.0626	0.2045	0.4284

Abbreviations: ALP = alkaline phosphatase, ALT = alanine aminotransferase, AST = aspartate aminotransferase, T. Bili = total bilirubin, CI = confidence interval.

Necropsy Findings:

Gross Lesions:

No gross lesions were observed in the vehicle control group, the riddelliine group or the heliotrine group immediately or 28-days post-exposure. In the immediate post-exposure group one out of five senecionine-exposed mouse had disseminated pinpoint white foci throughout all liver lobes, and three mice were emaciated.

Microscopic Findings

Immediate Post-Exposure Senecionine Group Microscopic Description:

Four out of five mice exposed to senecionine developed hepatocellular hypertrophy or cell swelling mainly in midzonal areas. The other senecionine-exposed mouse developed panlobular hepatocellular hypertrophy or cell swelling. Within areas of hepatocyte hypertrophy and swelling there was a combination of vacuolar degeneration and individual cell necrosis and groups of contiguous hepatocytes affected by coagulative necrosis. Individual cell necrosis was characterized by cellular enlargement or shrinkage, hypereosinophilic cytoplasm, and nuclear pyknosis or karyolysis. Foci of coagulative necrosis had pale eosinophilic cytoplasm, pale eosinophilic nuclei, but maintained cell borders and somewhat normal tissue architecture. Low to moderate numbers of neutrophils sometimes infiltrated areas of coagulative necrosis. See figure 4.3 for photomicrographs of the livers of senecionine-exposed mice.

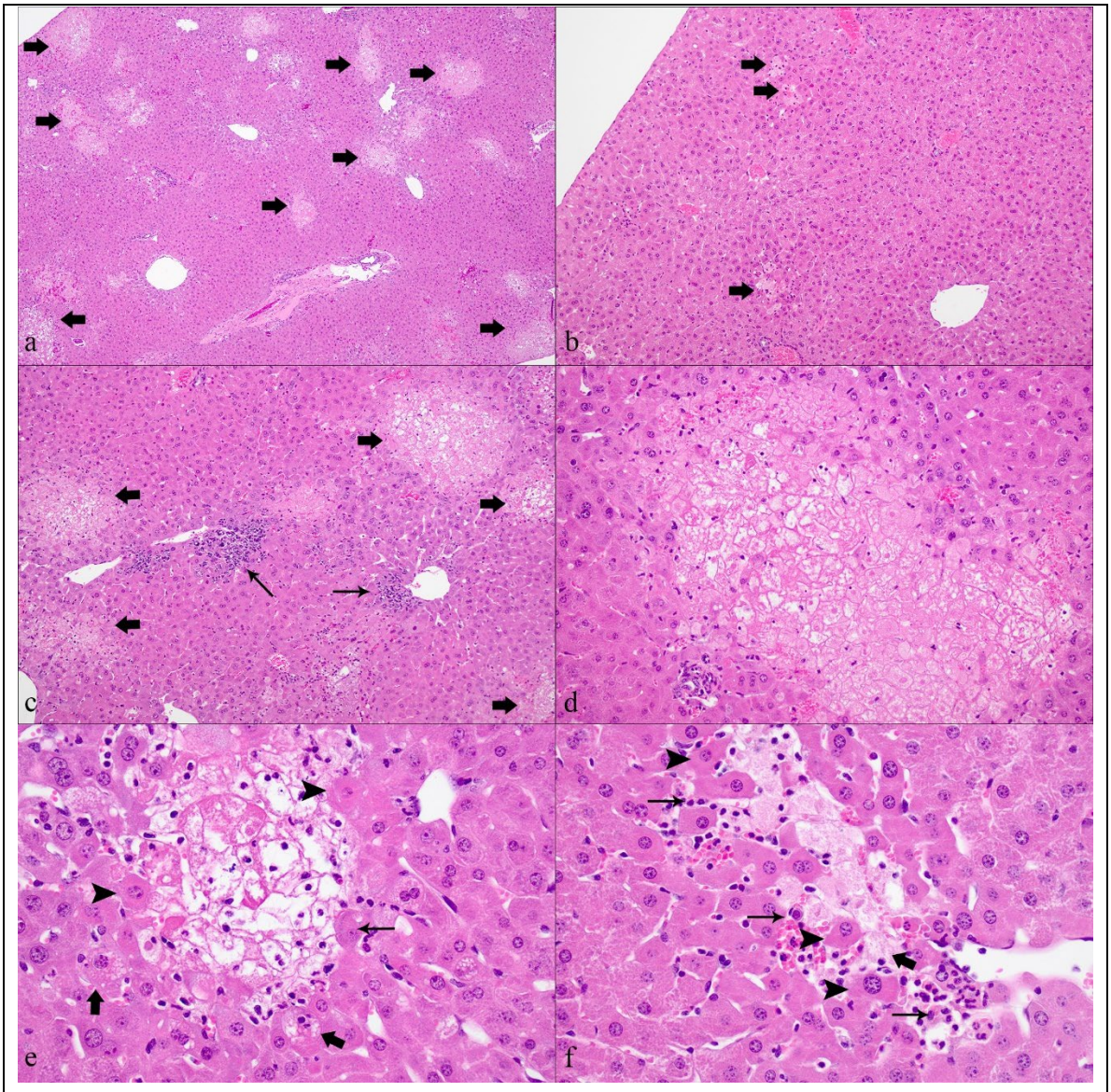

Figure 4.3 Images a-f: Liver from mice exposed to 0.137 mmol/kg/day senecionine for eight days and euthanized one day later. Hematoxylin and eosin.Image (a). Severe hepatic necrosis characterized by frequent randomly distributed areas of coagulative necrosis (arrows). Image (b). Multifocal areas of coagulative necrosis (arrows) are randomly distributed throughout the liver. Image (c). Multifocal random areas of coagulative necrosis affect up to 25% of the liver. There are basophilic areas in which contiguous hepatocytes undergo dystrophic mineralization (thin arrows). Image (d). Large area of coagulative necrosis. Hepatocytes maintain cellular architecture but have lost cytoplasmic and nuclear detail and coloration. Image (e). The center of the image is an area of coagulative necrosis. Hepatocytes adjacent to the area of necrosis have

hypereosinophilic cytoplasm (arrowheads), basophilic cytoplasmic stippling (thin arrow) or clear cytoplasmic vacuoles (arrows), characteristic of hepatocellular degeneration and necrosis. A few neutrophils infiltrate the periphery of this focus of hepatocellular necrosis. Image (f). Hepatocytes are focally replaced by cellular debris (lytic necrosis) (arrows). Adjacent hepatocytes have hypereosinophilic cytoplasm (arrowheads). Neutrophils infiltrate this focus of hepatocellular necrosis (thin arrows).

Immediate Post-Exposure Riddelliine Group:

Mice exposed to riddelliine developed hepatocellular hypertrophy and/or cell swelling affecting mainly centrilobular areas. Within areas of hepatocellular hypertrophy and/or cell swelling scattered individual hepatocytes were enlarged, hypereosinophilic and had pale or absent nuclei or shrunken with hypereosinophilic cytoplasm and nuclear pyknosis (individual cell necrosis) in all five mice. Occasional hepatocytes within areas of hypertrophy and/or swelling had multiple variably sized clear cytoplasmic vacuoles (vacuolar degeneration). One of the riddelliine-exposed mice had rare foci (0-1 per 10X field) of coagulative necrosis. See figure 4.4 for photo micrographs of the livers of riddelliine-exposed mice.

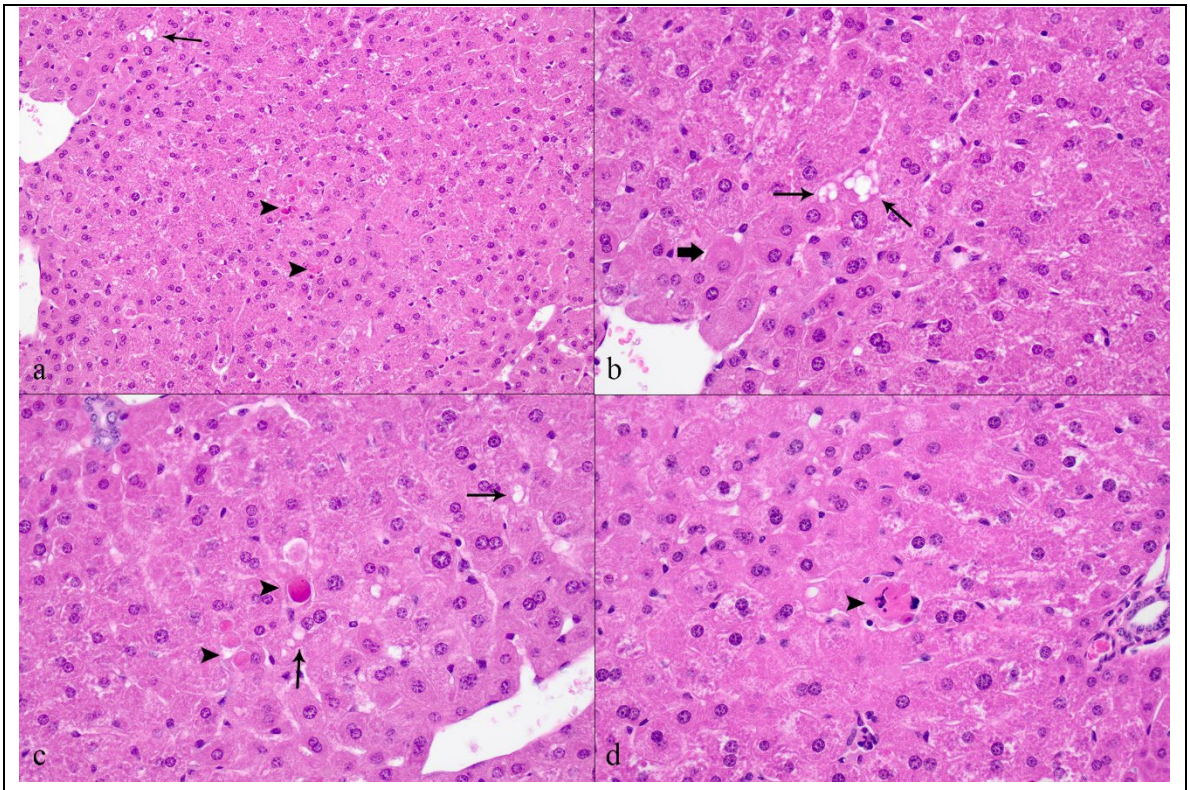

Figure 4.4. images a-d. Livers of mice exposed to 0.137 mmol/kg/day riddelliine for eight days and euthanized one day later. Hematoxylin and eosin. Image (a). Multifocal individual hepatocytes or small groups of contiguous hepatocytes undergo necrosis (arrowheads). Some hepatocytes have multiple clear cytoplasmic vacuoles (vacuolar degeneration) (thin arrow). Image (b). Hepatocytes have hypereosinophilic cytoplasm (arrow) or vacuolar degeneration (thin arrows) multifocally. Image (c). Individual hepatocytes undergo necrosis (arrowheads) Multifocally. Multiple hepatocytes are affected by vacuolar degeneration (thin arrows). Image (d). Individual hepatocytes undergo necrosis (arrowhead).

Immediate Post-Exposure Heliotrine Group:

Mice exposed to heliotrine did not develop lesions in the liver. The microscopic appearance of the livers of heliotrine-exposed mice was identical to the vehicle exposed control animals. See figure 4.5 for photomicrographs of the livers of heliotrine exposed mice.

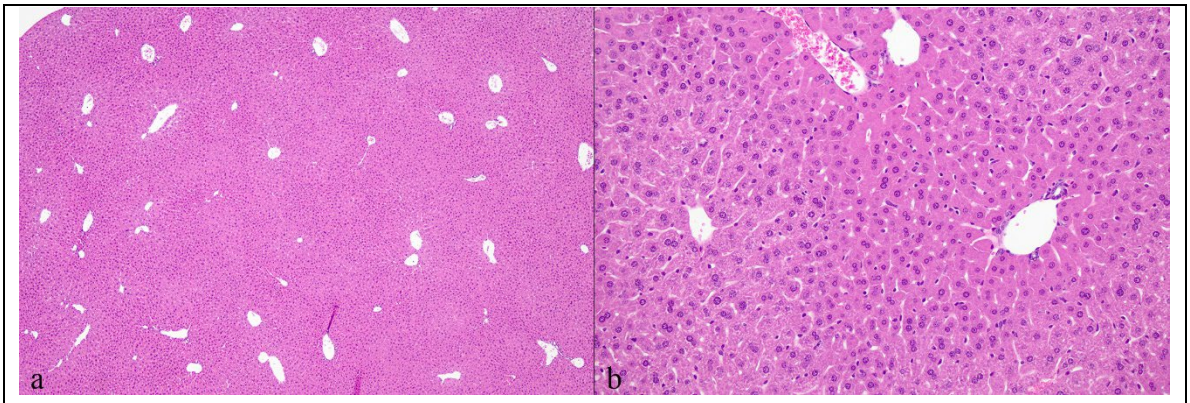

Figure 4.5 Images a-b: Liver from mice exposed to 0.137 mmol/kg/day heliotrine for eight days and euthanized one day later. Hematoxylin and eosin. Image (a). No microscopic abnormalities are observed. Image (b). No microscopic abnormalities are observed.

28-Day Post-Exposure Senecionine Group:

Mice exposed to senecionine had multifocal areas of hepatocellular hypertrophy and/or swelling. In rare foci of cellular hypertrophy and/or cell swelling, small numbers of individual necrotic hepatocytes were in seven out of ten mice, and rare foci of coagulative necrosis affecting contiguous groups of hepatocytes in three out of ten mice. In one of the mice, a pattern of differential staining resulting in increased cytoplasmic eosinophilia in centrilobular hepatocytes was observed. See figure 4.6 photomicrographs from the livers of senecionine-exposed mice at 28-days post-exposure.

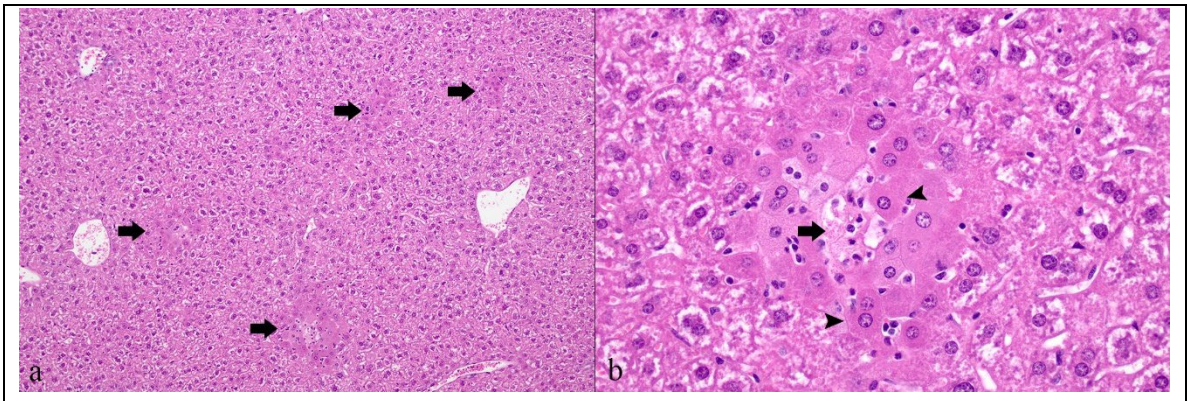

Figure 4.6 Images a-b: Liver from mice exposed to 0.137 mmol/kg/day senecionine for eight days and euthanized twenty-eight days later. Image (a). Multifocal randomly distributed areas of necrosis (arrows) are observed. Image (b). Foci of necrosis have a center of cell debris (arrow) and are surrounded by hepatocytes with increased cytoplasmic eosinophilia (arrowheads).

28-Day Post-Exposure Riddelliine Group:

One of the ten mice in the group exposed to riddelliine had rare foci (0-1 per 100x field) of coagulative necrosis affecting groups of contiguous hepatocytes. The remaining nine mice in this group had no gross or microscopic liver lesions and closely resembled the control group. See figure 4.7 photomicrographs from the livers of riddelliine-exposed mice at 28-days post-exposure.

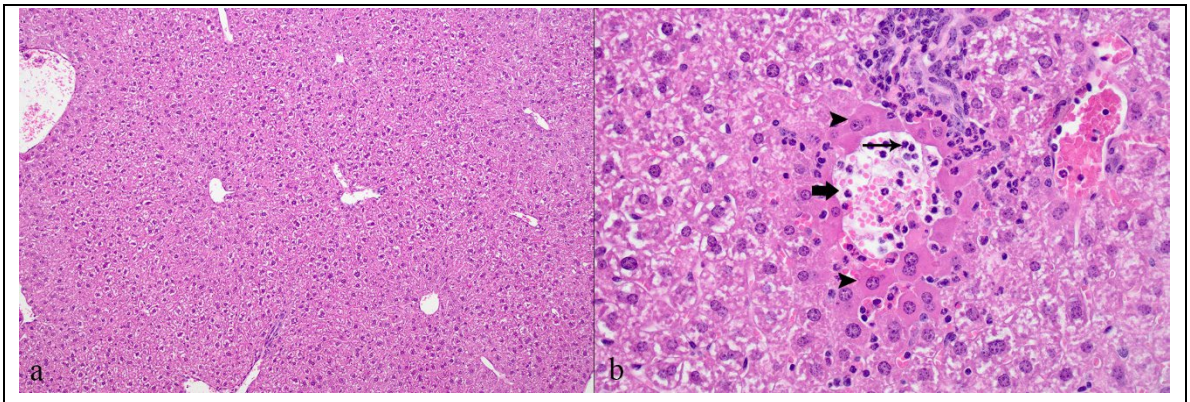

Figure 4.7. Images a-b: Riddelliine, 28-days post exposure group. Liver from mice exposed to 0.137 mmol/kg/day riddelliine for eight days and euthanized twenty-eight days later. Image a) Riddelliine exposed mouse. Liver. No microscopic lesions are observed. Image b) Riddelliine exposed mouse. Liver. A single focus of necrosis (arrow) was observed in one out of ten mice in this group. Hepatocytes adjacent to the area of necrosis have increased cytoplasmic eosinophilia.

28-day post-exposure heliotrine group:

Mice exposed to heliotrine had no gross or microscopic liver lesions. See figure 4.8 for photomicrographs from the livers of heliotrine-exposed mice at 28-days post-exposure.

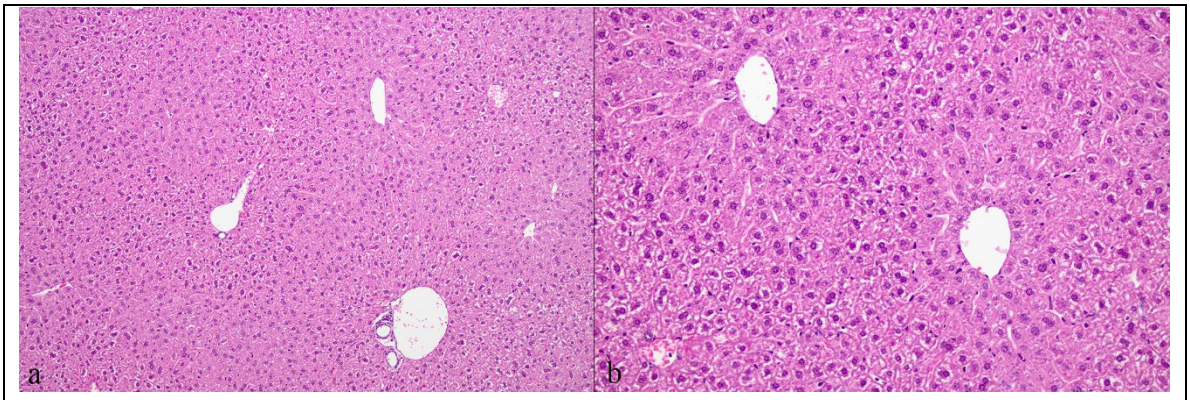

Figure 4.8 Images a-b: Liver from mice exposed to 0.137 mmol/kg/day heliotrine for eight days and euthanized twenty-eight days later. Image (a). No microscopic lesions are observed. Image (b). No microscopic lesions are observed.

Statistical Comparison of Hepatic Necrosis Scores:

Immediate Post-Exposure Group:

Hepatic necrosis scores were significantly different than the control group for mice exposed to senecionine and riddelliine at nine days ($p \leq 0.05$). Mice exposed to

senecionine had the most severe hepatic necrosis and the highest average hepatic necrosis score (3.2 ± 0.45). The average hepatic necrosis score for mice exposed to riddelliine was 1.2 ± 0.45. Mice exposed to heliotrine developed no hepatic necrosis and therefore the hepatic necrosis score for all these mice was zero. No hepatic necrosis was observed in control mice. Hepatic necrosis scores for the immediate post-exposure (9-day) group can be seen in table 4.6.

Table 4.6. Hepatic necrosis scores (0-4) for individual mice in the immediate post-exposure groups (n=5).

Senecionine	Riddelliine	Heliotrine	Control
3	1	0	0
3	2	0	0
4	1	0	0
3	1	0	0
3	1	0	0

28-Day Post-Exposure Group:

Only mice exposed to senecionine had necrosis scores that were statistically different than the control group ($p < 0.0001$). The mean necrosis score for senecionine exposed mice was 0.7 ± 0.48. The mean necrosis score for riddelliine was 0.1 ± 0.32, and for heliotrine and the control group the mean necrosis score was 0. All necrosis scores for the 28-day post-exposure group can be seen in table 4.7.

Table 4.7. Hepatic necrosis scores (0-4) for individual mice from the groups euthanized twenty-eight days post-exposure. Each PA group included ten mice. The control group included nine mice.

Senecionine	Riddelliine	Heliotrine	Control
1	0	0	0

1	1	0	0
1	0	0	0
0	0	0	0
0	0	0	0
0	0	0	0
1	0	0	0
1	0	0	0
1	0	0	0
1	0	0	-

Hepatic Pyrrole Concentration:

Statistical Analysis:

Immediate Post-Exposure Necropsy Group:

Mean hepatic pyrrole concentrations were significantly different than the control group for senecionine ($p < 0.0001$) and riddelliine ($p = 0.0009$), but not for heliotrine. Mean hepatic pyrrole concentrations were 335.4 ± 126.0 nmol/g for senecionine, 189.4 ± 35.65 nmol/g for riddelliine, 3.07 ± 1.13 nmol/g for heliotrine and 0.29 ± 0.41 nmol/g for the control group. The minimal concentration detected in the control group is likely due to cross-contamination during HPLC-MSMS analysis.

28-Day Post-Exposure Necropsy Group:

Mean hepatic pyrrole concentrations were significantly different than the control group for riddelliine ($p = 0.0029$), but not for senecionine or heliotrine. Mean hepatic pyrrole concentrations were 1.26 ± 1.36 nmol/g for riddelliine, 0.72 ± 0.18 nmol/g for senecionine, 0.18 ± 0.56 nmol/g for heliotrine and 0.03 ± 0.08 nmol/g for the control group.

Hepatic Pyrrole Concentration Comparisons Within Compounds Over Time:

Mean hepatic pyrrole concentrations were significantly different ($p < 0.0001$) between the immediate post-exposure group and the 28-day post-exposure group for senecionine, riddelliine and heliotrine. Pyrrole concentrations reduced nearly to zero for all compounds by 28 days post exposure. Mean hepatic pyrrole concentrations can be seen in table 4.8.

Table 4.8. Average hepatic pyrroles concentrations ± standard deviation immediately and 28 days post-exposure.

Hepatic pyrrole concentration (nmol/g)	Immediate	28-days post-exposure
Senecionine	335.4 ± 126.0	0.72 ± 0.18
Riddelliine	189.4 ± 35.65	1.26 ± 1.36
Heliotrine	3.09 ± 1.13	0.18 ± 0.56
Control	0.28 ± 0.41	0.03 ± 0.08

Spearman correlations of pyrrole concentrations with necrosis score for the immediate post-exposure group are as follows: r = 0.0.88, 95% confidence interval = 0.71 to 0.95, p-value < 0.0001.

Spearman correlations of pyrrole concentrations with necrosis score for the 28-day post-exposure group are as follows: r = 0.0.46, 95% confidence interval = 0.15 to 0.68, p-value = 0.0035.

Correlations Between Hepatic Pyrrole Concentration and Serum Biochemistry Concentrations:

In the immediate post-exposure group, hepatic pyrrole concentration had a strong positive correlation with ALT, and moderate positive correlations with AST, total bilirubin, and cholesterol. There were strong negative correlations with albumin and glucose (See table 4.9 for r, r-squared and p-values). Correlations were not statistically significant for ALP.

In the 28-day post-exposure group, hepatic pyrrole concentration had a weak positive correlation with AST. Correlations were not statistically significant for ALP, ALT, total bilirubin, albumin, glucose and cholesterol (See table 4.10 for r, r-squared and p-values).[58]

Table 4.9. Pearson correlation of serum biochemistry concentrations with hepatic pyrrole concentrations for immediate post-exposure group.

	ALP	ALT	AST	T. Bili	Albumin	Glucose	Cholesterol
R	0.6	0.88	0.69	0.68	-0.9	-0.71	0.69
R squared	0.36	0.77	0.48	0.47	0.82	0.5	0.47
P value (two tailed)	0.0054	<0.0001	0.0016	0.0012	<0.0001	0.0005	0.0048

Abbreviations: ALP = alkaline phosphatase, ALT = alanine aminotransferase, AST = aspartate aminotransferase, T. Bili = total bilirubin.

Table 4.10. Pearson correlation of serum biochemistry concentrations with hepatic pyrrole concentrations for 28-day post-exposure group.

	ALP	ALT	AST	T. Bili	Albumin	Glucose	Cholesterol
R	0.17	0.16	0.39	0.05	0.02	-0.27	-0.08

R squared	0.03	0.03	0.15	0.003	0.0003	0.07	0.006
P value (two tailed)	0.29	0.34	0.02	0.76	0.92	0.1	0.7

Abbreviations: ALP = alkaline phosphatase, ALT = alanine aminotransferase, AST = aspartate aminotransferase, T. Bili = total bilirubin.

RNAseq Hepatic Gene Expression:

Total RNA expression in liver was performed (25701 genes) for five mice from each group. Pairwise comparisons were performed between the control group and each PA group at two time points (immediately after exposure on day 9, and 28 days after exposure on day 37). Complete gene expression results can be seen in supplementary material.

Differentially Expressed Genes (DEGs):

Whole genome RNA expression was performed using liver for five mice from each group. Genes were classified as differentially expressed if there was a two-fold change compared to the control group and the false discovery rate (FDR) was less than or equal to 0.05.[59,60] Senecionine-exposed mice immediately post-exposure had a total of 3,006 differentially expressed genes (DEGs), with 1,857 upregulated genes and 1,149 downregulated genes. Riddelliine-exposed mice had 2,017 DEGs, with 1,127 upregulated and 890 downregulated genes immediately post-exposure. Heliotrine-exposed mice had a total of 112 DEGs, with 76 upregulated genes and 36 downregulated genes immediately post-exposure. The combined lists of differentially expressed genes for senecionine and

riddelliine included a total of 3,486 genes. Among this list of 3,486 DEGs, 1,535 were differentially regulated by both senecionine and riddelliine. Among this group, all but four DEGs were dysregulated in the same direction, up or down. The genes which were dysregulated in opposite directions included Ugtb37, Cndp1, and Nat8f6. In the 28-day post-exposure groups, senecionine-exposed mice had a total of 341 DEGs, with 244 upregulated genes and 97 downregulated genes. Riddelliine-exposed mice at 28 days post-exposure had a total of 179 DEGs with 123 upregulated and 56 downregulated genes. Heliotrine-exposed mice had a total of 111 DEGs with 59 upregulated and 52 downregulated genes at this time point. Venn diagrams showing a summary of DEGs which were unique or commonly upregulated or downregulated between PA groups can be seen in figure 4.10 below.

Table 4.11. Summary of differentially expressed genes for each compound group at day 9 and day 37.

Group	Total DEGs	Upregulated genes	Downregulated genes
Day 1 Senecionine	3006	1857	1149
Day 1 Riddelliine	2017	1127	890
Day 1 Heliotrine	112	76	36
Day 28 Senecionine	341	244	97
Day 28 Riddelliine	179	123	56
Day 28 Heliotrine	111	59	52

Upregulated Genes:

Immediately post-exposure, senecionine had 972 unique upregulated genes, riddelliine had 243 uniquely upregulated genes and heliotrine had 21. Forty-six genes were upregulated by all three PAs, 834 were upregulated by both senecionine and riddelliine, 5

were upregulated by senecionine and heliotrine and 4 were upregulated by riddelliine and heliotrine. In the 28-day post-exposure groups, senecionine had 153 unique upregulated genes, riddelliine had 25 uniquely upregulated genes and heliotrine had 21. Twenty-seven genes were upregulated by all three PAs, 62 were upregulated by both senecionine and riddelliine, 2 were upregulated by senecionine and heliotrine and 9 were upregulated by riddelliine and heliotrine.

Downregulated Genes:

Immediately post-exposure, senecionine had 490 unique downregulated genes, riddelliine had 231 uniquely downregulated genes, and heliotrine had 10. Eighteen genes were downregulated by all three PAs, 637 were downregulated by both senecionine and riddelliine, 4 were downregulated by senecionine and heliotrine and 4 were downregulated by riddelliine and heliotrine. In the 28-day post exposure groups, senecionine had 68 unique downregulated genes, riddelliine had 20 uniquely downregulated genes and heliotrine had 35. Eight genes were downregulated by all three PAs, 20 were downregulated by both senecionine and riddelliine, 1 was downregulated by senecionine and heliotrine and 8 were downregulated by riddelliine and heliotrine.

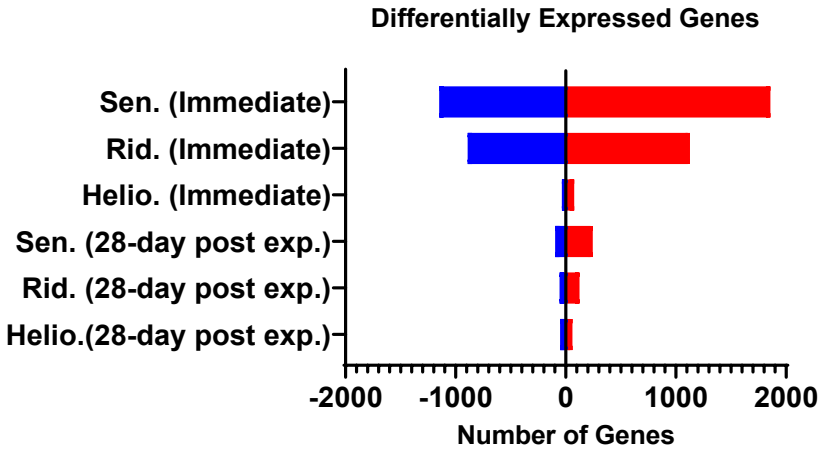

Figure 4.9. Differentially expressed genes detected in mice exposed to senecionine, riddelliine, or heliotrine, at two time points. Sen = senecionine, Rid. = riddelliine, Helio. = heliotrine. Immediate = immediate post-exposure group, 28-day post-exp. = 28-day post-exposure group.

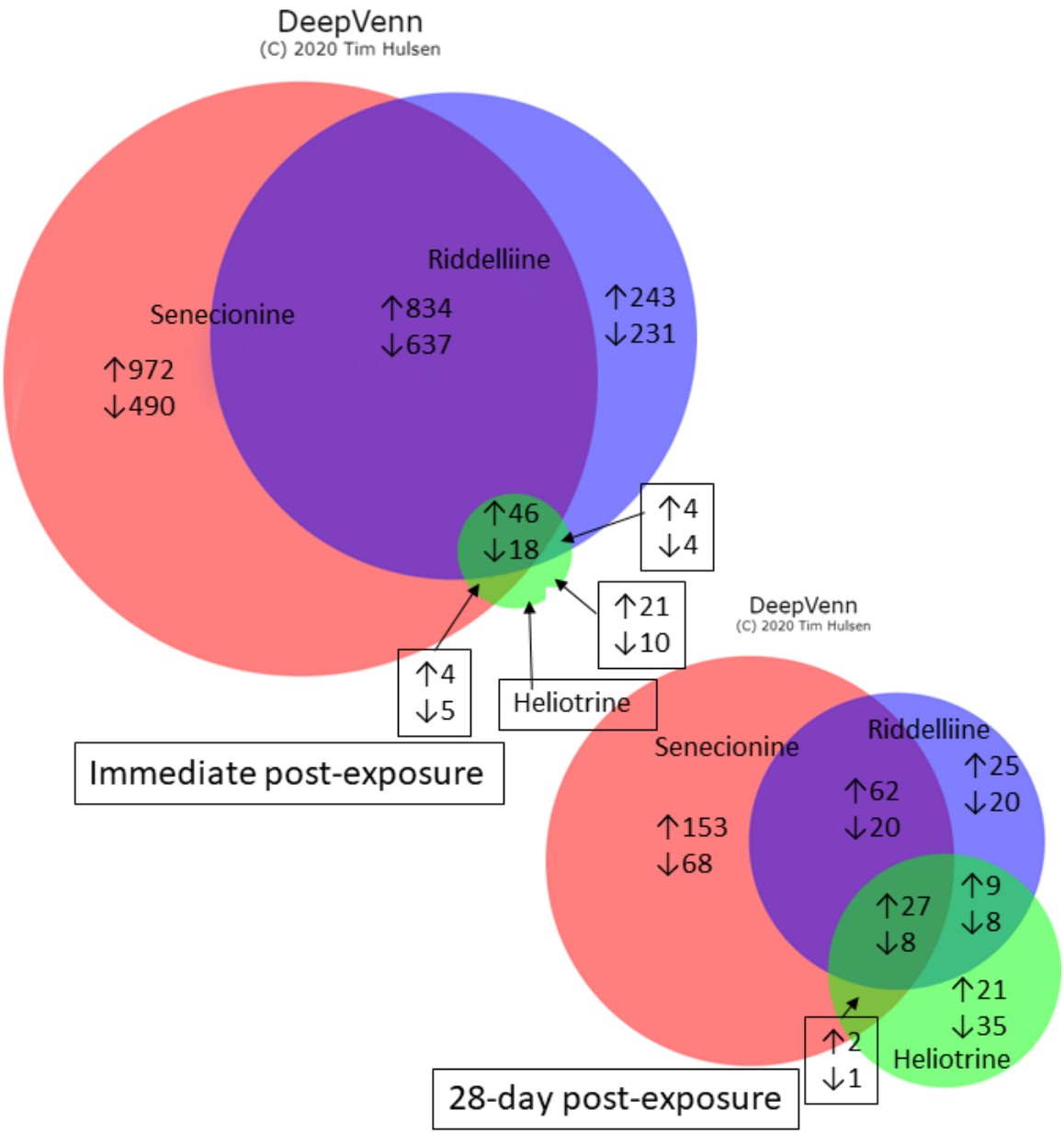

Figure 4.10. Venn diagrams of upregulated and downregulated genes immediately post-exposure, and 28-days post exposure. Upregulated genes are labeled with an up arrow (↑) and downregulated genes are labeled with a down arrow (↓).Senecionine is in light red, riddelliine is in blue and heliotrine is in green.

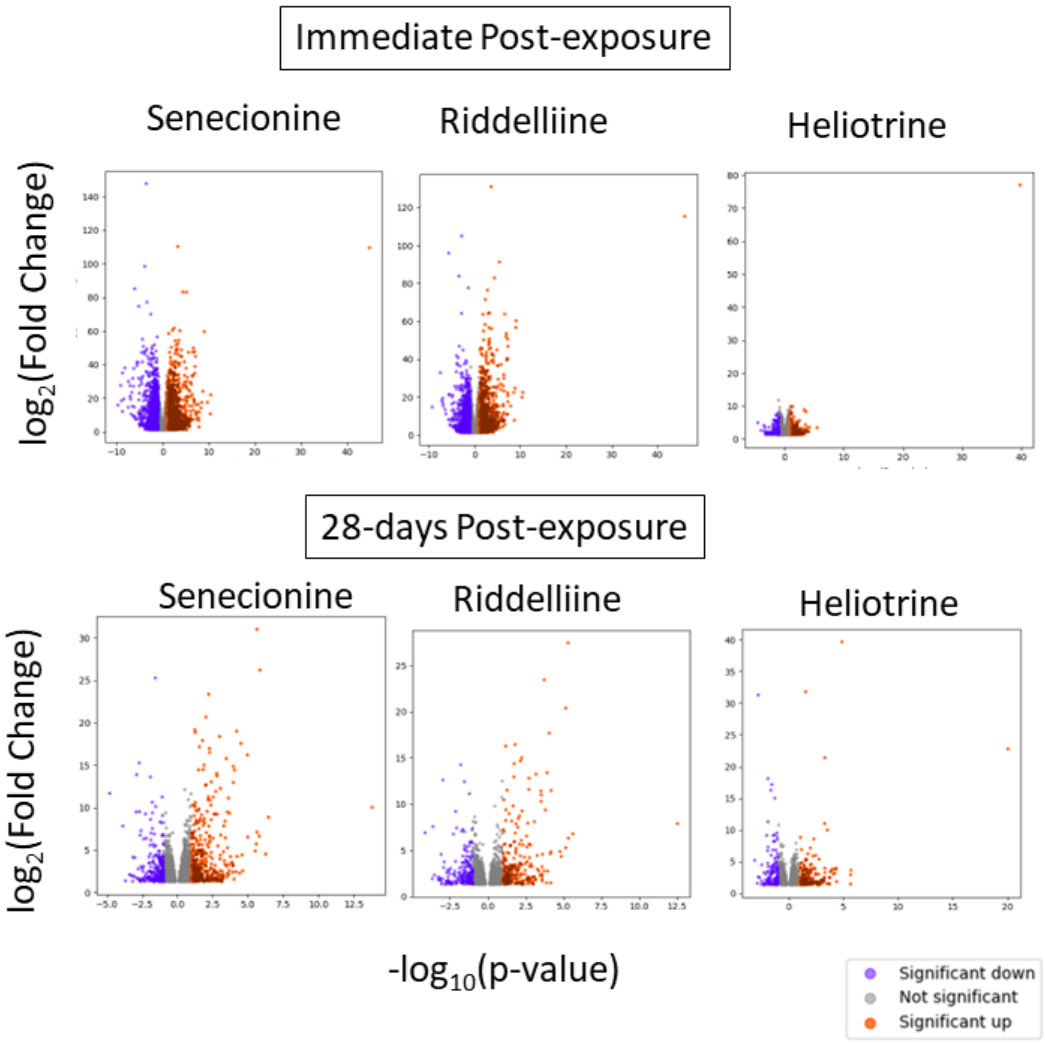

Figure 4.11. Volcano plots of differentially expressed genes at two time points. Day 9 is the immediate post-exposure group and day 37 is the 28-day post exposure group. The y axis is the log base 2 of the fold change compared to the control group. The x axis is the $\log_{10}$(p-value) calculated for the differentially expressed gene.

Top 25 Common DEGs for Senecionine and Riddelliine:

Table 12 shows the top 25 up or downregulated genes which were commonly dysregulated by senecionine and riddelliine immediately post-exposure. This list includes a wide variety of genes with different functions, many of which are not known to be related to PA-induced toxicosis or carcinogenicity. Genes from this list which may be of interest in the toxicogenomic study of PA toxicosis include the upregulated genes Cdkn1a, Cyp2a4, Gsta1, Cox6b2, and MMP2. Cdkn1a encodes Cyclin-Dependent Kinase Inhibitor 1A (P21), involved in the cell cycle, and regulated by p53. Upregulation of this gene may result in cell cycle arrest.[61] Cyp2a4 encodes the enzyme cytochrome P450, Family 2, Subfamily A, Polypeptide 4, which is a member of the family of enzymes responsible for bioactivation of PAs.[1,2] Gsta1 encodes for Glutathione S-Transferase, Alpha 1 (Ya), which is involved in phase 2 metabolism of PAs and other xenobiotics.[62] Cox6b2 encodes for the Cytochrome C Oxidase Subunit 6B2 protein, which is involved in electron transport in aerobic metabolism.[63] MMp12 encodes for a matrix metalloproteinase, a family of proteins involved in tissue repair and remodeling, among other functions. [64] Lactotransferrin had the greatest fold change at this time point for all three PAs. Lactotransferrin (Ltf) is involved in several biological processes including immune system function, iron homeostasis, proteolysis and others.[65,66]. The importance of lactotransferrin in PA exposure is unclear. In the group comprising the 25 most downregulated genes by both senecionine and riddelliine immediately post-exposure, includes a list of seemingly unrelated genes. The exception in this list is a number of genes that encode for major urinary proteins, namely Mup1, Mup2, Mup13, Mup7, Mup16, Mup12, Mup22, Mup18, Mup11, Mup19, Mup17 and Mup15. The major urinary

proteins are a group of proteins that have multiple roles including communication via urine derived scent marks.[67]

Table 4.12. The top 25 commonly up and down regulated genes which are dysregulated by senecionine and riddelliine on 1-day post exposure. Genes were ranked by fold change, and the numbers presented are log base 2 of the fold change.[68–71] Upregulated genes are red while downregulated genes are blue..

Name	Description	logFC (Sen. D9)	logFC (Rid. D9)	logFC (Hel. D9)
Ltf	lactotransferrin	44.85	45.97	39.83
Tekt5	tektin 5	10.43	10.52	3.78
Sprr1a	small proline-rich protein 1A	10.37	8.7	5.53
Zfp365	zinc finger protein 365	9.71	10.35	4.2
Cdkn1a	cyclin-dependent kinase inhibitor 1A (P21)	9.04	9.08	3.34
Psrc1	proline/serine-rich coiled-coil 1	8.76	8.85	3.54
Lif	leukemia inhibitory factor	8.48	7.89	2.76
Slc7a11	solute carrier family 7, member 11	7.86	6.15	4.09
Pierce1	piercer of microtubule wall 1	7.25	8.56	2.12
Cbr3	carbonyl reductase 3	7.03	9	1.67
Ly6d	lymphocyte antigen 6 complex, locus D	7.75	6.18	3.13
Inka2	inka box actin regulator 2	7.14	7.28	2.11
Eda2r	ectodysplasin A2 receptor	7.06	7.17	2.1
Tinag	tubulointerstitial nephritis antigen	6.36	6.46	3.4
Apln	apelin	8.32	5.17	2.58
Gpnmb	glycoprotein (transmembrane) nmb	7.97	4.53	3.5
Phlda3	pleckstrin homology like domain, family A, member 3	6.99	7.21	1.62
Ms4a4a	membrane-spanning 4-domains, subfamily A, member 4A	7.32	4.67	3.72
Sec14l5	SEC14-like lipid binding 5	6.78	7.23	1.65
Got1l1	glutamic-oxaloacetic transaminase 1-like 1	7.16	7.05	1.4
Ckap2	cytoskeleton associated protein 2	6.45	7.05	2.1
Gm37795	predicted gene, 37795	6.8	6.26	2.39
Mmp12	matrix metallopeptidase 12	6.72	6.39	2.12

Chil3	chitinase-like 3	7.81	3.67	3.55
Cyp2a4	cytochrome P450, family 2, subfamily a, polypeptide 4	6.89	7.27	0.87
Kcnb2	potassium voltage gated channel, Shab-related subfamily, member 2	-4.92	-4.53	-0.92
Chchd6	coiled-coil-helix-coiled-coil-helix domain containing 6	-4.21	-5.63	-0.56
Slc26a4	solute carrier family 26, member 4	-4.04	-5.42	-1.02
Tnfsf15	tumor necrosis factor (ligand) superfamily, member 15	-4.4	-4.57	-1.55
Mup7	major urinary protein 7	-6.54	-4.91	0.86
Saa2	serum amyloid A 2	-1.92	-4.39	-4.51
Adgrv1	adhesion G protein-coupled receptor V1	-6.08	-4.96	-0.3
Mup16	major urinary protein 16	-7.01	-4.44	0.04
Hamp2	hepcidin antimicrobial peptide 2	-5.14	-5.47	-1.25
Mup1	major urinary protein 1	-7.06	-4.79	-0.14
Syt1	synaptotagmin I	-6.03	-5.67	-0.38
Olfr541	olfactory receptor 541	-5.08	-5.25	-1.83
Mup12	major urinary protein 12	-7.36	-4.93	-0.08
Vmn1r90	vomeronasal 1 receptor 90	-6.35	-4.67	-1.37
Mup22	major urinary protein 22	-8.67	-3.76	-0.07
Cyp2b9	cytochrome P450, family 2, subfamily b, polypeptide 9	-4.45	-4.88	-3.48
Sun3	Sad1 and UNC84 domain containing 3	-6.13	-5.72	-1.27
Mup2	major urinary protein 2	-7.41	-6.46	-0.68
Nxph1	neurexophilin 1	-6.9	-6.99	-1.21
Mup18	major urinary protein 18	-8.36	-6.88	-0.12
Mup9	major urinary protein 9	-8.67	-6.27	-0.48
Mup11	major urinary protein 11	-8.17	-7.5	0.09
Mup19	major urinary protein 19	-8.91	-6.95	-0.11
Mup17	major urinary protein 17	-9.08	-7.16	-0.13
Mup15	major urinary protein 15	-9.67	-9.26	-0.08

Kyoto Encyclopedia of Genes and Genomes (KEGG) Pathway Analysis Immediately Post-Exposure:

A cutoff FDR of 0.05 was used to determine which KEGG pathways were affected. Particular attention was paid to KEGG pathways that were affected by both senecionine and riddelliine. Heliotrine only affected a single KEGG pathway, “Bile secretion”, at the immediate post-exposure time point, and did not affect any pathways in the 28-day post-exposure group. Senecionine and riddelliine affected 24 common KEGG pathways, many of which were related to metabolism and neoplasia (See figure 4.12). Senecionine affected 44 additional KEGG pathways and riddelliine affected 4 additional KEGG pathways. Special attention is paid to pathways involved in the metabolic pathways used for bioactivation (phase I metabolism) and phase II metabolism of PAs, and to pathways related to neoplasia. KEGG pathways which were of particular interest, based on previous knowledge of the toxic mechanism and carcinogenic effects of PAs include “Metabolic pathways”, “Pathways in cancer”, “Chemical carcinogenesis-receptor activation”, microRNAs in cancer, hepatocellular carcinoma, chemical carcinogenesis-DNA adducts”, “Metabolism of xenobiotics by cytochrome p450”, “Glutathione metabolism”, “P53 signaling pathway”, and “Pentose and glucuronate interconversions”. Senecionine caused differential expression in a greater number of genes in most KEGG pathways than riddelliine, with the exception being the “P53 signaling pathway”, in which both PAs affected 26 pathway genes, metabolism of xenobiotics by cytochrome p450 enzymes in which both riddelliine and senecionine affected 29 pathway genes, and drug metabolism-other enzymes, in which riddelliine affected 35 pathway genes and senecionine affected 34 pathway genes. Figure 12 shows enrichment scores for KEGG

pathways affected by senecionine and riddelliine immediately post-exposure. Figures 13-24 show heatmaps of the relevant KEGG pathways affected by senecionine and riddelliine. The only gene related to metabolism which was expressed differently by these two PAs was Ugt2b37 (UDP-glucuronosyltransferase 2B37), otherwise, all genes related to the metabolic pathways of PAs moved in the same direction for senecionine and riddelliine. The purpose of the following heatmaps in figures 13-24 is to show that senecionine and riddelliine had similar effects on gene expression as it related to functional analysis.

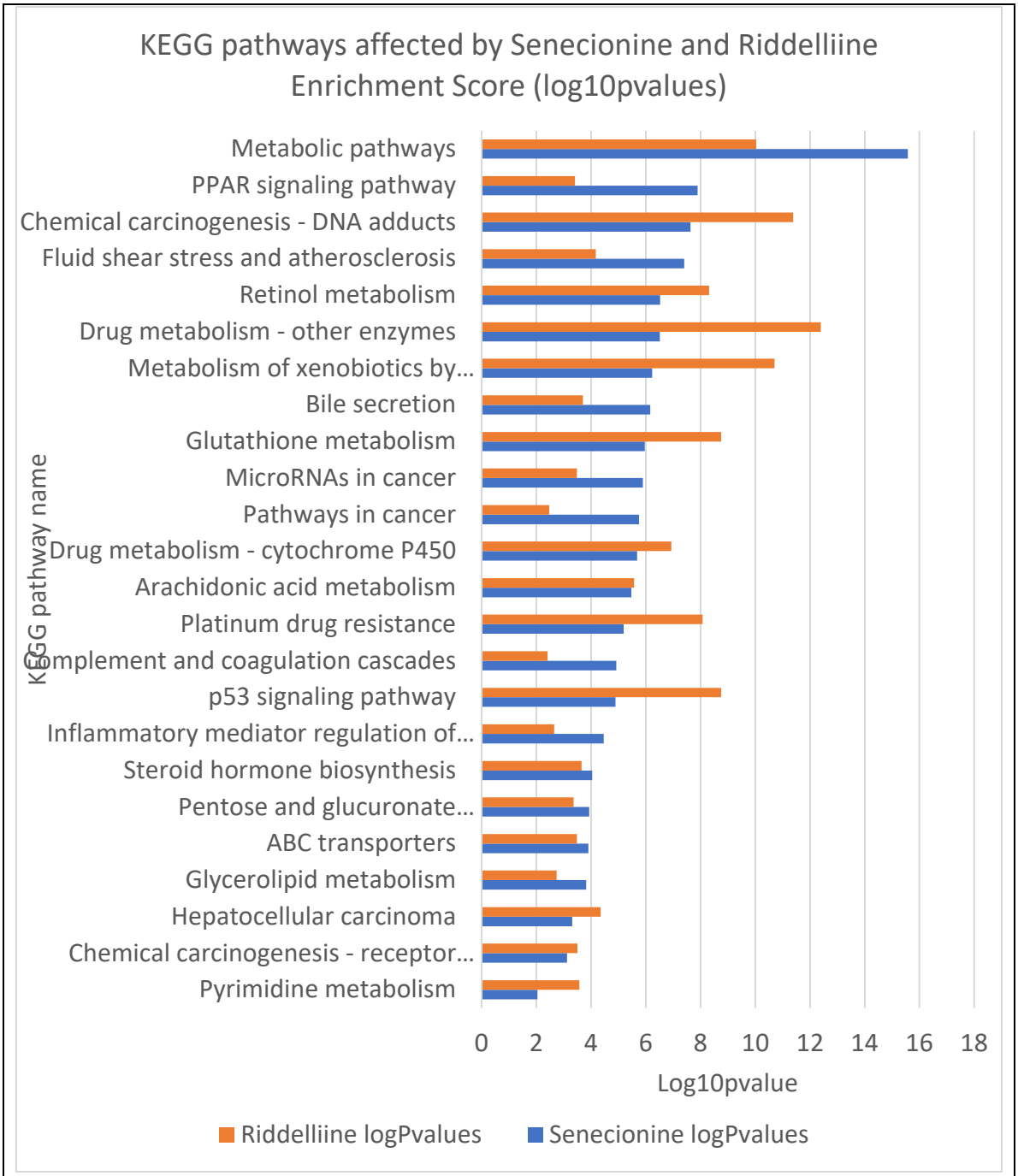

Figure 4.12. KEGG pathways affected by senecionine (orange bars) and riddelliine (blue bars) immediately post-exposure arranged in descending order by enrichment score. The x axis indicates the enrichment score in log10pvalue of the KEGG pathway for riddelliine (orange) or senecionine (blue). Heliotrine is left out of comparisons due to the relatively small number of DEGs seen in this group.

KEGG Pathways “Metabolic Pathways”:

Metabolic pathways had the largest number of DEGs from the senecionine (361 DEGs) and riddelliine (233 DEGs) groups. The enrichment score was 15.58 for senecionine compared to 10.03 for riddelliine. The majority of DEGs were regulated in the same direction up or down. Exceptions in which senecionine and riddelliine exposure caused dysregulation in opposite directions include the genes Nat8fc, Ugt2b37, and Cndp1 which were downregulated by senecionine but upregulated by riddelliine. Ugt2b37 encodes for UDP glucuronosyltransferase 2 family, polypeptide B37, which is predicted to enable glucuronosyltransferase activity.[72] Nat8fc and Cndp1 are unrelated to PA toxicosis and carcinogenesis. See figure 4.13 for a heatmap showing logFC values for riddelliine and senecionine. “Metabolic pathways” includes all genes found in other more focused pathways related to metabolism including “Drug metabolism-other enzymes”, “Metabolism of xenobiotics by cytochrome p450”, “Glutathione metabolism”, “Drug metabolism-cytochrome p450”, and “Pentose and glucuronate interconversions”. Heatmaps for these pathways showing Log_2FC values for senecionine and riddelliine can be seen below in figures 4.19, 4.20, 4.21, 4.22, and 4.24.

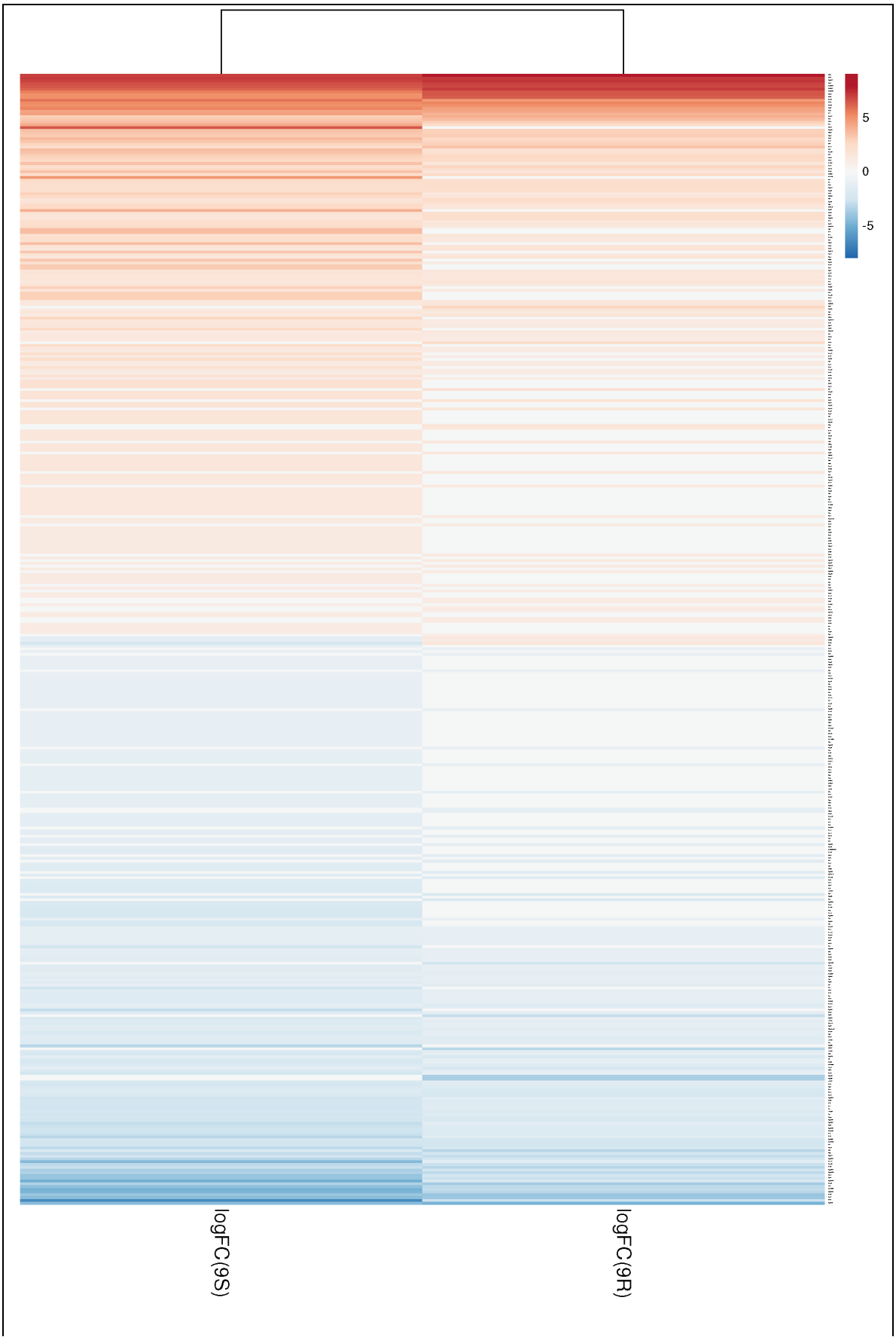
5
0
-5
logFC(9S)
logFC(9R)

Figure 4.13. Heatmap for riddelliine and senecionine showing DEGs in the "Metabolic pathways" pathway immediately post-exposure. Genes in blue are downregulated and genes in red are upregulated. Genes in white were excluded based FDR >0.05 or $log_2FC < 1$. logFC(9S) = Log_2 fold change for senecionine-exposed mice. logFC(9R) = Log_2 fold change for riddelliine-exposed mice.Three genes were differentially expressed in different directions and the remainder were differentially expressed in the same direction. logFC(9S) = Log_2 fold change for senecionine-exposed mice. logFC(9R) = Log_2 fold change for riddelliine-exposed mice.

KEGG Pathways, "Pathways in Cancer":

Pathways in cancer had the second largest number of DEGs for senecionine (122 DEGs) and riddelliine (72 DEGs). The enrichment score was 5.47 for senecionine compared to 2.47 for riddelliine. All genes which were differentially expressed by both riddelliine and senecionine changed in the same direction, up or down. A heatmap from this pathway can be seen in figure 14 below. "Pathways in cancer" includes many of the genes involved in other cancer related KEGG pathways including "Chemical carcinogenesis- receptor activation", "MicroRNAs in cancer", "Hepatocellular carcinoma", "Chemical carcinogenesis-DNA adducts", and "p53 signaling pathway". Heatmaps of these can be seen below in figures 4.15, 4.16, 4.17, 4.18, and 4.23.

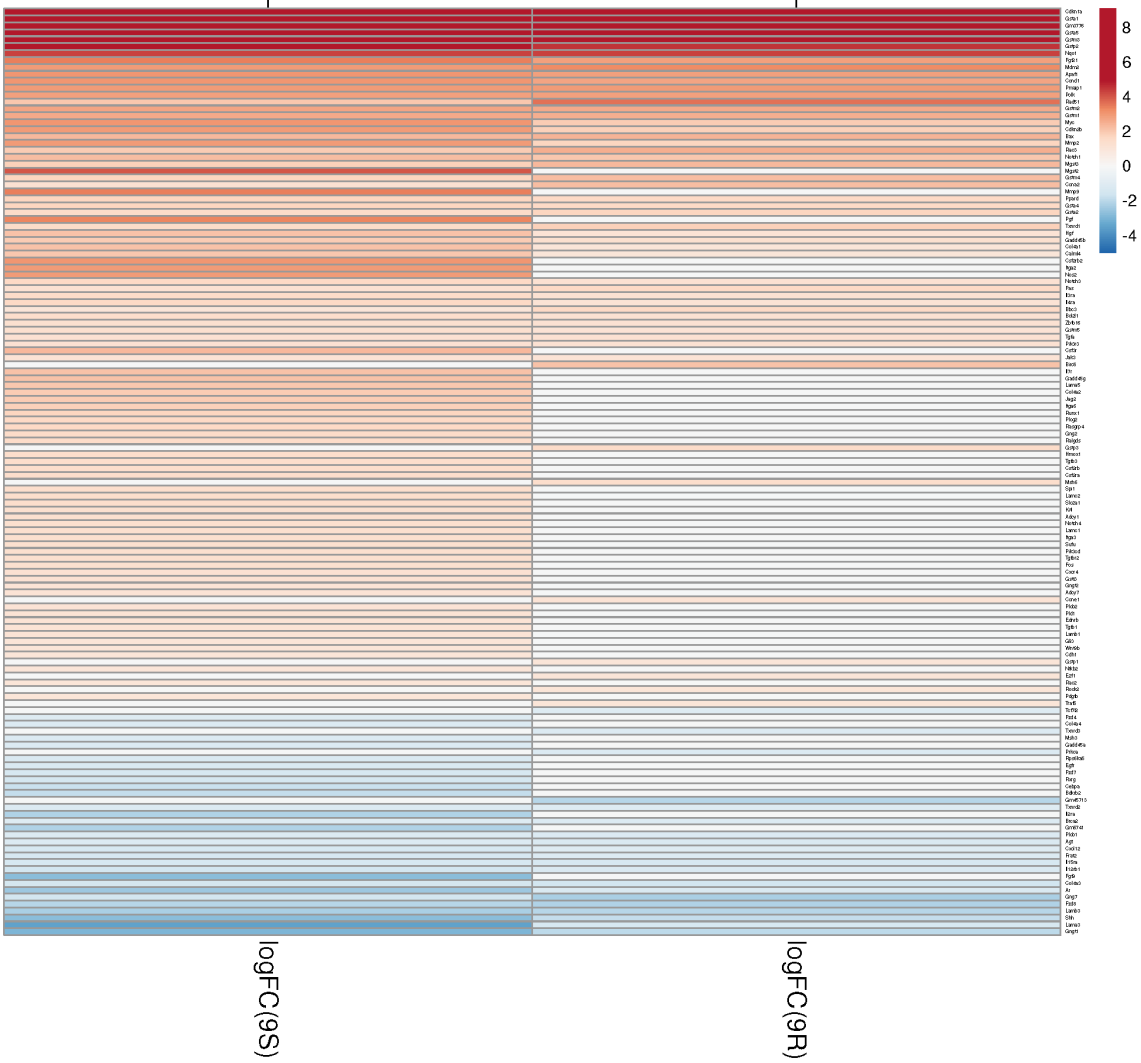

Figure 4.14. Heatmap showing differentially expression genes which affect the KEGG pathway “pathways in cancer” immediately post-exposure. Genes in blue are downregulated and genes in red are upregulated. Genes in white were excluded based on FDR >0.05 or $\log_2$FC < 1. logFC(9S) = Log base 2-fold change for senecionine-exposed mice. logFC(9R) = Log base 2 -fold change for riddelliine-exposed mice.

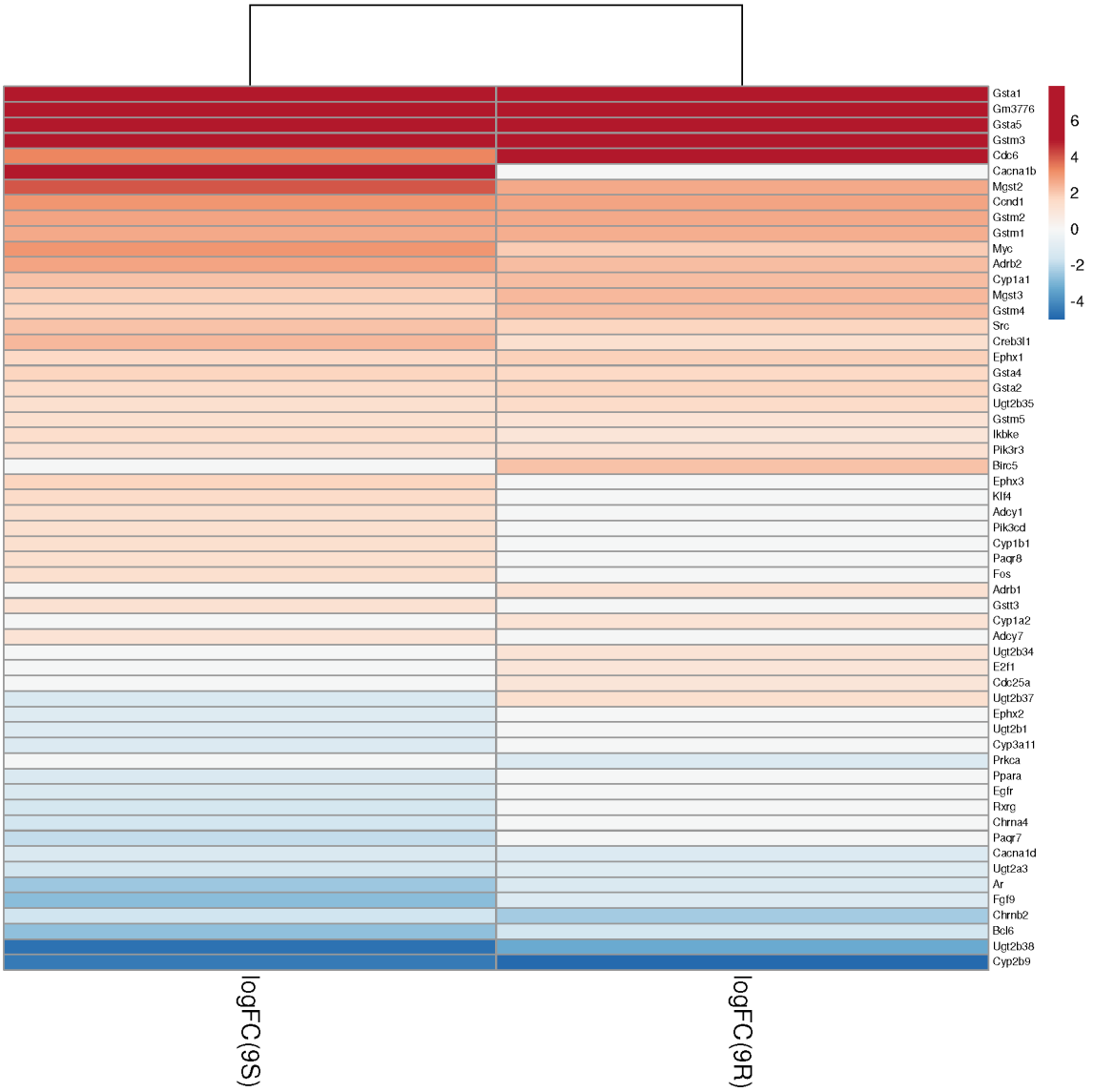

Figure 4.15. Heatmap showing differentially expression genes which affect the KEGG pathway “chemical carcinogenesis-receptor activation” immediately post-exposure. Genes in blue are downregulated and genes in red are upregulated. Genes in white were excluded based on FDR >0.05 or $\log_2$FC < 1. logFC(9S) = Log_2 fold change for senecionine-exposed mice. logFC(9R) = Log_2 fold change for riddelliine-exposed mice.

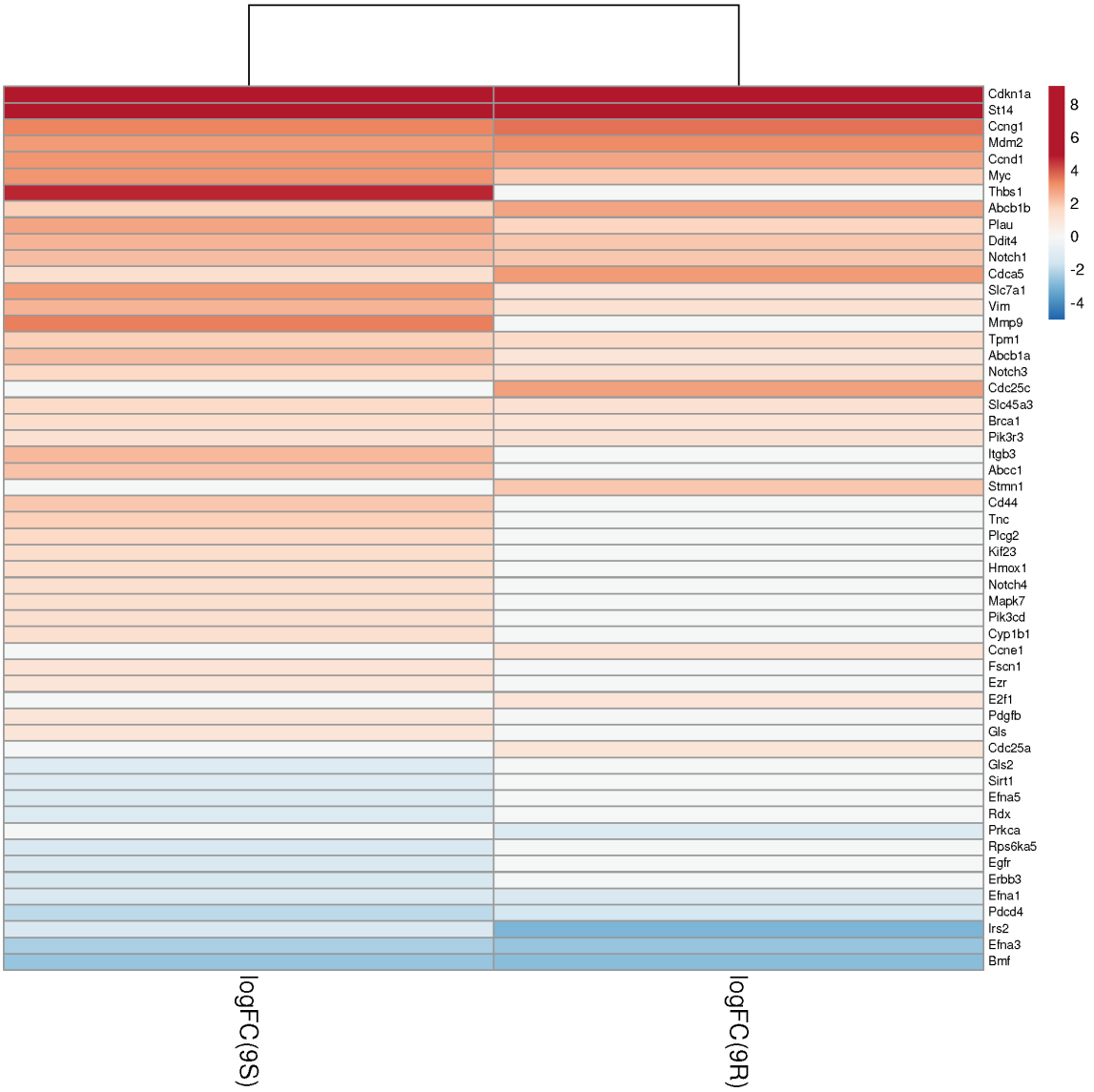

Figure 4.16 Heatmap showing differentially expression genes which affect the KEGG pathway “MicroRNAs in cancer” immediately post-exposure. Genes in blue are downregulated and genes in red are upregulated. Genes in white were excluded based on FDR >0.05 or $\log_2$FC < 1. logFC(9S) = Log_2 fold change for senecionine-exposed mice. logFC(9R) = Log_2 fold change for riddelliine-exposed mice.

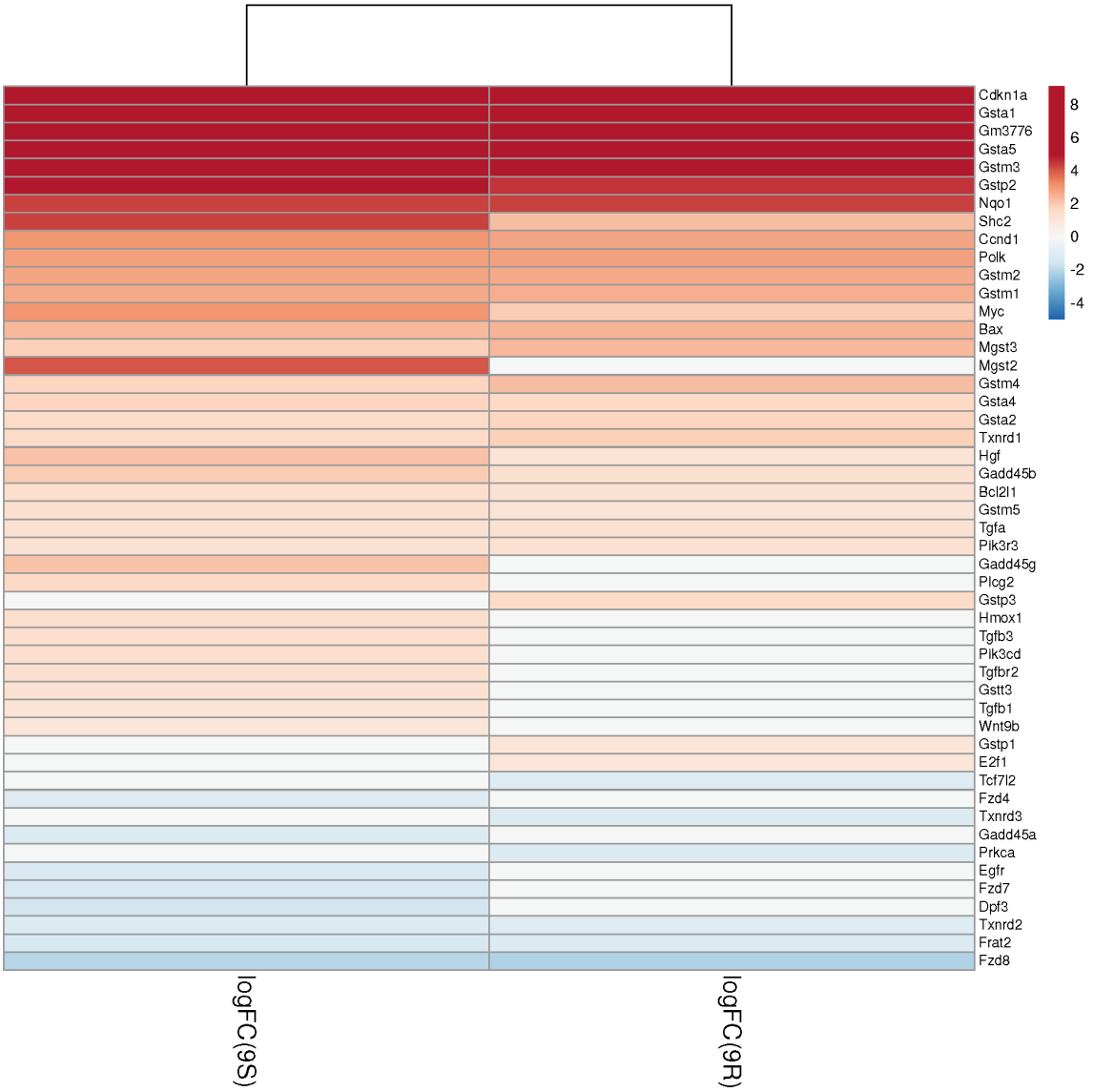

Figure 4.17. Heatmap showing differentially expression genes which affect the KEGG pathway “Hepatocellular carcinoma” immediately post-exposure. Genes in blue are downregulated and genes in red are upregulated. Genes in white were excluded based on FDR >0.05 or $log_2FC < 1$. logFC(9S) = Log_2 fold change for senecionine-exposed mice. logFC(9R) = Log_2 fold change for riddelliine-exposed mice.

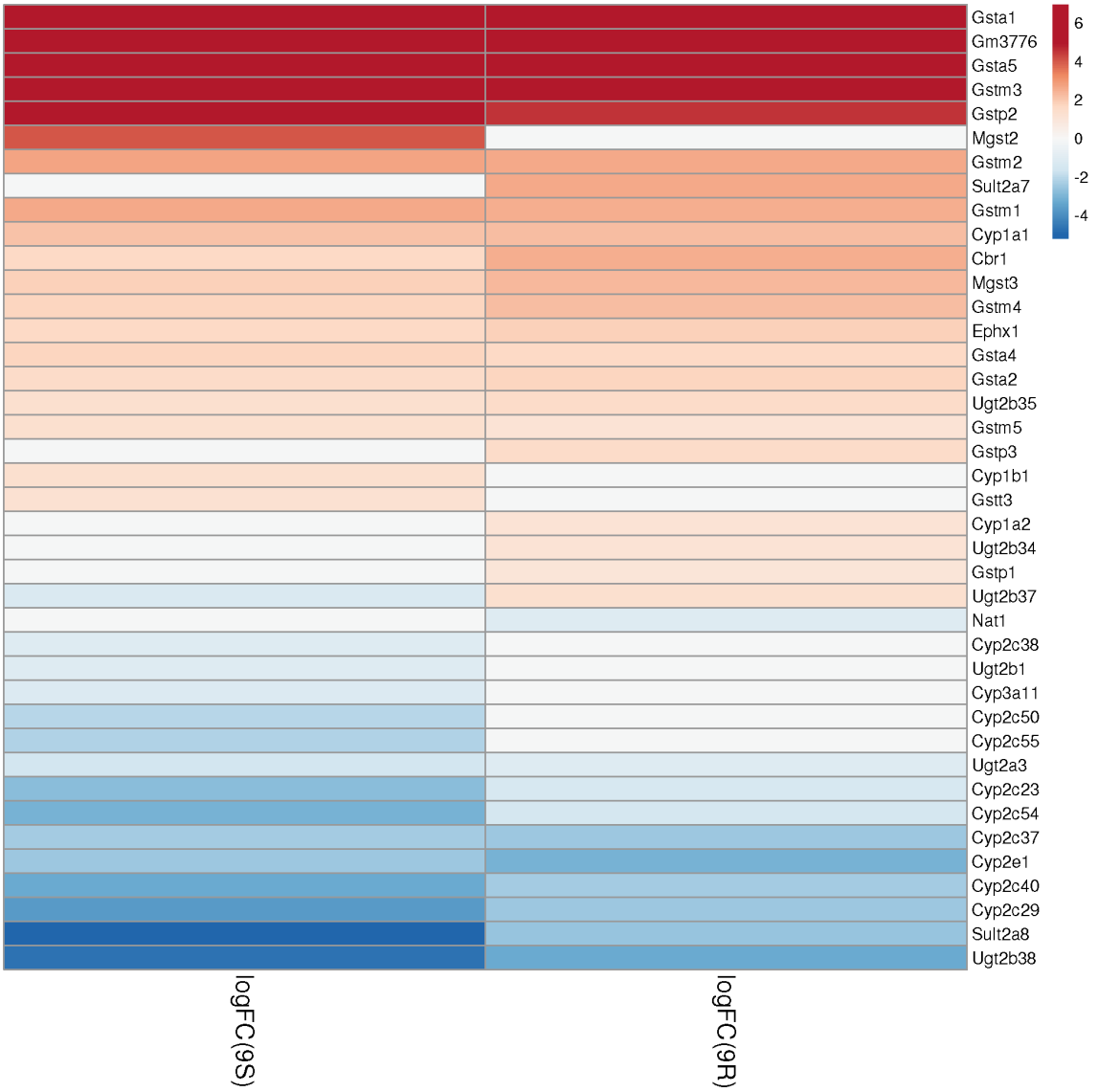

Figure 4.18. Heatmap showing differentially expression genes which affect the KEGG pathway “Chemical carcinogenesis-DNA adducts” immediately post-exposure. Genes in blue are downregulated and genes in red are upregulated. Genes in white were excluded based on FDR >0.05 or $\log_2$FC < 1. logFC(9S) = Log_2 fold change for senecionine-exposed mice. logFC(9R) = Log_2 fold change for riddelliine-exposed mice.

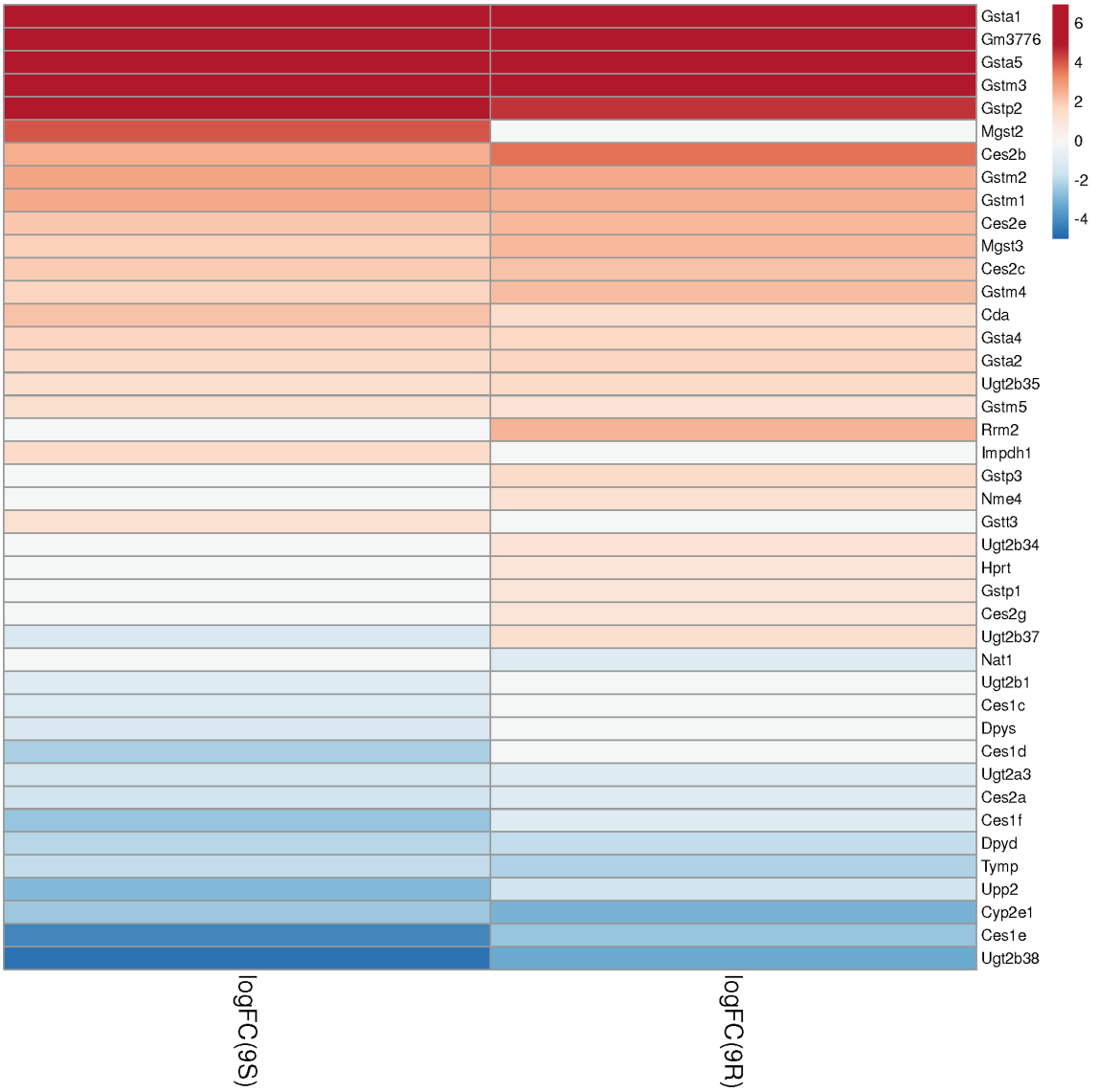

Figure 4.19. Heatmap showing differentially expression genes which affect the KEGG pathway “Drug metabolism-other enzymes” immediately post-exposure. Genes in blue are downregulated and genes in red are upregulated. Genes in white were excluded based on FDR >0.05 or $\log_2$FC < 1. logFC(9S) = Log_2 fold change for senecionine-exposed mice. logFC(9R) = Log_2 fold change for riddelliine-exposed mice.

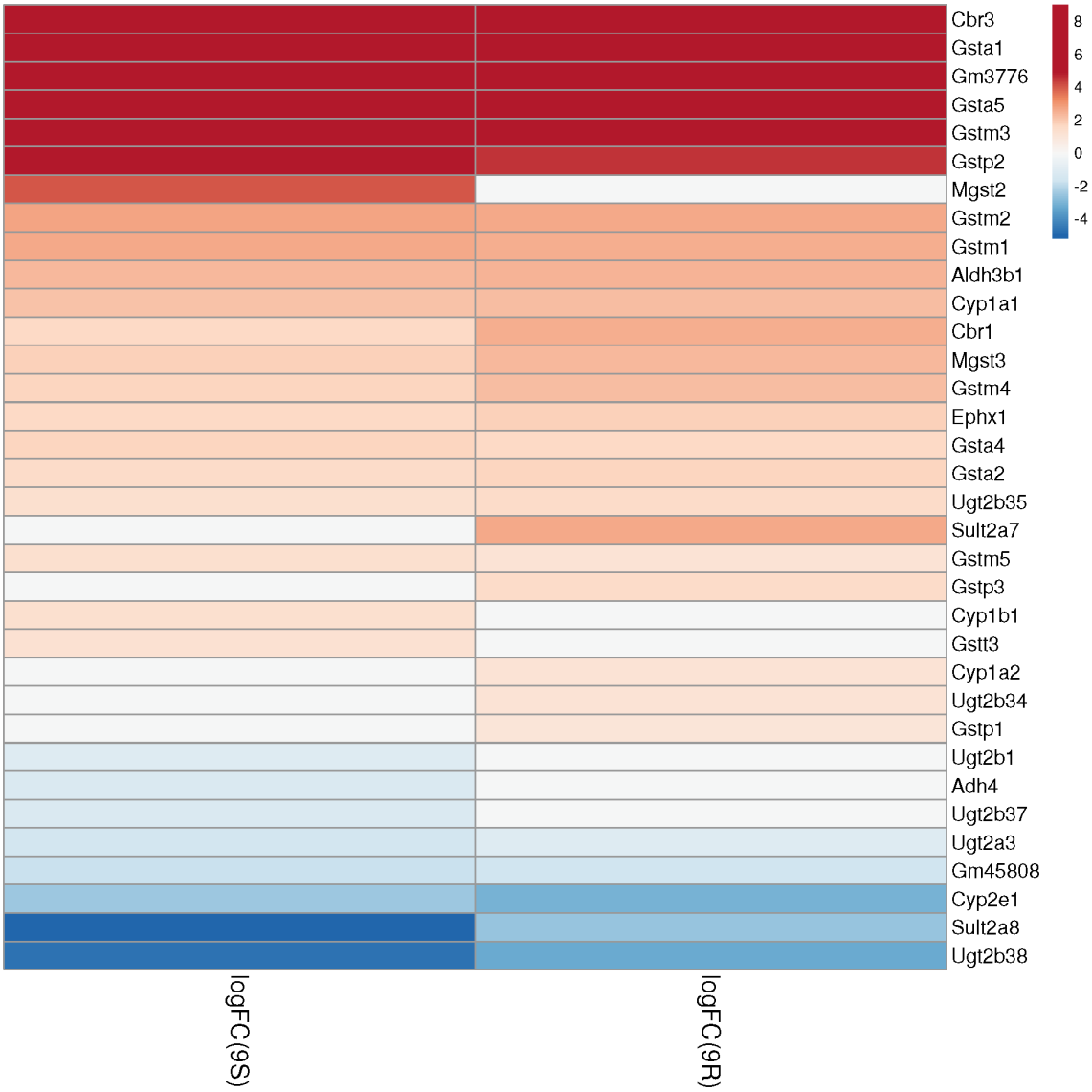

Figure 4.20. Heatmap showing differentially expression genes which affect the KEGG pathway “Metabolism of xenobiotics by cytochrome p450” immediately post-exposure. Genes in blue are downregulated and genes in red are upregulated. Genes in white were excluded based on FDR >0.05 or $log_2FC < 1$. logFC(9S) = Log_2 fold change for senecionine-exposed mice. logFC(9R) = Log_2 fold change for riddelliine-exposed mice.

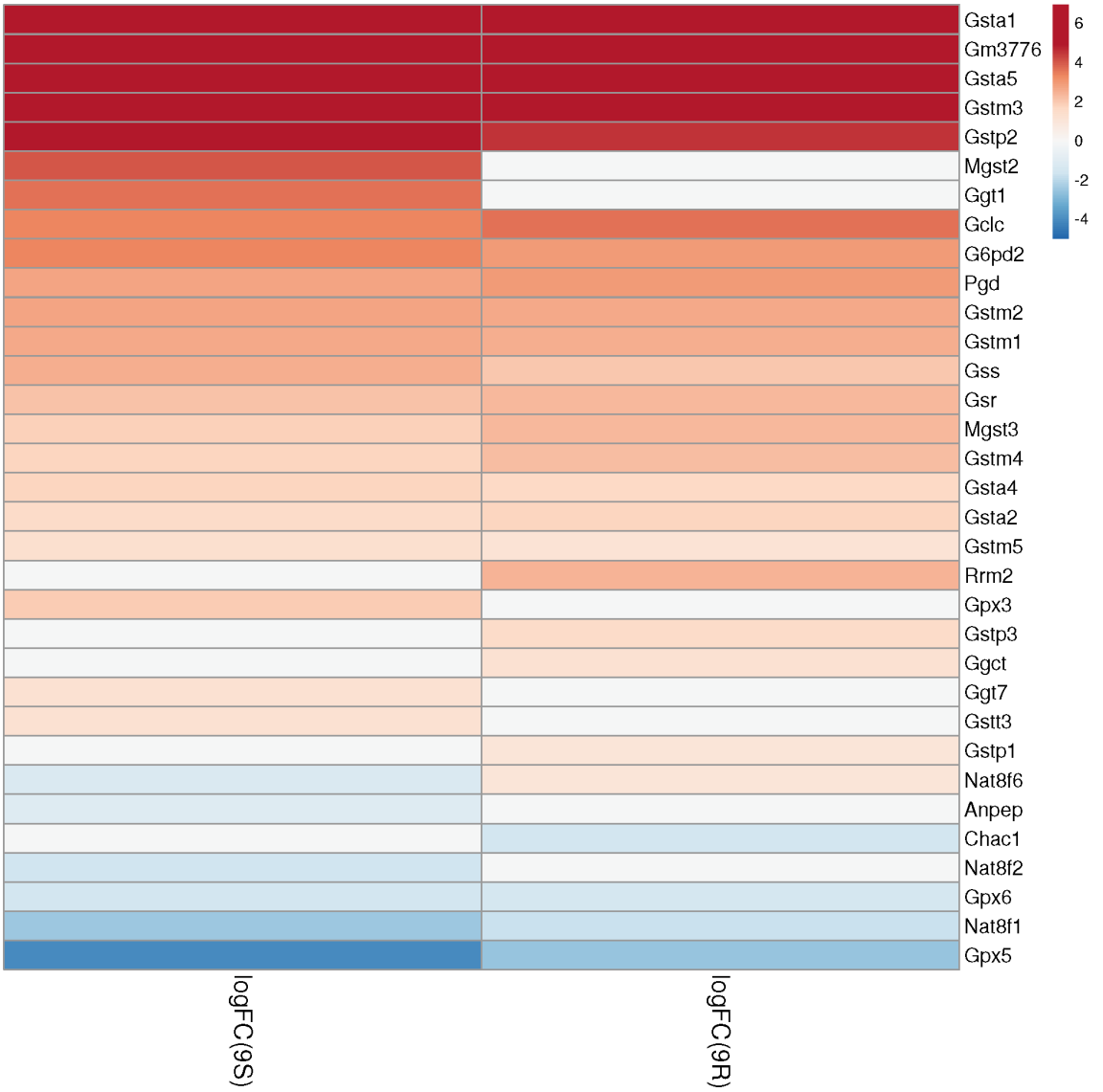

Figure 4.21. Heatmap showing differentially expression genes which affect the KEGG pathway “Glutathione metabolism” immediately post-exposure. Genes in blue are downregulated and genes in red are upregulated. Genes in white were excluded based on FDR >0.05 or $\log_2$FC < 1. logFC(9S) = Log base 2 fold change for senecionine-exposed mice. logFC(9R) = Log base 2 fold change for riddelliine-exposed mice.

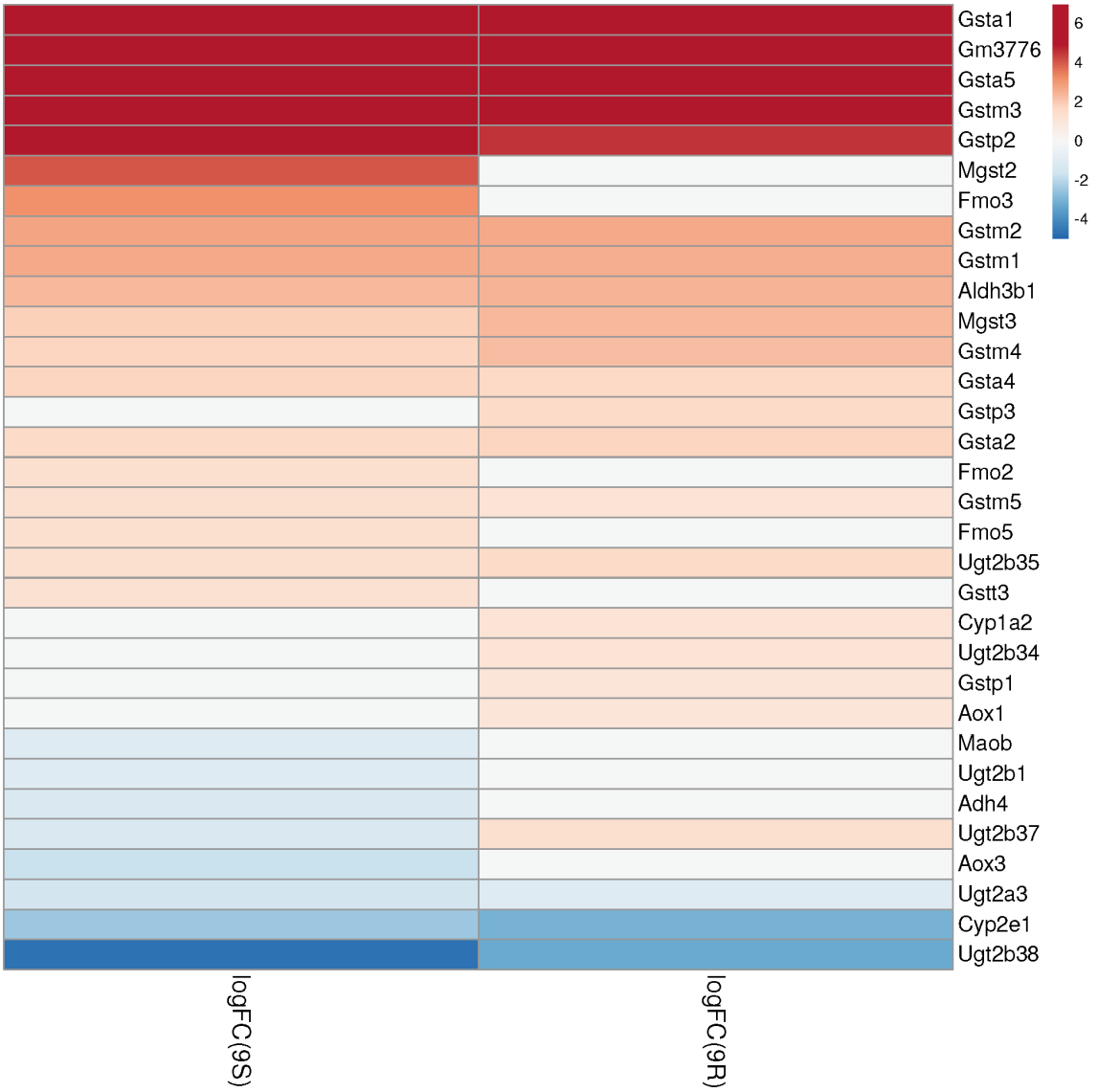

Figure 4.22. Heatmap showing differentially expression genes which affect the KEGG pathway “Drug metabolism-cytochrome p450”. Genes in blue are downregulated and genes in red are upregulated. Genes in white were excluded based on FDR >0.05 or $\log_2$FC < 1. logFC(9S) = Log base 2 fold change for senecionine-exposed mice. logFC(9R) = Log base 2 fold change for riddelliine-exposed mice.

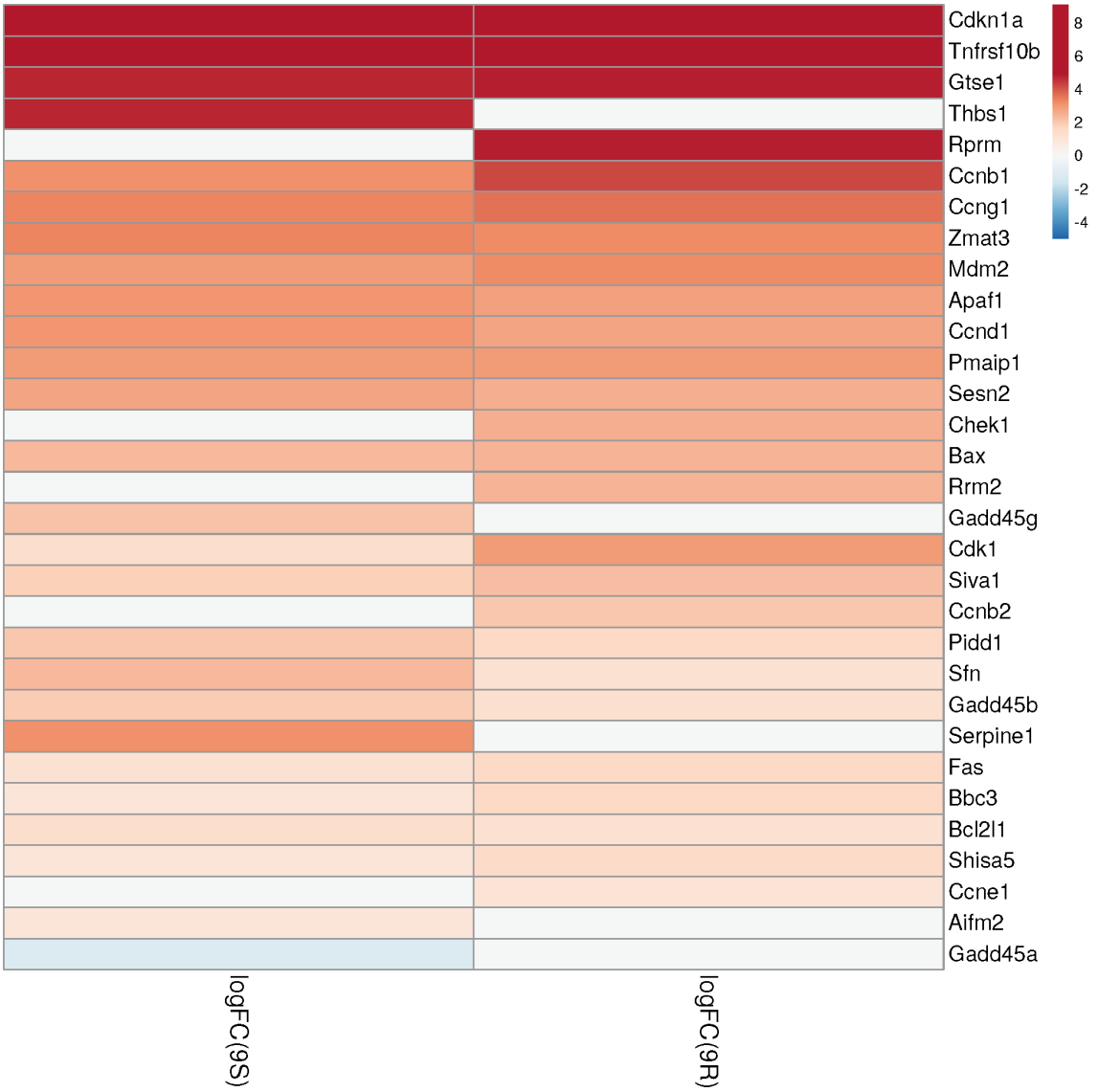

Figure 4.23. Heatmap showing differentially expression genes which affect the KEGG pathway “p53 signaling pathway” immediately post-exposure. Genes in blue are downregulated and genes in red are upregulated. Genes in white were excluded based on FDR >0.05 or $\log_2$FC < 1. logFC(9S) = Log base 2 fold change for senecionine-exposed mice. logFC(9R) = Log base 2 fold change for riddelliine-exposed mice.

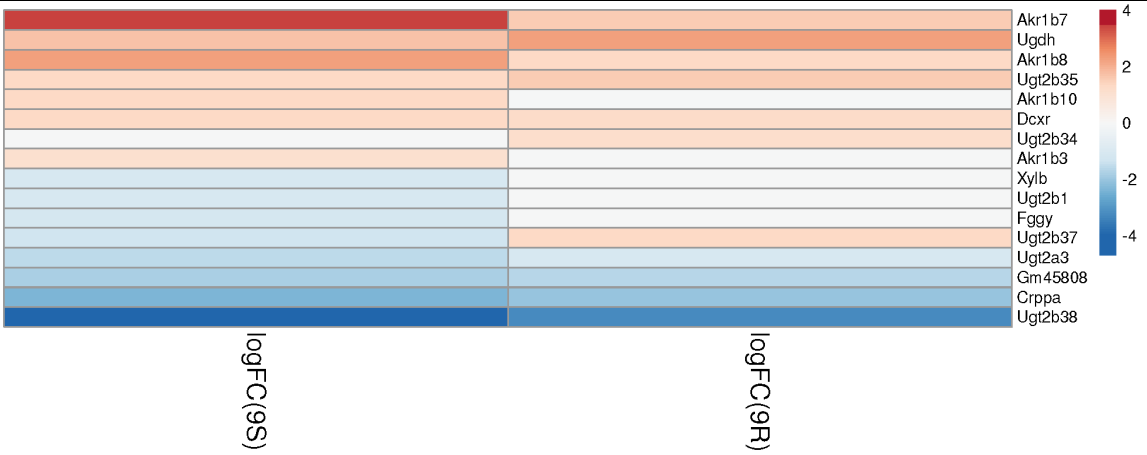

Figure 4.24. Heatmap showing differentially expression genes which affect the KEGG pathway "Pentose and glucuronate interconversions" immediately post-exposure. Genes in blue are downregulated and genes in red are upregulated. Genes in white were excluded based on FDR >0.05 or $\log_2$FC < 1. logFC(9S) = Log base 2 fold change for senecionine-exposed mice. logFC(9R) = Log base 2 fold change for riddelliine-exposed mice.

Gene Expression Related to Metabolism:

Phase 1 metabolism of PAs is the bioactivation step required for toxicity. The CYP450 enzymes are responsible for this metabolic step.[2,73] Twenty-four genes for CYP450 enzymes were differentially expressed immediately post-exposure in the senecionine and riddelliine. Fold changes for all CYP450 encoding genes can be seen in table 13. Cyp2a4, Cyp4f16, Cyp1a1, Cyp4f39, and Cyp2a5 were the upregulated CYP450 genes and Cyp2a4 had the greatest fold-change for riddelliine and senecionine immediately following exposure. Figures 4.26 and 4.27 show the fold change of the 24 differentially expressed CYP450 genes at the immediate post-exposure point, and at 28-days post-exposure. These genes all moved toward a reduced magnitude of fold-change during the 28-day period of recovery. Phase 2 metabolism of PAs is achieved mainly by glutathione conjugation. Glucuronidation also participates to a lesser extent.[73,74] Genes encoding for

proteins involved in glutathione conjugation and glucuronidation can be seen in table 14 below. Genes encoding for glutathione s-transferase and glutathione synthase were upregulated. Two glutathione peroxidase genes were down regulated. Genes encoding for UDP glucuronosyltransferase were both upregulated and downregulated. Ugt2b37, which encodes for UDP glucuronosyltransferase 2 family, polypeptide B37 was one of the few genes that was dysregulated in opposite directions by senecionine and riddelliine, with senecionine-exposure resulting in downregulation and riddelliine-exposure leading to upregulation.

Phase I Metabolism:

Twenty-four genes encoding for CYP450 enzymes were differentially expressed by mice exposed to senecionine and riddelliine. These genes all moved in the same direction, either up or down (See table 13 for differentially expressed genes involved in phase I metabolism of PAs). Upregulated CYP450 genes included Cyp2a4, Cyp4f16, Cyp1a1, Cyp4f39 and Cyp2a5. Heliotrine did not cause upregulation of any CYP450 genes, and only caused downregulation of one (Cyp2b9). See figures 4.26 and 4.27 below.

Table 4.13. Fold change (log base 2) for cytochrome p450 genes immediately post-exposure (day 9). Genes highlighted in red are upregulated and those in blue are downregulated.

Name	Description	logFC (Sen.)	logFC (Rid.)	logFC (Helio.)
Cyp2a4	cytochrome P450, family 2, subfamily a, polypeptide 4	6.89	7.27	0.87
Cyp4f16	cytochrome P450, family 4, subfamily f, polypeptide 16	3.19	2.68	0.55
Cyp1a1	cytochrome P450, family 1, subfamily a, polypeptide 1	2.11	2.27	0.61
Cyp4f39	cytochrome P450, family 4, subfamily f, polypeptide 39	1.22	2.90	-0.52
Cyp2a5	cytochrome P450, family 2, subfamily a, polypeptide 5	1.62	2.28	-0.06

Cyp2d9	cytochrome P450, family 2, subfamily d, polypeptide 9	-1.08	-1.09	-0.18
Cyp4a32	cytochrome P450, family 4, subfamily a, polypeptide 32	-1.15	-1.28	-0.39
Cyp4f15	cytochrome P450, family 4, subfamily f, polypeptide 15	-1.29	-1.27	-0.12
Cyp2u1	cytochrome P450, family 2, subfamily u, polypeptide 1	-1.92	-1.07	-0.12
Cyp17a1	cytochrome P450, family 17, subfamily a, polypeptide 1	-1.32	-2.03	-0.51
Cyp2c23	cytochrome P450, family 2, subfamily c, polypeptide 23	-2.71	-1.32	0.05
Cyp4a14	cytochrome P450, family 4, subfamily a, polypeptide 14	-2.44	-1.98	-1.00
Cyp2c54	cytochrome P450, family 2, subfamily c, polypeptide 54	-3.02	-1.41	-0.51
Cyp4a10	cytochrome P450, family 4, subfamily a, polypeptide 10	-2.57	-1.91	-0.81
Cyp2c37	cytochrome P450, family 2. subfamily c, polypeptide 37	-2.38	-2.49	-0.31
Cyp2d40	cytochrome P450, family 2, subfamily d, polypeptide 40	-3.23	-1.86	-0.68
Cyp46a1	cytochrome P450, family 46, subfamily a, polypeptide 1	-2.97	-2.29	-0.60
Cyp2e1	cytochrome P450, family 2, subfamily e, polypeptide 1	-2.48	-3.01	-0.21
Cyp2c40	cytochrome P450, family 2, subfamily c, polypeptide 40	-3.24	-2.36	-0.80
Cyp2c29	cytochrome P450, family 2, subfamily c, polypeptide 29	-3.63	-2.48	-0.30
Cyp4a12b	cytochrome P450, family 4, subfamily a, polypeptide 12B	-3.44	-3.09	0.61
Cyp2d13	cytochrome P450, family 2, subfamily d, polypeptide 13	-4.32	-2.32	-0.04
Cyp4a12a	cytochrome P450, family 4, subfamily a, polypeptide 12a	-5.02	-1.93	0.20
Cyp2b9	cytochrome P450, family 2, subfamily b, polypeptide 9	-4.45	-4.88	-3.48

Abbreviations: Sen. = senecionine, Rid = riddelliine, Helio. = heliotrine

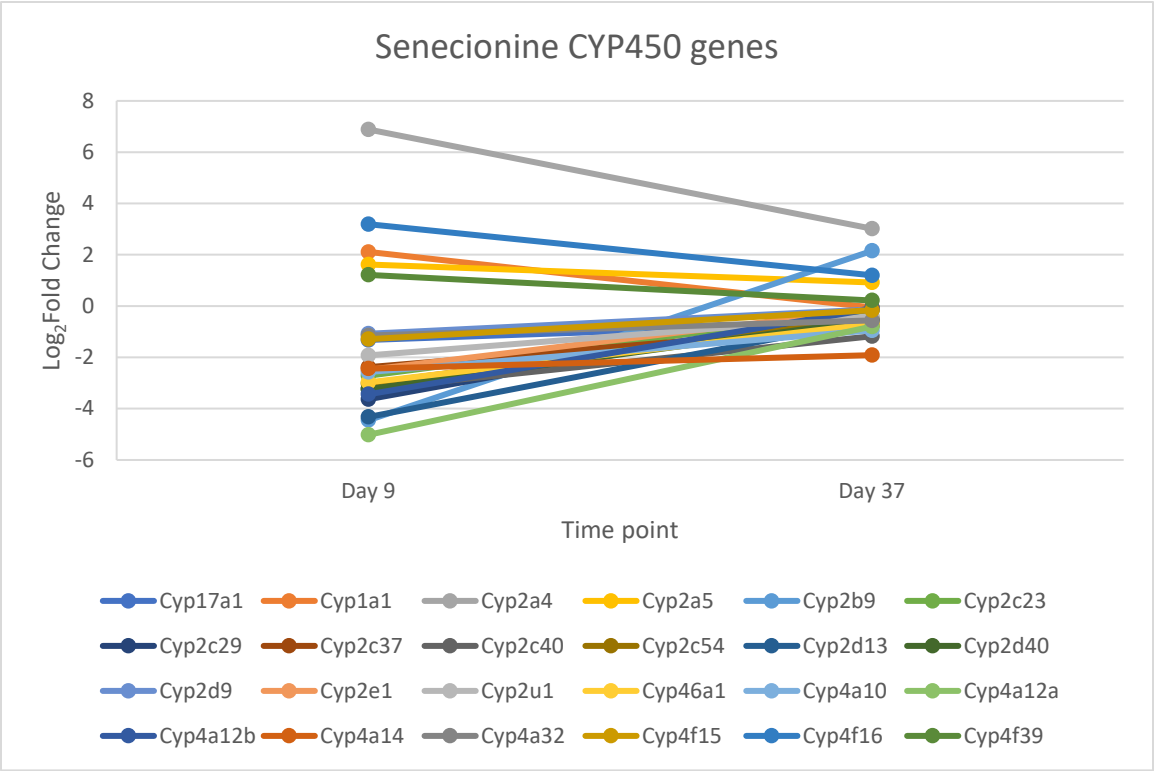

Figure 4.25. change of cytochrome p450 genes in mice exposed to senecionine at two time points, immediately post-exposure (day 9) and 28 days post-exposure (day 37).

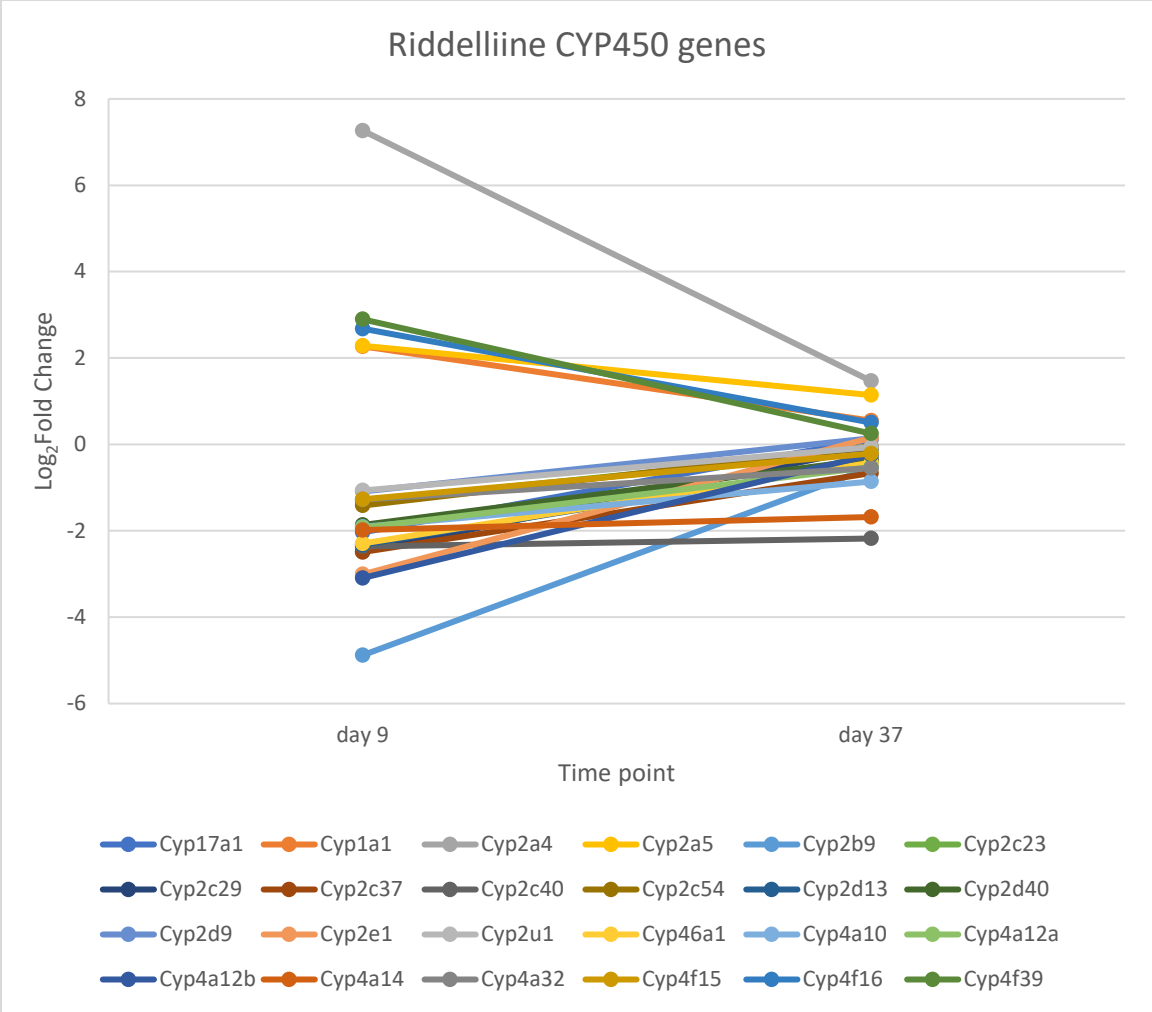

Figure 4.26. Log2fold change of cytochrome p450 genes in mice exposed to riddelliine at two time points, immediately post-exposure (day 9) and 28 days post-exposure (day 37).

Phase II Metabolism:

Glutathione binding is the main metabolic pathway for PAs, and glucuronidation contributes to a lesser degree.[2,74] The KEGG pathway "glutathione metabolism" was significantly affected by both senecionine and riddelliine. Genes encoding for glutathione s-transferase (Gsta1, Gsta2, Gsta4, Gsta5, Gstm1, Gstm2, Gstm3, Gstm4, Gstm5, Gstp2, Mgst3), glutathione synthase, and glutathione reductase were upregulated. Genes

encoding for glutathione peroxidase (Gpx5, Gpx6) were downregulated. Senecionine and riddelliine also affected the KEGG pathway "pentose and glucuronate interconversion", which is related to glucuronidation. Glucuronidation has only recently been identified as a contributor to phase II metabolism of PAs.[74] Differential expression of six genes encoding for UDP glucuronosyltransferases (Ugt2b35, Ugt2b34, Ugt2b1, Ugt2b37, Ugt2a3, and Ugt2b38) occurred with riddelliine and senecionine exposure. See table 14 for log fold changes of genes involved in phase II metabolism of PAs. The only genes involved in phase two metabolism which were dysregulated in mice exposed to heliotrine immediately post-exposure were Gstp2 and Ugt2b38.

Table 4.14. Fold change (log base 2) for genes involved in phase II metabolism immediately post-exposure. Upregulated genes are highlighted in red while downregulated genes are highlighted in blue.

Name	Description	logFC (Sen.)	logFC (Rid.)	logFC (Helio.)
Gsta1	glutathione S-transferase, alpha 1 (Ya)	6.69	6.94	1.17
Gstm3	glutathione S-transferase, mu 3	5.11	5.02	0.45
Gstp2	glutathione S-transferase, pi 2	5.35	4.56	1.84
Gsta5	glutathione S-transferase alpha 5	5.05	6.24	0.71
Gstm2	glutathione S-transferase, mu 2	2.73	2.65	-0.18
Gstm1	glutathione S-transferase, mu 1	2.62	2.56	0.09
Mgst3	microsomal glutathione S-transferase 3	1.86	2.32	-0.38
Gstm4	glutathione S-transferase, mu 4	1.79	2.27	-0.37
Gstm5	glutathione S-transferase, mu 5	1.35	1.16	-0.02
Gsta2	glutathione S-transferase, alpha 2 (Yc2)	1.59	1.80	-0.28
Gsr	glutathione reductase	2.15	2.34	0.03
Gss	glutathione synthetase	2.57	2.09	0.11
Gsta4	glutathione S-transferase, alpha 4	1.79	1.61	0.09
Gpx5	glutathione peroxidase 5	-4.03	-2.52	-0.05
Gpx6	glutathione peroxidase 6	-1.53	-1.42	-0.33
Ugt1a10	UDP glycosyltransferase 1 family, polypeptide A10	1.28	2.45	0.63

Ugt1a10	UDP glycosyltransferase 1 family, polypeptide A10	1.28	2.45	0.63
Ugt2b34	UDP glucuronosyltransferase 2 family, polypeptide B34	0.54	1.16	0.06
Ugt2b35	UDP glucuronosyltransferase 2 family, polypeptide B35	1.33	1.55	-0.19
Ugt2b37	UDP glucuronosyltransferase 2 family, polypeptide B37	-1.29	1.34	0.50
Ugt2a3	UDP glucuronosyltransferase 2 family, polypeptide A3	-1.55	-1.07	-0.13
Ugt3a2	UDP glycosyltransferases 3 family, polypeptide A2	-2.85	-1.70	-0.18
Ugt2b38	UDP glucuronosyltransferase 2 family, polypeptide B38	-4.69	-3.28	1.52
Ugt3a1	UDP glycosyltransferases 3 family, polypeptide A1	-4.35	-2.68	-0.39

Abbreviations: Sen. = senecionine, Rid = riddelliine, Helio. = heliotrine.

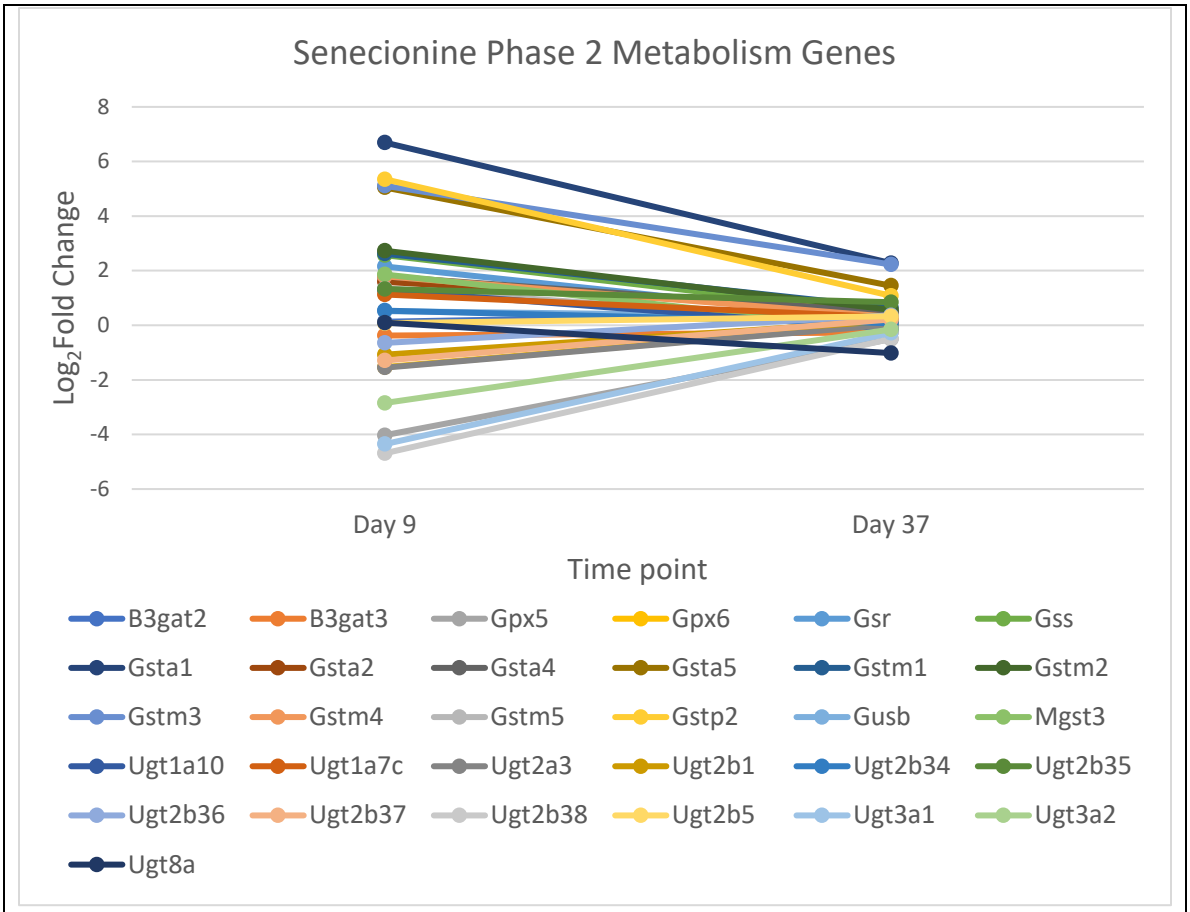

Figure 4.27. Log base 2-fold change of genes associated with phase 2 metabolism of PAs in senecionine-exposed mice.

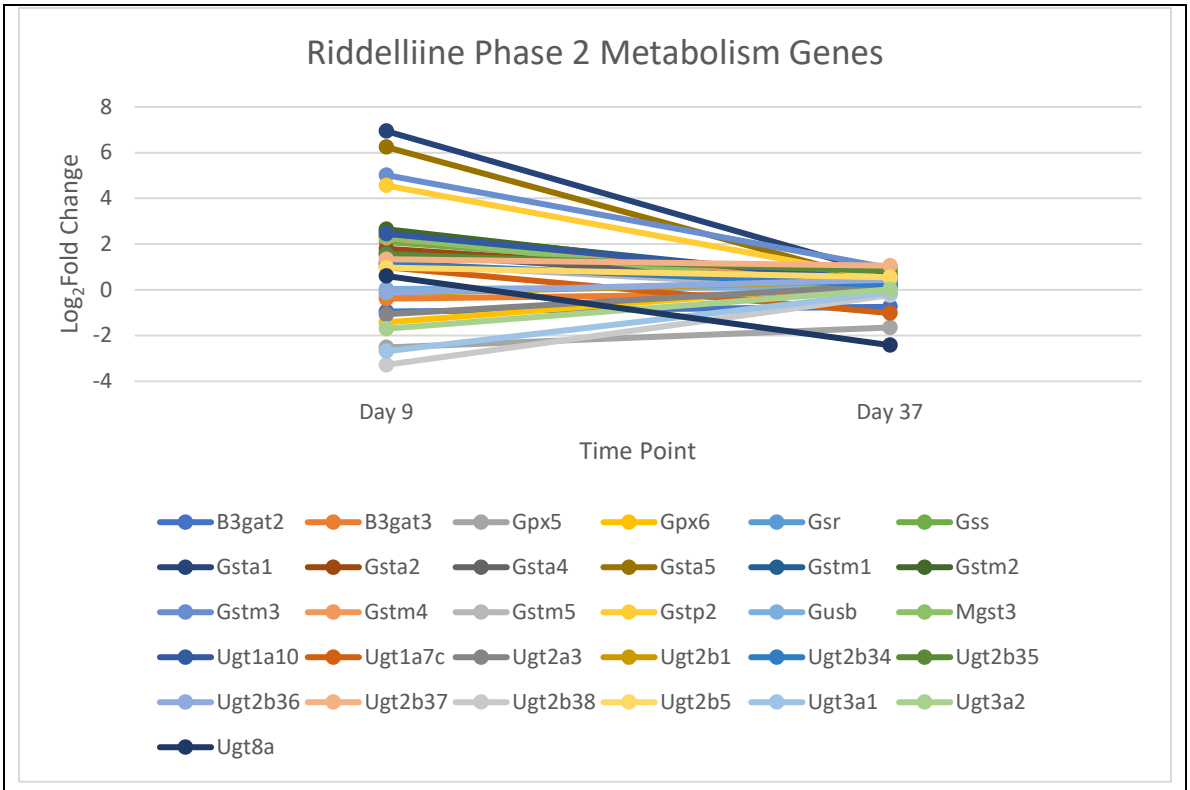

Figure 4.28. Log base 2-Fold change of genes associated with phase 2 metabolism of PAs for riddelliine-exposed mice.

Additional Metabolic Pathways:

The two main groups of hepatic transporters are the solute carrier (SLC) proteins and the ATP-binding cassette (ABC) proteins. The solute carrier (SLC) family of proteins has been shown to affect PA uptake in-vitro, indicating a potential role in PA toxicokinetics.[75] SLC genes were dysregulated in all three PA groups immediately post-exposure. Senecionine exposed mice had 99 SLC family genes which were dysregulated, while riddelliine-exposed mice had 66 and heliotrine exposed mice had 2. At 28-day post-exposure, senecionine-exposed mice had 8 dysregulated SLC genes, while riddelliine-exposed mice had none, and heliotrine-exposed mice had 1. Genes encoding

for ABC proteins were also dysregulated. Senecionine-exposed mice had 18 dysregulated ABC genes, riddelliine-exposed mice had 12, and heliotrine-exposed mice had one at the immediate post-exposure time point. After the 28-day recovery period, senecionine-exposed mice had two dysregulated ABC genes, while riddelliine exposed mice had two and heliotrine-exposed mice had none.

Heliotrine KEGG Pathways:

Heliotrine had no significant effect on KEGG pathways related to PA metabolism or neoplasia at either time point when an FDR cutoff of > 0.05 was applied.

Gene Ontology Terms, Immediate Post-Exposure Group:

Figure 4.29 below shows Gene Ontology terms which were affected by both senecionine and riddelliine. In this study, gene ontology was less illustrative of the toxic effects than KEGG pathway analysis.

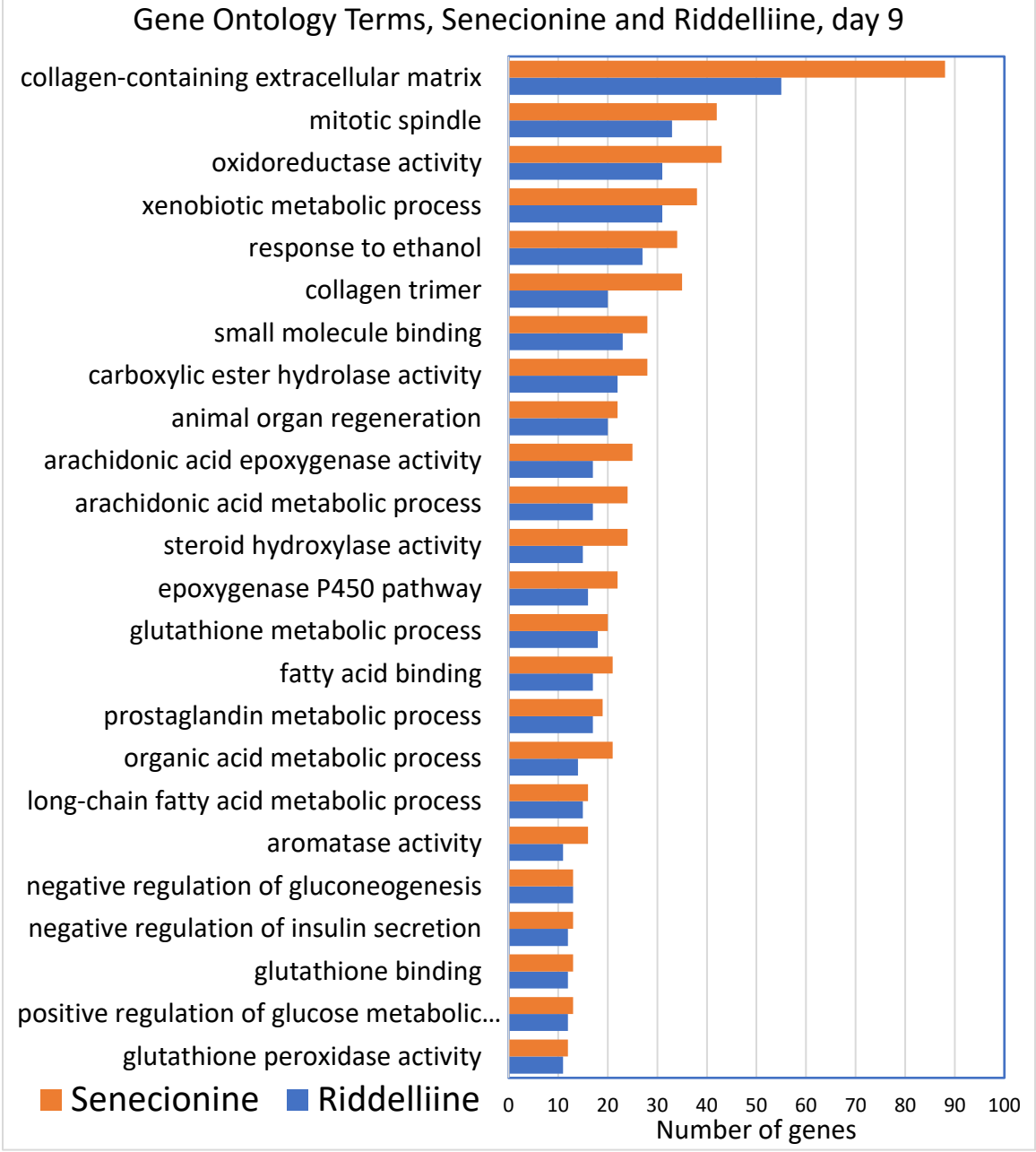

Figure 4.29. Gene Ontology (GO) terms affected by senecionine and riddelliine. The x axis shows the number of DEGs belonging to the GO term.

28-Day Post-Exposure (Day 37) Gene Expression Findings:

At the 28-day post-exposure time point senecionine-exposed mice had the greatest number of DEGs at 341, followed by riddelliine-exposed mice at 179, and heliotrine-exposed mice had the fewest at 111. The number of DEGs for senecionine and riddelliine was approximately ten percent of the number of DEGs immediately post exposure. For heliotrine, the number of DEGs was nearly the same, indicating that the DEGs in the heliotrine-exposed group occurred incidentally. Figure 10 shows Venn diagrams of the gene expression results for all 3 PAs at both time points.

Differentially Regulated Genes at Both Time-Points:

Senecionine:

In senecionine-exposed mice, 206 genes were upregulated and 68 were downregulated at both time points. Genes that were only differentially regulated immediately post-exposure included 1652 upregulated genes and 1081 downregulated genes. Genes that were only differentially regulated at 28-day post-exposure included 39 upregulated and 29 downregulated genes. See figure 4.30. KEGG pathways of interest which were significantly affected at both time-points include “p53 signaling pathway”, “proteoglycans in cancer”, “small cell lung cancer”, “bladder cancer”, and “MAPK signaling pathway”. The change in expression of cancer related genes affected by senecionine are shown in figure 4.33. Fold changes tended to move toward zero over time, indicating recovery after the toxic insult.

Riddelliine:

In riddelliine-exposed mice, 96 genes were upregulated and 29 were downregulated at both time points. Genes that were only differentially regulated immediately post-exposure included 1031 upregulated genes and 861 downregulated genes. Genes that were only differentially regulated at 28 days post-exposure included 27 upregulated and 27 downregulated genes. See figure 4.31. KEGG pathways of interest which were affected by riddelliine at both timepoints include “P53 signaling pathway”, “MicroRNAs in cancer”, “pathways in cancer” and “hepatocellular carcinoma”. The change in expression of cancer related genes affected by riddelliine are shown in figure 4.34. Fold changes tended to move toward zero over time, indicating recovery after the toxic insult.

Heliotrine:

In heliotrine-exposed mice, 14 genes were upregulated and 2 were downregulated at both day 9 and day 37. Genes that were only differentially regulated immediately post-exposure included 62 upregulated genes and 34 downregulated genes. Genes that were only differentially regulated at 28-day post-exposure included 45 upregulated and 50 downregulated genes. See figure 4.32. At the 28-day post-exposure time point, no KEGG pathways were significantly affected in the heliotrine-exposed group.

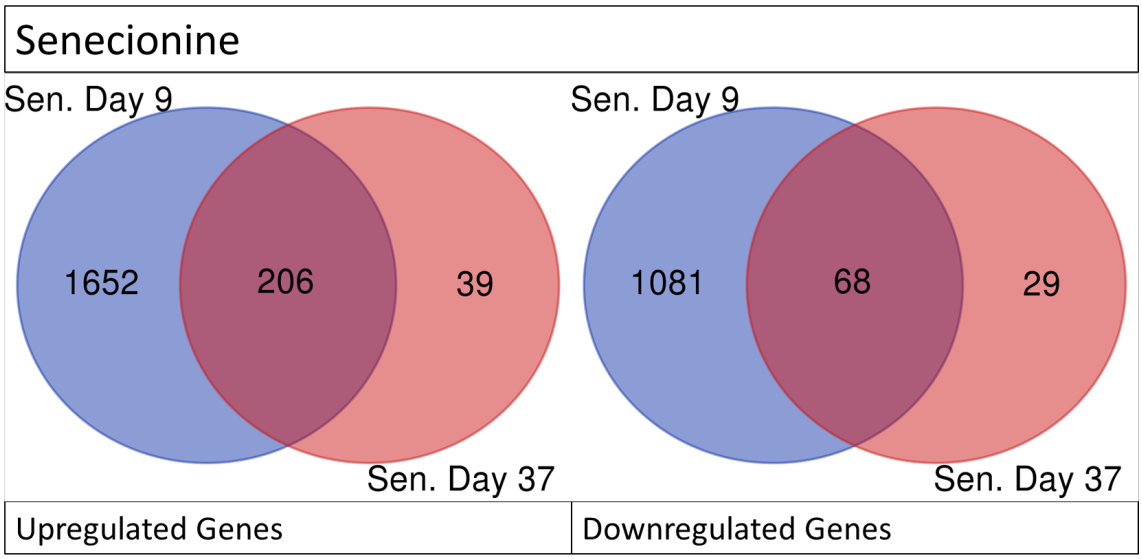

Figure 4.30 Venn diagram showing differentially expressed genes in mice exposed to senecionine immediately post-exposure (day 9) and 28 days post-exposure (day 37).

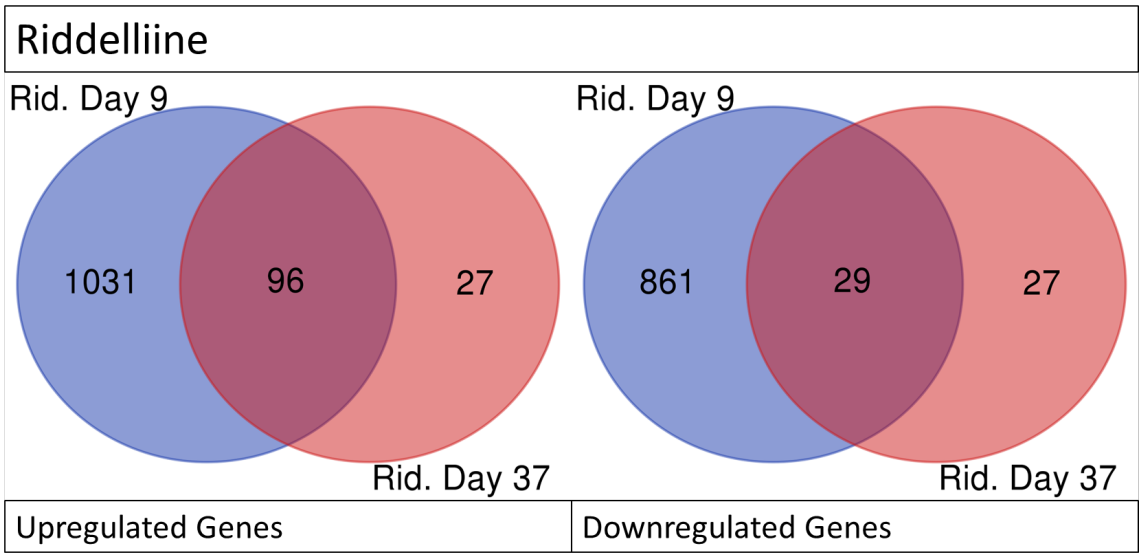

Figure 4.31 Venn diagram showing differentially expressed genes in mice exposed to riddelliine immediately post-exposure (day 9) and 28 days post-exposure (day 37).

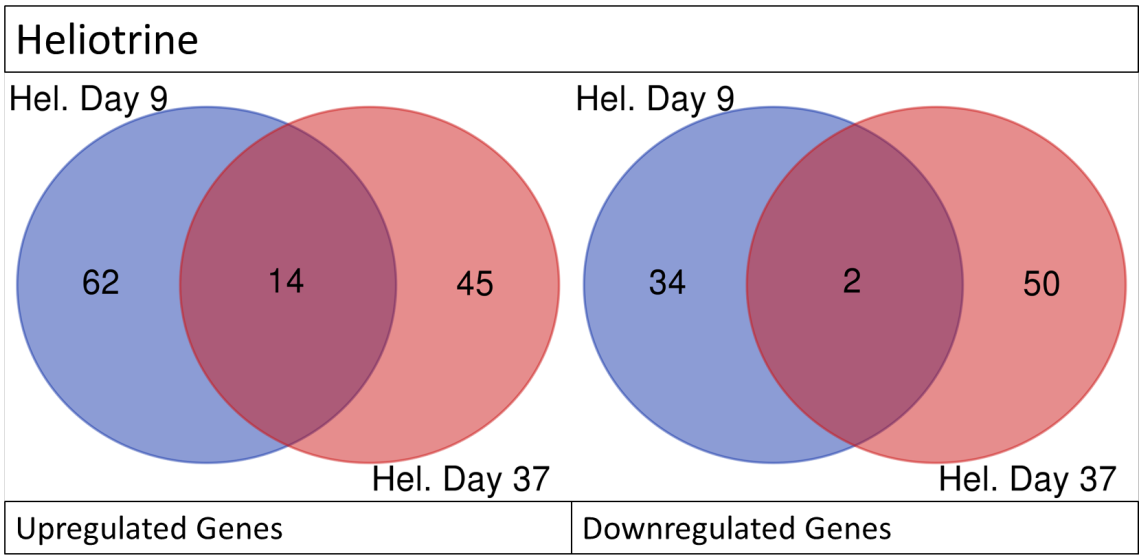

Figure 4.32 Differentially expressed genes in mice exposed to heliotrine immediately post-exposure (day 9) and 28 days post-exposure (day 37).

28-day Post-Exposure KEGG Pathway Analysis:

KEGG pathways affected by senecionine with FDR values less than 0.05 can be seen in table 15. Table 16 shows KEGG pathways in the senecionine group 28-day post-exposure which are of interest to this study but had FDR values greater than 0.05. KEGG pathways affected by riddelliine with FDR values less than 0.05 can be seen in table 4.17.

Table 4.15 KEGG pathways affected at 28 days post-exposure (day 37) by exposure to senecionine.

Senecionine 28-day post-exposure KEGG pathways	GeneRatio	BgRatio	FDR	Enrichment score
p53 signaling pathway	10/144	73/8907	5.67E-05	6.63
Platinum drug resistance	8/144	83/8907	0.0067	4.26
Proteoglycans in cancer	12/144	198/8907	0.0068	4.08

Viral protein interaction with cytokine and cytokine receptor	7/144	87/8907	0.024	3.3
Small cell lung cancer	7/144	95/8907	0.026	3.07
Endocrine resistance	7/144	94/8907	0.028	3.1
Cytokine-cytokine receptor interaction	13/144	286/8907	0.029	3.15
Bladder cancer	5/144	41/8907	0.029	3.32
MAPK signaling pathway	13/144	300/8907	0.03	2.95

KEGG pathways with FDR values greater than 0.05 were excluded. Table 17 shows tables which are of interest to this study but had FDR values greater than 0.05. GeneRatio = k/n where k is the number of DEGs in the senecionine group in the specific KEGG pathway and n is the number of DEGs in the senecionine group that are in any KEGG pathway. BgRatio = M/N where M is the total number of genes in the specified KEGG pathway and N is the total number of genes in all KEGG pathways. FDR and p values are calculated based on these ratios. The enrichment score is calculated using the pvalue and the gene ratio and BgRatio.

Table 4.16 KEGG pathways of interest that were excluded because of FDR > 0.05 at which include DEGs in the senecionine, 28-day post-exposure group.

Description	GeneRatio	BgRatio	FDR	Enrichment score
Pathways in cancer	17/144	540/8907	0.13	2.21
MicroRNAs in cancer	7/144	160/8907	0.18	1.82
Hepatocellular carcinoma	7/144	172/8907	0.23	1.67
Non-small cell lung cancer	4/144	73/8907	0.27	1.52
Chronic myeloid leukemia	4/144	78/8907	0.29	1.43
Chemical carcinogenesis - DNA adducts	4/144	85/8907	0.35	1.31

GeneRatio = k/n where k is the number of DEGs in the senecionine group in the specific KEGG pathway and n is the number of DEGs in the senecionine group that are in any KEGG pathway. BgRatio = M/N where M is the total number of genes in the specified KEGG pathway and N is the total number of genes in all KEGG pathways. FDR and p

values are calculated based on these ratios. Pathways are listed in order of pathway enrichment score.

Table 4.17. KEGG pathways of interest affected at 28 days post-exposure in the riddelliine group.

Description	GeneRatio	BgRatio	FDR	Enrichment score
p53 signaling pathway	11/70	73/8907	1.4E-09	11.12
Bladder cancer	6/70	41/8907	6.34E-05	6.16
Chronic myeloid leukemia	7/70	78/8907	0.0001	5.64
Thyroid cancer	5/70	36/8907	0.0004	5.09
Small cell lung cancer	7/70	95/8907	0.0003	5.06
Glioma	6/70	73/8907	0.0006	4.67
Melanoma	6/70	73/8907	0.0006	4.67
Non-small cell lung cancer	6/70	73/8907	0.0006	4.67
MicroRNAs in cancer	8/70	160/8907	0.000686	4.48
Platinum drug resistance	6/70	83/8907	0.0008	4.35
Colorectal cancer	6/70	88/8907	0.001	4.21
Pathways in cancer	14/70	540/8907	0.001	4.2
Endometrial cancer	5/70	58/8907	0.001	4.07
Endocrine resistance	6/70	94/8907	0.001	4.05
Proteoglycans in cancer	8/70	198/8907	0.002	3.82
Pancreatic cancer	5/70	75/8907	0.003	3.53
Cell cycle	6/70	125/8907	0.005	3.37
FoxO signaling pathway	6/70	133/8907	0.006	3.23
Breast cancer	6/70	146/8907	0.009	3.01
Prostate cancer	5/70	99/8907	0.01	2.98
Basal cell carcinoma	4/70	62/8907	0.01	2.86
Phenylalanine, tyrosine and tryptophan biosynthesis	2/70	8/8907	0.015	2.78
Hepatitis C	6/70	165/8907	0.015	2.74

JAK-STAT signaling pathway	6/70	169/8907	0.016	2.69
Hepatocellular carcinoma	6/70	172/8907	0.017	2.65
Thyroid hormone signaling pathway	5/70	121/8907	0.018	2.59
Cellular senescence	6/70	180/8907	0.019	2.55
Gastric cancer	5/70	149/8907	0.041	2.21

KEGG pathways with FDR values greater than 0.05 were excluded. GeneRatio=k/n where k is the number of DEGs in the riddelliine group in the specific KEGG pathway and n is the number of DEGs in the senecionine group that are in any KEGG pathway. BgRatio = M/N where M is the total number of genes in the specified KEGG pathway and N is the total number of genes in all KEGG pathways. FDR and p values are calculated based on these ratios. Enrichment score is calculated based on the pvalue, gene ratio and BgRatio.

Table 4.18. Heatmap showing log base 2 of the fold change (log_2FC) for genes from the KEGG pathway “Pathways in Cancer” that are significantly dysregulated by senecionine and riddelliine. Upregulated genes are highlighted red while downregulated genes are blue.

Gene	Description	logFC (Sen. D1)	logFC (Sen. D28)	logFC (Rid. D1)	logFC (Rid. D28)
Cdkn1a	cyclin-dependent kinase inhibitor 1A (P21)	9.04	3.98	9.08	3.52
Gsta1	glutathione S-transferase, alpha 1 (Ya)	6.69	2.28	6.94	0.65
Gm3776	predicted gene 3776	6.55	1.84	6.86	0.5
Gstp2	glutathione S-transferase, pi 2	5.35	1.08	4.56	0.48
Gstm3	glutathione S-transferase, mu 3	5.11	2.23	5.02	0.95
Gsta5	glutathione S-transferase alpha 5	5.05	1.45	6.24	0.25
Nqo1	NAD(P)H dehydrogenase, quinone 1	4.37	0.94	4.35	0.68
Mgst2	microsomal glutathione S-transferase 2	4.1	0.14	2.67	-1.31
Mmp9	matrix metallopeptidase 9	3.46	0.51	-0.51	-0.37

Fgf21	fibroblast growth factor 21	3.46	0.13	2.82	-1.21
Pgf	placental growth factor	3.38	0.28	2.7	2.04
Myc	myelocytomatosis oncogene	3.1	1.15	2	2.33
Apaf1	apoptotic peptidase activating factor 1	3.07	1.36	2.86	1.02
Ccnd1	cyclin D1	3.05	2.67	2.8	1.5
Csf2rb2	colony stimulating factor 2 receptor, beta 2, low-affinity (granulocyte-macrophage)	3.04	1.03	0.65	0.05
Mmp2	matrix metallopeptidase 2	3	1.84	1.76	1.47
Itga2	integrin alpha 2	2.95	0.38	0.55	0.38
Cdkn2b	cyclin dependent kinase inhibitor 2B	2.94	0.15	1.87	-0.07
Nos2	nitric oxide synthase 2, inducible	2.94	3.11	-1.59	0.81
Pmaip1	phorbol-12-myristate-13-acetate-induced protein 1	2.93	1.48	2.91	1.68
Mdm2	transformed mouse 3T3 cell double minute 2	2.91	1.24	3.26	1.04
Polk	polymerase (DNA directed), kappa	2.84	1.48	2.86	1.01
Gstm2	glutathione S-transferase, mu 2	2.73	0.57	2.65	0.16
Gstm1	glutathione S-transferase, mu 1	2.62	0.64	2.56	0.34
Csf3r	colony stimulating factor 3 receptor (granulocyte)	2.35	0.59	0.16	-0.3
Bax	BCL2-associated X protein	2.31	0.84	2.48	0.85
Notch1	notch 1	2.25	1.28	2.07	1.01
Il7r	interleukin 7 receptor	2.17	0.74	1.17	0.02
Col4a1	collagen, type IV, alpha 1	2.16	0.89	1.08	0.52
Gadd45g	growth arrest and DNA-damage-inducible 45 gamma	2.15	-0.66	0.46	0.99
Hgf	hepatocyte growth factor	2.13	0.61	1.17	-0.43
Rad51	RAD51 recombinase	2.08	1.01	3.63	1.44
Calml4	calmodulin-like 4	2.04	-0.03	1.01	-0.55
Lama5	laminin, alpha 5	2.03	0.91	0.69	0.19
Col4a2	collagen, type IV, alpha 2	1.99	1.04	0.8	0.67
Jag2	jagged 2	1.96	0.5	0.97	0.39
Gadd45b	growth arrest and DNA-damage-inducible 45 beta	1.93	0.81	1.33	-0.8
Rac3	Rac family small GTPase 3	1.91	0.58	2.56	0.05
Mgst3	microsomal glutathione S-transferase 3	1.86	-0.17	2.32	-0.17

Itga6	integrin alpha 6	1.84	0.39	0.81	-0.22
Gstm4	glutathione S-transferase, mu 4	1.79	0.31	2.27	0.27
Runx1	runt related transcription factor 1	1.79	0.23	0.09	-0.09
Gsta4	glutathione S-transferase, alpha 4	1.79	0.47	1.61	0.14
Ppard	peroxisome proliferator activator receptor delta	1.75	-1.09	1.66	-1.54
Plcg2	phospholipase C, gamma 2	1.69	0.59	0.69	-0.29
Il4ra	interleukin 4 receptor, alpha	1.65	0.14	1.17	0.07
Notch3	notch 3	1.62	0.36	1.28	0.2
Rasgrp4	RAS guanyl releasing protein 4	1.6	0.48	0.37	-0.51
Il3ra	interleukin 3 receptor, alpha chain	1.59	0	1.23	-0.35
Gsta2	glutathione S-transferase, alpha 2 (Yc2)	1.59	0.5	1.8	0.34
Gng2	guanine nucleotide binding protein (G protein), gamma 2	1.59	0.63	0.78	0.4
Txnrd1	thioredoxin reductase 1	1.56	0.61	1.81	0.37
Ralgds	ral guanine nucleotide dissociation stimulator	1.55	0.02	0.46	0.11
Hmox1	heme oxygenase 1	1.48	0.76	0.75	0.12
Tgfb3	transforming growth factor, beta 3	1.46	-0.28	0.26	1.05
Bcl2l1	BCL2-like 1	1.46	0.34	1.27	0.34
Csf2rb	colony stimulating factor 2 receptor, beta, low-affinity (granulocyte-macrophage)	1.46	0.27	0.55	-0.04
Csf2ra	colony stimulating factor 2 receptor, alpha, low-affinity (granulocyte-macrophage)	1.44	0.43	0.4	-0.23
Spi1	spleen focus forming virus (SFFV) proviral integration oncogene	1.42	0.6	0.69	-0.3
Lamc2	laminin, gamma 2	1.41	0.24	1.05	-0.1
Slc2a1	solute carrier family 2 (facilitated glucose transporter), member 1	1.41	0.01	0.93	0.04
Kitl	kit ligand	1.38	-0.76	0.59	-0.49
Adcy1	adenylate cyclase 1	1.38	0.47	-0.94	-0.05
Notch4	notch 4	1.37	0.51	0.2	0.37
Lamc1	laminin, gamma 1	1.36	0.52	0.7	0.12
Itga3	integrin alpha 3	1.36	0.1	0.36	-0.02

Sufu	SUFU negative regulator of hedgehog signaling	1.35	0.37	0.47	0
Gstm5	glutathione S-transferase, mu 5	1.35	0.04	1.16	-0.03
Zbtb16	zinc finger and BTB domain containing 16	1.33	-0.82	1.26	-1.2
Pik3cd	phosphatidylinositol-4,5-bisphosphate 3-kinase catalytic subunit delta	1.33	0.69	0.36	-0.07
Tgfbr2	transforming growth factor, beta receptor II	1.31	0.9	0.89	0.3
Fos	FBJ osteosarcoma oncogene	1.3	1.83	-0.22	0.48
Tgfa	transforming growth factor alpha	1.27	0.45	1.2	0.24
Cxcr4	chemokine (C-X-C motif) receptor 4	1.26	0.9	0.38	0.51
Pik3r3	phosphoinositide-3-kinase regulatory subunit 3	1.25	0.29	1.21	0.39
Fas	Fas (TNF receptor superfamily member 6)	1.25	0.02	1.63	0.1
Ccna2	cyclin A2	1.23	0.84	2.24	0.81
Gstt3	glutathione S-transferase, theta 3	1.21	-0.02	0.11	0.3
Jak3	Janus kinase 3	1.18	0.31	1.15	0.15
Gngt2	guanine nucleotide binding protein (G protein), gamma transducing activity polypeptide 2	1.17	0.52	0.64	0.12
Adcy7	adenylate cyclase 7	1.16	0.74	0.16	-0.13
Plcb2	phospholipase C, beta 2	1.15	0.33	0.6	-0.46
Pld1	phospholipase D1	1.14	0.15	0.66	-0.1
Ednrb	endothelin receptor type B	1.13	0.09	0.69	-0.03
Tgfb1	transforming growth factor, beta 1	1.12	0.55	0.52	0.01
Lamb1	laminin B1	1.1	0.17	0.65	0.03
Gli3	GLI-Kruppel family member GLI3	1.09	-0.34	0.17	-0.6
Bbc3	BCL2 binding component 3	1.08	-0.15	1.69	-0.11
Wnt9b	wingless-type MMTV integration site family, member 9B	1.08	0.5	0.79	0.15
Cdh1	cadherin 1	1.08	0.3	0.27	0.11
Nfkb2	nuclear factor of kappa light polypeptide gene enhancer in B cells 2, p49/p100	1.07	0.26	0.3	0.01
Rac2	Rac family small GTPase 2	1.03	0.69	0.23	-0.1

Pdgfb	platelet derived growth factor, B polypeptide	1.03	0.77	-0.29	0.79
Gstp3	glutathione S-transferase pi 3	0.96	0.37	1.52	0.29
Msh6	mutS homolog 6	0.95	0.56	1.43	0.3
Rock2	Rho-associated coiled-coil containing protein kinase 2	0.91	0.47	1.03	0.11
Gstp1	glutathione S-transferase, pi 1	0.61	0.09	1.07	0.29
Ccne1	cyclin E1	0.61	1.09	1.16	1.3
Traf5	TNF receptor-associated factor 5	0.55	0.01	1	0.22
Birc5	baculoviral IAP repeat-containing 5	0.5	-0.14	2.19	0.83
E2f1	E2F transcription factor 1	0.08	0.46	1.06	0.37
Prkca	protein kinase C, alpha	-0.54	0.33	-1.2	0
Gm45713	predicted gene 45713	-0.77	-0.28	-2.03	0.02
Tcf7l2	transcription factor 7 like 2, T cell specific, HMG box	-0.89	-0.42	-1.03	-0.3
Txnrd3	thioredoxin reductase 3	-0.93	-0.23	-1.13	0.04
Brca2	breast cancer 2, early onset	-1.06	-0.29	-1.1	-0.3
Fzd4	frizzled class receptor 4	-1.06	0.13	-0.86	0.23
Txnrd2	thioredoxin reductase 2	-1.11	-0.21	-1.02	-0.05
Col4a4	collagen, type IV, alpha 4	-1.13	-0.19	-0.95	-0.01
Agt	angiotensinogen (serpin peptidase inhibitor, clade A, member 8)	-1.13	-0.41	-1.28	-0.14
Msh3	mutS homolog 3	-1.13	-0.03	-0.92	0.09
Gadd45a	growth arrest and DNA-damage-inducible 45 alpha	-1.14	0.31	0.19	1.29
Plcb1	phospholipase C, beta 1	-1.15	-0.54	-1.15	-0.47
Rps6ka5	ribosomal protein S6 kinase, polypeptide 5	-1.22	-0.36	-0.85	-0.04
Egfr	epidermal growth factor receptor	-1.29	-0.25	-0.94	0.01
Frat2	frequently rearranged in advanced T cell lymphomas 2	-1.31	-0.4	-1.13	-0.02
Il15ra	interleukin 15 receptor, alpha chain	-1.32	-0.16	-1.32	-0.09
Cxcl12	chemokine (C-X-C motif) ligand 12	-1.35	-0.47	-1.07	-0.28
Fzd7	frizzled class receptor 7	-1.36	-0.04	-0.72	0.5
Rxrg	retinoid X receptor gamma	-1.44	-0.02	-0.8	-0.02
Col4a3	collagen, type IV, alpha 3	-1.48	-0.72	-1.59	-0.31

Il12rb1	interleukin 12 receptor, beta 1	-1.52	-0.23	-1.22	-0.51
Gng7	guanine nucleotide binding protein (G protein), gamma 7	-1.55	-0.71	-2.23	-0.43
Cebpa	CCAAT/enhancer binding protein (C/EBP), alpha	-1.71	-0.08	-0.93	0.36
Bdkrb2	bradykinin receptor, beta 2	-1.87	-1.29	-0.96	-1.63
Fzd8	frizzled class receptor 8	-2	-0.61	-2.2	0.11
Il2ra	interleukin 2 receptor, alpha chain	-2.15	-0.59	-0.81	-0.76
Gm5741	predicted gene 5741	-2.19	0.53	-0.98	0.21
Lamb3	laminin, beta 3	-2.27	-0.52	-2.08	-0.43
Ar	androgen receptor	-2.41	-1.78	-1.26	-1.24
Fgf9	fibroblast growth factor 9	-2.77	-0.13	-1.17	0.09
Shh	sonic hedgehog	-2.8	-0.82	-1.81	-0.88
Gngt1	guanine nucleotide binding protein (G protein), gamma transducing activity polypeptide 1	-2.94	-1	-1.94	-0.92
Lama3	laminin, alpha 3	-3.48	-1.06	-1.39	-0.67

Abbreviations: Rid. = riddelliine, Sen. = senecionine. D1 = Immediate post exposure, D28 = 28-days after exposure. LogFC = log base 2 fold change compared to the control group. Numbers in bold had false discovery rates (FDR) values greater than 0.05.

Table 4.19. Heatmap showing the log base 2 fold changes for genes that are classified in KEGG pathways related to cancer that are significantly dysregulated by senecionine and riddelliine. Upregulated genes are highlighted red while downregulated genes are blue.

Gene	Description	LogFC (Sen. D1)	LogFC (Sen. D28)	LogFC (Rid. D1)	LogFC (Rid. D28)
Cdkn1a	cyclin-dependent kinase inhibitor 1A (P21)	9.04	3.98	9.08	3.52
Cacna2d4	calcium channel, voltage-dependent, alpha 2/delta subunit 4	7.4	4.23	2.97	1.26
Gsta1	glutathione S-transferase, alpha 1 (Ya)	6.69	2.28	6.94	0.65
Gm3776	predicted gene 3776	6.55	1.84	6.86	0.5
Tnfrsf10b	tumor necrosis factor receptor superfamily, member 10b	6.22	3.62	6.4	3.07
Nrg1	neuregulin 1	5.36	3.39	4.39	1.24

Gstm3	glutathione S-transferase, mu 3	5.11	2.23	5.02	0.95
Gtse1	G two S phase expressed protein 1	4.72	2.8	4.89	2.73
Plk2	polo like kinase 2	4.07	1.99	3.79	1.58
Zmat3	zinc finger matrin type 3	3.36	2.22	3.22	1.74
Ccng1	cyclin G1	3.34	1.83	3.68	1.73
Cd63	CD63 antigen	3.31	1.29	2.55	0.26
Serpine1	serine (or cysteine) peptidase inhibitor, clade E, member 1	3.11	2.23	-1.02	1.24
Myc	myelocytomatosis oncogene	3.1	1.15	2	2.33
Apaf1	apoptotic peptidase activating factor 1	3.07	1.36	2.86	1.02
Ccnd1	cyclin D1	3.05	2.67	2.8	1.5
Mmp2	matrix metallopeptidase 2	3	1.84	1.76	1.47
Col1a1	collagen, type I, alpha 1	2.98	1.47	1.84	1.57
Pmaip1	phorbol-12-myristate-13-acetate-induced protein 1	2.93	1.48	2.91	1.68
Mdm2	transformed mouse 3T3 cell double minute 2	2.91	1.24	3.26	1.04
Polk	polymerase (DNA directed), kappa	2.84	1.48	2.86	1.01
Plau	plasminogen activator, urokinase	2.78	2.28	1.78	2.16
Dusp8	dual specificity phosphatase 8	2.58	1.96	1.75	0.52
Ptpn7	protein tyrosine phosphatase, non-receptor type 7	2.29	1.74	0.16	0.7
Notch1	notch 1	2.25	1.28	2.07	1.01
Abcb1a	ATP-binding cassette, sub-family B (MDR/TAP), member 1A	2.22	1.37	1.1	0.28
Lum	lumican	2.21	1.07	1.74	0.53
Src	Rous sarcoma oncogene	2.17	1.84	1.76	0.76
Cacnb3	calcium channel, voltage-dependent, beta 3 subunit	2	1.69	1.11	1.23
Col4a2	collagen, type IV, alpha 2	1.99	1.04	0.8	0.67
Ppard	peroxisome proliferator activator receptor delta	1.75	-1.09	1.66	-1.54
Dusp4	dual specificity phosphatase 4	1.75	1.32	0.33	0.82
Map3k20	mitogen-activated protein kinase kinase kinase 20	1.39	1.24	1.63	0.92
Fos	FBJ osteosarcoma oncogene	1.3	1.83	-0.22	0.48
Pak1	p21 (RAC1) activated kinase 1	1.13	1.09	1.04	0.13
Sult2a7	sulfotransferase family 2A, dehydroepiandrosterone (DHEA)-preferring, member 7	0.9	2.06	2.62	3.8

Cdkn2a	cyclin dependent kinase inhibitor 2A	0.54	2.2	-0.29	3.28
Hhip	Hedgehog-interacting protein	0.51	-0.81	-0.08	-1.64
Ntrk2	neurotrophic tyrosine kinase, receptor, type 2	0.41	3.27	0.92	1.93
Dusp2	dual specificity phosphatase 2	0.24	1.55	-0.08	0.41
Wnt5a	wingless-type MMTV integration site family, member 5A	0.15	-1.08	0.1	-0.38
Gpc3	glypican 3	-0.27	0.95	-1.29	2.2
Flt1	FMS-like tyrosine kinase 1	-0.32	-1.07	-0.34	-0.7
Hspb1	heat shock protein 1	-0.9	-1.06	0.37	-0.82
Gadd45a	growth arrest and DNA-damage-inducible 45 alpha	-1.14	0.31	0.19	1.29
Ar	androgen receptor	-2.41	-1.78	-1.26	-1.24
Fhit	fragile histidine triad gene	-2.58	-1.32	-2.48	-1.24
G6pc	glucose-6-phosphatase, catalytic	-2.89	-0.56	-2.56	-1.48
Camk4	calcium/calmodulin-dependent protein kinase IV	-3.07	-1.25	-2.51	-0.9
Lama3	laminin, alpha 3	-3.48	-1.06	-1.39	-0.67
Erbb4	erb-b2 receptor tyrosine kinase 4	-3.77	-1.4	-3.23	-0.79

Abbreviations: Rid. = riddelliine, Sen. = senecionine, LogFC = log base-2 fold change compared to the control group. D9 = day 9, immediately post-exposure. Fold changes moved towards zero after the 28-day recovery period.

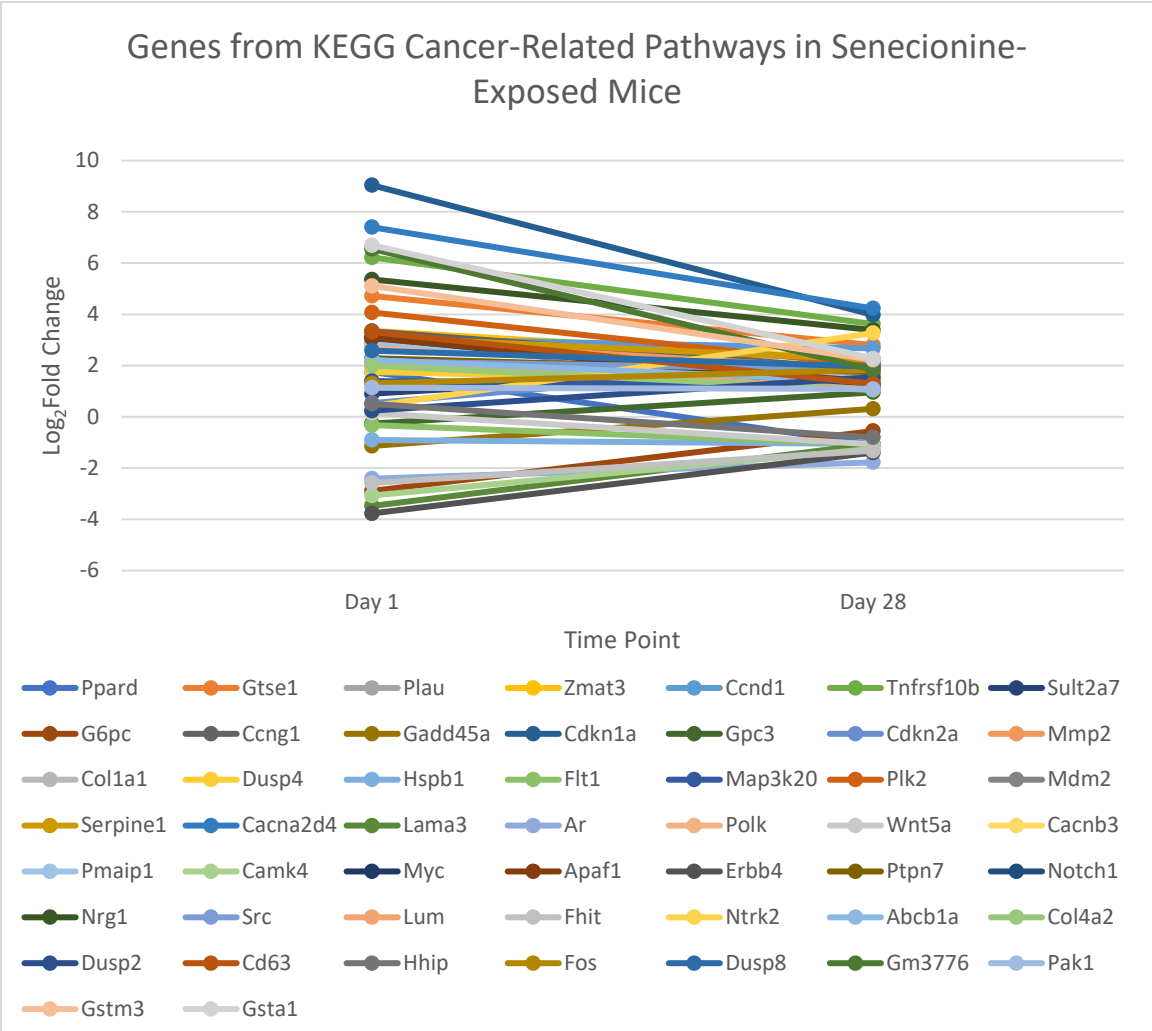

Figure 4.33 Senecionine-exposed mice. Genes from cancer related KEGG pathways which were dysregulated at at 28-days post-exposure. The change in log_2FC from day 1 (immediately post-exposure) to day 28 (28 days post-exposure), can be observed. Fold change moved toward zero for upregulated and downregulated genes.

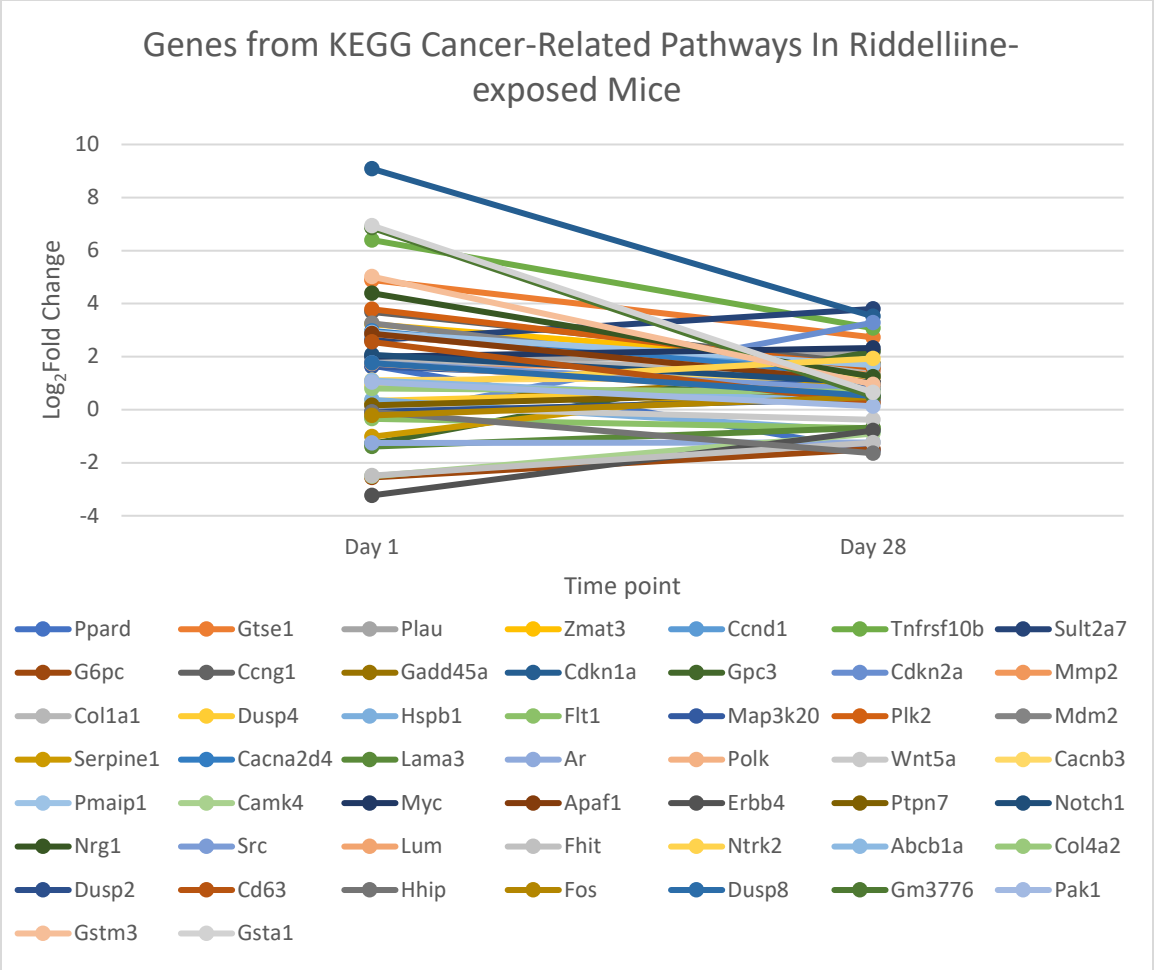

Figure 4.34. Riddelliine-exposed mice. Genes from cancer related KEGG pathways which were dysregulated at 28-days post-exposure. The change in log_2FC from day 1 (immediately post-exposure) to day 28 (28 days post-exposure), can be observed. Fold change moved toward zero for upregulated and downregulated genes.

Discussion:

PA toxicosis is an important problem for humans and animals. Exposure to PA containing plants occurs through contamination of feed or grain, consumption of herbal teas or supplements, or grazing. PAs are genotoxic carcinogens and therefore should be avoided whenever possible.[1,8,11] Studies using transcriptomic analysis to make direct

comparisons of the effects of PA exposure are few. Luckert et al. (2015) used whole genome sequencing to compare gene expression changes in four structurally unique PAs in vitro using human hepatocytes.[35] Other studies have analyzed gene expression changes induced by singular PAs in rat and mouse liver.[29,30,76,77] Evaluation of the transcriptome is a useful tool for investigating the effects of toxicants which may precede the development of morphologic lesions or serum biochemical changes.[78] This type of exposure is meant to replicate natural exposure as would occur in a contamination of grain or animal feed. The overall changes in clinical signs (weight loss), serum biochemistry assays, gross and microscopic lesions, hepatic pyrrole concentration and gene expression changes over time indicate an initial insult followed by a period of recovery. Senecionine and riddelliine caused similar changes in all assays evaluated. Both senecionine and riddelliine mainly caused dysregulation of genes related to metabolism and cancer, with fewer genes related to inflammation and other processes. Senecionine affected a substantially greater number of genes, as well as more marked changes in all other endpoints. Both riddelliine and senecionine resulted in initial dysregulation which was followed by a general reduction in the magnitude of the fold change towards zero at the second time point. At the 28-day post-exposure time point, senecionine caused dysregulation of a larger number of genes, but a greater proportion of the genes dysregulated by riddelliine were involved in KEGG pathways related to cancer. This may mean that riddelliine is more carcinogenic than senecionine, or that the severity of lesions caused by senecionine resulted in more lingering changes in gene expression, in addition to the genes involved in cancer development. The clinical signs, serum biochemical changes, and hepatic necrosis caused by senecionine were more severe than

riddelliine at both time points. Senecionine-exposed mice were the only group with significant serum biochemical changes and persistent liver necrosis at the 28-day post-exposure time-point. The senecionine-exposed group also had the most severe initial weight loss, serum biochemistry concentration changes and hepatic necrosis immediately after exposure. Senecionine caused larger foci of hepatic necrosis, compared to riddelliine which resulted in individual cell necrosis. Riddelliine-exposed mice completely recovered regarding clinical signs, serum biochemistry concentrations, and liver histopathology after the 28-day period of recovery. Importantly, senecionine exposure resulted in the greatest concentration of hepatic pyrroles in the immediate post-exposure necropsy group. Hepatic pyrroles are understood to be the main toxic metabolite that results in DNA damage and cell damage following PA bioactivation. The largest concentration occurring in senecionine-exposed mice most likely explains the reason senecionine exposure also had the most severe or marked changes in the other assays evaluated, including changes in gene expression. In the senecionine-exposed group there were persistent changes in serum biochemistry assays indicative of hepatocellular injury, as well as microscopic lesions of multifocal hepatic necrosis. The lesions and changes at the 28-day post exposure point were less severe than the immediate post-exposure changes. Riddelliine-exposed mice had the greatest average hepatic pyrrole concentration at this time point (1.26 +/- 1.36 nmol/g), but this was low compared to the initial measurement average (189.4 +/- 35.65 nmol/g). It is likely that the senecionine-exposed mice would also completely recover if additional time for recovery was allowed.

Mice exposed to heliotrine did not exhibit signs of toxicosis based on any of the assays used in this study. Oral LD50 information for heliotrine in mice is not available. Brown et al. (2015) found that heliotrine was the most hepatotoxic when administered to chicks by oral gavage.[47] Heliotrine is also reportedly toxic to rats, and has been shown to have deleterious in-vitro effects on human hepatocytes.[79,80] These differences in toxicity between species indicate that all PAs should be avoided when possible. One should not assume a specific PA is safe for consumption based on a study in a different species. The lack of hepatotoxicity in heliotrine-exposed mice is most likely due to a lack of biotransformation from the CYP450 enzymes present. If enhanced phase 2 metabolism was the reason for the lack of toxic effects, it would be expected that genes involved in metabolism and excretion would be upregulated in these mice, which was not the case. Comparisons regarding carcinogenic potential of the PAs tested is another important aspect of this experiment. Heliotrine is not carcinogenic at the dose administered (0.129 mmol/kg/day for eight days) based on the gene expression profile. Riddelliine is a known carcinogen, and as expected caused dysregulation of multiple pathways involved in the development of cancer. Senecionine has been considered as a carcinogen largely based on research performed on other PAs, including riddelliine. Senecionine was clearly the most toxic PA in this study, but based on the number of DEGs it was also the most genotoxic PA, even compared to riddelliine. Based on the similarity of the gene expression results observed following exposure to senecionine and riddelliine, these results strengthen the assertion that senecionine is likely carcinogenic to mice. Using the gene expression results to ascertain which PA, senecionine or riddelliine is more carcinogenic is a complex question which we will discuss. Senecionine affected multiple

pathways associated with cancer development at the early time point, but 28-day post-exposure senecionine affected fewer cancer related KEGG pathways than riddelliine. On the other hand, senecionine caused dysregulation of more individual genes from KEGG pathways related to cancer than riddelliine, therefore it could be argued that senecionine is as likely or even more likely than riddelliine to exert carcinogenic effects in mice. KEGG enrichment analysis accounts for the overall number of dysregulated genes to determine which pathways are significantly affected. Riddelliine had a smaller number of DEGs, but a greater proportion of those DEGs were members of KEGG pathways related to cancer development. Furthermore, in the senecionine-exposed group there were persistent changes in serum biochemistry assays indicative of hepatocellular injury, as well as microscopic lesions of multifocal hepatic necrosis. The changes in serum biochemistry and microscopic lesions were less severe than at the immediate post-exposure time point. The initial weight loss, alterations in serum biochemistry concentrations, lesions of hepatic necrosis, and hepatic pyrrole concentrations were most significant in magnitude in the senecionine-exposed group. These persistent changes most likely explain why the senecionine group also had the largest number of differentially expressed genes at 28 days post-exposure. The changes observed over time indicate that mice can fully recover following short duration hepatotoxic exposure to PAs. We speculate that if an additional time point was observed these mice most likely would have completely recovered regarding their gene expression profiles as well. Based on the common toxic mechanism observed in PA toxicosis, it is possible that other species may also recover following similar exposure of PAs, but additional studies are needed to confirm this. Direct comparison of the carcinogenicity of riddelliine and

senecionine would be best addressed by a side by side, long term carcinogenicity study with constant low dose exposure for the two-year duration of the experiment. Additional discussion and analysis of individual endpoints can be seen below.

Clinical Findings: Clinical Signs, Serum Biochemistry Data

Clinical Signs:

Senecionine exposed mice had the most severe clinical signs including weight loss, malaise, and alterations in serum biochemical assays indicative of hepatic insult. Weight loss and malaise were only observed during dosing. Riddelliine-exposed mice lost the second greatest amount of weight during dosing. Weight loss in the senecionine-exposed mice was more severe than expected and resulted in the need to shorten the dosing from the initially planned ten days to eight days. Heliotrine did not cause weight loss. A previous pilot study of senecionine described in chapter 2 showed that mice could tolerate this dose for ten days, but the mice in the pilot study ranged in age from 5-13 weeks as they were sourced from our breeding colony. In this study, all mice were seven weeks old at the start of dosing. The severe response illustrates the fact that young animals are more susceptible to PA toxicosis than adults.[2,81,82] After dosing was discontinued, animals in the 28-day post-exposure groups ceased to lose weight, and gradually began to gain weight. There was one mouse in the long term senecionine group that lost 0.82 g. after the 28-day recovery period, but all other animals gained weight. Mice exposed to riddelliine gained the smallest amount of weight, followed by senecionine, the control group, and heliotrine-exposed mice gained the largest amount. Average weight gain was not significantly different between senecionine and riddelliine. Weight gain in the heliotrine group was not significantly different than the control group.

Based on these changes, mice exposed to heliotrine did not experience immediate or delayed (28-day post-exposure) detrimental effects on body weight. Senecionine had the most severe immediate effects on body weight. Changes in weight over time again illustrate the fact that mice seem to recover following immediate post-exposure hepatotoxic doses of PAs.

Serum Biochemistry Data:

Immediate Post-Exposure Serum Biochemistry Data:

In the immediate post-exposure group, there were strong positive correlations between hepatic necrosis score and ALP, ALT, AST, total bilirubin, and cholesterol ($p < 0.0001$). Strong negative correlations were present between hepatic necrosis score and albumin and glucose ($p < 0.0001$). In the 28-day post-exposure group correlations between serum biochemistry values and hepatic necrosis score were weak or non-existent. Although nonspecific, serum concentrations of ALP, ALT, AST, total bilirubin, albumin, glucose and cholesterol can be useful indicators of hepatocellular injury from PAs depending on the clinical context. The important aspect of context is evidence of exposure, which can be proven by measuring the concentration of hepatic pyrroles. Other clinical scenarios which may indicate exposure to PA containing plants include visual detection of plant parts in stomach or rumen content, detection of plant material in hay, or observation of animals eating the plant. ALP, ALT, AST and total bilirubin are known indicators of hepatocellular injury, while albumin, glucose and cholesterol are indicators of hepatic function. Correlations between serum biochemistry assays and hepatic necrosis score, aside from cholesterol, are as expected.[83–86] Albumin concentrations were significantly decreased for mice exposed to senecionine and riddelliine in the immediate post-exposure

group. Glucose concentration was significantly reduced for senecionine and riddelliine. Serum glucose concentrations were significantly reduced immediately after exposure (day 9) for the groups exposed to senecionine and riddelliine. The most likely cause of glucose reduction is fasting due to inappetance.[83] Cholesterol was significantly increased for senecionine exposed mice, but the mean was based on only two values. Hypercholesterolemia can occur as a result of cholestasis, which could be present in this study, as indicated by the increase in ALP observed. Microscopic evidence of cholestasis was not present. Assays that can be indicators of liver damage in this study include total bilirubin, ALP, ALT, and AST. However, in chapter two, we demonstrated that AST may not be a good indicator in mice. Total bilirubin, ALT and ALP were significantly increased ($p \leq 0.05$) for riddelliine and senecionine. Mean ALT concentration was greatest for senecionine exposed mice, nearly doubling the value for riddelliine. AST concentration was significantly increased for mice exposed to senecionine.

28-Day Post-Exposure Serum Biochemistry Data:

In the 28-day post-exposure groups, ALP and ALT were significantly different than the control group for senecionine exposed mice, but not for riddelliine and heliotrine. Total protein and albumin were significantly increased in the heliotrine exposed group. BUN was significantly reduced for the senecionine and heliotrine groups. Cholesterol was significantly reduced for the riddelliine group. Sodium was significantly decreased for the heliotrine group. Elevations in ALP and ALT in senecionine-exposed mice are likely due to persistent hepatocellular necrosis which was observed microscopically. Abnormalities observed in heliotrine-exposed mice are likely unrelated to PA exposure, as these mice had not significant lesions, clinical signs, or even changes in gene expression at either

time point which would indicate hepatic insult. The decrease in cholesterol observed in riddelliine-exposed mice may also be unrelated to exposure, as there are no significant microscopic lesions which would indicate a hepatic cause. Lack of calorie intake may cause hypocholesterolemia, but these mice had not lost weight and had seemingly recovered from the PA exposure by all measures except some persistent gene expression changes.

Necropsy Findings:

Gross lesions in the immediate post exposure groups mainly included emaciation which was only observed in the mice immediately evaluated after exposure to senecionine and/or riddelliine. One of the senecionine-exposed mice in the immediate post-exposure group had multifocal pinpoint tan foci distributed throughout all liver lobes. In the 28-day post exposure group, mice recovered the lost weight and gained weight for the remainder of the experiment, and emaciation was not observed. Body weight data obtained at necropsy is discussed below.

Weight Data:

Final weights were measured after euthanasia and were therefore included in the necropsy data in addition to the clinical signs section. Senecionine exposed mice had the greatest average weight loss during dosing at 4.95 ± 1.05 g. Riddelliine was second at 2.67 ± 0.65 g, followed by heliotrine at 1.13 ± 0.4 g. Mice in the control group lost a small amount of weight (0.44 ± 0.54g) during dosing, which is attributed to inappetance and stress from gavaging. This effect of gavaging may also be the cause of weight loss in heliotrine-exposed mice as these mice did not have abnormalities in other assays to indicate toxicosis. Each PA group recovered their lost weight and eventually gained

weight over the 28-day recovery period. There were some statistically significant differences in weight gain over the course of the experiment. Senecionine and riddelliine-exposed mice gained significantly less weight than the control group. Riddelliine-exposed mice gained the smallest amount of weight, although not significantly different than senecionine. The reduced weight gain is attributable to PA-induced hepatic necrosis during growth and development. Although mice seemed to recover from exposure by nearly all endpoints measured, the reduced overall weight gain after a 28-day recovery period indicates that exposure may have lasting impacts on growth if it occurs in a young animal.

Liver Weights:

In the one-day post-exposure group, liver weights were significantly different for riddelliine and senecionine exposed mice compared to the control group, but not for heliotrine. Mean liver weight was greatest for mice exposed to riddelliine (1.524 g.), followed by senecionine (1.218 g.), and these values were statistically different ($p \leq 0.05$). Increases in liver weight can be associated with histologic changes including hepatocellular hypertrophy.[87] In. this case, senecionine and riddelliine-exposed mice had multifocal hepatocellular hypertrophy and/or swelling. Histologic lesions were most severe in senecionine-exposed mice, so the expectation would be for senecionine exposed mice to have the greatest liver weights. On the other hand, senecionine-exposed mice lost the greatest amount of weight which may have resulted in loss of liver weight. This could be the result of hepatocyte loss from necrosis. Hepatocyte atrophy could also contribute, but the microscopic appearance lesions of atrophy were not present. 28-day post-

exposure liver weights were not significantly different for any group including the control.

Calculation of liver to body weight ratio is performed to adjust for changes in body weight. In the immediate post-exposure necropsy group, liver to body weight ratio was greatest in riddelliine exposed mice at 0.074 ± 0.004, followed by senecionine at 0.073 ± 0.006. Heliotrine-exposed mice had liver to body weight ratios averaging at 0.044 ± 0.003 and control mice had an average ratio of 0.046 ± 0.001. Only senecionine and riddelliine were significantly different than the control group. The liver to body weight ratios for senecionine and riddelliine were not significantly different from each other. The increase in liver to body weight ratio in mice exposed to senecionine or riddelliine is most likely due to the presence of hepatocellular hypertrophy and/or cell swelling, which were observed microscopically in both groups.[87] At the 28 day post-exposure time point, there were no significant differences in liver to body weight ratio between any of the PA groups or the control group. The lack of significant differences after 28 days further supports the conclusion that mice recover following exposure to hepatotoxic doses of senecionine and riddelliine. In this study, liver to body weight ratio is preferable to liver weight alone due to weight loss in the senecionine and riddelliine-exposed mice.

Microscopic Findings:

Equimolar doses (0.129 mmol/kg/day) of senecionine, riddelliine and heliotrine were administered by gastric gavage. PA induced microscopic liver lesions differed in severity between the three PAs evaluated in this study. Senecionine clearly caused the most severe hepatic necrosis and is therefore, the most hepatotoxic among these three PAs.

Senecionine caused frequent foci of coagulative necrosis, mostly in midzonal areas with fewer foci in centrilobular and portal areas. Individual cell necrosis was also observed in senecionine-exposed mice. Riddelliine mainly caused individual cell necrosis. Hepatocellular hypertrophy/swelling was observed and mainly affected centrilobular areas. Heliotrine did not cause hepatocellular necrosis and is not hepatotoxic at the dose given in this study. Extrahepatic lesions were not observed for any of the PAs. Hepatic necrosis score had strong positive correlations with ALP, ALT, AST, total bilirubin, and cholesterol ($p < 0.0001$) in the immediate post-exposure group, which supports the validity of these serum biochemistry assays as indicators of hepatocellular injury in mice. In the 28-day post-exposure group the hepatocellular injury had resolved and correlations between serum biochemistry values and hepatic necrosis score were weak or non-existent. In chapter two, in a pilot study, mice were exposed to increasing doses of senecionine (2,4,8,15,30,45 mg/kg/day), riddelliine (4,8,15,30,45,90 mg/kg/day), and heliotrine (8,15, 30,45,90,180 mg/kg/day) for ten days and microscopic lesions were characterized. Mice exposed to senecionine developed hepatocellular hypertrophy and/or cell swelling with individual cell necrosis and multifocal necrosis starting in the midzonal areas and increasing to panlobular. Riddelliine exposed mice developed hepatocellular hypertrophy and/or cell swelling with individual cell necrosis and multifocal necrosis starting in the centrilobular areas and increasing to panlobular. Heliotrine-exposed mice did not develop lesions of cell swelling or necrosis at any dose given. The findings in the present study are similar the pilot study findings but lack the benefit of multiple doses to demonstrate the progression of lesions which may occur. The most likely reason for differences in severity and characterization of liver lesion is that mice in the current study

were uniformly seven weeks old at the start of dosing, whereas mice in the pilot study ranged from 5-13 weeks of age. Additionally, differences may be attributable to the different length of exposure compared to the pilot study from eight days to ten days. In the pilot study we detected differences in distribution of hepatocellular hypertrophy and/or swelling, and necrosis between PAs. The present study noted that riddelliine affected mainly centrilobular areas, senecionine mainly midzonal and heliotrine did not cause lesions. Our hypothesis for the cause of differing distribution within the lobule was that PAs are likely bioactivated by different CYP450 enzymes. Gene expression data which will be discussed below showed that expression levels of the genes encoding for CYP450 enzymes were nearly identical for senecionine and riddelliine, therefore different CYP450 distribution is an unlikely explanation. Alternate hypotheses for differences in distribution include differences in volatility of toxic metabolites or the presence of differing metabolites in addition to the measured pyrrole. Senecionine has been documented to produce an additional hepatotoxic metabolite, trans-4-hydroxy-2-hexenal, so both of these hypotheses are possible.[88]

Whole Genome RNA Sequencing:

Gene expression data was performed in this experiment to compare the carcinogenic, genotoxic, and metabolic effects of these PAs. Heliotrine was selected as an example of a relatively non-toxic PA in mice. Riddelliine was selected because of its status as a known carcinogen in mice and rats. The gene expression profile confirmed and strengthened evidence of riddelliines carcinogenicity and showed that this PA had a greater proportion of genes involved in KEGG pathways related to cancer at the 28-day post-exposure time point. Senecionine was selected because of its status as a hepatotoxic PA, with greater

hepatotoxicity than riddelliine, and relatively weaker evidence of carcinogenicity when compared to riddelliine. The overall gene expression profiles in mice exposed to senecionine and riddelliine were similar. The main pathways that were affected at the one-day post-exposure time point were those related to metabolism and cancer development, with fewer pathways related to inflammation. After the 28-day recovery period, gene expression levels in terms of fold change generally decreased toward a zero-fold change, indicating recovery following the initial injury. Senecionine had the greatest number of DEGs at both time points. Senecionine also caused the most severe hepatic necrosis and had the most marked serum biochemistry changed indicating hepatic insult. Further, it was the only PA with remaining hepatic necrosis at the 28-day post-exposure time point. For both riddelliine and senecionine, most of the DEGs immediately post-exposure had returned to normal following the 28-day recovery period, and those that were persistently dysregulated tended to have reduced in magnitude of the fold change at the second time point.

Heliotrine:

Heliotrine had no significant effect on KEGG pathways related to PA metabolism or neoplasia. Heliotrine exposure affected only a single KEGG pathway at the immediate post-exposure time point, namely “Bile secretion” in which only four genes were differentially expressed. At 28-days post exposure, no KEGG pathway was significantly affected in the heliotrine group. Mice in the heliotrine group had by far the smallest number of DEGs immediately post-exposure, with a total of 112 genes being dysregulated. At 28-days post exposure, heliotrine-exposed mice only had 111 DEGs. Heliotrine caused no histopathologic lesions or significant change in serum biochemical

assays. Taken with the information from chapters 2 and 3, this indicates that heliotrine has no effect in mice at the doses used in this study (0.129 mmol/kg/day or 40.36 mg/kg/day, for eight days) and in the previous chapters (8,15,30,45,90,180 mg/kg/day for 10 days). This contrasts with information on the toxic effects of heliotrine in other species. Brown et al. (2015) demonstrated that heliotrine was among the most hepatotoxic PAs when fed to California white chicks. Their study included comparisons with senecionine and riddelliine among other PAs.[47] Luckert et al. (2015) reported that heliotrine induced dysregulation of 1,806 genes in an in-vitro study using human hepatocytes.[35] Peterson and Jago (1980) demonstrated toxicity and teratogenicity caused by heliotrine in rats.[79] Heliotrine has also been shown to be carcinogenic to rats.[44] We hypothesized that lack of bioactivation by CYP450 enzymes is the most likely reason for lack of heliotrine toxicity in mice. The gene expression data confirmed that this is the most likely reason, as there was no dysregulation in pathways related to metabolism in heliotrine-exposed mice. Heliotrine did not cause upregulation of any CYP450 genes, and only caused downregulation of one (Cyp2b9). This indicates that heliotrine is not bioactivated in mice at the dose applied in this study. These differences warrant the use of caution when extrapolating experimental results from one species to another. It is prudent to avoid exposure to PAs with evidence of toxicity in any species. Our results indicate that heliotrine had no significant effect on gene expression under the exposure conditions used. The other endpoints in this study further support the conclusion heliotrine is not hepatotoxic to mice at the current dose and duration of exposure. The remaining discussion of gene expression data will focus on senecionine and riddelliine.

Senecionine and Riddelliine:

Senecionine and riddelliine had similar changes in gene expression and will be discussed together. These PAs represent two hepatotoxic PAs, and riddelliine is a known carcinogen. Our aim was to characterize gene expression in these PAs, which enables us to answer multiple questions. The strategy of performing gene expression at two time points is targeted at answering questions regarding carcinogenicity, in addition to recovery following PA exposure. Based on these similarities, senecionine is likely to be as carcinogenic as riddelliine. At the earlier, 1-day post exposure time-point senecionine-exposed mice had the largest number of DEGs at 3,006, and riddelliine-exposed mice had 2,007. Heliotrine-exposed mice had far fewer DEGs at 112. Riddelliine and senecionine had 1,535 common DEGs, nearly all of which were dysregulated in the same direction, either upregulated or downregulated. The genes which were dysregulated in opposite directions included Ugtb37, Cndp1, and Nat8f6. These genes respectively encode for the proteins UDP glucuronosyltransferase family 2 polypeptide B37, carnosine dipeptidase 1, and N-acetyltransferase 8 family member 6. These differences are likely of little consequence. Opposite expression of UDP glucuronosyltransferase 2 family could indicate a difference in the contribution of glucuronidation to metabolism of PAs between senecionine and riddelliine, but the other genes in the UDP glucuronosyltransferase family moved in the same directions for senecionine and riddelliine. Ugt2b35, Ugt1a10, and Ugt2b34 were upregulated and Ugt2a3, Ugt3a2, Ugt3a1, and Ugt2b38 were downregulated. Ugt2b1 was downregulated for senecionine, but not dysregulated for riddelliine. Glucuronidation is thought to play a minimal role in phase II metabolism of PAs, therefore this difference is likely unimportant.[74] Carnosine dipeptidase 1, and N-

acetyltransferase 8 family member 6 are unlikely to be related PA toxicosis based on current knowledge.[71] The shared gene expression patterns in mice exposed to senecionine and riddelliine 1-day post-exposure indicate that these PAs use the same mechanism of hepatotoxicity. Senecionine resulted in a greater number of DEGs, which may coincide with the increased severity of hepatotoxicity seen in this group. Mice were exposed to the same molar dose of riddelliine and senecionine, however in this study it appears that senecionine has greater hepatotoxic potential per mole than riddelliine. Senecionine-exposed mice exhibited the most severe weight loss and malaise compared to other groups. The presence of relatively severe hepatocellular degeneration and necrosis as well as weight loss when compared to riddelliine-exposed mice is the most likely reason for genes and pathways effected by senecionine and not riddelliine.

Functional Analysis of Gene Expression Data (KEGG Pathway Analysis):

One of the greatest challenges when using next generation sequencing and whole genome analysis to investigate a hypothesis is the large data sets that are obtained from such analyses. This challenge certainly was a factor in this experiment, particularly at the1-day post-exposure time point, immediate post-exposure time point in which thousands of genes were dysregulated in the senecionine and riddelliine exposed groups. Gene set enrichment analysis tools are currently the mainstay solution for taking large sets of DEGs and obtaining the relevant biological functions affected by the dysregulation. Pathway enrichment score calculations are performed using statistical software, but the calculation is based on the proportion of DEGs in the experimental set which fall into the pathway set. This calculation also factors in the overall number of DEGs in the experimental set to determine statistical significance.[89] There are multiple tools used for

pathway analysis. Among the most frequently used in current research are the Kyoto encyclopedia of genes and genomes (KEGG) and gene ontology (GO).[90–93] In this experiment both KEGG and GO pathway analyses were performed, however the KEGG pathway nomenclature was more consistent with the current body of literature regarding toxic mechanisms and carcinogenic effects of PAs. The false discovery rate (FDR) is a calculation based on the expected number of false positives in a data set. FDR is the cutoff measurement of choice when looking at large data sets, including genomic data from microarray and whole genome RNAseq.[60,94,95] In this study, gene expression as well as pathway enrichment was considered significant if the FDR was less than 0.05. Senecionine and riddelliine affected 24 common KEGG pathways, many of which were related to metabolism and neoplasia (See figure 12 for all pathways and their corresponding pathway enrichment scores). Senecionine affected 44 additional KEGG pathways and riddelliine affected 4 additional KEGG pathways. KEGG pathways affected by only senecionine or only riddelliine can be seen in supplemental data, but commonly affected pathways are the focus of this work. KEGG pathways involved in phase I and phase II metabolism of PAs, and to pathways related to neoplasia are of particular interest, as PAs are genotoxic carcinogens which require bioactivation by CYP450 enzymes.

Gene Expression Changes Related to Metabolism:

KEGG pathways related to PA metabolism which were affected by senecionine and riddelliine included “Metabolic pathways”, “Metabolism of xenobiotics by cytochrome p450”, “Drug-metabolism-cytochrome p450”, “Glutathione metabolism”, “Drug metabolism-other enzymes” and “Pentose and glucoronate interconversions”. Within

these pathways, the only gene which was expressed differently by these two PAs was Ugtb37 which was downregulated by senecionine and upregulated by riddelliine. Besides Ugtb37, all DEGs related to the metabolic pathways of PAs were dysregulated in the same direction for senecionine and riddelliine. PAs are bioactivated by CYP450 enzymes, which are found in the largest concentration in the liver.[73] The KEGG pathways "metabolic pathways", "metabolism of xenobiotics by cytochrome p450", and "drug-metabolism-cytochrome p450" were of particular interest in this study. Twenty-four genes encoding for CYP450 enzymes were differentially expressed by mice exposed to senecionine and riddelliine. These genes all moved in the same direction for senecionine and riddelliine, either up or downregulated (See table 13 for differentially expressed genes involved in phase I metabolism of PAs). The upregulated CYP450 genes are likely the main enzymes responsible for bioactivation of senecionine and riddelliine in mice. Upregulated CYP450 genes included Cyp2a4, Cyp4f16, Cyp1a1, Cyp4f39 and Cyp2a5. The greatest fold change was seen in Cyp2a4; therefore, Cyp2a4 is likely be the main CYP450 enzyme involved in bioactivation of these PAs in mice. Cyp2a4 was still upregulated in senecionine-exposed mice 28-day post-exposure. This may indicate continued bioactivation of senecionine which is compatible with the microscopic presence of multifocal hepatic necrosis. However, based on hepatic pyrrole concentration the toxic metabolite is no longer present. It has been shown that bioactivation of senecionine results in production of trans-4-hydroxy-2-hexenal, which is also hepatotoxic.[88] The effects of trans-4-hydroxy-2-hexenal on gene expression are not characterized, but it is possible that this metabolite, or other undiscovered toxic metabolites could explain the increased severity and persistence of hepatic necrosis, and

the greater number of DEGs induced by senecionine. A proteomic study using senecionine in mice similarly found that Cyp2a4 was the CYP450 enzyme that was most upregulated following acute (single-dose) exposure to senecionine.[33] A previous study showed that CYP2C, CYP2C12, CYP2C13, CYP2E1, CYP2E1, CYP3A2, CYP3A9, CYP3A18, CYP4A12, and CYP26 were the CYP450 enzymes responsible for phase 1 metabolism of riddelliine in rats.[30] In our study, gene expression indicated that Cyp2a4 is likely the main CYP450 enzyme responsible for bioactivation of riddelliine. These comparisons illustrate that which CYP450 enzymes are most important for PA bioactivation varies both by PA and by species. Phase II metabolism of PAs occurs mainly through glutathione binding. The KEGG pathway "glutathione metabolism" was significantly affected by both senecionine and riddelliine. Immediate post-exposure, genes encoding for glutathione s-transferase (Gsta1, Gsta2, Gsta4, Gsta5, Gstm1, Gstm2, Gstm3, Gstm4, Gstm5, Gstp2, Mgst3), glutathione synthase, and glutathione reductase were upregulated. The genes with the highest fold changes were Gsta1, Gsta5, Gstm3 and Gstp2, which encode for glutathione S-transferase, alpha 1 (Ya), glutathione S-transferase alpha 5, glutathione S-transferase, mu 3, and glutathione S-transferase, pi 2 respectively. These proteins likely have a primary role in phase 2 metabolism of PAs. In senecionine-exposed mice, Gsta1 and Gstm3 were upregulated at the 28-day post-exposure time point as well, although the fold changes were reduced in magnitude compared to the immediate post-exposure fold changes. Again, senecionine exposed mice were the only group with persistent hepatic necrosis at 28-days post-exposure, which may indicate the presence of ongoing metabolic bioactivation, phase 2 metabolism and excretion. Genes encoding for glutathione peroxidase (Gpx5, Gpx6) were downregulated.

These gene expression changes indicate that glutathione conjugation is the main pathway by which phase II metabolism of PAs occurs. Senecionine and riddelliine also affected the KEGG pathway "Pentose and glucuronate interconversion", which is related to glucuronidation. Glucuronidation has recently been noted as a contributor to phase II metabolism of PAs.[74] Differential expression of six genes encoding for UDP glucuronosyltransferases (Ugt2b35, Ugt2b34, Ugt2b1, Ugt2b37, Ugt2a3, and Ugt2b38) occurred with riddelliine and senecionine exposure. The fold changes of genes encoding for UDP glucuronosyltransferases were relatively small compared to genes related to glutathione conjugation, and fewer genes related to glucuronidation were significantly affected. This indicates that glucuronidation plays a relatively small role in phase II metabolism compared to glutathione conjugation. See table 14 for log fold changes of genes involved in phase II metabolism of PAs. Members of the ATP-binding cassette (ABC) family of proteins are implicated in cellular excretion of xenobiotics, and other studies have shown that they are upregulated following PA exposure.[73,75] The ABC family of proteins have been referred to as phase 3 metabolism pathways for PAs.[30] In our study, senecionine-exposed mice had 12 dysregulated genes which encode for proteins in the ATP-binding cassette family, and riddelliine-exposed mice had eight. This further supports the assertion that ATP-binding cassette proteins are involved in metabolism of PAs.

Gene Expression Changes Related to Neoplasia:

Senecionine and riddelliine affected multiple KEGG pathways related to cancer development. There was overlap between these two PAs within each affected pathway, but senecionine-exposure generally resulted in a greater number of DEGs. When

senecionine and riddelliine dysregulated common genes, the direction of dysregulation was in the same direction for these PAs with few exceptions. Both senecionine and riddelliine significantly affected the KEGG pathway “Pathways in cancer” immediately post-exposure. Senecionine caused dysregulation of 122 genes in this pathway and riddelliine affected 72 genes. Sixty of these genes were affected by both senecionine and riddelliine. Senecionine affected 62 unique genes and riddelliine affected 12 unique genes, so the total number of genes in this pathway affected by senecionine and/or riddelliine was 134. The direction of the dysregulation was the same for all DEGs affected by both riddelliine and senecionine and most fold changes were similar. Of the 134 genes affected by senecionine and/or riddelliine in this pathway, 101 were upregulated and 33 were downregulated. “Pathways in cancer” is an umbrella pathway which includes many genes that are involved in other cancer related KEGG pathways. These smaller and more focused cancer related pathways are comprised of smaller subsets of genes within the “pathways in cancer” set. These pathways that include smaller numbers of genes are useful for making direct comparisons between senecionine and riddelliine. Additional KEGG pathways related to cancer which were affected by both senecionine and riddelliine immediately post-exposure include “Chemical carcinogenesis-DNA adducts”, “Chemical carcinogenesis-receptor activation”, “Hepatocellular carcinoma”, “P53 signaling pathway”, and “MicroRNAs in cancer”. Within the pathway “Chemical carcinogenesis-DNA adducts” senecionine and riddelliine commonly dysregulated 26 genes, all genes moved in the same direction either up or down and had similar fold changes. Senecionine affected eight unique genes and riddelliine affected six. The KEGG pathway “Chemical carcinogenesis-receptor

activation" had 32 genes which were affected by both riddelliine and senecionine. PAs are chemical carcinogens, and riddelliine and senecionine had similar effects on the "Chemical carcinogenesis" pathways. All these genes moved in the same direction and the fold changes were similar. Senecionine affected eight unique genes and riddelliine affected seven unique genes in this pathway. The KEGG pathway "hepatocellular carcinoma" had 27 genes that were affected by both senecionine and riddelliine. These commonly affected genes moved in the same direction and had similar fold-changes. Senecionine affected 16 and riddelliine affected 7 unique genes in this pathway. Twenty-one genes in the KEGG pathway "P53 signaling pathway" were affected by both senecionine and riddelliine. These commonly affected genes moved in the same direction, all were upregulated with similar fold-changes. Senecionine affected 5 unique genes, riddelliine also affected five unique genes in this pathway. All but one of these genes were upregulated. Only Gadd45a was downregulated, and this gene was only significantly affected by senecionine. Gadd45 proteins are involved in tumorigenesis, playing roles in DNA repair, cell cycle control, and others.[96,97] The KEGG pathway "microRNAs in cancer" had 24 genes commonly affected by riddelliine and senecionine, all of which moved in the same direction and had similar fold-changes. Senecionine affected 24 unique genes and riddelliine affected 6 unique genes in this pathway. At 28-day post-exposure senecionine affected fewer cancer related KEGG pathways than riddelliine, but senecionine caused a greater number of DEGs within these cancer related pathways. When comparing the KEGG pathways affected by senecionine and riddelliine 28-day post-exposure it is important to understand the calculations that bioinformatics software uses to determine statistical significance. At first glance, we can easily note that

riddelliine had a statistically significant affect (FDR < 0.05) on 22 KEGG pathways related to cancer (table 17). Whereas senecionine only affected five KEGG pathways related to cancer (table 15). Closer inspection of the individual genes from these pathways shows that senecionine affected as many or more genes in many of the same cancer-related pathways as riddelliine, and that many of these genes affected by both senecionine and riddelliine moved in the same direction with similar fold change numbers. Statistical significance in pathway analysis depends not only on the genes which are dysregulated, but also on the proportion of these genes that fall into a pathway and the proportion of genes in a specific pathway in relation to the entire genome. The calculations for the p-values, FDR, and pathway enrichment score are performed by statistical software (DESeq2) but the GeneRatio and BgRatio are components of that calculation. DESeq2 uses the Wald test for determination of statistical significance for differentially expressed genes as well as pathway enrichment.[56,98] GeneRatio = k/n where k is the number of DEGs in the senecionine group in the specific KEGG pathway and n is the number of DEGs in the senecionine group that are in any KEGG pathway. BgRatio = M/N where M is the total number of genes in the specified KEGG pathway and N is the total number of genes in all KEGG pathways. Therefore, the reason for the lack of statistical significance in the senecionine group for the cancer-related pathways is that senecionine caused a greater number of DEGs, which resulted in a larger denominator in the GeneRatio. The fact that senecionine caused the greatest number of DEGs could be taken to mean that senecionine was the most genotoxic PA in this study. KEGG pathways of interest in the 28-day post-exposure senecionine group that were excluded due to FDR value can be seen in table 17. Two KEGG pathways which illustrate this point well are

the “Pathways in cancer” and Hepatocellular carcinoma” pathways. Riddelliine caused differential expression of 14 genes in the “pathways in cancer” pathway, compared to 17 DEGS in this pathway in senecionine exposed mice, but riddelliine had an FDR for this pathway of 0.0009 compared to 0.12 for senecionine. In the “Hepatocellular carcinoma” pathway senecionine affected 7 genes, while riddelliine affected 6, however riddelliine had an FDR of 0.017 compared to the FDR for senecionine of 0.22. The logic behind these statistical tests is that if there are a greater number of DEG’s, then the chance of a false positive result in each pathway is greater, if by false positive we mean a KEGG pathway being affected by random change. Comparisons were made of genes from these cancer related pathways and make comparisons between senecionine and riddelliine regarding gene expression. Given the statistical results, it is reasonable to state that riddelliine is more carcinogenic than senecionine, however closer inspection of individual genes within these pathways may indicate that senecionine is equally or even more carcinogenic. Senecionine caused the largest number of DEGs at both time points and affected many of the same genes as riddelliine. Senecionine also caused the most severe microscopic lesions in the livers of these mice. Senecionine was the only PA that caused hepatic necrosis a full 28 days after dosing had ceased. Senecionine also caused the most severe clinical affects, with weight loss in this group leading to the need to reduce the dosing period from ten to eight days, and the most significant effects on serum biochemical assays related to liver damage and liver function. Senecionine-exposed mice also had the greatest concentration of hepatic pyrroles immediately post-exposure, which are understood to be the main toxic metabolite responsible for cell damage and DNA damage. Riddelliine had a slightly greater hepatic pyrrole concentration than senecionine

after the 28-day recovery period but this difference likely not biologicaly relevant as the amount of pyrrole was very low. When all endpoints are considered, senecionine is likely to be carcinogenic in mice. Senecionine is also the most hepatotoxic PA in this study. Riddelliines carcinogenicity has been established previously, and it may be more carcinogenic than the PAs in this study based on the delayed changes in gene expression observed 28 days after dosing.[6,99] Previous studies have shown that riddelliine has the potential to induce greater concentrations of hepatic pyrroles that other PAs including senecionine, but this did not occur in this study.[47] There are important differences in this study including mouse sourcing, uniform age, and species which can provide potential explanations for these differences. Overall similarity in the gene expression profiles of senecionine and riddelliine both immediately following exposure and after a 28-day period of recovery, indicates similar genotoxic and carcinogenic activity between these two PAs in mice. The ideal way to compare carcinogenic potential between senecionine and riddelliine would be with side by side, long-term carcinogenicity studies lasting two years and using a variety of doses.

Selected Individual Genes of Interest:

Genes related to the development of neoplasia are of interest in this experiment, particularly those genes which were dysregulated after the 28-day period of recovery. Some additional genes which were notably dysregulated or are related to PA metabolism will also be discussed. In the immediate post-exposure group, Ltf, which encodes for lactotransferrin had by far the greatest fold change increase for all three PAs immediately post-exposure, even heliotrine which by most other measures had little to no affect. Lactotransferrin mainly functions in the immune system having antimicrobial, anti-

inflammatory and even anticancer effects. The anticancer effects include induction of apoptosis and blocking the transition from the G1 to S phase of the cell cycle.[65,66,69] Additional studies found that lactotransferrin resulted in tumor inhibition in squamous cell carcinomas, and the lactotransferrin activated mucosal immunity in tumor-bearing mice.[100,101] Previous work has not described Ltf as being involved in PA toxicosis.

At the 28-day post-exposure time point there were fewer DEGs. Among the main interests in this experiment were comparisons of carcinogenicity between these PAs. KEGG pathways provide curated lists of genes involved in various disease processes, including cancer development. By selecting genes of interest from cancer related KEGG pathways, we can provide further insight into the carcinogenic effects of senecionine and riddelliine. At 28-days post-exposure, within the KEGG pathways related to cancer, there were 21 genes that were dysregulated by both senecionine and riddelliine (see table 18), these genes moved in the same direction with similar fold changes. Notable upregulated genes and their products in relation to the development of cancer in this group include Cdkn1a (cyclin-dependent kinase inhibitor 1A (P21)), Tnfrsf10b (tumor necrosis factor receptor superfamily, member 10b), Gtse1 (G two S phase expressed protein 1), Ccnd1 (cyclin D1), Zmat3 (zinc finger matrin type 3), Ccng1 (cyclin G1), Pmaip1 (phorbol-12-myristate-13-acetate-induced protein 1), Plk2 (polo like kinase 2), Col1a1 (collagen, type I, alpha 1), Mmp2 (matrix metallopeptidase 2), Mdm2 (transformed mouse 3T3 cell double minute 2), Polk (polymerase kappa), and Notch1 (notch 1). These genes are involved in processes such as cell division, cell cycle inhibitors, cell differentiation, apoptosis, p53 signaling and extracellular matrix deposition and remodeling.[71] Mdm2 has been identified as a protoconcogene.[102] Downregulated genes in KEGG pathways related

to cancer which are of interest include Flt1 (FMS-like tyrosine kinase 1) also known as VEGFR1, Fhit (fragile histidine triad gene), Ppard (peroxisome proliferator activator receptor delta). Fhit is purportedly susceptible to damage and is associated with various cancers. Fhit has been shown to be overexpressed in human colorectal cancer.[103–105] Ppard is upregulated in a variety of tumor types and has been shown to play a role in regulation of metastasis.[106,107] Riddelliine exposed mice had six dysregulated genes from KEGG pathways related to cancer which were not significantly affected in the senecionine group. See table 19 for a heatmap showing the genes from KEGG pathways related to cancer which were only dysregulated in mice exposed to riddelliine. KEGG cancer-related pathway genes which were only affected by riddelliine include Cdkn2a, Myc, Gpc3, and Gadd45a which were all upregulated, and downregulation of G6pc and Hhip. Cdkn2a encodes for the protein cyclin dependent kinase inhibitor 2A which inhibits cell proliferation and invasion. Myc encodes for myelocytomatosis oncogene, which has been associated with hemotopoietic neoplasms and lymphoma. Gpc3 encodes for glypican 3 which is overexpressed in some hepatocellular carcinomas.[71] Gadd45a encodes for growth arrest and DNA-damage-inducible 45 alpha. This protein has been associate with various environmental stresses and drug therapies, and is a target for p53 related proteins p63 and p73. Mice with deficient Gadd45a have increased genomic instability and may be prone to neoplasia..[96] G6pc encodes for glucose-6-phosphatase, which is involved in the pentose phosphate pathway.[108] Hhip encodes for hedgehog-interacting protein, the human ortholog of which is downregulated in human colorectal cancer.[109] Mice exposed to senecionine had an additional 26 dysregulated genes which fall into KEGG pathways related to cancer development. See table 20 for a complete list

of KEGG genes related to cancer which were only dysregulated in the senecionine group at 28-day post-exposure. Upregulated genes in this group which are of particular interest and their products include Nrg1 (neuregulin 1), Ntrk2 (neurotrophic tyrosine kinase, receptor, type 2), Gsta1 (glutathione S-transferase, alpha 1 (Ya)), Gstm3 (glutathione S-transferase, mu 3), Dusp8 (dual specificity phosphatase 8), Src (Rous sarcoma oncogene), Fos (FBJ osteosarcoma oncogene), Ptpn7 (protein tyrosine phosphatase, non-receptor type 7) , Dusp2 (dual specificity phosphatase 2), Dusp4 (dual specificity phosphatase 4), Map3k20 (mitogen-activated protein kinase kinase kinase 20), Pak1 (p21 (RAC1) activated kinase 1), and Lum (lumican). Pak1 is involved in cell motility, survival, proliferation, transformation and other functions and has been associated with a variety of tumor types.[110] Pak1 silencing has been shown to result in decreased cell proliferation.[111] Src has been identified as a proto-oncogene.[112] Fos has been identified as an oncogene.[113] Ntrk2, Dusp2, Dusp4, Dusp8, Ptpn7, Map3k20 are involved in the MAP kinase4 pathway, which is associated with the development of various neoplasms.[114–116] Lum is predicted to be involved in regulation of TGF-beta, and RNA polymerase II, and in humans has been associated with pancreatic cancer development and other disease processes.[117,118] Nrg1 dysregulation has been identified as an oncogenic driver gene.[119,120] Downregulated genes from KEGG pathways related to cancer in senecionine-exposed mice at 28-day post-exposure include Hspb1 (heat shock protein 1), Lama3 (laminin, alpha 3), Flt1 (FMS-like tyrosine kinase 1), Wnt5a (wingless-type MMTV integration site family, member 5A), Erbb4 (erb-b2 receptor tyrosine kinase 4). Dysregulation of the human ortholog of Hspb1 has been identified in a variety of cancers. Hspb1 is supports cancer development by suppressing apoptosis and senescence, and

increasing expression of genes related to metastasis.[121–123] Laminin alpha 3 is downregulated in certain human skin cancers.[124,125] Flt1 encodes for a member of the VEGFR family, which are mediators of angiogenesis in cancer.[71,126] Wnt5a and other Wnt gene products are implicated in oncogenesis and associated with a variety of human cancers, particularly with human colorectal cancer. Wnt5a binds to a variety of receptors to activate the non-canonical Wnt pathway. This pathway acts independent of β-catenin and contributed to cell proliferation and migration.[71,127–130] Ppard, which encodes the protein peroxisome proliferator activator receptor delta, was up regulated immediately post-exposure and downregulated at 28-day post-exposure in senecionine and riddelliine-exposed mice. Peroxisome proliferator activator receptor delta is involved in metabolism, inflammation and the development of neoplasia. Peroxisome proliferator activator receptor delta promotes inflammation in the colon directly contributing to neoplastic disease. Ppard is also upregulated in tumor associated macrophages in ovarian cancer. [106,131–133] Senecionine and riddelliine both affected multiple pathways and genes related to cancer development.

After ingestion, PAs are metabolized by cytochrome p450 enzymes to didehydropyrrolizidine alkaloids, which are reactive electrophiles and can form covalent bonds with cellular macromolecules including DNA or RNA or cellular proteins. As the toxic metabolite is highly reactive, the covalent binding is nonspecific and which cell components are damaged most likely results from the concentration of the pyrrole in the cell and its proximity to the cellular substrate after bioactivation. Extensive work has proven that riddelliine is a carcinogen in mice and rats and is a likely human carcinogen.[6] The relatively small number of studies on PA toxicosis using transcriptomic tools have

consistently found that PA exposure results in dysregulation of pathways related to metabolism, cancer development, the cell cycle, and p53 signaling.[30–32,35] This study confirms these findings.

Conclusions:

In conclusion, senecionine and riddelliine exposure resulted in similar changes in gene expression in mice, although senecionine caused a greater number of DEGs both immediately following exposure and after a 28-day period of recovery. The overall similarity in the gene expression profiles of senecionine and riddelliine indicates similar hepatotoxic, genotoxic, and carcinogenic activity between these two PAs. Senecionine caused more severe hepatic necrosis, more significant changes in serum biochemistry assays indicating liver injury and had the greatest concentration of hepatic pyrroles immediately post-exposure. Riddelliine was the second most toxic PA based on these measures. Functional pathway analysis revealed gene expression changes relating to metabolism and cancer development. These similarities indicate that senecionine has similar carcinogenic potential when compared to riddelliine. Heliotrine had no significant effect on mice in this study. The next reasonable steps for this research include using proteomics to verify that gene expression results in the production of predicted proteins. In addition, performing transcriptomics following exposure to additional PAs would be beneficial.

References:

1. Fu, P. P., Xia, Q., Lin, G. & Chou, M. W. Pyrrolizidine Alkaloids—Genotoxicity, Metabolism Enzymes, Metabolic Activation, and Mechanisms. *Drug Metabolism Reviews* 36, 1–55 (2004).
2. Stegelmeier, B. L. *et al.* Pyrrolizidine alkaloid plants, metabolism and toxicity. *J Nat Toxins* 8, 95–116 (1999).
3. Mattocks, A. R. *Chemistry and toxicology of pyrrolizidine alkaloids*. (Academic Press, 1986).
4. Moreira, R., Pereira, D. M., Valentão, P. & Andrade, P. B. Pyrrolizidine Alkaloids: Chemistry, Pharmacology, Toxicology and Food Safety. *Int J Mol Sci* 19, 1668 (2018).
5. Chen, T., Mei, N. & Fu, P. P. Genotoxicity of pyrrolizidine alkaloids. *J Appl Toxicol* 30, 183–196 (2010).
6. National Toxicology Program. Toxicology and carcinogenesis studies of riddelliine (CAS No. 23246-96-0) in F344/N rats and B6C3F1 mice (gavage studies). *Natl Toxicol Program Tech Rep Ser* 1–280 (2003).
7. Green, C. E., Segall, H. J. & Byard, J. L. Metabolism, cytotoxicity, and genotoxicity of the pyrrolizidine alkaloid senecionine in primary cultures of rat hepatocytes. *Toxicology and Applied Pharmacology* 60, 176–185 (1981).
8. Phillips, D. H. & Arlt, V. M. Genotoxicity: damage to DNA and its consequences. *EXS* 99, 87–110 (2009).
9. Medical Definition of GENOTOXIC. https://www.merriam-webster.com/medical/genotoxic.

10. Ren, N., Atyah, M., Chen, W.-Y. & Zhou, C.-H. The various aspects of genetic and epigenetic toxicology: testing methods and clinical applications. *Journal of Translational Medicine* 15, 110 (2017).
11. Nohmi, T. Thresholds of Genotoxic and Non-Genotoxic Carcinogens. *Toxicol Res* 34, 281–290 (2018).
12. Griffin, D. S. & Segall, H. J. Genotoxicity and cytotoxicity of selected pyrrolizidine alkaloids, a possible alkenal metabolite of the alkaloids, and related alkenals. *Toxicol Appl Pharmacol* 86, 227–234 (1986).
13. Williams, G. M., Laspia, M. F. & Dunkel, V. C. Reliability of the hepatocyte primary culture/DNA repair test in testing of coded carcinogens and noncarcinogens. *Mutat Res* 97, 359–370 (1982).
14. Mori, H. *et al.* Genotoxicity of a Variety of Pyrrolizidine Alkaloids in the Hepatocyte Primary Culture-DNA Repair Test Using Rat, Mouse, and Hamster Hepatocytes. *Cancer Research* 45, 3125–3129 (1985).
15. Yang, Y.-C. *et al.* Development of a 32P-Postlabeling/HPLC Method for Detection of Dehydroretronecine-Derived DNA Adducts in Vivo and in Vitro. *Chem. Res. Toxicol.* 14, 91–100 (2001).
16. Chou, M. W. *et al.* Riddelliine N-oxide is a phytochemical and mammalian metabolite with genotoxic activity that is comparable to the parent pyrrolizidine alkaloid riddelliine. *Toxicol Lett* 145, 239–247 (2003).
17. Brink, N. G. The mutagenic activity of the pyrrolizidine alkaloid heliotrine in Drosophila melanogaster II. Chromosome rearrangements. *Mutation*

Research/Fundamental and Molecular Mechanisms of Mutagenesis 8, 139–146 (1969).

18. Clark, A. M. The mutagenic activity of some pyrrolizidine alkaloids in Drosophila. *Z Vererbungsl* 91, 74–80 (1960).
19. Alderson, T. & Clark, A. M. Interlocus specificity for chemical mutagens in Aspergillus nidulans. *Nature* 210, 593–595 (1966).
20. Yamanaka, H. *et al.* Mutagenicity of pyrrolizidine alkaloids in the Salmonella/mammalian-microsome test. *Mutation Research/Genetic Toxicology* 68, 211–216 (1979).
21. Wehner, F. C., Thiel, P. G. & van Rensburg, S. J. Mutagenicity of alkaloids in the Salmonella/microsome system. *Mutat Res* 66, 187–190 (1979).
22. Rubiolo, P. *et al.* Mutagenicity of pyrrolizidine alkaloids in the Salmonella typhimurium/mammalian microsome system. *Mutation Research Letters* 281, 143–147 (1992).
23. Richardson, S. J., Bai, A., Kulkarni, A. A. & Moghaddam, M. F. Efficiency in Drug Discovery: Liver S9 Fraction Assay As a Screen for Metabolic Stability. *Drug Metab Lett* 10, 83–90 (2016).
24. Mei, N., Heflich, R. H., Chou, M. W. & Chen, T. Mutations Induced by the Carcinogenic Pyrrolizidine Alkaloid Riddelliine in the Liver cII Gene of Transgenic Big Blue Rats. *Chem. Res. Toxicol.* 17, 814–818 (2004).
25. Mei, N., Guo, L., Fu, P. P., Heflich, R. H. & Chen, T. Mutagenicity of comfrey (Symphytum Officinale) in rat liver. *Br J Cancer* 92, 873–875 (2005).

26. Comfrey. in *Drugs and Lactation Database (LactMed®)* (National Institute of Child Health and Human Development, 2006).

27. Aubrecht, J. & Caba, E. Gene expression profile analysis: an emerging approach to investigate mechanisms of genotoxicity. *Pharmacogenomics* 6, 419–428 (2005).

28. Youns, M., Hoheisel, J. D. & Efferth, T. Toxicogenomics for the Prediction of Toxicity Related to Herbs from Traditional Chinese Medicine. *Planta Med* 76, 2019–2025 (2010).

29. Guo, L., Mei, N., Dial, S., Fuscoe, J. & Chen, T. Comparison of gene expression profiles altered by comfrey and riddelliine in rat liver. *BMC Bioinformatics* 8, S22 (2007).

30. Mei, N., Guo, L., Liu, R., Fuscoe, J. C. & Chen, T. Gene expression changes induced by the tumorigenic pyrrolizidine alkaloid riddelliine in liver of Big Blue rats. *BMC Bioinformatics* 8 Suppl 7, S4 (2007).

31. Abdelfatah, S. *et al.* Pyrrolizidine alkaloids cause cell cycle and DNA damage repair defects as analyzed by transcriptomics in cytochrome P450 3A4-overexpressing HepG2 clone 9 cells. *Cell Biol Toxicol* 38, 325–345 (2022).

32. Ebmeyer, J. *et al.* Hepatotoxic pyrrolizidine alkaloids induce DNA damage response in rat liver in a 28-day feeding study. *Arch Toxicol* 94, 1739–1751 (2020).

33. Wang, W. *et al.* A TMT-based shotgun proteomics uncovers overexpression of thrombospondin 1 as a contributor in pyrrolizidine alkaloid-induced hepatic sinusoidal obstruction syndrome. *Arch Toxicol* 96, 2003–2019 (2022).

34. Li, Y.-H. *et al.* Toxicoproteomic assessment of liver responses to acute pyrrolizidine alkaloid intoxication in rats. *Journal of Environmental Science and Health, Part C* 36, 65–83 (2018).

35. Luckert, C., Hessel, S., Lenze, D. & Lampen, A. Disturbance of gene expression in primary human hepatocytes by hepatotoxic pyrrolizidine alkaloids: A whole genome transcriptome analysis. *Toxicology in Vitro* 29, 1669–1682 (2015).

36. Hirono, I., Mori, H. & Culvenor, C. C. Carcinogenic activity of coltsfoot, Tussilago farfara l. *Gan* 67, 125–129 (1976).

37. Hirono, I., Mori, H., Yamada, K., Hirata, Y. & Haga, M. Carcinogenic activity of petasitenine, a new pyrrolizidine alkaloid isolated from Petasites japonicus Maxim. *J Natl Cancer Inst* 58, 1155–1157 (1977).

38. Hirono, I., Mori, H. & Haga, M. Carcinogenic activity of Symphytum officinale. *J Natl Cancer Inst* 61, 865–869 (1978).

39. Hirono, I. *et al.* Induction of hepatic tumors in rats by senkirkine and symphytine. *J Natl Cancer Inst* 63, 469–472 (1979).

40. Hirono, I., Ueno, I., Aiso, S., Yamaji, T. & Haga, M. Carcinogenic activity of Farfugium japonicum and Senecio cannabifolius. *Cancer Letters* 20, 191–198 (1983).

41. Rao, M. S. & Reddy, J. K. Malignant neoplasms in rats fed lasiocarpine. *Br J Cancer* 37, 289–293 (1978).

42. Johnson, W. D., Robertson, K. A., Pounds, J. G. & Allen, J. R. Dehydroretronecine-induced skin tumors in mice. *J Natl Cancer Inst* 61, 85–89 (1978).

43. Harris, P. N. & Chen, K. K. Development of hepatic tumors in rats following ingestion of Senecio longilobus. *Cancer Res* 30, 2881–2886 (1970).

44. Schoental, R. Pancreatic islet-cell and other tumors in rats given heliotrine, a monoester pyrrolizidine alkaloid, and nicotinamide. *Cancer Res* 35, 2020–2024 (1975).

45. 15th Report on Carcinogens. *National Toxicology Program* https://ntp.niehs.nih.gov/whatwestudy/assessments/cancer/roc.

46. Culvenor, C., Edgar, J., Smith, L. & Tweeddale, H. Dihydropyrrolizines. III. Preparation and reactions of derivatives related to pyrrolizidine alkaloids. *Aust. J. Chem.* 23, 1853 (1970).

47. Brown, A. Relative Toxicity of Select Dehydropyrrolizidine Alkaloids and Evaluation of a Heterozygous P53 Knockout Mouse Model for Dehydropyrrolizidine Alkaloid Induced Carcinogenesis. *All Graduate Theses and Dissertations* (2015) doi:https://doi.org/10.26076/7997-d859.

48. Brown, A. W. *et al.* The comparative toxicity of a reduced, crude comfrey (Symphytum officinale) alkaloid extract and the pure, comfrey-derived pyrrolizidine alkaloids, lycopsamine and intermedine in chicks (Gallus gallus domesticus). *J Appl Toxicol* 36, 716–725 (2016).

49. Hoppers, A. *et al.* A Robust, Streamlined, Enzyme-based DNA Library Preparation Method Amenable to a Wide Range of DNA Inputs. *J Biomol Tech* 30, S2 (2019).

50. Sato, M. P. *et al.* Comparison of the sequencing bias of currently available library preparation kits for Illumina sequencing of bacterial genomes and metagenomes. *DNA Res* 26, 391–398 (2019).

51. Senabouth, A. *et al.* Comparative performance of the BGI and Illumina sequencing technology for single-cell RNA-sequencing. *NAR Genom Bioinform* 2, lqaa034 (2020).

52. Andrews, S. Babraham Bioinformatics - FastQC A Quality Control tool for High Throughput Sequence Data. https://www.bioinformatics.babraham.ac.uk/projects/fastqc/.

53. Krueger, F. Trim Galore: a wrapper tool around Cutadapt and FastQC to consistently apply quality and adapter trimming to FastQ files, with some extra functionality for MspI-digested RRBS-type (Reduced Representation Bisufite-Seq) libraries. https://xz6kg9rb2j.search.serialssolutions.com/?url_ver=Z39.88-2004&rft.atitle=Trim+Galore%3A+a+wrapper+tool+around+Cutadapt+and+FastQC+to+consistently+apply+quality+and+adapter+trimming+to+FastQ+files%2C+with+some+extra+functionality+for+MspI-digested+RRBS-type+%28Reduced+Representation+Bisufite-Seq%29+libraries&rft.aufirst=F&rft.aulast=Krueger&rft.date=2014.

54. Dobin, A. *et al.* STAR: ultrafast universal RNA-seq aligner. *Bioinformatics* 29, 15–21 (2013).

55. Liao, Y., Smyth, G. K. & Shi, W. The Subread aligner: fast, accurate and scalable read mapping by seed-and-vote. *Nucleic Acids Res* 41, e108 (2013).

56. Love, M. *et al.* DESeq2: Differential gene expression analysis based on the negative binomial distribution. (2023) doi:10.18129/B9.bioc.DESeq2.

57. Kim, H.-Y. Analysis of variance (ANOVA) comparing means of more than two groups. *Restor Dent Endod* 39, 74–77 (2014).

58. Akoglu, H. User's guide to correlation coefficients. *Turk J Emerg Med* 18, 91–93 (2018).

59. Dalman, M. R., Deeter, A., Nimishakavi, G. & Duan, Z.-H. Fold change and p-value cutoffs significantly alter microarray interpretations. *BMC Bioinformatics* 13, S11 (2012).

60. Jung, K., Friede, T. & Beißbarth, T. Reporting FDR analogous confidence intervals for the log fold change of differentially expressed genes. *BMC Bioinformatics* 12, 288 (2011).

61. Gartel, A. L. & Tyner, A. L. The Role of the Cyclin-dependent Kinase Inhibitor p21 in Apoptosis.

62. Liu, H. *et al.* Downregulation of Glutathione S-transferase A1 suppressed tumor growth and induced cell apoptosis in A549 cell line. *Oncology Letters* 16, 467–474 (2018).

63. Little, A. G., Lau, G., Mathers, K. E., Leary, S. C. & Moyes, C. D. Comparative biochemistry of cytochrome c oxidase in animals. *Comparative Biochemistry and Physiology Part B: Biochemistry and Molecular Biology* 224, 170–184 (2018).

64. Murphy, G. & Nagase, H. Progress in matrix metalloproteinase research. *Molecular Aspects of Medicine* 29, 290–308 (2008).

65. Vorland, L. H. Lactoferrin: A multifunctional glycoprotein. *APMIS* 107, 971–981 (1999).

66. González-Chávez, S. A., Arévalo-Gallegos, S. & Rascón-Cruz, Q. Lactoferrin: structure, function and applications. *International Journal of Antimicrobial Agents* 33, 301.e1-301.e8 (2009).

67. Beynon, R. J. & Hurst, J. L. Multiple roles of major urinary proteins in the house mouse, Mus domesticus. *Biochemical Society Transactions* 31, 142–146 (2003).

68. Oiki, S., Hiyama, E., Gotoh, T. & Iida, H. Localization of Tektin 1 at both acrosome and flagella of mouse and bull spermatozoa. *Zoolog Sci* 31, 101–107 (2014).

69. Berlutti, F. *et al.* Antiviral properties of lactoferrin--a natural immunity molecule. *Molecules* 16, 6992–7018 (2011).

70. Laity, J. H., Lee, B. M. & Wright, P. E. Zinc finger proteins: new insights into structural and functional diversity. *Curr Opin Struct Biol* 11, 39–46 (2001).

71. National Center for Biotechnology Information. https://www.ncbi.nlm.nih.gov/.

72. Phlda3 - Gene - NCBI. https://www.ncbi.nlm.nih.gov/gene/?term=Phlda3.

73. Xu, J. *et al.* Pyrrolizidine alkaloids: An update on their metabolism and hepatotoxicity mechanism. *Liver Research* 3, 176–184 (2019).

74. He, Y.-Q. *et al.* Glucuronidation, a new metabolic pathway for pyrrolizidine alkaloids. *Chem Res Toxicol* 23, 591–599 (2010).

75. Enge, A.-M., Kaltner, F., Gottschalk, C., Braeuning, A. & Hessel-Pras, S. Active Transport of Hepatotoxic Pyrrolizidine Alkaloids in HepaRG Cells. *Int J Mol Sci* 22, 3821 (2021).

76. Buermans, H. P. J. *et al.* Microarray analysis reveals pivotal divergent mRNA expression profiles early in the development of either compensated ventricular hypertrophy or heart failure. *Physiological Genomics* 21, 314–323 (2005).

77. Wang, Z. *et al.* Proteomic characterization of the possible molecular targets of pyrrolizidine alkaloid isoline-induced hepatotoxicity. *Environmental Toxicology and Pharmacology* 34, 608–617 (2012).

78. Ellinger-Ziegelbauer, H., Aubrecht, J., Kleinjans, J. C. & Ahr, H.-J. Application of toxicogenomics to study mechanisms of genotoxicity and carcinogenicity. *Toxicol Lett* 186, 36–44 (2009).

79. Peterson, J. E. & Jago, M. V. Comparison of the toxic effects of dehydroheliotridine and heliotrine in pregnant rats and their embryos. *J Pathol* 131, 339–355 (1980).

80. Sullman, S. F. & Zuckerman, A. J. The Effect of Heliotrine, a Pyrrolizidine Alkaloid, on Human Liver Cells in Culture. *Br J Exp Pathol* 50, 361–370 (1969).

81. Stegelmeier, B. L. Pyrrolizidine Alkaloid–Containing Toxic Plants (Senecio, Crotalaria, Cynoglossum, Amsinckia, Heliotropium, and Echium spp.). *Veterinary Clinics: Food Animal Practice* 27, 419–428 (2011).

82. Stegelmeier, B. L., Colegate, S. M. & Brown, A. W. Dehydropyrrolizidine Alkaloid Toxicity, Cytotoxicity, and Carcinogenicity. *Toxins (Basel)* 8, 356 (2016).

83. McClure, D. E. Clinical pathology and sample collection in the laboratory rodent. *Vet Clin North Am Exot Anim Pract* 2, 565–590, vi (1999).

84. Senior, J. R. Alanine aminotransferase: a clinical and regulatory tool for detecting liver injury-past, present, and future. *Clin Pharmacol Ther* 92, 332–339 (2012).

85. Panteghini, M. Aspartate aminotransferase isoenzymes. *Clin Biochem* 23, 311–319 (1990).

86. Xu, Q., Lu, Z. & Zhang, X. A novel role of alkaline phosphatase in protection from immunological liver injury in mice. *Liver* 22, 8–14 (2002).

87. Sellers, R. S. *et al.* Society of Toxicologic Pathology position paper: organ weight recommendations for toxicology studies. *Toxicol Pathol* 35, 751–755 (2007).

88. Segall, H. J., Wilson, D. W., Dallas, J. L. & Haddon, W. F. Trans-4-Hydroxy-2-Hexenal: a Reactive Metabolite from the Macrocyclic Pyrrolizidine Alkaloid Senecionine. *Science* 229, 472–475 (1985).

89. Subramanian, A. *et al.* Gene set enrichment analysis: A knowledge-based approach for interpreting genome-wide expression profiles. *Proceedings of the National Academy of Sciences* 102, 15545–15550 (2005).

90. Du, J. *et al.* KEGG-PATH: Kyoto encyclopedia of genes and genomes-based pathway analysis using a path analysis model. *Mol. BioSyst.* 10, 2441–2447 (2014).

91. Du, J. *et al.* A decision analysis model for KEGG pathway analysis. *BMC Bioinformatics* 17, 407 (2016).

92. Kanehisa, M., Goto, S., Sato, Y., Furumichi, M. & Tanabe, M. KEGG for integration and interpretation of large-scale molecular data sets. *Nucleic Acids Res* 40, D109-114 (2012).

93. Gene Ontology Consortium. The Gene Ontology (GO) database and informatics resource. *Nucleic Acids Research* 32, 258D – 261 (2004).

94. Benjamini, Y. & Hochberg, Y. Controlling the False Discovery Rate: A Practical and Powerful Approach to Multiple Testing. *Journal of the Royal Statistical Society: Series B (Methodological)* 57, 289–300 (1995).

95. Benjamini, Y. Discovering the False Discovery Rate. *Journal of the Royal Statistical Society Series B: Statistical Methodology* 72, 405–416 (2010).

96. Rosemary Siafakas, A. & Richardson, D. R. Growth arrest and DNA damage-45 alpha (GADD45alpha). *Int J Biochem Cell Biol* 41, 986–989 (2009).

97. Tamura, R. E. *et al.* GADD45 proteins: central players in tumorigenesis. *Curr Mol Med* 12, 634–651 (2012).

98. Love, M. I., Huber, W. & Anders, S. Moderated estimation of fold change and dispersion for RNA-seq data with DESeq2. *Genome Biology* 15, 550 (2014).

99. Chan, P. NTP technical report on the toxicity studies of Riddelliine (CAS No. 23246-96-0) Administered by Gavage to F344 Rats and B6C3F1 Mice. *Toxic Rep Ser* 27, 1-D9 (1993).

100. Wang, W.-P. *et al.* Activation of Intestinal Mucosal Immunity in Tumor-bearing Mice by Lactoferrin. *Japanese Journal of Cancer Research* 91, 1022–1027 (2000).

101. Wolf, J. S. *et al.* Oral Lactoferrin Results in T Cell–Dependent Tumor Inhibition of Head and Neck Squamous Cell Carcinoma In vivo. *Clinical Cancer Research* 13, 1601–1610 (2007).

102. Haines, D. S. The mdm2 Proto-Oncogene. *Leukemia & Lymphoma* 26, 227–238 (1997).

103. Wierzbicki, P. *et al.* Fragile histidine triad (FHIT) gene is overexpressed in colorectal cancer. *Journal of physiology and pharmacology : an official journal of the Polish Physiological Society* 60 Suppl 4, 63–70 (2009).

104. FHIT fragile histidine triad diadenosine triphosphatase [Homo sapiens (human)] - Gene - NCBI. https://www.ncbi.nlm.nih.gov/gene/2272.

105. Fhit fragile histidine triad gene [Mus musculus (house mouse)] - Gene - NCBI. https://www.ncbi.nlm.nih.gov/gene/14198.

106. Ppard peroxisome proliferator activator receptor delta [Mus musculus (house mouse)] - Gene - NCBI. https://www.ncbi.nlm.nih.gov/gene/19015.

107. Zuo, X. *et al.* Metastasis regulation by PPARD expression in cancer cells. *JCI Insight* 2, e91419.

108. Song, J., Sun, H., Zhang, S. & Shan, C. The Multiple Roles of Glucose-6-Phosphate Dehydrogenase in Tumorigenesis and Cancer Chemoresistance. *Life (Basel)* 12, 271 (2022).

109. Fu, F., Zhang, Y., Feng, J. & Nie, Y. Bioinformatics analysis of hedgehog interacting protein in colorectal cancer: a study based on GEO data and TCGA data. *BMC Gastroenterology* 23, 278 (2023).

110. Yao, D. *et al.* P21-Activated Kinase 1: Emerging biological functions and potential therapeutic targets in Cancer. *Theranostics* 10, 9741–9766 (2020).

111. Zhang, Z.-L. *et al.* Effect of PAK1 gene silencing on proliferation and apoptosis in hepatocellular carcinoma cell lines MHCC97-H and HepG2 and cells in xenograft tumor. *Gene Ther* 25, 284–296 (2018).

112. Dehm, S. M. & Bonham, K. SRC gene expression in human cancer: the role of transcriptional activation. *Biochem. Cell Biol.* 82, 263–274 (2004).

113. Fuchs, B. & Pritchard, D. J. Etiology of Osteosarcoma. *Clinical Orthopaedics and Related Research (1976-2007)* 397, 40–52 (2002).

114. Fang, J. Y. & Richardson, B. C. The MAPK signalling pathways and colorectal cancer. *The Lancet Oncology* 6, 322–327 (2005).

115. Santarpia, L., Lippman, S. M. & El-Naggar, A. K. Targeting the MAPK–RAS–RAF signaling pathway in cancer therapy. *Expert Opinion on Therapeutic Targets* 16, 103–119 (2012).

116. Stramucci, L., Pranteda, A. & Bossi, G. Insights of Crosstalk between p53 Protein and the MKK3/MKK6/p38 MAPK Signaling Pathway in Cancer. *Cancers* 10, 131 (2018).

117. Ping Lu, Y., Ishiwata, T. & Asano, G. Lumican expression in alpha cells of islets in pancreas and pancreatic cancer cells. *The Journal of Pathology* 196, 324–330 (2002).

118. Li, X. *et al.* Extracellular lumican inhibits pancreatic cancer cell growth and is associated with prolonged survival after surgery. *Clin Cancer Res* 20, 6529–6540 (2014).

119. NRG1 neuregulin 1 [Homo sapiens (human)] - Gene - NCBI. https://www.ncbi.nlm.nih.gov/gene/3084.

120. Severson, E. *et al.* RNA Sequencing Identifies Novel NRG1 Fusions in Solid Tumors that Lack Co-Occurring Oncogenic Drivers. *J Mol Diagn* 25, 454–466 (2023).

121. Rizvi, S. F., Hasan, A., Parveen, S. & Mir, S. S. Untangling the complexity of heat shock protein 27 in cancer and metastasis. *Arch Biochem Biophys* 736, 109537 (2023).

122. Huo, Q., Wang, J. & Xie, N. High HSPB1 expression predicts poor clinical outcomes and correlates with breast cancer metastasis. *BMC Cancer* 23, 501 (2023).

123. Nagaraja, G. M., Kaur, P. & Asea, A. Role of Human and Mouse HspB1 in Metastasis. *Current Molecular Medicine* 12, 1142–1150 (2012).

124. Kariya, Y. *et al.* Localization of laminin alpha3B chain in vascular and epithelial basement membranes of normal human tissues and its down-regulation in skin cancers. *J Mol Histol* 39, 435–446 (2008).

125. PubChem. Lama3 - laminin, alpha 3 (house mouse). https://pubchem.ncbi.nlm.nih.gov/gene/Lama3/mouse.

126. Carmeliet, P. VEGF as a key mediator of angiogenesis in cancer. *Oncology* 69 Suppl 3, 4–10 (2005).

127. Coupe, N. *et al.* WNT5A-ROR2 axis mediates VEGF dependence of BRAF mutant melanoma. *Cell Oncol (Dordr)* 46, 391–407 (2023).

128. Ma, Z. *et al.* Interferon-dependent SLC14A1+ cancer-associated fibroblasts promote cancer stemness via WNT5A in bladder cancer. *Cancer Cell* 40, 1550-1565.e7 (2022).

129. Ma, L. *et al.* [PDS5B inhibits the proliferation of A549 human lung cancer cells via downregulation of Wnt5a]. *Xi Bao Yu Fen Zi Mian Yi Xue Za Zhi* 39, 15–20 (2023).

130. Zhan, T., Rindtorff, N. & Boutros, M. Wnt signaling in cancer. *Oncogene* 36, 1461–1473 (2017).

131. Lien, C.-F. *et al.* Peroxisome proliferator-activated receptor δ improves the features of atherosclerotic plaque vulnerability by regulating smooth muscle cell phenotypic switching. *Br J Pharmacol* 180, 2085–2101 (2023).

132. Fan, L. *et al.* Transcription factors KLF15 and PPARδ cooperatively orchestrate genome-wide regulation of lipid metabolism in skeletal muscle. *J Biol Chem* 298, 101926 (2022).

133. Liu, Y. *et al.* Rapid acceleration of KRAS-mutant pancreatic carcinogenesis via remodeling of tumor immune microenvironment by PPARδ. *Nat Commun* 13, 2665 (2022).

CHAPTER V CONCLUSIONS

Despite the large body of knowledge regarding the toxic effects of PAs, exposure continues to negatively impact both human and animal health. Given the worldwide distribution, and frequency of exposure, it is somewhat surprising many in the general population are not aware of the risks these toxins pose. Recommendations for maximum acceptable exposure limits have been created by governmental organizations in the United States, Europe and others.[1,2] Given their classification as genotoxic carcinogens, it could be argued that no exposure should be considered safe.[3] Exposure in people can occur from contamination of grain, contaminated animal products such as milk, honey and eggs, herbal teas, supplements or phytomedicines.[4–7] Animal exposure happens as a result of contaminated hay or grain, or grazing of PA containing plants. Animal exposure has the potential to affect human health through secondary poisoning as PAs contaminate animal products causing economic losses to agricultural producers, and detrimental effects on the food supply. These impacts on human and animal health justify the resources used for PA research.

A major cause of human PA exposure is ingestion of herbal teas, remedies, supplements, and phytomedicines. Among commercial products, teas are among the most common source of exposure. Evidence from the research performed herein strengthens the body of literature regarding the hepatotoxic, genotoxic and carcinogenic effects of PAs. This information may help prevent exposure in people who would otherwise be unaware of the risks posed by PA containing herbal products. These individuals may

consume these products as part of an effort to live healthy lifestyles by relying on natural products. Any PA exposures may be causing unnecessary harm to themselves and even more harm to their highly susceptible children.

Review of Experimental Results:

In our first experiment, C57BL6/j mice were exposed to varying doses of riddelliine, senecionine, seneciphylline, lasiocarpine, heliotrine, riddelliine N-oxide, and senecionine N-oxide at varying doses (1,2,4,8,15,30,45,90,180,360 mg/kg/day) for ten days. The results of this experiment led to several important conclusions. Comparison of severity of hepatotoxicity between these PAs ranked senecionine, senecionine N-oxide, and seneciphylline as the most hepatotoxic, while riddelliine and its N-oxide were in the intermediate group, and lasiocarpine and heliotrine were the least hepatotoxic. In mice heliotrine did not cause hepatic necrosis even at 180 mg/kg/day. Lasiocarpine caused minimal periportal hepatocellular degeneration and necrosis only at 30 mg/kg/day, which was the greatest dose tolerated. At doses higher than 30 mg/kg/day, lasiocarpine caused severe malaise and inappetance in the mice. Clearly lasiocarpine has additional toxic effects in mice, but these were not detected by histopathology in this study. This study found that PAs cause different hepatic distributions of hypertrophy, degeneration, and necrosis. Differing distributions of hepatic necrosis between PAs is a novel finding. Riddelliine, senecionine, seneciphylline, senecionine N-oxide and riddelliine N-oxide caused a pattern of degeneration and necrosis that affected specific lobular zones at lower affective doses, but progressed to a panlobular distribution as dose was increased. Serum concentrations of ALT and ALP had strong positive correlations with hepatic necrosis severity scores. Riddelliine induced substantially greater concentrations of hepatic

pyrroles than all other PAs at most doses. This was also found by Brown et al. (2015) when California white chicks were exposed to riddelliine and other various PAs.[8] Notably, the increase in accumulation of pyrroles, the main toxic metabolite of PAs, did not correlate with severity of hepatic necrosis. This ability to induce greater concentrations of hepatic pyrroles may represent a unique trait by which riddelliine could be more carcinogenic than other PAs in some circumstances.

The second experiment was designed to compare carcinogenicity of five PAs. Heterozygous p53 knockout male mice were exposed to riddelliine, senecionine, seneciphylline, heliotrine and lasiocarpine. Brown et al. (2015) performed an experiment in which a heterozygous p53 knockout mouse model was exposed to various doses of riddelliine. They found a significant dose related trend in the development of neoplasms. They determined that this mouse model and the conditions in which they were exposed and observed were potentially useful in PA carcinogenicity research.[9] Mice were necropsied one year later, and gross and microscopic lesions were compared. Comparison with the control group of the relative frequency of neoplasia development did not detect significant differences for any PA using Dunnett's test with a poly-k mortality correction. Dunnett's test is said to be somewhat conservative, and the poly-k correction was necessary because groups had substantial differences in average mortality.[10,11] Riddelliine is used as a positive control for carcinogenicity. Although not statistically significant, the riddelliine-exposed group developed the greatest number of liver hemangiosarcomas which are the neoplasm of interest in male mice.[12] A variety of neoplasms developed in every group including the control group. The lack of statistical significance indicates that these tumors may be due to the genetic predisposition of the

mouse model to neoplasia and not the PA exposure. An additional lesion which developed in mice was the presence of heterotopic bone within the liver. This lesion is referred to as osseous metaplasia. In their initial studies, Brown et al. (2015) also observed this lesion following riddelliine exposure.[8] This lesion was most prevalent in mice exposed to senecionine and seneciphylline, followed by riddelliine. A singular focus of heterotopic bone was observed in the liver of one of the lasiocarpine exposed mice, while none of the heliotrine-exposed mice or control mice had this finding. This order is the same as the severity of hepatotoxicity observed in experiment 1. Leading to the conclusion that this is likely an aberrant response to hepatocellular injury that is most likely specific to this transgenic mouse model. Because this seems to be a unique finding in a single mouse model, it may not be prudent to use additional resources to further investigate the pathogenesis of the lesion. On the other hand, production of bone matrices is an important area of biomedical research, and others may judge that this lesion warrants additional research.

Experiment three compared whole genome RNA expression in mice at two time points, after exposure to riddelliine, senecionine and heliotrine. Mice were gavaged with these PAs for eight days. The first group was euthanized the day after dosing and the second group was euthanized 28-days later. Riddelliine was selected as a prototypical carcinogenic and hepatotoxic PA. Senecionine was compared to riddelliine because it is more hepatotoxic than riddelliine. Heliotrine was selected as a minimally toxic or non-toxic PA. Heliotrine had minimal effects on gene expression both immediately and after 28 days of recovery. Senecionine-exposure resulted in the greatest number of DEGs at both time points. Both senecionine and riddelliine affected genes associated with

neoplasia and metabolism. Senecionine also caused the most severe hepatic necrosis, the greatest hepatic pyrrole concentrations, and the most significant increases in serum biochemical assays related to hepatic injury. The similarity in gene expression profiles and the established fact that riddelliine is carcinogenic in male mice indicate that senecionine is also carcinogenic to mice. This study represents a possible alternative to traditional long-term carcinogenicity studies for PAs. Using riddelliine as a standard for comparison, it may be possible to predict whether a PA is likely to be carcinogenic. The changes in expression of genes related to phase I and II metabolism of PAs for riddelliine and senecionine support the proposed mechanism of bioactivation and toxicity. Comparison of gene expression at two timepoints, immediately after dosing and then after a 28-day period of recovery, provided useful information as well. After 28 days of recovery, the number of DEGs had reduced to approximately ten percent of the initial number. Further, fold changes of genes that were dysregulated at both times moved toward a zero-fold change after 28 days. This indicates that the genetic effects of PA exposure may resolve with time. This result is good news for people who have been regularly ingesting PA-contaminated teas or supplements. The results of this toxicogenomic study further illustrate the vast amount of information that can be obtained by adding gene expression profiles to toxicologic studies. Using these tools in vivo also enables correlation with histopathology, serum biochemical assays, and detection of the toxic metabolite in tissue. PA studies are a particularly useful example of this utility as there is already a large amount of knowledge regarding their toxic mechanism and metabolic pathways. Toxicogenomic tools should be considered whenever designing toxicologic studies, particularly those in which the mechanisms are not fully understood.

The combined results of these experiments illustrate several important concepts. Individual PAs vary in their toxic effects in mice. Variation in hepatotoxicity, and toxicogenomic effects are clearly illustrated with statistical significance. Although not statistically significant, there were differences in the frequency of neoplasm development between PAs as well, and it is likely that individual PAs are not equally carcinogenic. Important differences between PAs which were characterized in these studies include severity of hepatotoxicity, distribution of hepatic necrosis within the liver, concentration of hepatic pyrroles induced, and induced changes in gene expression. Gene expression profile comparisons between two toxic PAs, riddelliine and senecionine indicate that PAs use common metabolic mechanisms to induce their toxic effects. Also, using the established carcinogenicity of riddelliine, shorter and simpler comparative experiments can be used to determine whether an additional PA is likely to be carcinogenic. Results of such comparative studies should be viewed considering the established fact that PAs that are non-toxic to some species can be toxic in others. In other words, negative results for carcinogenicity hold less weight than positive results. The results of heliotrine exposure in mice provide an illustrative example of this principle. Based on the results of all three experiments, heliotrine is non-toxic to mice at the doses used in each experiment. Brown et al. (2015) found that heliotrine was the most hepatotoxic PA when administered to California white chicks.[8] Additionally, in a large outbreak of PA poisoning in Afghanistan resulting in hepatic veno-occlusive disease in thousands of people and killing approximately 1,600 of those affected, heliotrine was the predominant PA in the contaminated grain.[13,14] Lack of toxicity in a single species should not lead to the assumption that an individual PA is safe for consumption.

Next Steps for research:

There are still many important questions regarding PA toxicosis which deserve attention. The reason for the differing lobular distributions of hepatocyte hypertrophy, degeneration and necrosis between PAs should be investigated. A reasonable hypothesis to explain the differences in distribution is that the CYP450 enzymes that toxify the PA are distributed differently within the liver. However, CYP450 gene expression between senecionine and riddelliine were nearly identical. Senecionine initially affected midzonal hepatocytes while riddelliine initially affected centrilobular areas. Mapping of CYP450 enzyme gene and protein expression within the liver would address this hypothesis and provide useful information for other toxicologic studies. Performing gene expression on hepatocytes in the different lobular zones, centrilobular, midzonal and periportal, could help determine if the distribution is in fact related to CYP450 enzymes, or if there is another cause. If CYP450 enzyme distribution is not the reason, structurally specific PA production of different toxic metabolites is the most likely theory.

Further studies comparing carcinogenic potential should be performed. The heterozygous p53 mouse model proved challenging for comparison of PA-induced neoplasia. The development of spontaneous/background neoplasms in the control group led to a lack of statistical significance for all PA groups. In Brown et al.'s (2015) initial carcinogenicity study, the heterozygous p53 knockout mice were purchased from different laboratory, and the purchased mice were all 9 weeks old when dosing was started. Additionally, all 49 mice were dosed simultaneously, enabling better statistical modeling and there was not a substantial difference in mortality between groups. In the experiment described here mice were obtained by breeding to reduce the cost of the

experiment. Breeding these mice necessitated using a range of ages from 5-13 weeks, and the size of the experiment required the compounds to be staggered and completed over a period of years. It is the authors opinion that if additional long-term carcinogenicity studies are to be performed on PAs, it would be wise to use a typical two-year exposure in a genetically unaltered mouse model. In 2006 the NTP discontinued the use of genetically modified animal models in carcinogenicity studies because of too many background tumors.[15] Additional two year carcinogenicity studies would be useful in proving that riddelliine is not unique in its carcinogenic potential. When these studies are performed, toxicogenomic tools should be performed to further characterize the genomic changes responsible for PA-induced cancer development. Establishing clear genomic mechanisms for carcinogenicity could enable comparative studies using in vitro methods to evaluate a large number of PAs in a short period of time and make predictions based on comparison to those PAs that are known carcinogens.

Proteomic studies in conjunction with RNAseq are needed to clarify which proteins are involved in toxicity and strengthen conclusions regarding upregulation and downregulation of genes responsible for phase 1 and phase 2 metabolism and cancer development. Last, further research into the development of fast and easy PA detection tools to enable regular screening of certain food items is important to help prevent human exposure to PAs.

Further characterization of the toxic effects of lasiocarpine in mice are also indicated. Our experiments would seemingly indicate that lasiocarpine was among the least toxic PAs, however it must be noted that mice could not tolerate doses greater than 30 mg/kg/day. Additional studies with varying doses and additional serum biochemical

assays to evaluate effects on other organs may provide the answer as to what caused such severe malaise in lasiocarpine-exposed mice. Similarly, additional dosing studies using greater doses of heliotrine in mice should be performed to determine the toxic dose in mice. All things are toxic and the dose determines the poison.[16] Given that mice are one of the most commonly used animal models in PA research, determining the toxic oral dose for heliotrine and other PAs would be helpful for future experiments.

References:

1. Ma, C. *et al.* Determination and regulation of hepatotoxic pyrrolizidine alkaloids in food: A critical review of recent research. *Food and Chemical Toxicology* **119**, 50–60 (2018).
2. World Health Organization and Food and Agriculture Organization of the United Nations. Safety evaluation of certain food additives and contaminants: supplement 2: pyrrolizidine alkaloids, prepared by the eightieth meeting of the Joint FAO/WHO Expert Committee on Food Additives (JECFA). https://www.who.int/publications-detail-redirect/9789240012677.
3. Phillips, D. H. & Arlt, V. M. Genotoxicity: damage to DNA and its consequences. *EXS* **99**, 87–110 (2009).
4. Bodi, D. *et al.* Determination of pyrrolizidine alkaloids in tea, herbal drugs and honey. *Food Addit Contam Part A Chem Anal Control Expo Risk Assess* **31**, 1886–1895 (2014).
5. Edgar, J. A. & Smith, L. W. Transfer of pyrrolizidine alkaloids into eggs: food safety implications. (1998).

6. Hoogenboom, L. a. P. *et al.* Carry-over of pyrrolizidine alkaloids from feed to milk in dairy cows. *Food Addit Contam Part A Chem Anal Control Expo Risk Assess* **28**, 359–372 (2011).
7. Bari, M. S. *et al.* Ethnomedicinal uses, phytochemistry, and biological activities of plants of the genus Gynura. *J Ethnopharmacol* **271**, 113834 (2021).
8. Brown, A. Relative Toxicity of Select Dehydropyrrolizidine Alkaloids and Evaluation of a Heterozygous P53 Knockout Mouse Model for Dehydropyrrolizidine Alkaloid Induced Carcinogenesis. *All Graduate Theses and Dissertations* (2015) doi:https://doi.org/10.26076/7997-d859.
9. Heterozygous p53 knockout mouse model for dehydropyrrolizidine alkaloid-induced carcinogenesis. *J Appl Toxicol* **35**, 1557–1563 (2015).
10. Hothorn, L. A. & Hasler, M. The Dunnett procedure with possibly heterogeneous variances. Preprint at https://doi.org/10.48550/arXiv.2303.09222 (2023).
11. Schaarschmidt, F., Sill, M. & Hothorn, L. A. Poly-k-trend tests for survival adjusted analysis of tumor rates formulated as approximate multiple contrast test. *J Biopharm Stat* **18**, 934–948 (2008).
12. National Toxicology Program. Toxicology and carcinogenesis studies of riddelliine (CAS No. 23246-96-0) in F344/N rats and B6C3F1 mice (gavage studies). *Natl Toxicol Program Tech Rep Ser* 1–280 (2003).
13. Kakar, F. *et al.* An Outbreak of Hepatic Veno-Occlusive Disease in Western Afghanistan Associated with Exposure to Wheat Flour Contaminated with Pyrrolizidine Alkaloids. *J Toxicol* **2010**, 313280 (2010).

14. Molyneux, R. J., Gardner, D. L., Colegate, S. M. & Edgar, J. A. Pyrrolizidine alkaloid toxicity in livestock: a paradigm for human poisoning? *Food Addit Contam Part A Chem Anal Control Expo Risk Assess* **28**, 293–307 (2011).
15. Toxicology/Carcinogenicity. *National Toxicology Program* https://ntp.niehs.nih.gov/whatwestudy/testpgm/cartox.
16. Grandjean, P. Paracelsus Revisited: The Dose Concept in a Complex World. *Basic Clin Pharmacol Toxicol* **119**, 126–132 (2016).

APPENDIX CURRICULUM VITAE

Michael J Clayton, DVM, Diplomate ACVP

783 South 1500 West,

Logan, Utah 84321
mjclaytondvm@gmail.com
801-867-9374

Education:

Date	Institution	Degree
2017-present	Utah Veterinary Diagnostic & Utah State University, Department of Animal, Dairy and Veterinary Sciences and USDA, ARS Poisonous Plant Research Laboratory, Logan, UT	Diplomate ACVP (passed phase 2 examination Aug. 2021), PhD (anticipated Sep. 2023) Relative Toxicity, Carcinogenicity and Toxicogenomics of Select Dehydropyrrolizidine Alkaloids in C57BL6/j Mice and Heterozygous p53 Knockout Mice
2008-2012	Washington State University College of Veterinary Medicine. Pullman, WA. *Phi zeta*	Doctor of Veterinary Medicine
2005-2008	University of Utah, College of Science. Salt Lake City, UT	Bachelor of Science, Biology

Professional Experience:

July 2017-present **Veterinary Anatomic Pathology resident and PhD Student**,

Utah State University, Utah Veterinary Diagnostic Laboratory, Logan,

UT

- Perform gross necropsies
- Perform histopathology on biopsy specimens
- Research, teaching, and coursework
- Lectures: endocrine system for veterinary systemic pathology, integument for veterinary histology

Veterinarian and Chief of Staff

Nov 2012-June 2017 Alcor Cresta Veterinary Hospital (A subsidiary of Cottonwood Animal Hospital), Midvale, UT

- Management, human resources, budgeting, client retention, conflict resolution, and all other duties necessary in the operation of a small animal veterinary clinic
- Perform physical examinations, surgeries, and dental procedures, and diagnose and treat medical conditions

May 2012-Nov 2012 **Associate Veterinarian**

Cottonwood Animal Hospital, Salt Lake City, UT

- Perform physical examinations, surgeries, dental procedures, and diagnose and treat medical conditions

Professional Activities and Associations:

- ACVP, member since 2021
- AAVLD, member since 2021
- AVMA, member since 2008

Publications:

- Clayton MJ, Kelly EJ, Mainenti M, Wilhelm A, Torchetti MK, Killian ML, Van Wettere AJ. Pandemic lineage 2009 H1N1 influenza A virus infection in farmed mink in Utah. J Vet Diagn Invest. 2022 Jan;34(1):82-85.
- Clayton MJ, Davis TZ, Knoppel EL, Stegelmeier BL. Hepatotoxic Plants that Poison Livestock. Vet Clin North Am Food Anim Pract. 2020 Nov;36(3):715-723.
- Eckstrand CD, Baldwin TJ, Rood KA, Clayton MJ, Lott JK, Wolking RM, Bradway DS, Baszler T. An outbreak of SARS-CoV-2 with high mortality in mink (Neovison vison) on multiple Utah farms. PLoS Pathog. 2021 Nov 12;17(11)

Conference Presentations:

- Comparison of Acute Dehydropyrrolizidine Alkaloid Toxicosis in C57BL6/J Mice Gavaged with Riddelliine, Riddelliine N-oxide, Senecionine, Senecionine N-oxide, Lasiocarpine, or Heliotrine. *Clayton MJ, Van Wettere AJ , Hall JO , Stegelmeier BL*. ACVP 2022 annual meeting, poster presentation and oral presentation.
- Outbreak of SARS-CoV-2 infection in farmed mink in Utah, 64th AAVLD Diagnostic Pathology Slide Seminar, 2021 USAHA/AAVLD annual meeting
- Characterization and Comparison of Acute Dehydropyrrolizidine Alkaloid Toxicosis in C57BL Mice Gavaged with Riddelliine, Senecionine, Seneciphylline or Lasiocarpine. *Clayton MJ, Knoppell E, Van Wettere AJ , Hall JO , Stegelmeier BL*. ACVP 2020 annual meeting, virtual poster presentation and short oral presentation.
- Toxicosis in Mice Gavaged With Riddelliine, Senecionine, Seneciphylline, or Lasiocarpine. 2020 USU ADVS Student Research Symposium, oral presentation.
- H1N1 Pandemic Lineage Influenza A In Farmed Mink In Utah. *Clayton M, Kelly EJ, Mainenti M, Wilhelm A, Torchetti MK, Killian ML , Van Wettere AJ*. ACVP 2019 annual meeting, poster presentation.
- Relative Carcinogenicity of Five Dehydropyrrolizidine Alkaloids in Heterozygous p53 Knockout Mice. *Clayton MJ, Van Wettere AJ, Hall JO, Stegelmeier BL*. 2019 USU ADVS Student Research Symposium, poster presentation.
- Hypotrichosis In Angus Calves Caused By Presumptive Bovine Viral Diarrhea Virus Infection In a Utah Beef Herd. *Clayton M, Firth P, Hullinger GA, Hall JO, Van Wettere AJ*. ACVP 2018 annual meeting, poster presentation.

Additional Honors and Awards:

- 1st place, Young Investigator Award, Industrial and Toxicologic Pathology, ACVP 2022 Annual Conference. Comparison of Acute Dehydropyrrolizidine Alkaloid Toxicosis in C57BL6/J Mice Gavaged with Riddelliine, Riddelliine N-oxide, Senecionine, Senecionine N-oxide, Lasiocarpine, or Heliotrine.
- 1st place, 64th Annual AAVLD Diagnostic Pathology Slide Seminar, case presentation titled “Outbreak of SARS-CoV-2 infection in farmed mink in Utah”
- Graduate Student Teacher of the Year, USU College of Agriculture and Applied Sciences, 2020
- Utah State University, Dept. of Animal, Dairy and Veterinary Science, Student Research Symposium, 1st place PhD oral presentation, 2020 and 2021
- 2019 Wendy J. Coe Memorial Graduate Student/Resident Travel Award
- Phi Zeta, Washington State University College of Veterinary Medicine, Class of 2012

- Washington State University College of Veterinary Medicine Class Rank: Class of 2012, 22 of 96
- Washington State University College of Veterinary Medicine Dean's List, Spring 2010